

2021-2022 CALIFORNIA CURRENT ECOSYSTEM STATUS REPORT

*A report of the NOAA California Current Integrated Ecosystem Assessment Team (CCIEA)
to the Pacific Fishery Management Council, March 13, 2022*

Edited by: Chris Harvey, Toby Garfield, Gregory Williams, and Nick Tolimieri
Northwest and Southwest Fisheries Science Centers, NOAA

With contributions from:

Kelly Andrews, Dan Ayres, Morgan Ball, Tracie Barry, Jack Barth, Rozy Bathrick, Jessie Beck, Eric Bjorkstedt, Steven Bograd, Jerry Borchert, Caren Braby, Brian Burke, Ryan Carle, Jason Cope, Jeff Cowen, David Demer, Heidi Dewar, Lynn deWitt, Blake Feist, John Field, Jennifer Fisher, Mary Fisher, Zachary Forster, Thomas Good, Christina Grant, Correigh Greene, Elliott Hazen, Daniel Holland, Mary Hunsicker, Matthew Hunter, Kym Jacobson, Michael Jacox, Jaime Jahncke, Elizabeth Jaime, Mike Johns, Tim Jones, Christy Juhasz, Stephen Kasperski, Su Kim, Dan Lawson, Andrew Leising, Kirsten Lindquist, Nate Mantua, Sharon Melin, Stephanie Moore, Cheryl Morgan, Barbara Muhling, Stuart Munsch, Catherine Nickels, Karma Norman, Rachael Orben, Julia Parrish, Scott Pearson, Amanda Phillips, Stephen Pierce, Jessica Porquez, Antonella Preti, Roxanne Robertson, Jan Roletto, Dan Rudnick, Lauren Saez, Keith Sakuma, Jameal Samhouri, Jarrod Santora, Isaac Schroeder, David Sherer, Kayleigh Somers, Beckye Stanton, Kevin Stierhoff, William Sydeman, Andrew Thompson, Sarah Ann Thompson, Duy Trong, Peter Warzybok, Brian Wells, Curt Whitmire, Samantha Zeman, Vanessa Zubkousky-White, Juan Zwolinski

2021-2022 CALIFORNIA CURRENT ECOSYSTEM STATUS REPORT

TABLE OF CONTENTS

MAIN REPORT

<u>Section</u>	<u>Page</u>
1 INTRODUCTION	1
2 CLIMATE AND OCEAN DRIVERS	2
3 FOCAL COMPONENTS OF ECOLOGICAL INTEGRITY	7
4 FISHERY LANDINGS, REVENUE, AND ACTIVITY	15
5 HUMAN WELLBEING	18
6 SYNTHESIS	22

SUPPLEMENTARY MATERIALS

<u>Appendix</u>	<u>Page</u>
A LIST OF CONTRIBUTORS TO THIS REPORT, BY AFFILIATION	S-1
B LIST OF FIGURE AND DATA SOURCES FOR THE MAIN REPORT	S-2
C CHANGES IN THIS YEAR'S REPORT	S-4
D SUMMARY INFOGRAPHICS FOR THE 2022 ECOSYSTEM STATUS REPORT	S-8
E DEVELOPING INDICATORS OF LONG-TERM CLIMATE CHANGE	S-10
F CLIMATE AND OCEAN INDICATORS	S-15
G SNOWPACK, STREAMFLOW, AND STREAM TEMPERATURE	S-24
H REGIONAL FORAGE AVAILABILITY	S-29
I COASTAL PELAGIC SPECIES DATA FROM SPRING 2021	S-32
J INDICATORS OF SALMON RETURNS	S-33
K HIGHLY MIGRATORY SPECIES (HMS)	S-40
L CALIFORNIA SEA LION PUP INDICATORS	S-42
M SEABIRD PRODUCTIVITY, DIET, AT-SEA DENSITY, AND MORTALITY	S-44
N HARMFUL ALGAL BLOOMS	S-51
O STATE-BY-STATE FISHERY LANDINGS AND REVENUES	S-54
P POTENTIAL FOR SPATIAL INTERACTIONS AMONG OCEAN-USE SECTORS	S-60
Q SOCIAL VULNERABILITY OF FISHING-DEPENDENT COMMUNITIES	S-64
R FLEET DIVERSIFICATION INDICATORS FOR MAJOR WEST COAST PORTS	S-65
S FISHERY REVENUE CONCENTRATION	S-66
T FISHERIES PARTICIPATION NETWORKS	S-68
U REFERENCES	S-73

2021-2022 CALIFORNIA CURRENT ECOSYSTEM STATUS REPORT

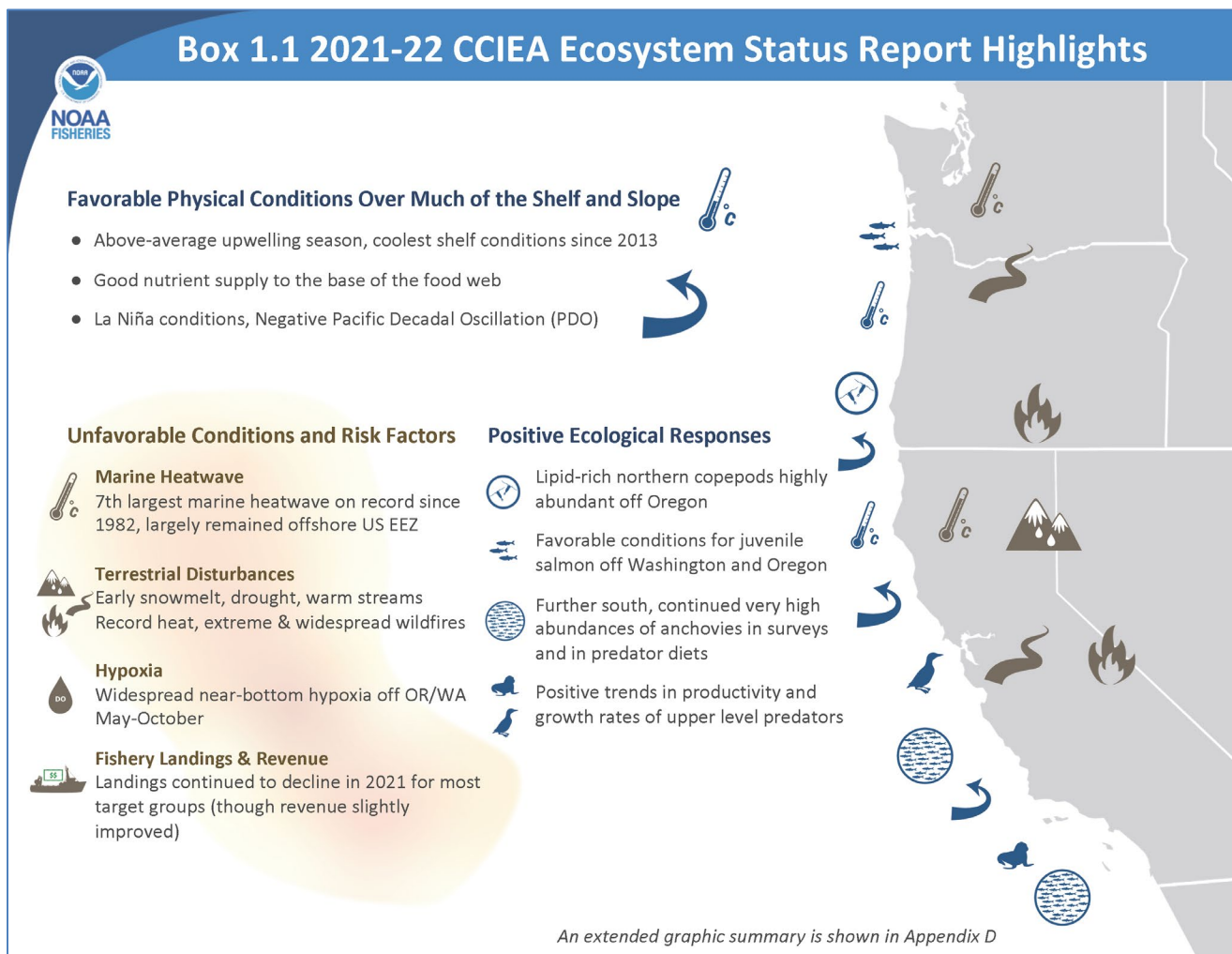
A report of the NOAA California Current Integrated Ecosystem Assessment Team (CCIEA) to the Pacific Fishery Management Council, March 13, 2022

Editors: Dr. Chris Harvey (NWFSC), Dr. Toby Garfield (SWFSC), Mr. Greg Williams (PSMFC), and Dr. Nick Tolimieri (NWFSC)

1 INTRODUCTION

Section 1.4 of the 2013 Fishery Ecosystem Plan (FEP) established a reporting process wherein NOAA provides the Pacific Fishery Management Council (Council) with a yearly update on the status of the California Current Ecosystem (CCE), as derived from environmental, biological, economic and social indicators. NOAA's California Current Integrated Ecosystem Assessment (CCIEA) team is responsible for this report. This is our 10th report, with prior reports in 2012 and 2014-2021.

This report summarizes CCE status based on data and analyses that generally run through 2021 and some that extend into 2022. Highlights are summarized in the infographic in Box 1.1. Appendices provide additional information or clarification, as requested by the Council and its committees and advisory bodies.



1.1 SAMPLING LOCATIONS

We generally refer to areas north of Cape Mendocino as the “Northern CCE,” Cape Mendocino to Point Conception as the “Central CCE,” and south of Point Conception as the “Southern CCE.” Figure 1.1a shows sampling areas for most regional oceanographic data. Key transects are the Newport Line off Oregon, the Trinidad Head Line off northern California, and CalCOFI lines further south. This sampling is complemented by basin-scale observations and models. Figure 1.1a also shows sampling areas for most biological indicators. Freshwater ecoregions in the CCE are shown in Figure 1.1b, and are the basis by which we summarize indicators for snowpack, flows, and stream temperatures.

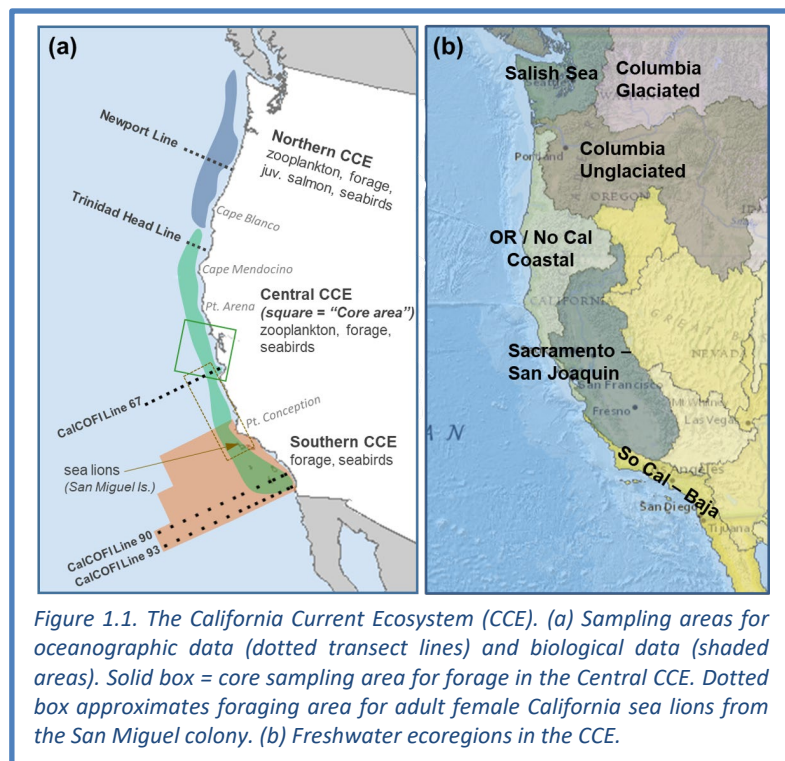


Figure 1.1. The California Current Ecosystem (CCE). (a) Sampling areas for oceanographic data (dotted transect lines) and biological data (shaded areas). Solid box = core sampling area for forage in the Central CCE. Dotted box approximates foraging area for adult female California sea lions from the San Miguel colony. (b) Freshwater ecoregions in the CCE.

1.2 COVID IMPACTS ON DATA COLLECTION

The COVID-19 pandemic impacted most West Coast data collection programs in 2020, which affected many indicator time series (Harvey et al. 2021a,b). The pandemic had far fewer effects on research in 2021, thanks to improved COVID conditions during 2021 field seasons and preparedness and adaptability of researchers and vessel crews. COVID-related effects on surveys, sample processing, and data are noted in the report as needed, and are summarized at the end of Appendix C. The CCIEA team is available to advise on interpretation of indicators, and we acknowledge that uncertainty in some indicators has been exacerbated by COVID-driven constraints on research.

2 CLIMATE AND OCEAN DRIVERS

After six years of variability dominated by the massive 2013-2016 marine heatwave, a large El Niño, and subsequent heatwaves, environmental conditions in the CCE in 2020-2021 appear to have returned to conditions similar to those prior to 2013. This return is manifested in the suite of environmental indices suggesting strong upwelling, an increased expanse of cool water over the shelf and slope, and La Niña conditions. Even with this return, a new marine heatwave was present in 2021, though it remained well offshore of our coastline except for a brief incursion in early June. On land, record-high air temperatures, severe drought, wildfires, reduced snowpack, and lower, warmer streamflow affected many regions. These observations are detailed in the following sections.

2.1 BASIN-SCALE INDICATORS

We use three indices to characterize large-scale physical ecosystem states in the North Pacific. The Oceanic Niño Index (ONI) describes the equatorial El Niño Southern Oscillation (ENSO). An ONI above 0.5°C indicates El Niño conditions, which often lead to lower primary production, weaker upwelling, poleward transport of equatorial waters and species, and more southerly storm tracks in the CCE. An ONI below -0.5°C means La Niña conditions, which create atmospheric pressure conditions that lead to upwelling-favorable winds that drive productivity in the CCE. The Pacific Decadal Oscillation

(PDO) describes North Pacific sea surface temperature (SST) anomalies that may persist for many years. Positive PDOs are associated with warmer SST and lower productivity in the CCE, while negative PDOs indicate cooler SST and are associated with higher productivity. The North Pacific Gyre Oscillation (NPGO), an index of sea surface height, indicates changes in circulation that affect source waters for the CCE. Positive NPGOs are associated with strong equatorward flow and higher salinity, nutrients, and chlorophyll-*a*. Negative NPGOs are associated with decreased subarctic source water and lower CCE productivity.

Basin-scale indices suggest average to above-average conditions for productivity in 2021: the ONI and PDO remained negative, while the NPGO transitioned from negative to neutral. The negative ONI illustrates the La Niña conditions that existed throughout 2021 (Figure 2.1.1, top). As of January 2022, NOAA forecasts a 67% chance of La Niña remaining through March-May, and a 51% chance of a transition to ENSO-neutral conditions in April-June. The PDO remained negative for a second consecutive year, reaching some of the lowest recorded values and continuing a trend of decreasing values since 2016 (Figure 2.1.1, middle). In late 2019 and early 2020 the NPGO reached its lowest value since 1993; through 2020 and 2021, NPGO rose to a neutral value (Figure 2.1.1, bottom). This indicates that the general circulation in the CCE transitioned to average. Taken together, these indices represent cool coastal conditions favorable for primary productivity. Seasonal values for all indices are in Appendix F.1.

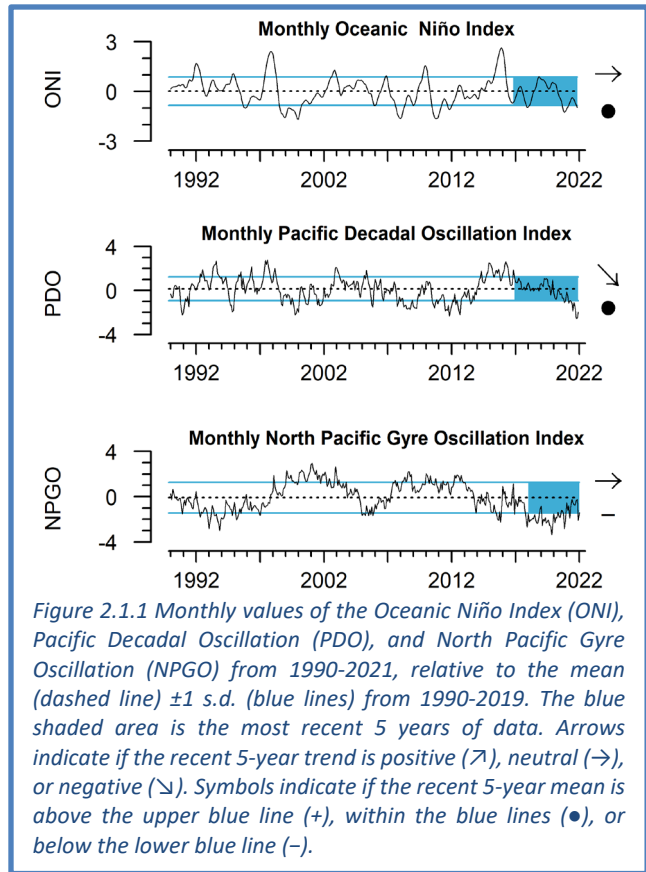


Figure 2.1.1 Monthly values of the Oceanic Niño Index (ONI), Pacific Decadal Oscillation (PDO), and North Pacific Gyre Oscillation (NPGO) from 1990-2021, relative to the mean (dashed line) ± 1 s.d. (blue lines) from 1990-2019. The blue shaded area is the most recent 5 years of data. Arrows indicate if the recent 5-year trend is positive (\nearrow), neutral (\rightarrow), or negative (\searrow). Symbols indicate if the recent 5-year mean is above the upper blue line (+), within the blue lines (\bullet), or below the lower blue line (-).

The northeast Pacific continues to experience large marine heatwaves in surface waters. The 2021 marine heatwave formed in April and reached its maximum size, approximately 4.1 million km², in August (Figure 2.1.2). It was the 7th largest heatwave by area and the 6th longest in duration since monitoring began in 1982. However, except for a ~1-week intrusion in June to the California and southern Oregon coasts, the feature largely remained offshore of the CCLME and outside of the US

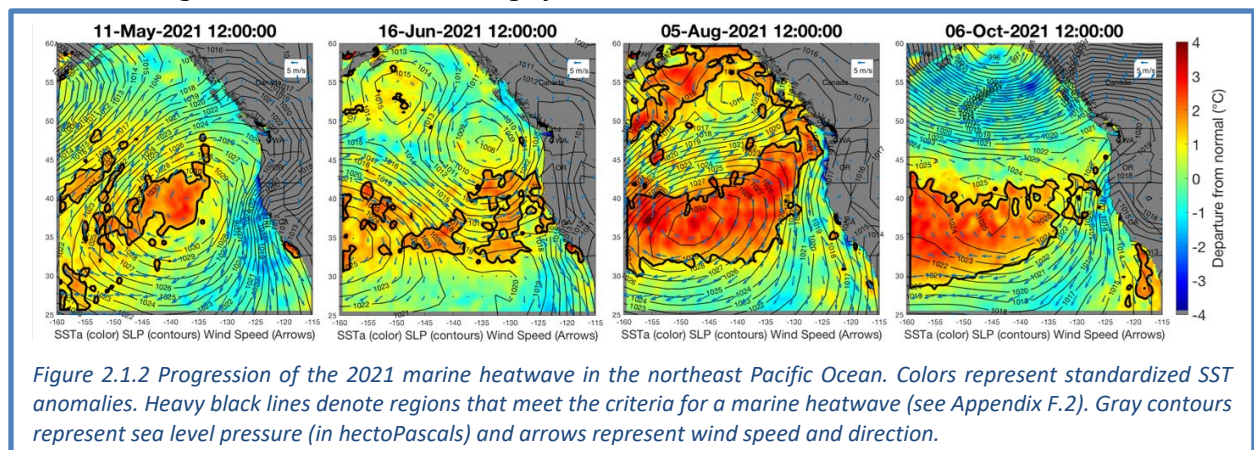


Figure 2.1.2 Progression of the 2021 marine heatwave in the northeast Pacific Ocean. Colors represent standardized SST anomalies. Heavy black lines denote regions that meet the criteria for a marine heatwave (see Appendix F.2). Gray contours represent sea level pressure (in hectoPascals) and arrows represent wind speed and direction.

EEZ, unlike heatwaves in many previous years. A contributing factor to the 2021 heatwave remaining offshore was moderately strong and relatively constant upwelling along the West Coast for much of the year. The short intrusion to California and Oregon coastal waters in early June exactly coincided with one of the few major wind reversal events of the upwelling season. The heatwave eventually broke apart in December. Additional information on the 2021 marine heatwave is in Appendix F.2.

Subsurface temperatures were cooler than average in 2021 along much of the West Coast. Off Newport, Oregon, temperatures in most of the upper 100 m were ~ 0.5 to 1.0°C cooler than average from winter through June (Figure 2.1.3, top). In the Southern California Bight, the water column in early 2021 was warm nearshore and cool further offshore. At CalCOFI station 90.30 (off Dana

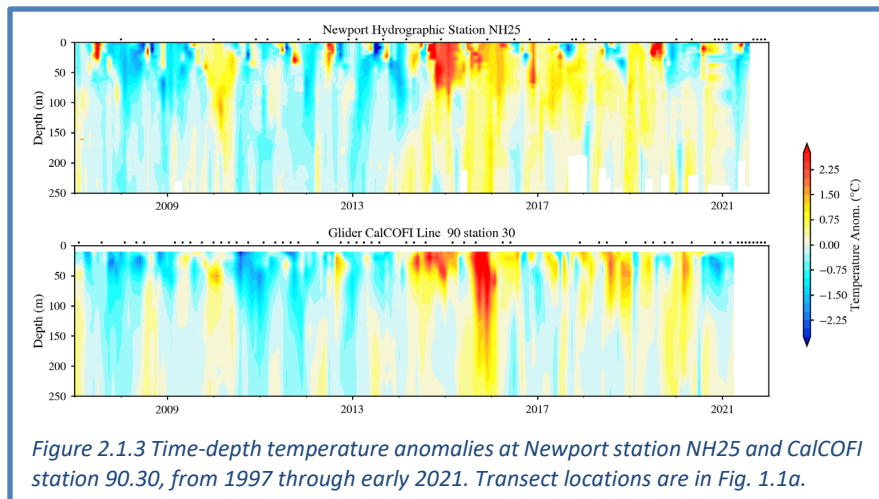


Figure 2.1.3 Time-depth temperature anomalies at Newport station NH25 and CalCOFI station 90.30, from 1997 through early 2021. Transect locations are in Fig. 1.1a.

Point), the water column was cool in spring (Figure 2.1.3, bottom), and offshore anomalies remained cool while inshore anomalies were warm (Appendix F, Figure F.1.5). Subsurface temperatures off Monterey Bay also were average or below-average for most of 2021 (Figure F.1.4). In contrast, warm anomalies $>1^\circ\text{C}$ dominated the water column off San Diego in winter and spring (not shown).

2.2 UPWELLING AND HABITAT COMPRESSION

Upwelling is a major driver of coastal productivity in the CCE. It occurs when equatorward coastal winds force deep, cold, nutrient-rich water to the surface. The greatest upwelling in the CCE occurs off central California and typically peaks in June. Here, we present two upwelling indices: vertical flux of water (Cumulative Upwelling Transport Index; CUTI) and of nitrate (Biologically Effective Upwelling Transport Index; BEUTI) (Jacox et al. 2018).

Numerous strong upwelling events occurred in 2021, with peaks ≥ 1 s.d. above the mean at 39°N and 45°N , (Figure 2.2.1). Many were followed by relaxation events that allowed for retention of nutrients that spurred coastal production. Upwelling events in February may have provided an early injection of nutrients, helping to “pre-condition” the system before the transition into the productive season for the coastal food web. Upwelling in May off central California was the strongest of the past 30 years.

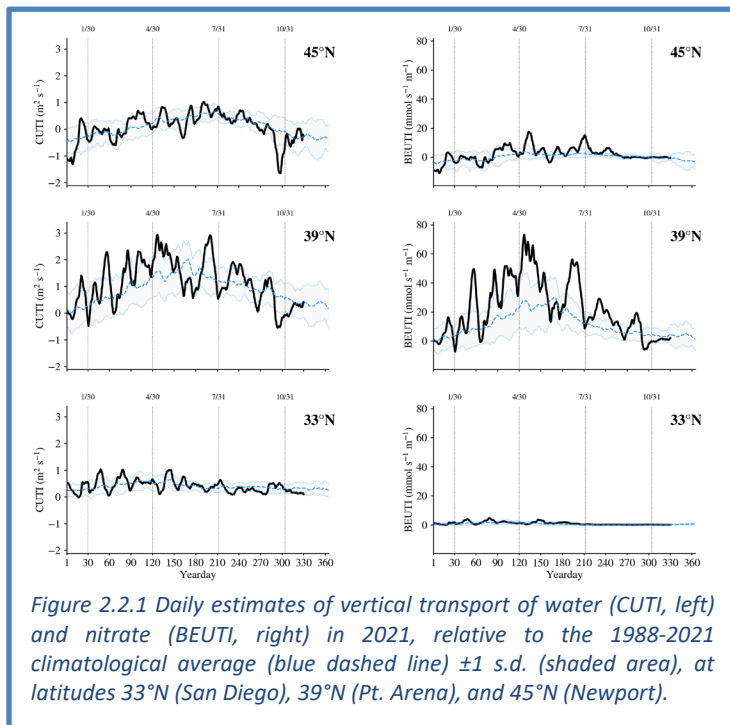


Figure 2.2.1 Daily estimates of vertical transport of water (CUTI, left) and nitrate (BEUTI, right) in 2021, relative to the 1988-2021 climatological average (blue dashed line) ± 1 s.d. (shaded area), at latitudes 33°N (San Diego), 39°N (Pt. Arena), and 45°N (Newport).

Santora et al. (2020) developed the habitat compression index (HCI) to describe how much cool, productive water is available adjacent to the coast. HCI ranges from 0 (= complete coverage of warm offshore water in the region) to 1 (= cool water fully extending 150 km from the coast). Off central California, cool coastal habitat has been expanding since 2016 (Figure 2.2.2), and winter and spring HCI values in 2021 were above the long-term means. Similarly, cool coastal habitat generally has been stable or expanding over the past five years off northern California, Oregon and Washington (Appendix F.3).

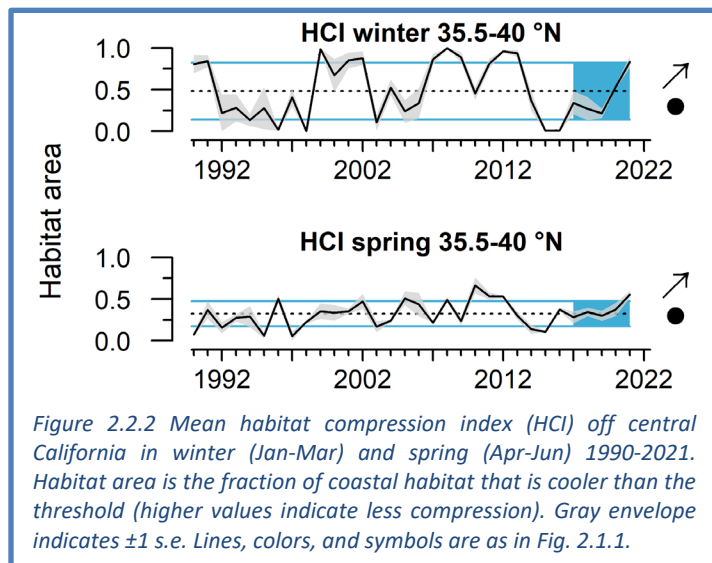


Figure 2.2.2 Mean habitat compression index (HCI) off central California in winter (Jan-Mar) and spring (Apr-Jun) 1990-2021. Habitat area is the fraction of coastal habitat that is cooler than the threshold (higher values indicate less compression). Gray envelope indicates ± 1 s.e. Lines, colors, and symbols are as in Fig. 2.1.1.

2.3 HYPOXIA AND OCEAN ACIDIFICATION

Dissolved oxygen (DO) is influenced by processes such as currents, upwelling, air-sea exchange, primary production, and respiration. Low DO (hypoxia) can compress habitat and cause stress or die-offs in sensitive species (Chan et al. 2008). Station NH05 off Newport, Oregon experienced sustained near-bottom hypoxia in 2021 (Figure 2.3.1, top). Near-bottom DO values were below the hypoxia threshold from late May through October 2021, which was the longest hypoxic period of the time series. Additional DO data from the Northern CCE are in Appendix F.4. DO values for CalCOFI in 2021 were not available at this writing.

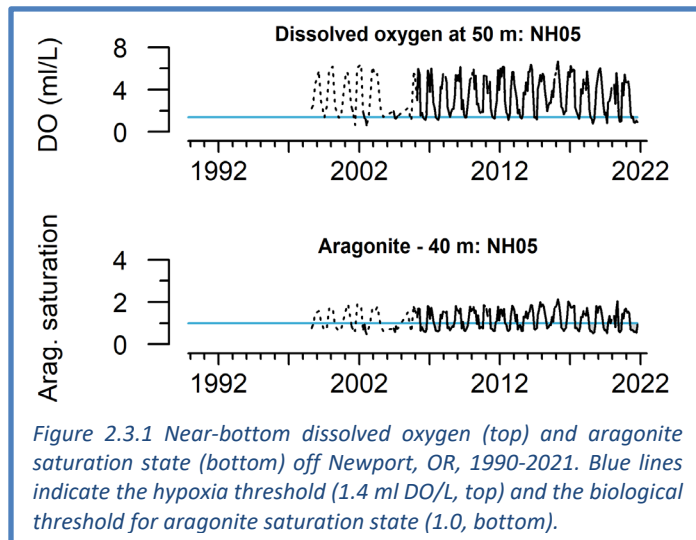


Figure 2.3.1 Near-bottom dissolved oxygen (top) and aragonite saturation state (bottom) off Newport, OR, 1990-2021. Blue lines indicate the hypoxia threshold (1.4 ml DO/L, top) and the biological threshold for aragonite saturation state (1.0, bottom).

Ocean acidification, caused by increased anthropogenic CO_2 , reduces pH and dissolved carbonate in seawater and is stressful to many marine species (Feely et al. 2008, Busch and McElhany 2016). At station NH05 off Newport, levels of aragonite (a form of calcium carbonate) were favorable in winter, but in summer and fall they dropped below 1.0 (Figure 2.3.1, bottom), which is corrosive for many shell-forming organisms. While this is a typical seasonal pattern at this station, the corrosive period in 2021 was longer than normal (see details in Appendix F.4).

2.4 SNOWPACK AND HYDROLOGY

Snow-water equivalent (SWE) is the water content in snowpack, which supplies cool freshwater to streams in spring, summer and fall and is critical for salmon production (Appendix E, Appendix J.2). SWE in 2021 exhibited major geographic differences: winter storms tended to track north, resulting in high snowpack in the northern Cascades (125-200% of the 30-yr median) and low snowpack in the Sierra Nevada (0-50% of median). On April 1, 2021, SWEs were above average or average in northern ecoregions, but below average to the south (Figure 2.4.1). After April 1, rapid warming led to major SWE deficits in most ecoregions. Conditions worsened as air temperatures rose to extremes:

June-to-August mean air temperatures in 2021 were the highest recorded in California, Idaho, and Oregon, and second-highest for Washington, and soil moisture content was extremely low throughout the West. These conditions set up severe to exceptional drought in late spring and summer. Hot, dry conditions triggered disastrous wildfires, drew reservoirs far below capacity, and forced hatchery managers in the Sacramento/San Joaquin River region to truck many smolts to San Francisco Bay instead of releasing them in-river (Appendix J.2).

As of February 1, 2022, SWE in the West is mixed (Appendix G). The annual benchmark measure of SWE will be on April 1, 2022.

At the ecoregion scale, stream flows were generally average to below-average in 2021 (Appendix G). Here, we further summarize streamflows at the finer scale of river basins representing Chinook salmon evolutionarily significant units (ESUs). Results are shown in quad plots, which indicate if flows over the last five years were above or below average, and if they had increasing or decreasing trends. Overall, both maximum and minimum flows show evidence of widespread recent declines (Figure 2.4.2). One-day maximum flows for 10 of 16 ESUs had significant declining trends from 2017-2021, and recent average maximum flows in 7 ESUs also fell below long-term averages during that period (Figure 2.4.2, left; Appendix G). ESUs with significant below-average maximum

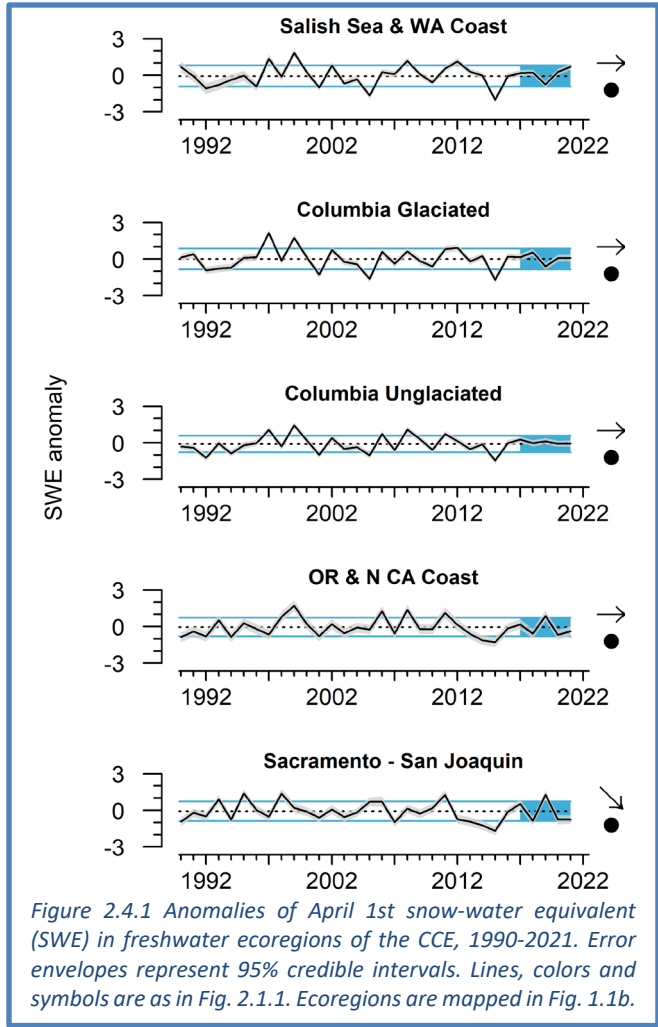


Figure 2.4.1 Anomalies of April 1st snow-water equivalent (SWE) in freshwater ecoregions of the CCE, 1990-2021. Error envelopes represent 95% credible intervals. Lines, colors and symbols are as in Fig. 2.1.1. Ecoregions are mapped in Fig. 1.1b.

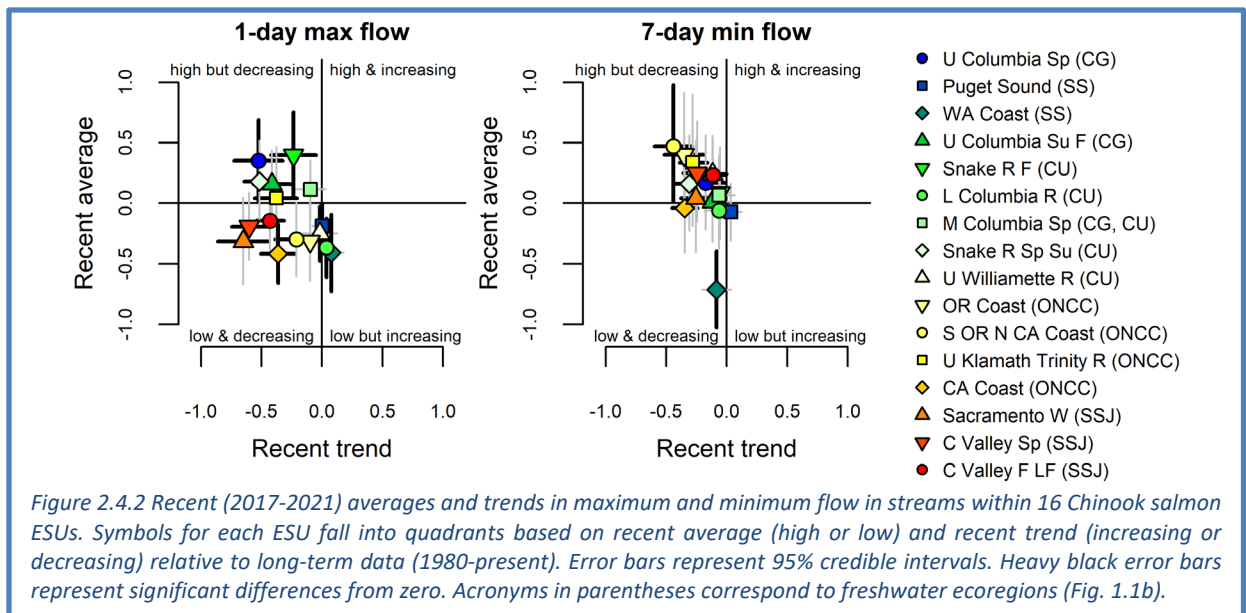


Figure 2.4.2 Recent (2017-2021) averages and trends in maximum and minimum flow in streams within 16 Chinook salmon ESUs. Symbols for each ESU fall into quadrants based on recent average (high or low) and recent trend (increasing or decreasing) relative to long-term data (1980-present). Error bars represent 95% credible intervals. Heavy black error bars represent significant differences from zero. Acronyms in parentheses correspond to freshwater ecoregions (Fig. 1.1b).

flows were mostly in the Pacific Northwest. Some ESUs (Snake River Fall and Upper Columbia Spring) have been above average in recent years, but have downward trends. Declining recent trends were even more apparent for seven-day minimum flows, with all but 5 ESUs exhibiting strong negative trends, and the rest exhibiting no trend (Figure 2.4.2, right; Appendix G). Recent average minimum flows were at or above the time series averages for all but the Washington Coast ESU.

3 FOCAL COMPONENTS OF ECOLOGICAL INTEGRITY

In general, ecological indicators suggest average to above-average feeding conditions in 2021 in much of the CCE, with signs of high productivity of nutritious zooplankton, continued high abundance of anchovy, mostly healthy groundfish stocks, and positive productivity signals for several top predators. Signals for coho salmon returns in 2022 are encouraging, but mixed for Chinook salmon.

3.1 COPEPODS AND KRILL

Copepod biomass anomalies represent variation in northern copepods (cold-water crustacean zooplankton rich in wax esters and fatty acids) and southern copepods (smaller species with lower fat content and nutritional quality). Northern copepods usually dominate the summer zooplankton community along the Newport Line (Figure 1.1a), while southern copepods dominate in winter.

In 2021, lipid-rich northern copepods were highly abundant along the Newport Line, reaching >1 s.d. above the mean in spring-summer before their regular seasonal decline in fall (Figure 3.1.1, top). The spring-summer anomaly was among the highest of the 26-year time series. Northern copepod biomass has increased steadily since the extreme lows of the 2014-2016 heatwave. Southern copepod biomass was below-average in much of 2021, continuing a negative trend since the heatwave (Figure 3.1.1, bottom). These values suggest above-average feeding conditions for pelagic fishes off central Oregon in spring and summer of 2021. La Niña events and a negative PDO generally favor northern copepods (Keister et al. 2011, Fisher et al. 2015). Positive northern copepod anomalies generally correlate with stronger returns of Chinook salmon to Bonneville Dam and coho salmon to coastal Oregon (Peterson et al. 2014).

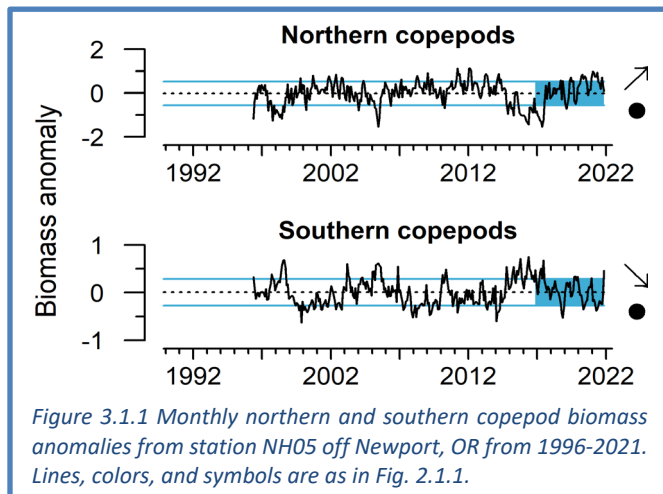


Figure 3.1.1 Monthly northern and southern copepod biomass anomalies from station NH05 off Newport, OR from 1996-2021. Lines, colors, and symbols are as in Fig. 2.1.1.

Krill are among the most important prey groups in the CCE. The species *Euphausia pacifica* is sampled year-round off Trinidad Head (Figure 1.1a). Mean length of adult *E. pacifica* is an indicator of productivity at the base of the food web, krill condition, and energy content for predators. *E. pacifica* lengths in spring and summer of 2021 were above average, then fell below average in fall (Figure 3.1.2, top). These seasonal changes are consistent with observations prior to the 2014-2016 heatwave. Krill lengths have generally increased since the onset of that

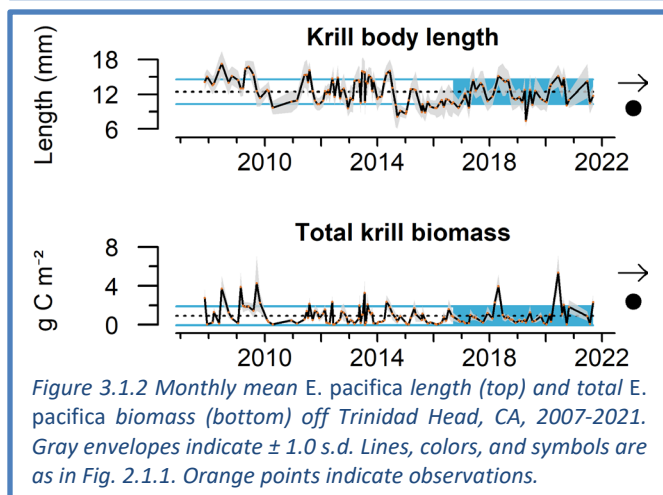


Figure 3.1.2 Monthly mean *E. pacifica* length (top) and total *E. pacifica* biomass (bottom) off Trinidad Head, CA, 2007-2021. Gray envelopes indicate ± 1.0 s.d. Lines, colors, and symbols are as in Fig. 2.1.1. Orange points indicate observations.

heatwave, except in 2019 when growth may have been reduced by El Niño conditions.

Based on recommendations from the Council SSC-ES, we added a metric of total *E. pacifica* biomass from two offshore Trinidad Head stations, where adults dominate the catch. *E. pacifica* biomass in 2021 was mostly within ± 1 s.d. of the time series average, but down from the exceptionally high biomasses of the summer of 2020 (Figure 3.1.2, bottom). COVID-19 led to some cancelled cruises and delays in sample processing in 2020 and 2021, but the data shown are from stations that are highly representative of *E. pacifica* sizes off Trinidad Head (Robertson and Bjorkstedt 2020).

3.2 REGIONAL FORAGE AVAILABILITY

The regional surveys that produce CCE forage data use different gears and survey designs, which makes regional comparisons difficult. In past reports, we developed cluster analysis methods to identify regional shifts in forage composition (Thompson et al. 2019a). Those plots are shown here; see the caption of Figure 3.2.1 for how to interpret the plots. Related time series are in Appendix H.

Northern CCE: The Northern CCE survey off Washington and Oregon (Figure 1.1a) targets juvenile salmon in surface waters, and also samples surface-oriented fishes, squid and jellies. The composition of this near-surface community has changed several times since the onset of marine heatwave conditions in 2014-2016, but the community has remained relatively stable since 2018 (Figure 3.2.1). This community is characterized by variable but roughly average catches of most salmon and high abundances of market squid and water jellies (though market squid catches were lower here in 2021 than in recent years). Pompano, which were common during the 2014-2016 marine heatwave, were not caught in June 2021. Time series of catches from this survey are in Appendix H.1. Juvenile salmon time series are discussed further in Section 3.3.

Central CCE: Data shown here are from the “Core Area” of a nearly coastwide survey (Figure 1.1a) that targets pelagic young-of-the-year (YOY) rockfishes, but also samples other pelagic species. The forage community in this region, centered just off Monterey Bay, has had a relatively stable structure since 2018, and a defining trait has been high abundance of adult anchovy (Figure 3.2.2). Adult anchovy remained very abundant at these stations in 2021, while no adult Pacific sardine were

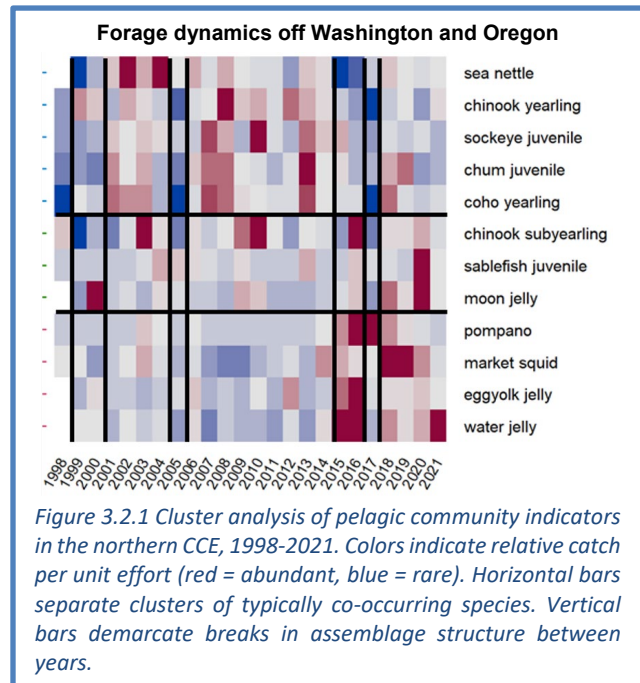


Figure 3.2.1 Cluster analysis of pelagic community indicators in the northern CCE, 1998-2021. Colors indicate relative catch per unit effort (red = abundant, blue = rare). Horizontal bars separate clusters of typically co-occurring species. Vertical bars demarcate breaks in assemblage structure between years.

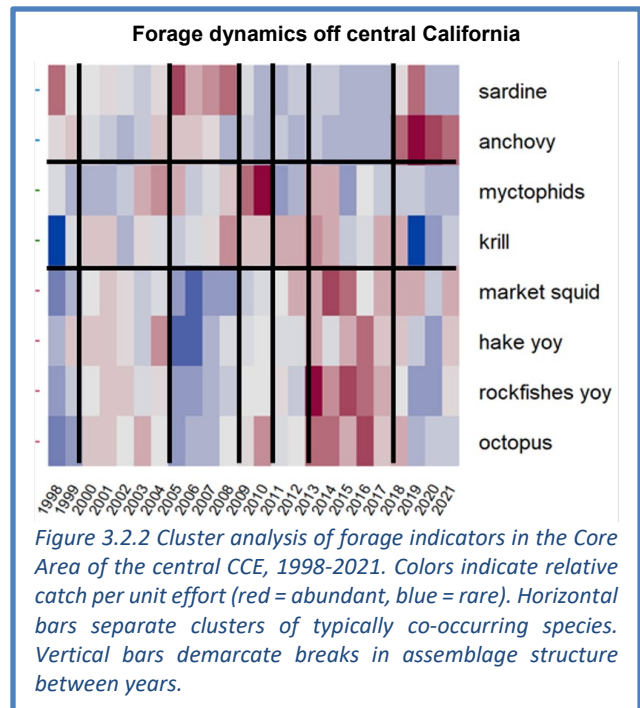


Figure 3.2.2 Cluster analysis of forage indicators in the Core Area of the central CCE, 1998-2021. Colors indicate relative catch per unit effort (red = abundant, blue = rare). Horizontal bars separate clusters of typically co-occurring species. Vertical bars demarcate breaks in assemblage structure between years.

encountered. Catches of YOY rockfishes, sanddabs, and Pacific hake increased from the very low levels of 2019-2020, but remained well below the peaks associated with the 2014-2016 marine heatwave. Market squid catches were above average. Time series of catch data are in Appendix H.2. The high occurrences of anchovy and rarity of sardine are consistent with findings from a NMFS acoustics and trawl survey for coastal pelagic species, conducted between the U.S./Mexico border and San Francisco Bay in spring 2021 (Appendix I).

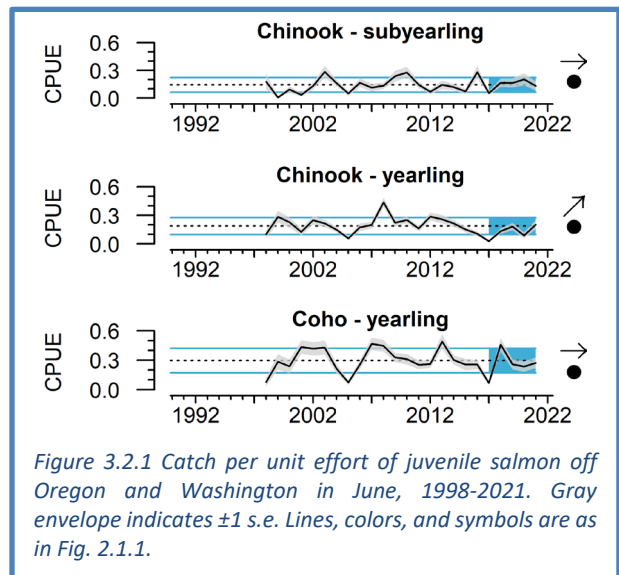
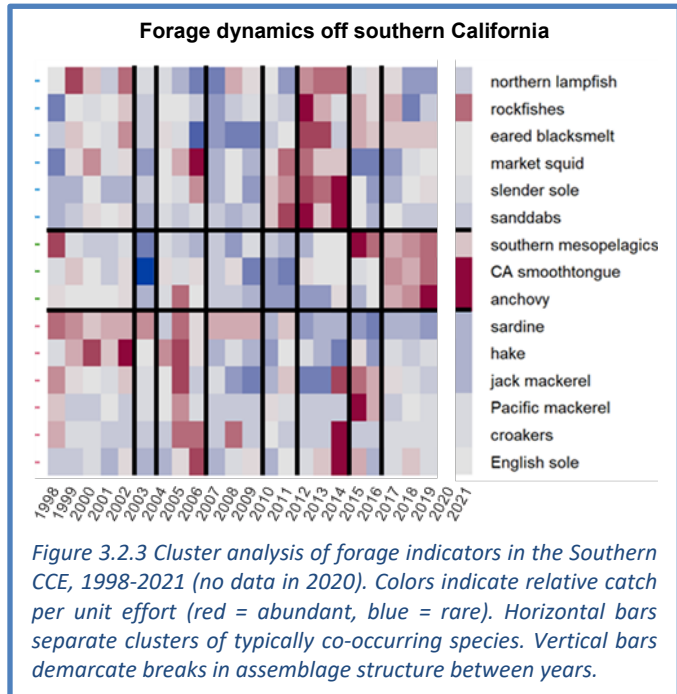
Southern CCE: Forage data for the Southern CCE come from CalCOFI larval fish surveys (Figure 1.1a). The spring 2021 assemblage clustered with the assemblages of 2017-2019 (Figure 3.2.3; no data for 2020 due to COVID-19). These years were characterized by extremely high abundances of anchovy and southern mesopelagic fishes. Similar to previous years, coastal pelagic species such as sardine, jack mackerel, and Pacific mackerel were rare in 2021 (see also Appendix I). Rockfish larvae, however, increased to their highest level since 2012, and market squid paralarvae were close to average abundance. Time series of catches are available in Appendix H.3.

Pyrosomes: Pyrosomes (warm-water pelagic tunicates) were highly abundant in the Central and Southern CCE in 2021, as they have generally been since the series of marine heatwaves began in 2014 (see Appendix H.2). Pyrosome catches in the Southern California Bight were the highest since sampling began in 1983. They were less abundant north of Cape Mendocino, but were present on the Trinidad Head line throughout the 2021 sampling season and were observed at least as far north as Newport in April 2021.

3.3 SALMON

Juvenile salmon abundance: Catches of juvenile coho and Chinook salmon from surveys during June in the Northern CCE (Figure 1.1a) are indicators of salmon survival during their first few weeks at sea. In 2021, catches of juvenile subyearling Chinook salmon, juvenile yearling Chinook salmon, and juvenile yearling coho salmon were all very close to time series averages (Figure 3.2.1). Juvenile yearling Chinook salmon catches have been trending upward over the most recent five years of data, while subyearling Chinook salmon and juvenile coho salmon catches have varied over the most recent five years, but show no significant trend.

Spotlight tables: Long-term associations between oceanographic conditions, food web structure, and salmon productivity support qualitative



outlooks of returns of Chinook salmon to Bonneville Dam and smolt-to-adult survival of Oregon Coast coho salmon (Burke et al. 2013, Peterson et al. 2014). These relationships are depicted in the “stoplight table” in Table 3.3.1, which includes many indicators shown elsewhere in this report (PDO, ONI, SST, deep temperature, copepods, juvenile salmon catch). In 2021, this suite of ecosystem indicators was the most favorable for northern California Current salmon productivity in the last decade (Table 3.3.1) and the second most favorable of the 1998-2021 time series, after only 2008. Marine conditions in 2021 are consistent with good marine survival for coho salmon returning to this area in 2022. For Chinook salmon returning to the Columbia Basin in 2022, indicators for the dominant smolt year (2020) reflect a mix of good, intermediate and poor conditions. A related quantitative model that uses the stoplight indicators in Table 3.3.1 estimates that for most Chinook salmon returning to the Snake and Upper Columbia rivers in 2022, smolt-to-adult survival will be close to the average of the last ten cohorts (Appendix J.1). Predicted survival for Chinook salmon smolts that went to sea in 2021 (and will dominate returns in 2023) is greater than the average from the last ten cohorts (Appendix J.1).

Table 3.3.1 "Stoplight" table of conditions for smolt years 2012-2021 for coho salmon originating in coastal Oregon and Chinook salmon from the Columbia Basin. Green = "good," yellow = "intermediate," and red = "poor," relative to the full time series (1998-present). Chinook salmon from smolt year 2020 and coho salmon from smolt year 2021 (columns outlined in blue) represent the dominant age classes likely to return to their respective spawning rivers in 2022.

ECOSYSTEM INDICATORS		2012	2013	2014	2015	2016	2017	2018	2019	2020	2021
CLIMATE & ATMOSPHERIC	PDO (SUM; Dec-Mar)	Green	Yellow	Yellow	Red	Red	Red	Yellow	Red	Yellow	Green
	PDO (SUM; May-Sep)	Green	Yellow	Red	Red	Red	Red	Yellow	Red	Yellow	Green
	ONI (AVG; Jan-Jun)	Green	Yellow	Yellow	Red	Red	Yellow	Green	Red	Red	Green
LOCAL PHYSICAL	SST NDBC Buoys (°C; May-Sep)	Yellow	Red	Red	Red	Red	Yellow	Red	Red	Yellow	Green
	Upper 20 m T (°C; Nov-Mar)	Green	Yellow	Green	Red	Red	Red	Yellow	Red	Green	Green
	Upper 20 m T (°C; May-Sep)	Green	Red	Red	Red	Yellow	Yellow	Yellow	Red	Red	Green
	Deep Temp (°C; May-Sep)	Green	Yellow	Red	Red	Yellow	Red	Red	Red	Red	Green
	Deep Salinity (May-Sept)	Yellow	Yellow	Red	Red	Yellow	Yellow	Green	Yellow	Red	Green
LOCAL BIOLOGICAL	Copepod richness	Green	Green	Yellow	Red	Red	Red	Yellow	Yellow	Green	Green
	N copepod biomass	Green	Green	Green	Red	Red	Red	Yellow	Green	Green	Green
	S copepod biomass	Yellow	Green	Yellow	Red	Red	Red	Yellow	Yellow	Yellow	Green
	Biological transition	Yellow	Green	Green	Red	Red	Red	Yellow	Yellow	Green	Yellow
	Nearshore Ichthyoplankton	Green	Yellow	Red	Yellow	Red	Yellow	Yellow	Red	Green	Green
	Nearshore & offshore Ichthyoplankton	Green	Green	Yellow	Red	Red	Red	Red	Red	Red	Yellow
	Chinook salmon juvenile catch	Green	Green	Yellow	Yellow	Red	Red	Yellow	Yellow	Red	Yellow
	Coho salmon juvenile catch	Red	Green	Yellow	Yellow	Yellow	Red	Green	Yellow	Yellow	Yellow

In the 2020 report, we introduced an indicator-based table to provide some broad, qualitative, ecosystem context for returns of fall Chinook salmon to the Central Valley. Natural-area Central Valley Fall Chinook salmon returns are correlated with fall egg incubation temperature and February streamflow in the Sacramento River, and the abundance and diet of common murrelets at Southeast Farallon Island (Friedman et al. 2019). For adult salmon returning in 2022, signals are mixed, both within and across age classes. The dominant age class (age-3, from the 2019 brood year) had relatively favorable parent escapement, but suboptimal egg incubation temperature and very poor winter flows for newly hatched juveniles (Table 3.3.2). Other cohorts had low to very low parent escapement, unfavorably warm egg incubation temperatures, and very poor flow for early juveniles except in the 2018 brood year. Common murre diets in recent years have been near the long-term

average, but that average is near zero, and abundant anchovies in the Central CCE (Figure 3.2.2) may be buffering salmon from murre predation near Southeast Farallon Island (see Appendix M.2). Additional details on this salmon stoplight table are in Appendix J.2. This table is best viewed as general context, as some of the underlying assumptions and descriptors require further data and validation.

Table 3.3.2 Conditions for natural-area Central Valley fall Chinook salmon returning in 2022, from brood years 2017-2020. See text for explanation of indicators. Bold type indicates age-3 Chinook salmon, the dominant age class of returns to the Central Valley.

Spawning Escapement (t=0)	Incubation Temperature (Oct-Dec t=0)	February Median Flow (t+1)	Seabird Marine Predation Index (t+1)	Chinook Age in Fall 2022
2017: 17,851 (very low)	11.7°C (poor)	5,525 cfs (very low)	Near average	5
2018: 71,689 (low)	11.7°C (poor)	21,700 cfs (high)	Near average	4
2019: 121,600 (met goal)	11.3°C (suboptimal)	6,030 cfs (very low)	Near average	3
2020: 100,100 (low)	11.5°C (poor)	6,015 cfs (very low)	Near average	2

The Council’s Habitat Committee, Salmon Technical Team, and others including CCIEA scientists are developing more comprehensive stoplight tables for Sacramento River Fall Chinook salmon and Klamath River Fall Chinook salmon, which were the focus of recent rebuilding plans. The stoplight tables feature indicators from throughout the stocks’ life histories, spanning brood years 1983-2020. Indicators in recent years for both stocks have been mixed (Appendix J.2). The 2020 brood years (smolts in 2021) in both systems experienced very poor freshwater conditions, so much so that most Sacramento River hatchery fish were released in estuarine or marine waters to reduce heat stress. Marine habitat conditions for both the 2019 and 2020 brood years showed some improvements compared to brood years 2012-2018 (Appendix J.2).

Thiamine deficiency: In 2020 and 2021, Mantua et al. (2021) documented widespread thiamine deficiency as a new stressor in Central Valley Chinook salmon. They suspect that this stressor is linked with the recent dominance of anchovy in the marine food web that supports these salmon (e.g., Figure 3.2.2). Thiamine deficiency can lead to high mortality in early life stages of Chinook salmon. Multiple effective treatments are being used at hatcheries in the Central Valley, which should limit impacts on hatchery populations. However, there are no clear treatment options for naturally spawning populations. We suspect that thiamine deficiency has negatively impacted early life stage survival rates for natural-origin Central Valley Chinook salmon from brood years 2020 and 2021. At present, anchovy abundance is not represented in Table 3.3.2 or the stoplight tables in Appendix J.2.

3.4 GROUND FISH STOCK ABUNDANCE AND FISHING INTENSITY

We regularly present the status of groundfish biomass and fishing pressure based on the most recent stock assessments. This year’s report includes newly updated information for 18 stocks and substocks, along with the most recent values for other stocks assessed since 2013.

The vast majority of recently assessed stocks are near or above stock status target reference points, but two substocks—copper rockfish from southern California (Figure 3.4.1, main) and quillback rockfish from California (Figure 3.4.1, inset)—were below the limit reference point (i.e., to the left of the red line). For management purposes, however, copper rockfish from the southern and northern California substocks are combined, and California copper rockfish as a whole are not considered overfished. Yelloweye rockfish are still rebuilding toward the target reference point. China rockfish in California are notably below the target reference point but above the limit reference point.

Overfishing occurs when catches exceed overfishing limits (OFLs), but not all stocks are managed by OFLs. Therefore, we present fishing intensity relative to a proxy fishing limit that is based on a stock’s

spawning potential (Figure 3.4.1, y-axis). Most stocks are well below the target fishing intensity level, but fishing intensity was well above target levels for quillback rockfish substocks in California and Oregon (Figure 3.4.1, inset). The vermilion/sunset rockfish substock in California and the vermilion rockfish substock in Oregon were close to the fishing intensity target in 2020, the most recent year measured. Some stocks showed sharp declines in fishing intensity in 2020 that can be attributed to lower fishing effort during the onset of the COVID-19 pandemic.

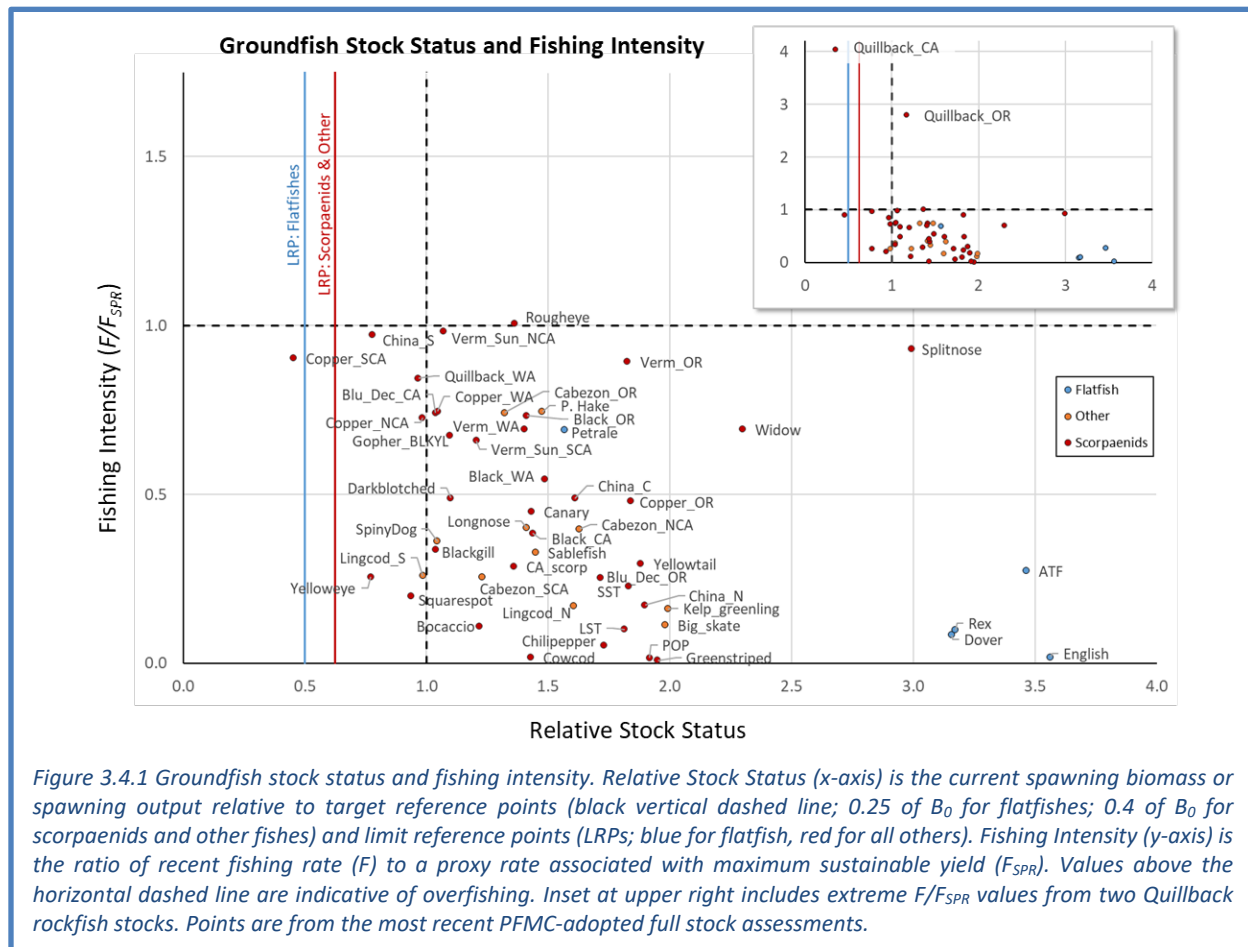


Figure 3.4.1 Groundfish stock status and fishing intensity. Relative Stock Status (x-axis) is the current spawning biomass or spawning output relative to target reference points (black vertical dashed line; 0.25 of B_0 for flatfishes; 0.4 of B_0 for scorpaenids and other fishes) and limit reference points (LRPs; blue for flatfish, red for all others). Fishing Intensity (y-axis) is the ratio of recent fishing rate (F) to a proxy rate associated with maximum sustainable yield (F_{SPR}). Values above the horizontal dashed line are indicative of overfishing. Inset at upper right includes extreme F/F_{SPR} values from two Quillback rockfish stocks. Points are from the most recent PFMC-adopted full stock assessments.

Last year’s report (Harvey et al. 2021a) featured new analyses on spatial distributions of groundfish relative to different ports through 2019. We were unable to update those analyses because the NMFS groundfish bottom trawl survey was cancelled in 2020 due to COVID-19, and data from the 2021 survey are still being processed. We will update those analyses in future reports.

3.5 HIGHLY MIGRATORY SPECIES (HMS)

Last year’s report included assessment-based estimates of biomass and recruitment of several HMS stocks that occur in the CCE. The only updated assessment this year is for blue marlin. Biomass and recruitment time series for all stocks are in Appendix K. Biomasses range from below average (e.g., yellowfin tuna, bigeye tuna) to above average (e.g., skipjack) relative to the full assessment periods. Recent biomass trends ranged from weakly negative to weakly positive. Recruitment estimates were within ± 1 s.d. of long-term averages, and generally had increasing trends with high uncertainty.

This year, we introduce diet indicators for albacore into the report. Quantitative estimates of HMS diets complement forage surveys (Section 3.2), lend insight into how forage varies in space and time, and provide direct measures of forage use by HMS. Albacore stomachs provided by commercial and

recreational fishers in Washington, Oregon and northern California reveal that YOY anchovy, krill, saury, and YOY rockfishes were among the dominant prey in recent years (Figure 3.5.1). Like other predators, albacore appear to be consuming more anchovy and fewer juvenile rockfishes in the last few

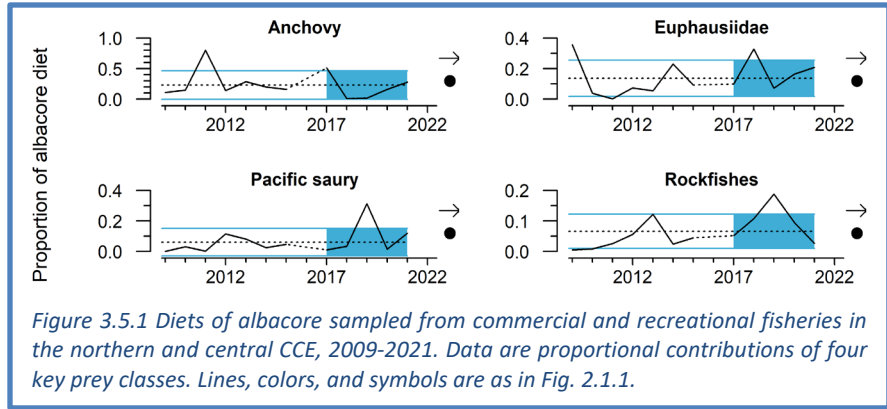


Figure 3.5.1 Diets of albacore sampled from commercial and recreational fisheries in the northern and central CCE, 2009-2021. Data are proportional contributions of four key prey classes. Lines, colors, and symbols are as in Fig. 2.1.1.

years. The proportion of sardine in albacore diets was above average in 2020 and 2021 (though it was <10% of the analyzed prey in both years; data not shown). This contrasts with forage and CPS surveys, which have not had recent increases in sardine catches (Section 3.2; Appendix I), but it is consistent with some observations of larval sardines off Washington and Oregon in May 2021 (Appendix H.1). Additional information on albacore diets, as well as swordfish diets off central and southern California, is in Appendix K. HMS diet information will be augmented in future reports.

3.6 MARINE MAMMALS

Sea lion production: California sea lion pup counts and condition at San Miguel Island are positively correlated with prey availability in the Central and Southern CCE, and are especially high when energy-rich prey like sardines, anchovy or mackerel have high occurrence in adult female sea lion diets (Melin et al. 2012a). Pup count relates to prey availability and nutritional status for gestating females from October to June. Pup growth from birth to age 7 months is related to prey availability to lactating females from June to February. These are robust indicators of prey quality and abundance even when the sea lion population is at or near carrying capacity (Appendix L).

The 2021 cohort was the fifth consecutive year of above-average pup counts (Figure 3.6.1), and continued the rebound since the relatively low counts in 2015-2016. Pups were in good condition: pup weights were above average in September 2021, and similar to weights observed in 2016-2019, suggesting good availability of high-quality prey during summer in the adult female foraging area (rectangle in Figure 1.1a). This is consistent with the estimates of high anchovy abundance from surveys of forage communities of the Central and Southern CCE in 2021 (Section 3.2). Pup growth through February 2022 had not yet been measured as of this writing.

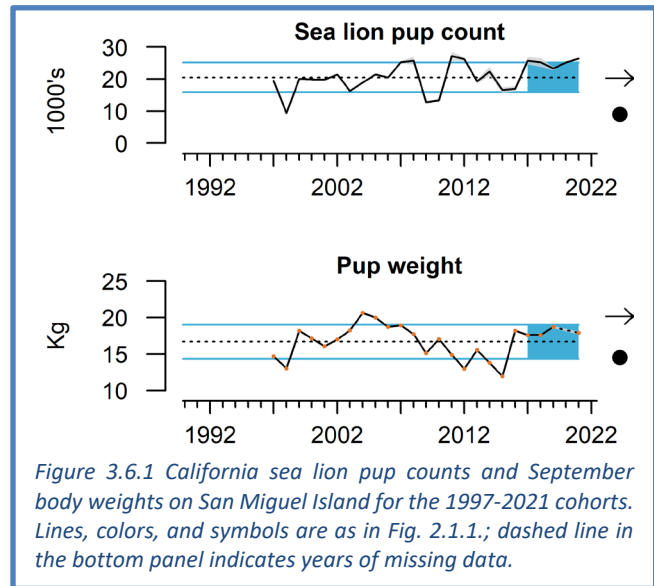


Figure 3.6.1 California sea lion pup counts and September body weights on San Miguel Island for the 1997-2021 cohorts. Lines, colors, and symbols are as in Fig. 2.1.1.; dashed line in the bottom panel indicates years of missing data.

Whale entanglement: Reports of whale entanglements along the West Coast increased in 2014 and even more in the next several years, particularly for humpback whales. While ~50% of reports cannot be attributed to a specific source, Dungeness crab gear has been the most common source identified in this period. The dynamics of entanglement risk and reporting are complex, and are affected by shifts in ocean conditions and prey fields, changes in whale populations, changes in distribution and timing of fishing effort, and increased public awareness.

Based on preliminary data, West Coast entanglement reports were higher in 2021 than pre-2014, but below the peak years of 2015-2018 (Figure 3.6.2). Humpback whales continued to be the most common species reported. Most reports were in California, but reported entanglements involved gear from all three West Coast states; this includes several reports from Mexico of humpback whales in gear confirmed from each state. Reported entanglements in 2021 involved a wide range of sources, including: commercial Dungeness crab from all three states; CA large-mesh drift gillnet gear; CA experimental box crab gear; CA commercial spiny lobster gear; commercial spot prawn gear; recreational hook and line gear; and other gillnet fisheries. No confirmed entanglements occurred in sablefish fixed gear.

Significant actions were taken in 2021 to reduce entanglement risk. California implemented closures and delays of commercial and recreational Dungeness crab seasons, while Washington and Oregon implemented late-season restrictions in commercial Dungeness crab fisheries. Other factors continue to present obstacles to risk reduction, including derelict gear, foraging by whales in nearshore waters under certain ecosystem conditions, and growth of some whale populations. COVID-19 likely continued to affect observations, reporting, and responses.

3.7 SEABIRDS

Seabird indicators (productivity, density, diet, and mortality) are a portfolio of metrics that reflect population health and condition of seabirds, as well as links to lower trophic levels and other conditions in the CCE. The species we report on here and in Appendix M represent a breadth of foraging strategies, life histories, and spatial ranges.

Fledgling production and diet: Seabird colonies on Southeast Farallon Island off central California experienced average to above-average productivity in 2021 (Figure 3.7.1). Cassin's auklet, common murre, pigeon guillemot and rhinoceros auklet continued to rebound from lows in 2019. Anchovies again dominated diets of piscivorous birds at this colony, while

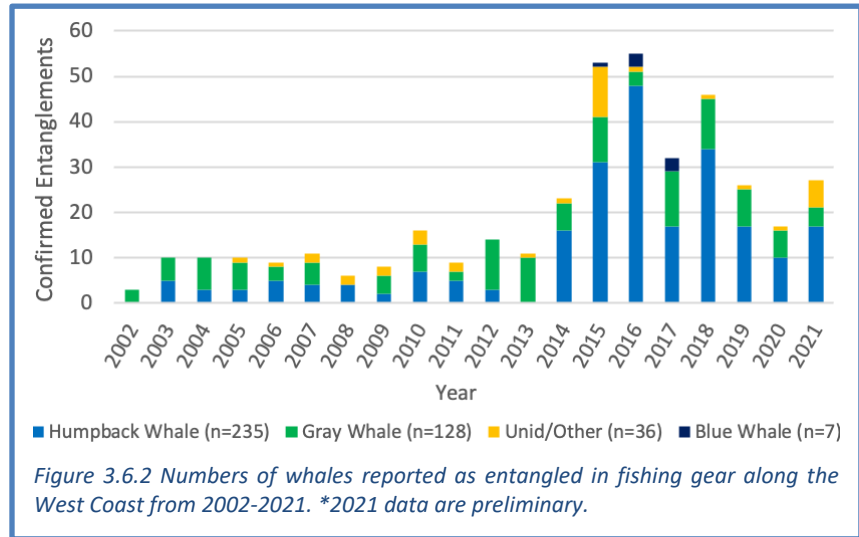


Figure 3.6.2 Numbers of whales reported as entangled in fishing gear along the West Coast from 2002-2021. *2021 data are preliminary.

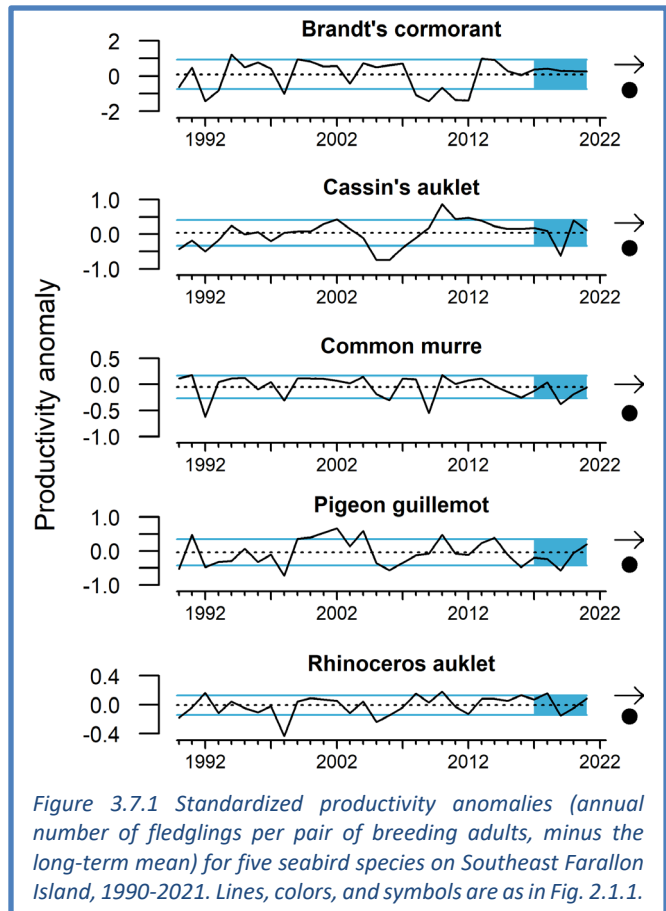


Figure 3.7.1 Standardized productivity anomalies (annual number of fledglings per pair of breeding adults, minus the long-term mean) for five seabird species on Southeast Farallon Island, 1990-2021. Lines, colors, and symbols are as in Fig. 2.1.1.

juvenile rockfish consumption remained low (Appendix M). Further north at Yaquina Head, Oregon, fledgling production in 2021 was above-average for two cormorant species and average for common murre (Appendix M). Diets of common murre chicks at Yaquina Head were typical for most prey groups, but showed increases in some species, including juvenile Pacific salmon (Appendix M).

Mortality: Monitoring of dead beachcast birds by citizen scientists returned to normal effort levels in 2021, after COVID-19 restrictions reduced or precluded data collection in 2020. No unusual mortality events were evident in the three beach monitoring programs in 2021 (Appendix M). Preliminary data from the Central and Northern CCE suggest elevated levels of beachcast northern fulmars in late 2021; data collection is ongoing to determine if this or other species' mortality rates will remain elevated in the fall 2021-winter 2022 period.

3.8 HARMFUL ALGAL BLOOMS (HABS)

Blooms of the diatom *Pseudo-nitzschia* spp. can produce domoic acid, a toxin that can affect coastal food webs and lead to shellfish fishery closures when shellfish tissue levels exceed regulatory limits (Appendix N). Domoic acid levels in shellfish were generally improved for most of the West Coast in 2021 compared to 2020 (Figure 3.8.1), perhaps related to the cooler temperatures associated with a negative PDO and La Niña; however, elevated levels associated with a persistent northern California “hotspot” (Trainer et al. 2020) were again observed. *Pseudo-nitzschia* cell counts varied around typical levels along most of the coast, except off Oregon where they were more abundant than normal; however, for the most part, cells produced only small amounts of domoic acid. Even so, exceedances of domoic acid were detected in razor clams from northern California to the Canadian border in early 2021 (Figure 3.8.1), due to legacy toxin from a fall 2020 HAB event that had not yet depurated from shellfish tissues. This resulted in closures of state, tribal and recreational razor clam fisheries, along with shortened seasons and/or evisceration orders for crab fisheries in all three coastal states. Because crab fisheries are highly connected to many other fisheries on the West Coast (Section 5.4), HAB impacts on crab fisheries can have indirect effects on participation in Council-managed fisheries. Details of the locations and timings of HAB-related fishery delays and closures are in Appendix N.

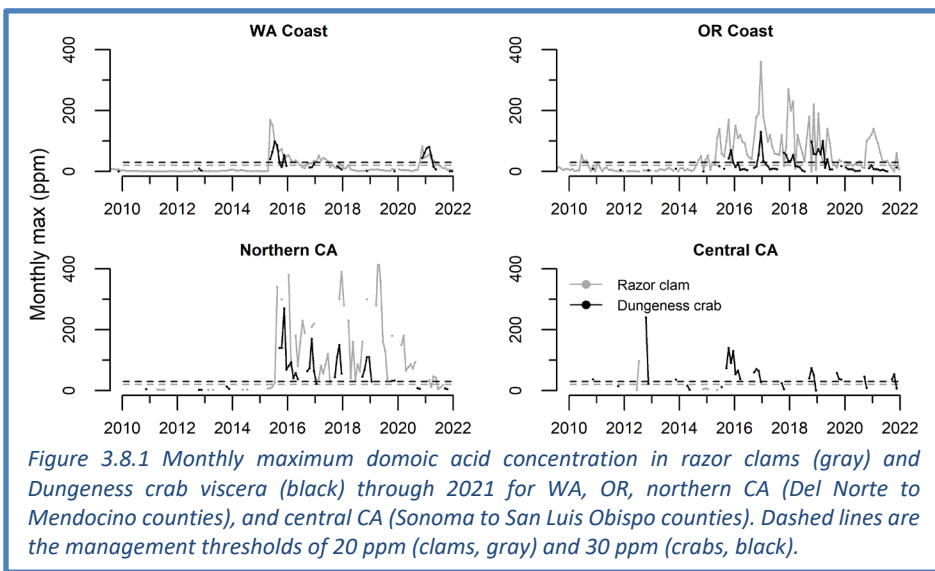


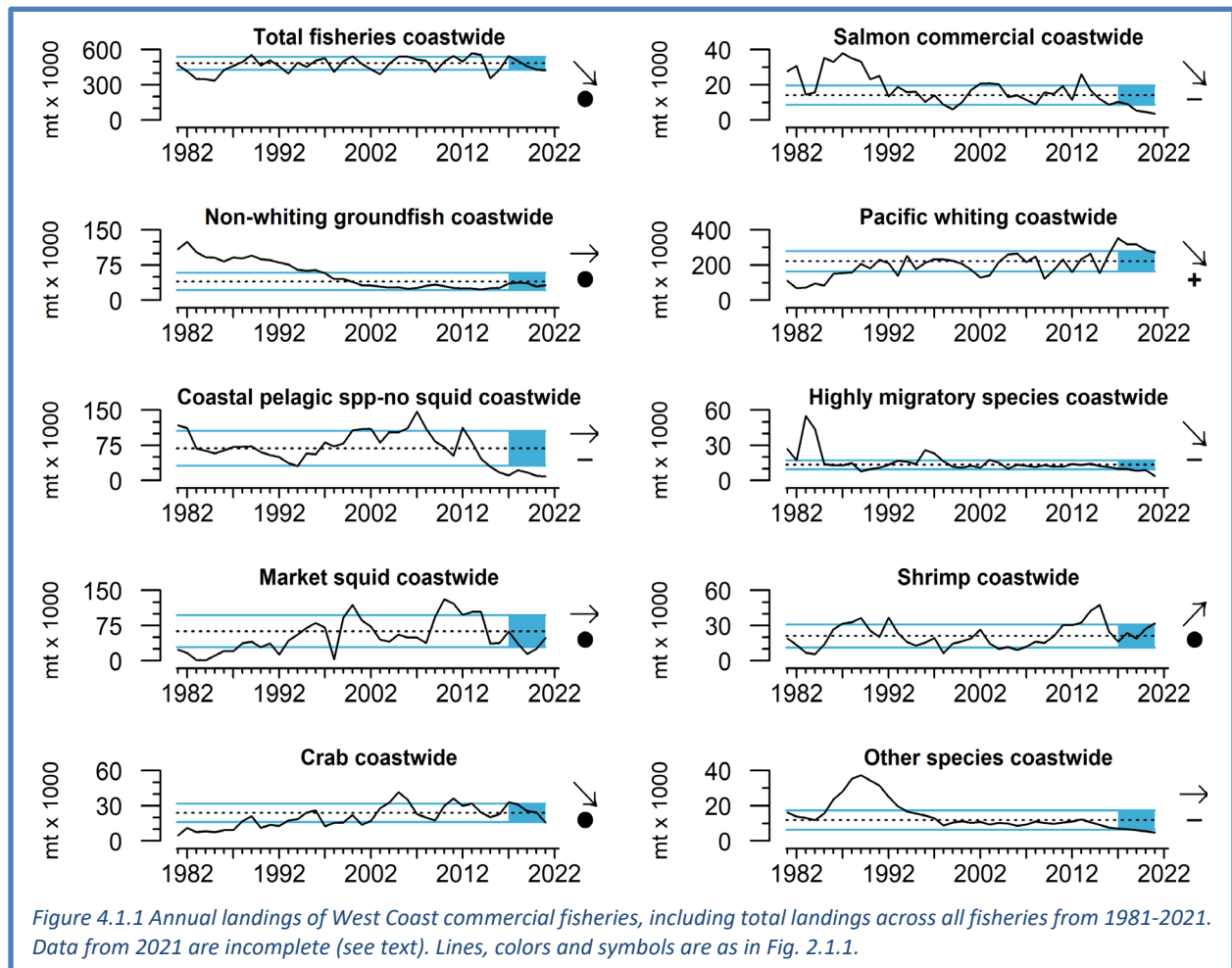
Figure 3.8.1 Monthly maximum domoic acid concentration in razor clams (gray) and Dungeness crab viscera (black) through 2021 for WA, OR, northern CA (Del Norte to Mendocino counties), and central CA (Sonoma to San Luis Obispo counties). Dashed lines are the management thresholds of 20 ppm (clams, gray) and 30 ppm (crabs, black).

4 FISHERIES LANDINGS, REVENUE, AND ACTIVITY

4.1 COASTWIDE LANDINGS AND REVENUE BY MAJOR FISHERIES

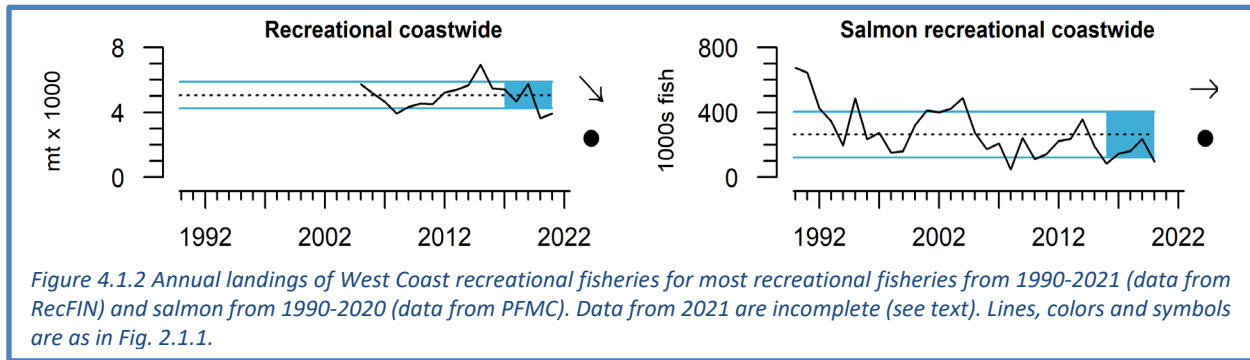
Fishery landings are indicators of ecosystem services provided by the CCE, and also reflect removals from the biophysical system. Coastwide total landings in 2021 continued a downward trend since 2017, largely tracking changes in Pacific whiting (= hake) over the past five years (Figure 4.1.1). In 2021, landings from six of nine commercial management groups decreased compared to 2020: HMS

(-57%), crab (-36%), salmon (-22%), CPS finfish (-13%), other species (-11%), and whiting (-6%). Landings of market squid (+94%), shrimp (+16%), and non-whiting groundfish (+9%) increased in 2021 relative to 2020. The recent 5-year averages for salmon, CPS finfish, HMS, and other species were at or near time series lows dating back to 1981, while whiting landings remained above average despite their recent declining trend. Shrimp were the only major fishery to show a significant increase in landings over the last 5 years, though market squid landings increased sharply since the relative low in 2019. State-by-state landings are in Appendix O.



Although total revenue for West Coast commercial fisheries decreased from 2017–2021, total revenue was actually 6% greater in 2021 than in 2020 (see Appendix O). Revenue for 6 of 9 target target groups increased in 2021 compared to 2020: market squid (+96%), Pacific whiting (+44%), non-whiting groundfish (+18%), other species (+11%), salmon (+6%) and shrimp (+4%). In contrast, HMS (-35%), crab (-15%) and CPS finfish (-15%) generated less revenue in 2021 than in 2020. Variation in price-per-pound is at least partly involved in these dynamics; for example, shrimp revenues experienced relatively little change from 2017-2021 (Appendix O), despite a concurrent increase in landings (Figure 4.1.1). Meanwhile, whiting landings decreased by 6% from 2020 to 2021, but whiting revenue increased 44% in the same year-on-year period. Coastwide and state-level revenue data are in Appendix O, and additional analyses related to revenues are in Section 5.

Recreational landings data are complete through October 2021. Large decreases in recreational albacore landings in Oregon and Washington in 2020 and Washington in 2021 heavily influenced the overall decreasing trend for the last five years (Figure 4.1.2, left; excludes salmon, Pacific halibut, and



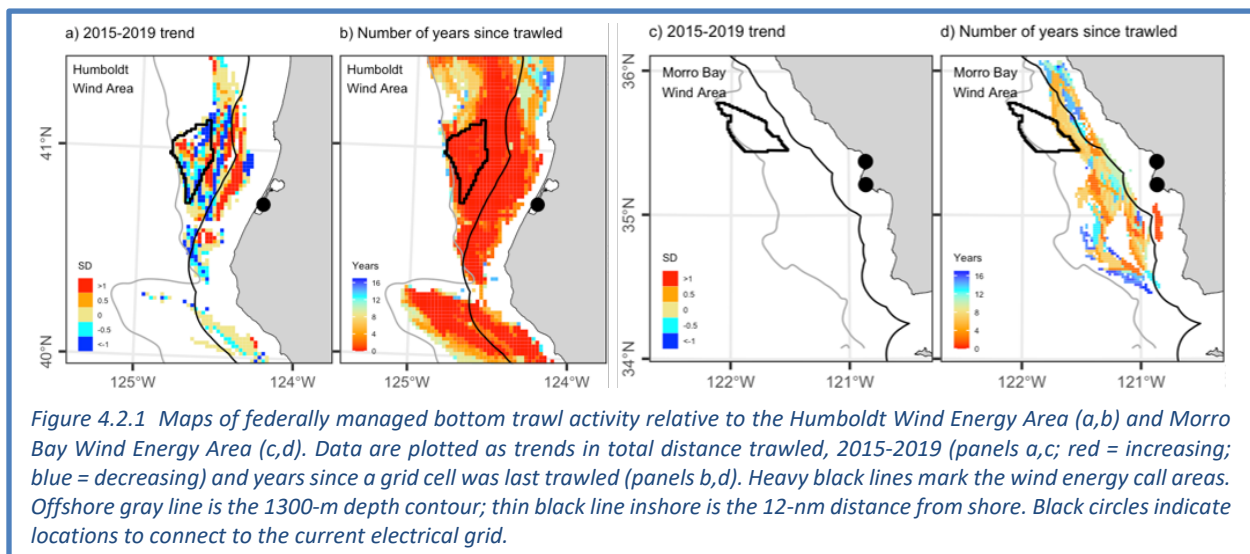
California HMS). Coastwide recreational landings of Chinook and coho salmon increased from 2017-2019, but declined steeply in 2020 (Figure 4.1.2, right); however, estimates of recreational salmon landings in 2020 may be compromised by sampling restrictions in some months due to the COVID-19 pandemic. State-by-state recreational landings and details are in Appendix O.

4.2 POTENTIAL INTERACTIONS BETWEEN FISHERIES ACTIVITIES AND OTHER OCEAN USE SECTORS

New ocean-use sectors of the economy (e.g., renewable energy and aquaculture) are becoming a reality off the West Coast, particularly with new offshore Wind Energy Area (WEA) designations. This presents an urgent need to identify sources of conflict and trade-offs that might occur with existing uses (especially commercial fisheries), essential fish habitats, protected species, and other managed resources. Ecosystem indicators and related analyses may be helpful in this regard.

To illustrate these concepts, we mapped two previously developed fisheries indicators and examined them in and around the newly established WEAs in California, as well as the Wind Energy Planning Area in Oregon. We compiled non-confidential logbook set and retrieval coordinates from the limited-entry/catch share groundfish bottom trawl fishery from 2002-2019. These data were mapped to a 2x2-km grid, and used to calculate (1) the most recent 5-year trend in total distance trawled in each grid cell, and (2) the number of years since trawling occurred within each grid cell.

Within the Humboldt WEA (HWEA), annual distance trawled from 2015-2019 increased primarily in a central band, especially in the westernmost region (Figure 4.2.1a, red cells), and decreased elsewhere (blue cells). There were large areas with increasing trends in distance trawled between HWEA and the grid-connecting locations onshore. Nearly all grid cells within and surrounding HWEA have had at least some bottom trawling activity within the last five years (Figure 4.2.1b). The Morro



Bay WEA (MWEA) did not have any non-confidential (≥ 3 vessels within a grid cell) trawling activity within the last five years (Figure 4.2.1c). A small band of grid cells shoreward of the southeastern boundary of MWEA has had trawling activity within the last five years (Figure 4.2.1d). Further information is in Appendix P.

Off Oregon, increasing trends in distance trawled from 2015-2019 were observed in several patches >12 nm offshore (Figure 4.2.2, left). The largest increases were off central Oregon, while decreasing trends were most concentrated at the southern and northern borders, where wind speeds off Oregon are highest and lowest, respectively. Highlighting the spatial breadth of fisheries off Oregon, a very large number of grid cells have been trawled recently between the 12-nm offshore and 1300-m depth contours (Figure 4.2.2, right), with the most notable exception off central Oregon, where EFH Conservation Areas are located and bottom trawling has been prohibited since 2006.

These spatial indicators only account for federal limited-entry/catch shares groundfish bottom trawl fisheries, but provide a framework for identifying the likelihood of overlap and conflicts between fisheries operations, scientific surveys, and offshore wind energy sites. Other fisheries will be included as data becomes available. Further information is in Appendix P.

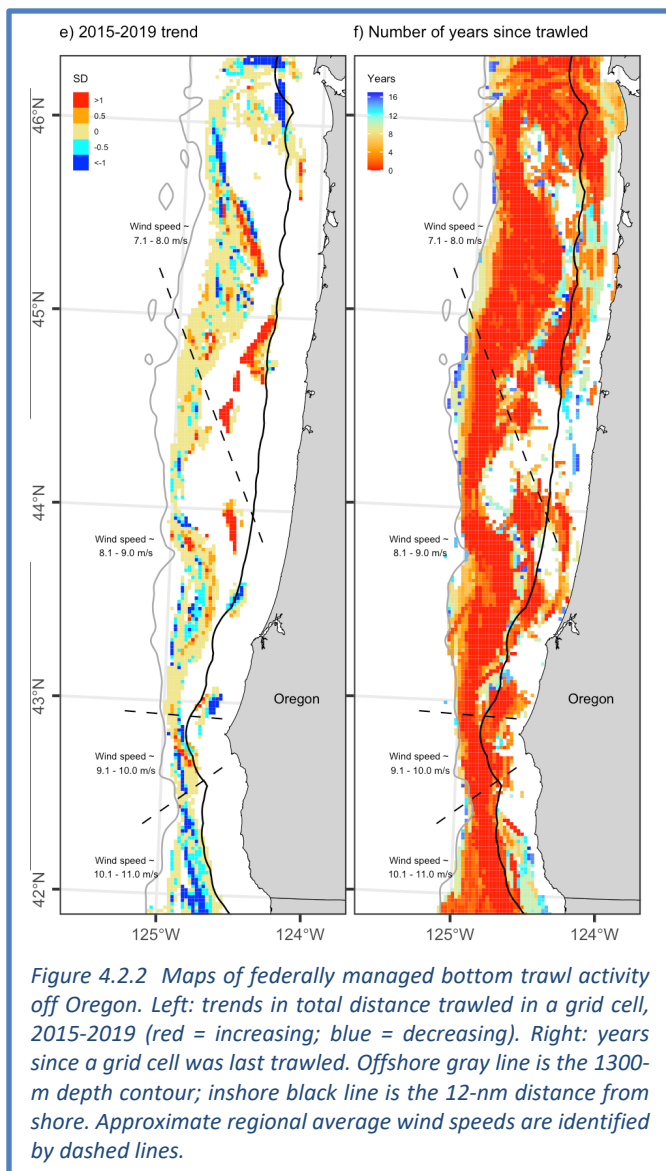


Figure 4.2.2 Maps of federally managed bottom trawl activity off Oregon. Left: trends in total distance trawled in a grid cell, 2015-2019 (red = increasing; blue = decreasing). Right: years since a grid cell was last trawled. Offshore gray line is the 1300-m depth contour; inshore black line is the 12-nm distance from shore. Approximate regional average wind speeds are identified by dashed lines.

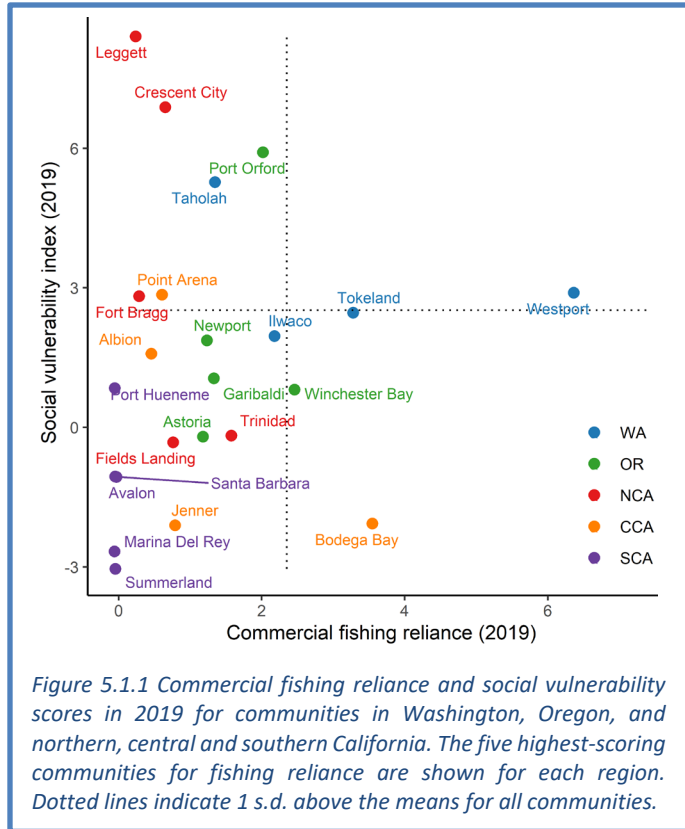
5 HUMAN WELLBEING

This section features an expanding suite of indicators and analyses of human wellbeing in fishing communities. These indicators and analyses relate to the risk profiles and adaptive capacities of coastal communities in the face of various pressures. We are working to develop indicators that help track progress toward meeting National Standard 8 (NS-8) of the Magnuson-Stevens Act. NS-8 states that fisheries management measures should “provide for the sustained participation of [fishing] communities” and “minimize adverse economic impacts on such communities.”

5.1 SOCIAL VULNERABILITY

The Community Social Vulnerability Index (CSVI) is a generalized metric that aggregates information from social vulnerability data (demographics, poverty, housing, labor force structure, etc.; Jepson and Colburn 2013). We monitor CSVI in communities that are highly reliant upon fishing. The commercial fishing reliance index reflects *per capita* engagement in commercial fishing (landings, revenues, permits, processing, etc.) in each West Coast fishing community ($n \approx 250$).

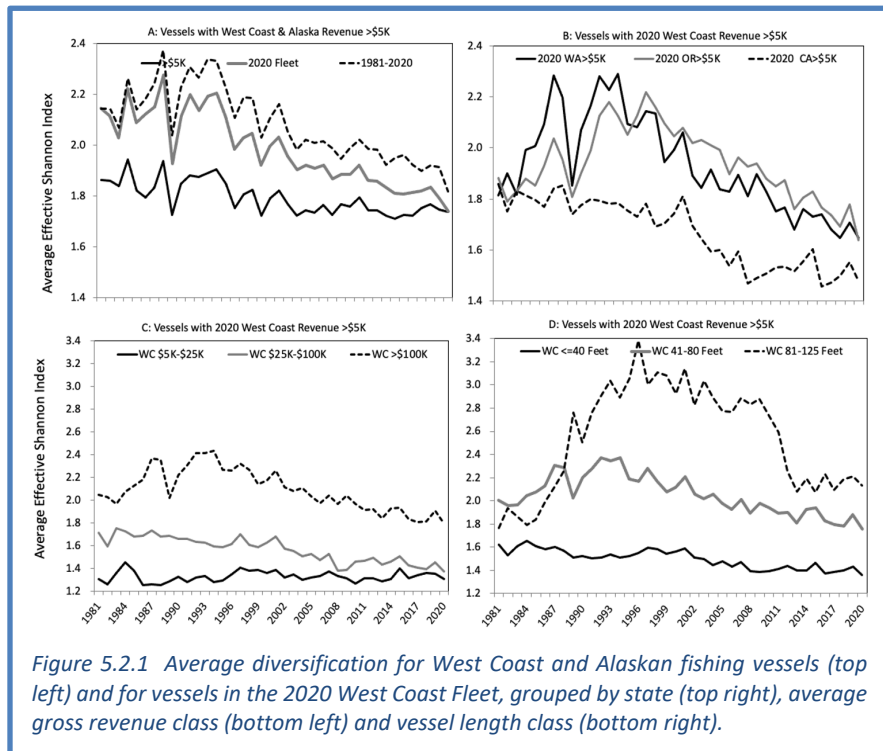
Figure 5.1.1 plots CSVI updated through 2019 against commercial fishing reliance for communities that are among the most reliant on commercial fishing in different regions of the West Coast. Communities in the upper right quadrant are those with relatively high social vulnerability (vertical axis) and commercial fishing reliance (horizontal axis). In 2019, Westport, WA and Tokeland, WA fell within or closest to the upper right quadrant, while Port Orford, OR and Ilwaco, WA were just outside of it. Communities that score highly in both indices may be especially socially vulnerable to downturns in commercial fishing. Fishing reliance can be volatile: communities can move left on the x-axis in years with reduced landings, and may thus appear to be less dependent on commercial fishing when in fact they have actually just experienced a difficult year; therefore, these results should be interpreted with care. These data are difficult to groundtruth and require further study. Additional details are in Appendix Q.



5.2 DIVERSIFICATION OF FISHERY REVENUES

Interannual variability in fishing revenue can be reduced by diversifying activities across multiple fisheries or regions.

According to the Effective Shannon Index that we use to measure fishery revenue diversification, the fleet of vessels that fished the West Coast and Alaska in 2020 was less diverse on average than at any time in the prior 40 years (Figure 5.2.1a, solid gray line). Diversification rates for most categories of West Coast vessels have been trending down for several years, and diversification declined in 2020 for all categories of West Coast vessels (Figure 5.2.1b-d). California, Oregon and Washington fleets saw 5%, 8% and 4% decreases in



average diversification in 2020 relative to 2019 (Figure 5.2.1b). Declines in diversification from 2019 to 2020 were also widely observed at the scale of individual ports (Appendix R).

Declines in diversification are due both to entry and exit of vessels and changes for individual vessels. Less diversified vessels have been more likely to exit; vessels that remain have become less diversified, at least since the mid-1990s; and newer entrants generally have been less diversified. Within the average trends are wide ranges of diversification levels and strategies, and some vessels remain highly diversified. Further information can be found in Appendix R.

5.3 PORT-LEVEL REVENUE CONCENTRATION

As a potential indicator to track progress toward meeting NS-8, we use a metric called the Theil Index to assess geographic concentration of fishing revenues. The index estimates the difference between observed revenue concentrations and what they would be if they were perfectly equally distributed across ports; higher values indicate greater concentration in a subset of ports. We calculate the Theil Index for total fisheries and for specific management groups, at the scale of the 21 port groups previously established for the economic Input-Output model for Pacific Coast fisheries (IO-PAC; Leonard and Watson 2011).

Figure 5.3.1 shows annual Theil Index values for total commercial fishing revenue (heavy black line) and six management groups. The total revenue trend is relatively flat over the 40-year time period, with relatively low values in each year, suggesting that total fishery revenue has not experienced marked changes in geographic concentration. A slight uptick in Theil value for total revenue occurred in 2020 (the most recent year of data analyzed). The separate management groups all increased from 2019 to 2020 as well. Individual management groups show distinctions in the overall degree of geographic concentration. CPS and HMS fisheries have had the highest Theil values for most of the last decade, indicating those groups currently have relatively high concentration of revenue in a smaller number of port groups.

Management groups also show distinct patterns of change over time. Their values for groundfish (heavy orange line) have increased gradually for decades as groundfish revenue became concentrated in northern port groups (Appendix S). HMS revenues (heavy blue line) follow a more U-shaped trend, from high revenue concentration in southern ports in the early 1980s, to more equal distribution in the middle of the time period, and back to high values in the 2000s and 2010s as HMS revenues became more concentrated in northern port groups (Appendix S). Crab revenues exhibit short-term variability in geographic concentration, but overall have become more equally distributed coastwide since the 1990s. CPS and salmon show relatively high short-term variability, while shrimp revenue concentration has varied at decadal scales. This index may provide the Council with relevant information on particular fisheries and port groups where revenue concentrations are changing, as a basis for evaluating tradeoffs related to NS-8 considerations.

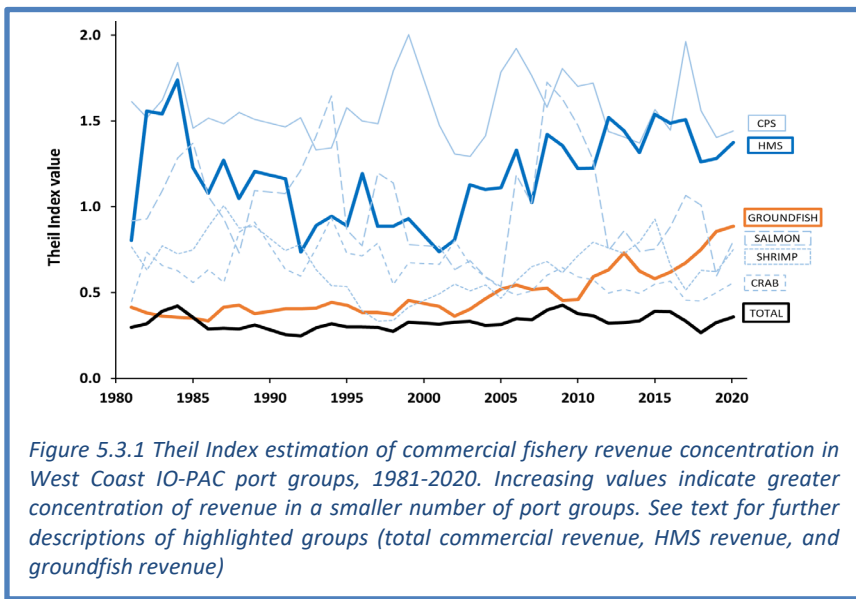


Figure 5.3.1 Theil Index estimation of commercial fishery revenue concentration in West Coast IO-PAC port groups, 1981-2020. Increasing values indicate greater concentration of revenue in a smaller number of port groups. See text for further descriptions of highlighted groups (total commercial revenue, HMS revenue, and groundfish revenue)

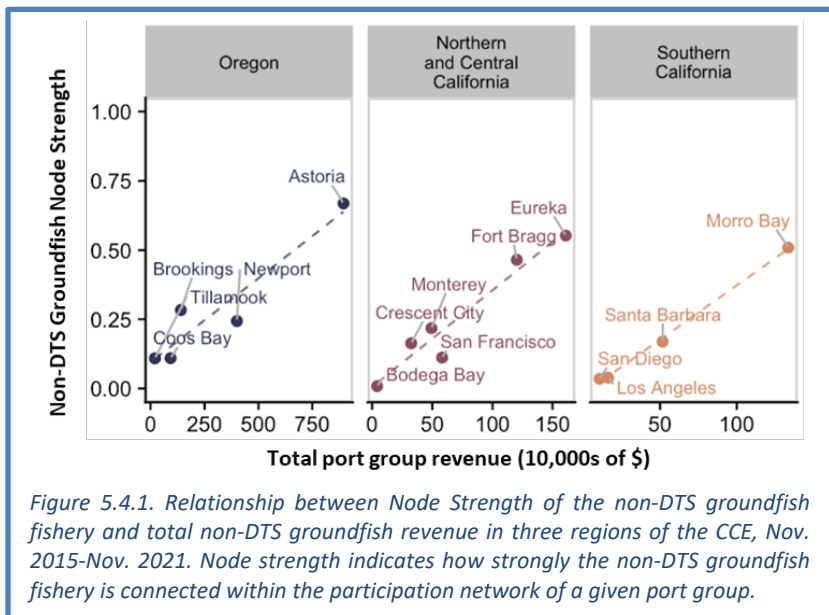
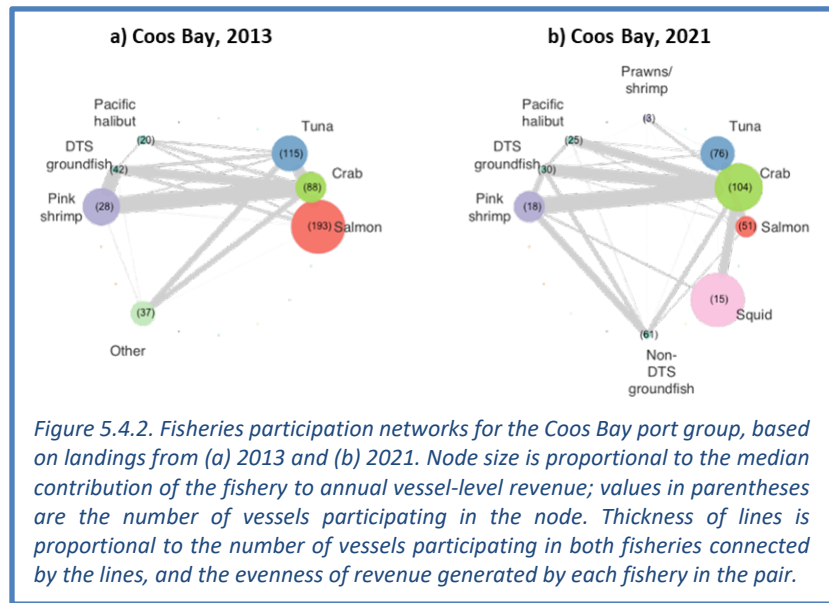
HMS revenues (heavy blue line) follow a more U-shaped trend, from high revenue concentration in southern ports in the early 1980s, to more equal distribution in the middle of the time period, and back to high values in the 2000s and 2010s as HMS revenues became more concentrated in northern port groups (Appendix S). Crab revenues exhibit short-term variability in geographic concentration, but overall have become more equally distributed coastwide since the 1990s. CPS and salmon show relatively high short-term variability, while shrimp revenue concentration has varied at decadal scales. This index may provide the Council with relevant information on particular fisheries and port groups where revenue concentrations are changing, as a basis for evaluating tradeoffs related to NS-8 considerations.

5.4 FISHERIES PARTICIPATION NETWORKS

As fishers diversify their harvest portfolios, they create connections between fisheries, even when ecological links between the target species are weak or absent. In last year's report (Harvey et al. 2021a,b), we introduced fisheries participation networks (Fuller et al. 2017, Fisher et al. 2021) as a way to represent this information. In these networks, fisheries are depicted as nodes, and pairs of nodes are connected by lines that integrate information about vessels participating in both fisheries. Changes in network structure over time reflect changes in the ecology of adjacent coastal waters, as well as the legacy of management, markets, and other factors.

To illustrate, we first compare two participation networks for the Coos Bay port group, one based on 2013 data (Figure 5.4.1a) and the other on 2021 data (Figure 5.4.1b). The networks reveal that tuna, crab, salmon, and pink shrimp fisheries consistently generate relatively large proportions of revenue and are connected to multiple other fisheries. Participation in all fisheries changed over time, and the number of links in the network increased ~50% from 2013 to 2021 (19 vs 28). Perhaps the most substantial change was the emergence of a lucrative and highly connected squid fishery, which began in 2016 as the 2014-2016 marine heatwave pushed market squid to the north. Other changes include declines in participation in fisheries for salmon, tuna, and the Dover sole-thornyhead-sablefish complex (DTS); and increased participation in the crab fishery, which has strong cross-participation in fisheries like pink shrimp, DTS groundfish, non-DTS groundfish, and squid. Overall, these observations suggest that some fisheries are staples of the Coos Bay port group, and track changes in vessel participation in fisheries due to a variety of as-yet unexplored factors (e.g., environmental, market-based, regulatory, etc.).

In Figure 5.4.2, we use a similar assessment of participation networks to explore the potential for knock-on effects of regulatory changes to the non-DTS groundfish fishery in California and Oregon (e.g., rebuilding of quillback rockfish). We examined how strongly this fishery was



connected to other fisheries using a network statistic called Node Strength, where a fishery with high Node Strength is more strongly connected (through shared vessel participation) to other fisheries in the network. Node Strength and port-level revenue for the non-DTS groundfish fishery were positively correlated (Figure 5.4.2), implying that revenue is a reasonable proxy for how strongly connected the non-DTS groundfish fishery is to other fisheries. Regulatory (or other) changes to the non-DTS groundfish fishery will likely have direct and substantial impacts on any community that generates a large amount of revenue from it. However, Node Strengths for some port groups (e.g., Brookings) fell above the best-fit line of the relationship between Node Strength and revenue, while others (e.g., Newport) fell below the line. This may indicate that indirect effects of regulatory changes to the non-DTS groundfish fishery (like spillover into other fisheries) are disproportionately more likely in communities like Brookings than those like Newport. Such information may be useful in considering effects of management actions in the context of NS-8. Additional analyses and information on fisheries participation networks are in Appendix T.

6 SYNTHESIS

In many respects, 2021 in the California Current was “a tale of three ecosystems” (Box 1.1, Appendix D). On the positive side, a second consecutive year of cool ocean conditions and strong upwelling supported favorable feeding conditions and good productivity for marine species. And yet, these improved conditions were bound on one side by yet another marine heatwave (which mostly stayed well offshore in 2021), and on the other side by another year of extreme heat, drought and fire throughout the West. These conditions present both opportunities and challenges to fishery participants and managers still dealing with the stresses of the COVID pandemic.

NOAA’s Climate Prediction Center (CPC) expects La Niña or ENSO-neutral conditions to extend into summer 2022, and because PDO generally lags ENSO indices, negative PDO conditions seem likely to extend into summer as well. However, CPC also predicts that a large region of anomalously warm offshore water will continue into at least June. On land, although heavy precipitation from October 2021 through January 2022 (the time of this writing) provided some needed relief, the CPC expects drought conditions to continue into 2022 in most of our region.

The CCIEA team remains committed to providing and updating these indicators in the most timely manner possible, and working together with the Council, committees and advisory bodies to “connect the dots” among these indicators with robust and informative analyses. Given the clear importance of climate variability and change on our fisheries, Council activities, and the ecosystem as a whole, we are taking first steps toward developing useful climate change indicators by introducing a “climate change appendix” (Appendix E). We have intentionally kept this new appendix simple and open-ended, and have emphasized both information and engagement. This is because climate change indicators are a tool that the CCIEA team and the Council must co-develop in order for the indicators to effectively support managers and participants, within and across FMPs; to support strategic management choices related to the FEP, including follow-ups to the Climate and Communities Initiative; and to help us better understand interactions among mixed uses in a changing ocean, including offshore renewable energy.

SUPPLEMENTARY MATERIALS TO THE 2021-2022 CALIFORNIA CURRENT ECOSYSTEM STATUS REPORT

Appendix A LIST OF CONTRIBUTORS TO THIS REPORT, BY AFFILIATION

NWFSC, NOAA Fisheries

Mr. Kelly Andrews
Dr. Brian Burke
Dr. Jason Cope
Mr. Jeff Cowen
Dr. Blake Feist
Dr. Correigh Greene
Dr. Thomas Good
Dr. Chris Harvey (co-editor)
Dr. Daniel Holland
Dr. Mary Hunsicker
Dr. Kym Jacobson
Ms. Su Kim
Dr. Stephanie Moore
Dr. Stuart Munsch
Dr. Karma Norman
Dr. Jameal Samhour
Dr. Kayleigh Somers
Dr. Nick Tolimieri (co-editor)
Mr. Curt Whitmire

AFSC, NOAA Fisheries

Dr. Stephen Kasperski
Dr. Sharon Melin
Ms. Elizabeth Jaime

SWFSC, NOAA Fisheries

Dr. Eric Bjorkstedt
Dr. Steven Bograd
Dr. David Demer
Dr. Heidi Dewar
Ms. Lynn deWitt
Dr. John Field
Dr. Newell (Toby) Garfield (co-editor)
Dr. Elliott Hazen
Dr. Michael Jacox
Dr. Andrew Leising
Dr. Nate Mantua
Dr. Catherine Nickels
Dr. Antonella Preti
Mr. Keith Sakuma
Dr. Jarrod Santora
Dr. Kevin Stierhoff
Dr. Andrew Thompson
Dr. Brian Wells
Dr. Juan Zwolinski

California State Polytechnic University, Humboldt

Ms. Roxanne Robertson

Oregon State University

Dr. Jack Barth
Ms. Jennifer Fisher
Ms. Cheryl Morgan
Dr. Rachael Orben
Dr. Stephen Pierce
Ms. Jessica Porquez
Ms. Samantha Zeman

NOAA Fisheries West Coast Region

Mr. Dan Lawson
Ms. Lauren Saez

Pacific States Marine Fishery Commission

Ms. Amanda Phillips
Mr. Gregory Williams (co-editor)

University of California-San Diego

Dr. Ralf Goericke
Dr. Dan Rudnick

University of California-Santa Cruz

Dr. Barbara Muhling
Dr. Isaac Schroeder

University of Washington

Ms. Mary Fisher

California Department of Public Health

Ms. Christina Grant
Mr. Duy Trong
Ms. Vanessa Zubkousky-White

California Department of Fish and Wildlife

Ms. Christy Juhasz

CA Office of Env. Health Hazard Assessment

Dr. Beckye Stanton

Oregon Department of Fish and Wildlife

Dr. Caren Braby
Mr. Matthew Hunter

Washington Department of Fish and Wildlife

Mr. Dan Ayres
Mr. Zachary Forster
Dr. Scott Pearson

Washington Department of Health

Ms. Tracie Barry
Mr. Jerry Borchert

BeachCOMBERS (U.S. Fish and Wildlife Service)

Mr. David Sherer

Beach Watch (Greater Farallones Association)

Ms. Kirsten Lindquist
Ms. Jan Roletto

Coastal Observation and Seabird Survey Team

Dr. Tim Jones
Dr. Julia Parrish

Farallon Institute

Dr. William Sydeman
Ms. Sarah Ann Thompson

Oikonos Ecosystem Knowledge

Ms. Rozy Bathrick
Ms. Jessie Beck
Mr. Ryan Carle

Point Blue Conservation Science

Dr. Jaime Jahncke
Dr. Mike Johns
Mr. Peter Warzybok

Wildlands Conservation Science

Mr. Morgan Ball

Appendix B LIST OF FIGURE AND DATA SOURCES FOR THE MAIN REPORT

Figure 2.1.1: Oceanic Niño Index data are from the NOAA Climate Prediction Center (https://origin.cpc.ncep.noaa.gov/products/analysis_monitoring/ensostuff/ONI_v5.php). PDO data are from N. Mantua, NMFS/SWFSC, and are served on the CCIEA ERDDAP server (https://oceanview.pfeg.noaa.gov/erddap/tabledap/cciea_OC_PDO.html). North Pacific Gyre Oscillation data are from E. Di Lorenzo, Georgia Institute of Technology (<http://www.o3d.org/npgo/>).

Figure 2.1.2: Standardized sea surface temperature anomaly plots were created by A. Leising, NMFS/SWFSC, using SST data from NOAA's optimum interpolation sea surface temperature analysis (OISST; <https://www.ncdc.noaa.gov/oisst>); SST anomaly calculated using climatology from NOAA's AVHRR-only OISST dataset. MHW conditions are delineated by values of the normalized SST + 1.29 SD from normal. Methods for tracking and classifying heatwaves are described in Thompson et al. 2019b and at <https://www.integratedecosystemassessment.noaa.gov/regions/california-current/cc-projects-blobtracker>.

Figure 2.1.3: Newport Hydrographic (NH) line temperature data from J. Fisher, NMFS/NWFSC, OSU. Glider data along CalCOFI lines are from Daniel Rudnick and obtained from <https://spraydata.ucsd.edu/projects/CUGN/>.

Figure 2.2.1: Daily 2021 values of BEUTI and CUTI are provided by M. Jacox, NMFS/SWFSC; detailed information about these indices can be found at <https://go.usa.gov/xG6Jp>.

Figure 2.2.2: Habitat compression index estimates developed and provided by J. Santora, NMFS/SWFSC, and I. Schroeder, NMFS/SWFSC, UCSC.

Figure 2.3.1: Newport Hydrographic (NH) line dissolved oxygen data are from J. Fisher, NMFS/NWFSC, OSU. CalCOFI data from <https://calcofi.org>. CalCOFI data before 2021 are from the bottle data database, while 2021 data are preliminary CTD from the CalCOFI CTD archive.

Figure 2.4.1: Snow-water equivalent data were derived from the California Department of Water Resources snow survey (<http://cdec.water.ca.gov/>) and the Natural Resources Conservation Service's SNOTEL sites in WA, OR, CA and ID (<http://www.wcc.nrcs.usda.gov/snow/>).

Figure 2.5.1: Minimum and maximum streamflow data were provided by the US Geological Survey (<http://waterdata.usgs.gov/nwis/sw>).

Figure 3.1.1: Copepod biomass anomaly data were provided by J. Fisher, NMFS/NWFSC, OSU.

Figure 3.1.2. Krill data were provided by E. Bjorkstedt, NMFS/SWFSC and Humboldt State University (HSU), and R. Robertson, Cooperative Institute for Marine Ecosystems and Climate (CIMEC) at HSU.

Figure 3.2.1: Pelagic forage data from the Northern CCE from B. Burke, NMFS/NWFSC and C. Morgan, OSU/CIMRS. Data are derived from surface trawls taken during the NWFSC Juvenile Salmon & Ocean Ecosystem Survey (JSOES; <https://www.fisheries.noaa.gov/west-coast/science-data/ocean-ecosystem-indicators-pacific-salmon-marine-survival-northern>).

Figure 3.2.2: Pelagic forage data from the Central CCE were provided by J. Field, K. Sakuma, and J. Santora, NMFS/SWFSC, from the SWFSC Rockfish Recruitment and Ecosystem Assessment Survey (<https://go.usa.gov/xGMfR>).

Figure 3.2.3: Pelagic forage larvae data from the Southern CCE were provided by A. Thompson, NMFS/SWFSC, and derived from spring CalCOFI surveys (<https://calcofi.org/>); data were not collected in 2020 due to survey cancellations associated with the COVID pandemic.

Figure 3.3.1: Data for at sea juvenile salmon provided by B. Burke, NMFS/NWFSC and C. Morgan, OSU/CIMRS. Derived from surface trawls taken during the NWFSC Juvenile Salmon and Ocean Ecosystem Survey (JSOES).

Figure 3.4.1: Groundfish stock status data provided by J. Cope, NMFS/NWFSC, derived from NOAA Fisheries stock assessments. .

Figure 3.5.1: Albacore diet data provided by H. Dewar, C. Nickels, and A. Preti, NMFS/SWFSC.

Figure 3.6.1: California sea lion data provided by S. Melin, NMFS/AFSC, with additional data collection and interpretation by E. Jaime, NMFS/AFSC, and M. Ball, Wildlands Conservation Science.

Figure 3.6.2: Whale entanglement data provided by D. Lawson and L. Saez, NMFS/WCR.

Figure 3.7.1: Seabird fledgling production data at nesting colonies on Southeast Farallon provided by J. Jahncke and P. Warzybok, Point Blue Conservation Science.

Figure 3.8.1: WA domoic acid data are provided by the Washington State Department of Health, OR data from the OR Department of Agriculture, and CA data from the California Department of Public Health.

Figure 4.1.1: Data for commercial landings are from PacFIN (<http://pacfin.psmfc.org>) and NORPAC (North Pacific Groundfish Observer Program).

Figure 4.1.2: Data for recreational landings are from RecFIN (<http://www.recfin.org/>) and the CDFW Pelagic Fisheries and Ecosystem Data Sharing index).

Figure 4.2.1: Data for total distance trawled by federally managed bottom-trawl fisheries were provided by J. McVeigh, NMFS/NWFSC, West Coast Groundfish Observer Program. Boundaries of WEAs from California Offshore Wind Energy Gateway (<https://caoffshorewind.databasin.org/>). Figures created by K. Andrews, NMFS/NWFSC.

Figure 5.1.1: Community social vulnerability index (CSVI) and commercial fishery reliance data provided by K. Norman, NMFS/NWFSC, and A. Phillips, PSMFC, with data derived from the US Census Bureau's American Community Survey (ACS; <https://www.census.gov/programs-surveys/acs/>) and PacFIN (<http://pacfin.psmfc.org>), respectively.

Figure 5.2.1: Fishery diversification estimates were provided by D. Holland, NMFS/NWFSC, and S. Kasperski, NMFS/AFSC.

Figure 5.3.1: Theil Index and annual commercial fishery revenue data provided by K. Norman, NMFS/NWFSC, and A. Phillips, PSMFC, with data derived from PacFIN (<http://pacfin.psmfc.org>).

Figure 5.4.1: Fishery Participation Network data and analyses provided by J. Samhour, M. Fisher, UW, and A. Phillips, PSMFC, with data derived from PacFIN (<http://pacfin.psmfc.org>).

Table 3.3.1: Stoplight table of indicators and projected 2022 salmon returns courtesy of B. Burke and K. Jacobson, NMFS/NWFSC, and J. Fisher, C. Morgan, and S. Zeman, OSU/CIMRS (<https://www.fisheries.noaa.gov/west-coast/science-data/ocean-ecosystem-indicators-pacific-salmon-marine-survival-northern>).

Table 3.3.2: Table of indicators and qualitative outlook for 2022 Chinook salmon returns to the Central Valley courtesy of N. Mantua and B. Wells, NMFS/SWFSC.

Appendix C CHANGES IN THIS YEAR'S REPORT

Below we summarize major changes in the 2021-2022 Ecosystem Status Report. As in past reports, many of these changes are in response to requests and suggestions received from the Council and advisory bodies (including those related to FEP Initiative 2, “Coordinated Ecosystem Indicator Review” (March 2015, Agenda Item E.2.b), or in response to annual reviews of indicators and analyses by the SSC-Ecosystem Subcommittee (SSC-ES). We also note items we have added and information gaps that we have filled since last year’s report (Harvey et al. 2021a). Finally, we note impacts of COVID-19 on research that supports this report.

Request/Need/Issue	Response/Location in document
<p>Increase use of maps and other graphics to illustrate the cumulative effects of multiple environmental indicators on biological components (Habitat Committee request, March 2016, as part of FEP Initiative on Coordinated Ecosystem Indicator Review)</p>	<p>We have introduced a summary infographic to begin the report (Page 1, Box 1.1), which replaces a list of bullet points. We also have an expanded 2-page summary infographic in Appendix D. We hope that this helps to better summarize the large amount of information in the report, and we look forward to feedback on how to improve the graphic and link it to web-based tools for exploring Council-relevant indicators throughout the year.</p>
<p>Request to add an indicator of krill biomass to complement the krill size indicator from the Trinidad Head hydrographic line (March 2021, Agenda Item 1.1.b, Supplement SSC Report 1)</p>	<p>We have added a time series of total krill biomass from the Trinidad Head transect in Section 3.1 of the report. This analysis was reviewed by the SSC-ES in September 2021. The data are from two stations that are representative of biomass trends on the transect as a whole (see Robertson and Bjorkstedt 2020), and these stations also experienced comparably less disruption in sampling and sample processing effort during the COVID-19 pandemic.</p> <p>The krill biomass index has also been added as a prey metric to the Klamath River fall Chinook salmon “stoplight table” (see Appendix J.2).</p>
<p>Cumulative concerns over the interpretation of salmon escapement indicators</p>	<p>The CCIEA team and SSC have had many discussions over the years about our escapement indicators for Chinook and coho salmon ESUs. The data we have included in past reports were typically 1-2 years out of date. Also, we struggled with how to link them to ecosystem conditions while accounting for factors such as harvest, component stock dynamics, changes in hatchery contributions, etc. Last year the SSC noted that our describing escapement as “high” or “low” relative to our time series averages was not based on reference points for biologically healthy stocks (March 2021, Agenda Item 1.1.b, Supplement SSC Report 1). We are thus discontinuing inclusion of escapement indicators from the Main Report and Supplement until informative, acceptable alternatives are identified.</p>

Request/Need/Issue	Response/Location in document
Groundfish availability to different West Coast ports	In the 2021 ecosystem status report, we introduced a fishery-independent analysis describing groundfish spatial distributions and potential port-level availability. The SSC-ES reviewed this work in September 2021. We did not include the analysis this year because of lack of new data: the NMFS groundfish bottom trawl survey was cancelled in 2020 due to COVID-19, and data from the 2021 survey were not yet available. We will update this work in next year’s report and incorporate SSC-ES recommendations.
The report needs CPS information, beyond what is provided in the forage community analyses (Section 3.2, Appendix H)	For the first time, we have included information from the NMFS / SWFSC’s annual acoustic and trawl surveys of CPS, in Appendix I. The CPS survey group is still analyzing and interpreting data from the 2021 surveys, so the information in Appendix I is limited to the spring 2021 survey, which spanned from the US/Mexico border to San Francisco Bay. We will continue to develop this section and identify potential CPS spatial and temporal indicators for future reports.
Improvements to indicator-based model projections of Chinook salmon returns to the Columbia River basin	Our Supplementary material has generally included a model that estimates returns of Chinook salmon to Bonneville Dam in the year to come, based on ecosystem indicators in the Northern CCE salmon “stoplight table” (Table 3.3.1). The SSC-ES reviewed this work in September 2019, along with an alternative approach that predicts smolt-to-adult survival ratios (SARs). The SSC-ES encouraged further development of these methods, and we have focused on the SAR approach in Appendix J.1. The updated model provides outlooks for four ESUs rather than the more generic “spring Chinook” and “fall Chinook” salmon outlooks previously provided. The approach has multiple alternative model structures and provides SAR estimates with 95% prediction intervals. We will continue to update this approach and work to incorporate SSC-ES recommendations.
The report needs HMS information; NMFS Fisheries Science Centers might look at predator-prey links between HMS and CCE prey (Ecosystem Workgroup request, September 2016, as part of FEP Initiative on Coordinated Ecosystem Indicator Review)	This year, we introduce albacore diets from fishery-dependent sampling of albacore stomachs from 2009-2021 (Section 3.5 and Appendix K.2). The albacore time series is the longest contemporary time series of HMS diet information in the CCE that we know of. In future reports, we will add additional species (including swordfish and thresher shark), though sample processing of those species has been severely delayed by COVID-19.

Request/Need/Issue	Response/Location in document
Offshore wind energy seems likely to emerge as a major human activity in the CCE	We have adapted the spatial and temporal analysis of seafloor contact by bottom trawl gear (reviewed by the SSC-ES in September 2019) to determine how recent, non-confidential activity by the federally managed limited-entry groundfish bottom trawl fleet overlaps with wind energy call areas off California and prospective wind energy areas off Oregon (Section 4.2 and Appendix P). We shared this analysis with Council staff prior to submission of this report, as we are aware of other analyses of fishery activity in relation to wind energy planning, and we do not want to cause any confusion. We anticipate future versions of this report incorporating fishing activities indicators in relation to a mix of ocean uses, and hope to coordinate our approach with the Marine Planning Committee and other interested committees and advisory bodies.
Changes in fishery participation networks analyses	Last year’s report introduced fishery participation networks as tools for describing and measuring the extent to which vessels participate in multiple fisheries and thus create networks of interconnected fishery practices, at the scale of IO-PAC port groups. The approach was reviewed by the SSC-ES in January 2021 and again in September 2021. SSC-ES discussions provided a number of suggestions on both the underlying approach and different topics to address. This year’s report features two analyses, in Section 5.4 and Appendix T. The first follows from the suggestion by the SSC-ES to examine a series of network diagrams to explore change over time for port groups (in this case, Coos Bay, OR). The second addresses the SSC-ES’s conclusion that network metrics could provide insight into how vessels, fisheries or ports respond to change (in this case, relationships between a network metric called Node Strength and port-level fishing revenue).
Evaluate which indicators in this report are sufficient and useful for tracking the effects of climate change, and whether there is a need to develop new or different indicators as part of this report (March 2021, Agenda Item I.2.b, Supplemental EAS Report 1)	In response to this suggestion from the EAS and subsequent and related discussion at the March 2021 PFMC meeting, we developed a short “climate change appendix,” Appendix D in this year’s report, to offer some general suggestions about types of indicators to consider (based in part on data availability and in part on prediction/forecasting skill and confidence), along with three examples of indicators and presentation. These are not intended to be final products: we believe that the indicators that ultimately end up in the report should be co-developed within Council process.

Request/Need/Issue	Response/Location in document
<p>COVID-19 impacts on West Coast surveys and related research in 2021</p>	<p>COVID-19 impacts on research are noted throughout the document. A general summary as of this writing is:</p> <ul style="list-style-type: none"> • Overall, far fewer cancellations or effort reductions on surveys in 2021 than in 2020. • Krill sampling: no cruises in early 2021 off Trinidad Head (Section 3.1) and delays in sample processing. • Forage sampling: the Rockfish Recruitment and Ecosystem Assessment Survey (RREAS), which provides data for Central CCE forage (Section 3.2, Appendix H.2) was forced to cover more area due to cancellation of a related survey off Washington and Oregon in spring 2021. This resulted in some loss of ship time in the central and southern areas of the RREAS (see Figure 1.1a). • HMS diets (Section 3.5, Appendix L): limited access to lab has slowed processing of HMS stomach contents, particularly species other than albacore. • Whale entanglement: reduced capacity for observations, reporting and responses in 2021.

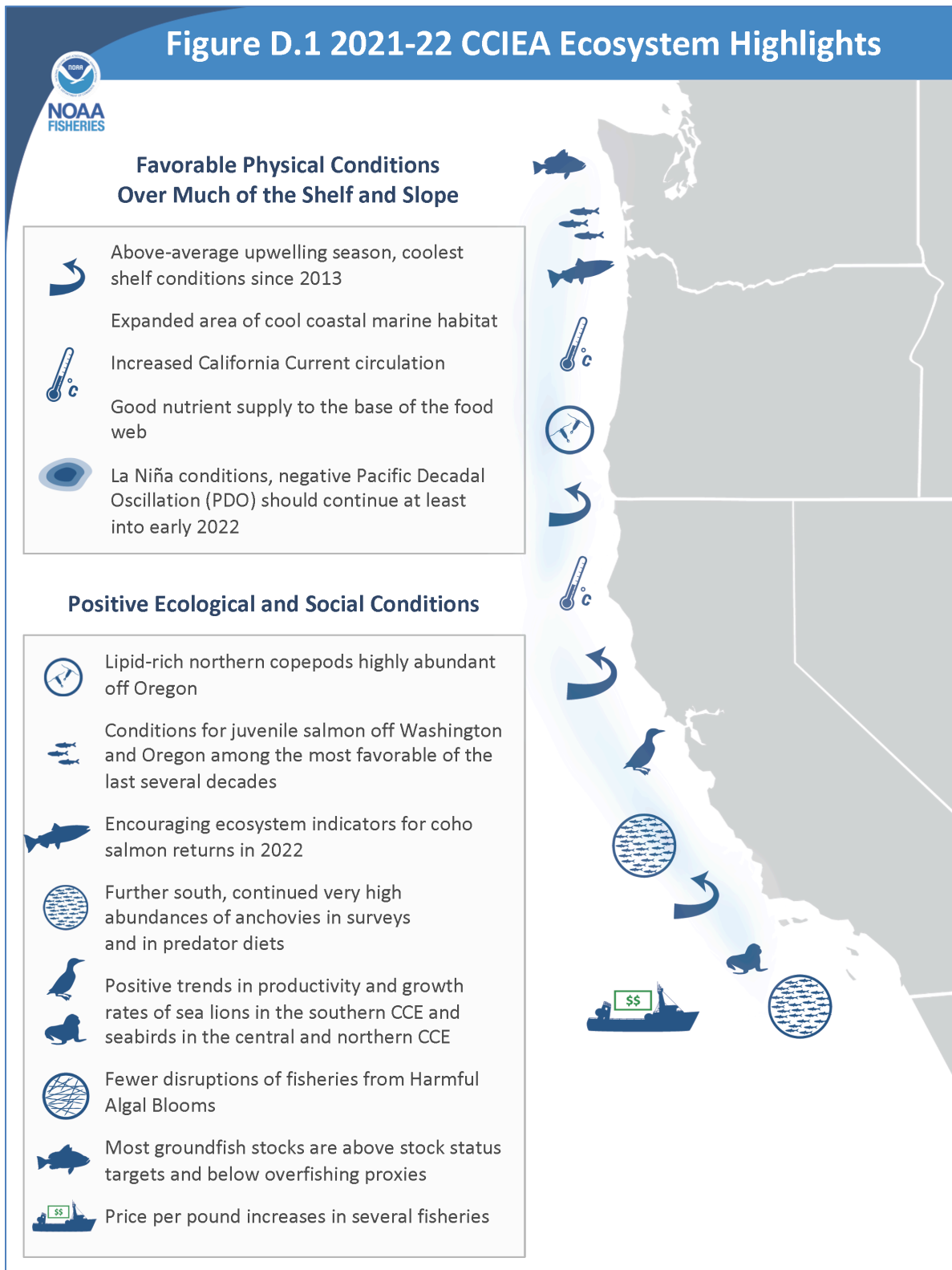


Figure D.2 2021-22 CCIEA Ecosystem Highlights



Unfavorable Conditions/Risk Factors

- 

Marine Heatwave
7th largest marine heatwave since 1982, largely stayed offshore and outside US EEZ
- 

Terrestrial Disturbances
Early snowmelt, drought, warm streams
Record heat, extreme & widespread wildfires
- 

Central Valley Salmon
Poor freshwater conditions
Potential thiamine deficiency in natural-area fish
- 

Hypoxia
Widespread near-bottom hypoxia off OR/WA May-October
- 

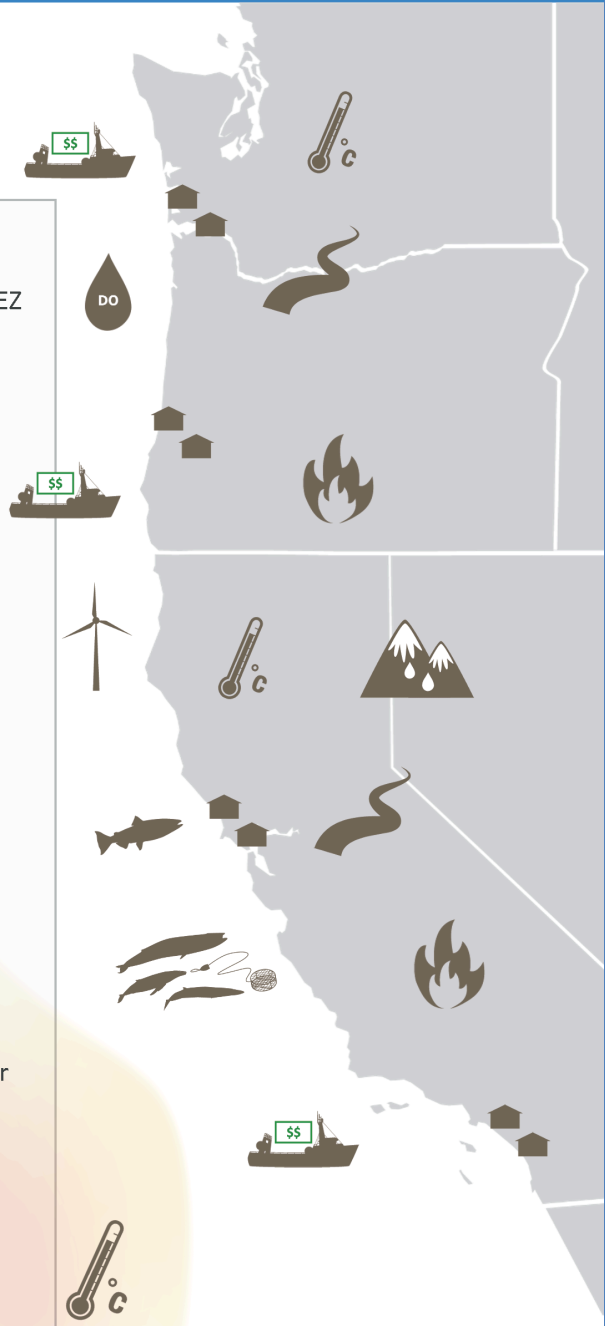
Whale Entanglement
Still above average in 2021
- 

Mixed Ocean Uses
Indicators show clear overlap in bottom trawl fishing and potential wind energy areas off Oregon and northern California
- 

Fishery Landings & Revenue
Landings continued to decline in 2021 for most target groups
- 

Coastal Communities
Lower fishery revenue diversification, higher revenue concentration
- 

COVID Pandemic Stressors
Continued effects and complexities

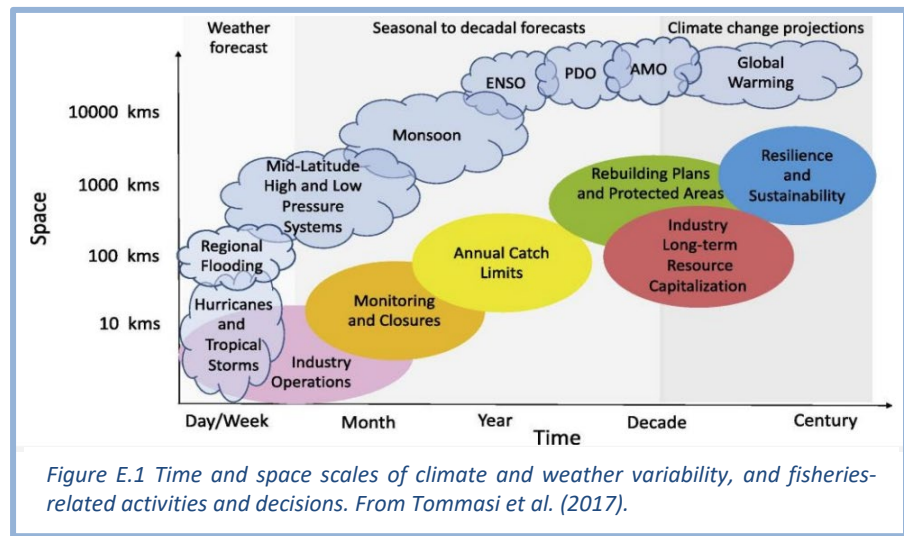


Appendix E DEVELOPING INDICATORS OF LONG-TERM CLIMATE CHANGE

This “climate change appendix” is meant solely as a conversation starter. It stems from a recommendation by the EAS that the CCIEA team could incorporate climate change information into the Ecosystem Status Report for Council management considerations (Supplemental EAS Report 1, March 2021, Agenda item I.2.b). Any such future climate change information that we could provide will necessarily hinge on the CCIEA’s stock in trade: indices of various ecosystem parameters, interpretive analyses and narratives, and (where possible) information on the ability to make skilled forecasts or future projections. We are eager to incorporate this type of information further into our reports, as Council needs, CCIEA team workload, and page limits allow.

This first iteration of a climate change appendix is divided into two parts: first, we propose a common vocabulary and framework for defining the scales of future variability, and how well (and how confidently) different categories of indices can be used to predict future states of the CCE. Second, we offer some examples of how we might present climate change indicators and interpretations, beyond the standard indicator presentations normally found in our reports.

To anticipate changes in climate drivers in time and space, along with responses in fisheries and other ecosystem components (Figure E.1), it is critical to understand different time scales of predictability, what predictions are based on, and sources of uncertainty. This helps to clarify the types of information that forecasting tools are capable (or incapable) of providing to support fisheries activities and management.



Time scales of climate/ocean forecasts and projections can be divided into a series of categories:

- **Nowcasts/Hindcasts.** Nowcasts/hindcasts typically try to describe the exact state of a variable or index at a specific time and space, up to the current date. (*Example: on January 10th, it was 12°C at the surface, 100 km west of Newport.*) Nowcasts/hindcasts are based on observations, but are usually supplemented by models and statistical tools. We can generally provide more up-to-date and confident nowcasts for physical indices than for biological or biogeochemical indicators, which tend to have delays in sample processing or lower spatial or temporal resolution.
- **Seasonal Forecasts.** Seasonal forecasts typically try to describe an index in terms of a limited range of values over the next few months to a year. (*Example: two months from now, it will be 10°C ±2°C at the surface in Monterey Bay.*) They are typically based on either persistence (forward projection of the most recent observations), statistical modeling techniques, or coupled climate and biogeochemical models. Confidence is based on factors such as how well past forecasts have performed, and our understanding of current conditions (nowcasts).
- **Decadal Forecasts.** Decadal forecasts typically try to describe an index in terms of its statistical probability over relatively broad spatial scales at some future point from a year to ten years in the future. (*Example: we are currently in year 8 of a positive phase of the PDO, which has a roughly decadal cycle; thus, in 5 years, there is a 75% chance we will be in a negative PDO phase.*) Decadal

forecasts are based on knowledge of past cycles, statistical models, and coupled climate and biogeochemical models. Like seasonal forecasts, confidence is based on factors like past forecast performance and knowledge of the state of the climate at the time forecasts are made.

- **Climate Projections:** Climate projections typically try to predict the overall statistical state of an index at scales of decades to centuries in the future. *(Example: under the B1 and A1B greenhouse gas emission scenarios, a given region of the ocean will warm by X to Y°C by 2100.)* Climate projections are based on output from global climate models, which can be scaled down to regional levels with additional modeling tools. Climate projections are meant to capture the influence of long-term changes in forcing (such as atmospheric CO₂ levels). Therefore, confidence reflects how well we can anticipate the general direction and magnitude of future change, not our ability to predict conditions at a specific place and time.

The descriptions above mainly apply to climate and ocean physics and chemistry. We can add further observations, statistics, and modeling tools to also make forecasts and projections of how different marine species, habitats, or food webs will respond, for example with changes in productivity, spatial distributions, or interactions between species. Confidence in those forecasts and predictions tends to be lower than for physical and chemical processes.

Critically, our degree of confidence in the various forecasting scales stems from the nature of the different forecasts, what kind of information they are actually forecasting, and the methods wrapped into such forecasts. A useful step could be to more precisely define our confidence around forecasts of indicators that are in the present ecosystem status report, or indicators and forecasting tools that the Council may find valuable for future reports or other Council uses. For example, we could bring Council representatives, CCIEA members and other experts together to workshop a table similar to the coarse, non-exhaustive, hypothetical example in Table E.1:

Table E.1: Hypothetical examples of forecast/projection confidence for different types of indices. Colors represent proposed levels of confidence (green = “high confidence”; yellow = “moderate confidence”; red = “low confidence”) for different combinations of index type and forecast/projection. These are generalizations, as a starting point for further discussion.

Index	Description	Nowcast/ hindcast	Seasonal Forecast	Decadal Forecast	Climate Projection
Type I	Very well sampled, most dynamics understood (example: some physical indices)	High Confidence (Green)	Moderate Confidence (Yellow)	Moderate Confidence (Yellow)	High Confidence (Green)
Type II	Well sampled, some dynamics understood, impacts of long-term change can be estimated (examples: some biological and biogeochemical indices)	High Confidence (Green)	Moderate Confidence (Yellow)	Low Confidence (Red)	Moderate Confidence (Yellow)
Type III	Not well sampled, dynamics less well understood (examples: hydrology, many biological and fisheries indices)	Moderate Confidence (Yellow)	Low Confidence (Red)	Low Confidence (Red)	Low Confidence (Red)

We conclude this appendix with three examples of climate change indicator analyses that are related to the California Current. Their predictability ranges from short-term seasonal forecasts (e.g., the “early warning index of ecosystem state”) to long-term projection (snowpack and sea level rise). They are presented in a different format than is typical of our report. The new format is intended to help the conversation move forward: we mean for them to be engaging and understandable. We hope they are a basis for climate change indicator summaries that provide useful information on status, predictability, and relevance to the Council, to West Coast communities, and to researchers.

Early warning index of ecosystem state



Status and trend:  Within normal range of variability

Why it matters:

Large changes in this “state index” may signal potential for a regime shift in the biological community

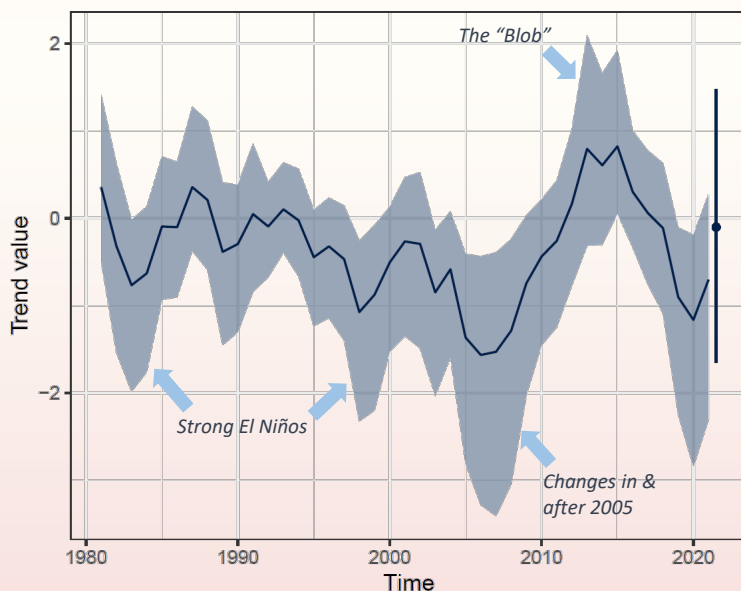
What is measured:

Biological variability in the central and southern CCE, and the probability of switching regimes after a climate stress

Future predictability:

Up to one year in advance with moderate confidence.
Predictions beyond one year will have very low confidence.

Description: The California Current has dozens of long-term datasets on the abundance of various species. Using a statistical tool called Dynamic Factor Analysis, we looked across these datasets to see if they have any similarities in their patterns of change over time. A single pattern emerged that can be used to describe an essential signal of variability in the biological data; we call this the “ecosystem state index.” We can see if its behavior tracks patterns of change in the environment, and if those changes are predictable as an “early warning” of pending change.¹



The ecosystem state index (left, blue trend within estimates of uncertainty) summarizes information across marine species and life stages that respond quickly to climate variability. The community response to recent climate events like the 2014-2016 marine heatwave (the “Blob”) has not exceeded normal biological variability within the ecosystem over the past four decades. For example, the responses to two strong El Niño events (1982–1983 and 1997–1998) and to unusually low productivity conditions (2005) appear similar in magnitude and duration to the response to the 2014-2016 marine heatwave.

Reliable 1-year forecasts of ecosystem state (the dot at the right in the figure) are possible, based on skilled predictions of upwelled nitrate. Operationalizing these forecasts will help us distinguish short-term periods of unusual dynamics or variability from more enduring “state shifts” into novel regimes of ecosystem structure or productivity.

¹Hunsicker et al., in press. PLoS Climate.

Focus area:

Snowpack in Central California

A predictor of Central Valley Chinook salmon returns



Status and trend:

Declining recently, but last 5 years not atypical

Why it matters:

Returns of Sacramento River fall Chinook salmon track snowpack levels from two years prior

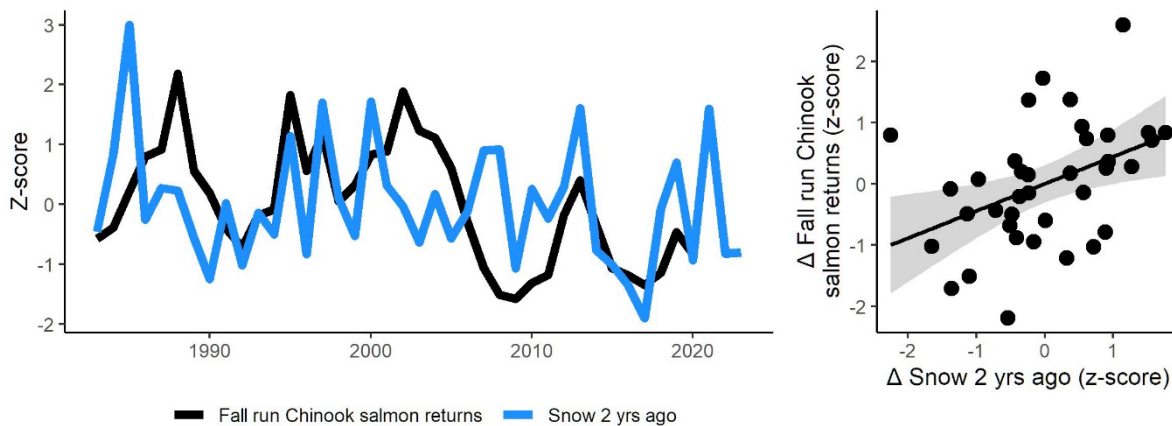
What is measured:

Snowpack in the mountains of the Sacramento / San Joaquin ecoregion, correlated with Sac River fall Chinook salmon returns

Future predictability:

Snowpack in Central California will show a decreasing trend, but with high variability from year to year. Confidence: high

Description: Cold, wet weather means cold, flowing water throughout the Sacramento—San Joaquin basin, even after substantial water regulation. In this system, snowpack generally indicates the extent of cold, wet conditions during the seasonal time period when Fall Run Chinook salmon inhabit this watershed. When water is cold and flows are high, egg survival increases; juveniles use habitats more and for longer seasonal windows; juveniles can grow larger, survive better, and avoid predators; and hatcheries truck fewer juveniles downriver. As most returning Sacramento Fall Run Chinook are three years old, **adult returns in a given year are correlated with snowpack two years prior**, as shown in these two figures:



As described in Munsch et al. (2022)¹, the Central Valley is a highly modified, warming system where people have eroded the climate resilience of salmon via loss of habitat and life history diversity. As a consequence, salmon production is liable to track snowpack increasingly tightly in the coming years. **If so, adult returns will decrease in 2022 and 2023 relative to 2021, based on the snowpack dynamics two years prior.** Unfortunately, snowpack remains difficult to predict with skill beyond a few months into the future, though we do expect average snowpack to decline in the long-term as climate change continues.

¹Munsch et al. 2022. DOI: 10.1111/gcb.16029

Sea level rise and coastal flooding risk

Status and trend:



Mixed. Rising in some areas, falling in others; highly variable

Why it matters:

Sea level rise and coastal flooding pose a threat to fisheries operations and port infrastructure

What is measured:

Effective sea level rise relative to coastal topography

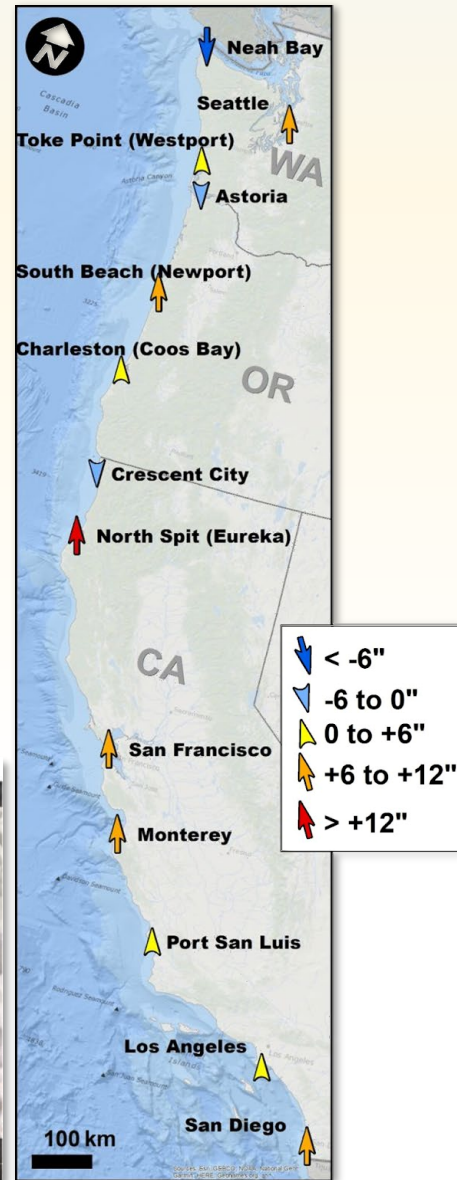
Future predictability:

Sea level rise: confidence is **high** for nowcasts and **moderate** for seasonal and decadal forecasts. Coastal flooding: expected to vary interannually but increase long-term (**high** confidence)

Description: Flooding is a risk in coastal communities, and this risk is increasing in many places due to climate change. Coastal flooding is driven by sea level rise, local geomorphology and topography, anomalous tides, and storm events. A key discussion point of the Climate and Communities Initiative was damage to coastal infrastructure in Northern California and Oregon during winter storms. Assessing impacts on port infrastructure and the probability of coastal flooding in the face of climate change is critical to promoting climate readiness in those communities.

Sea level data from tide stations are used to characterize past trends and to predict future increases. **Sea level trends vary widely on the West Coast (see map at right), ranging from decreases (-6" per century at Neah Bay) to increases (+18" per century at Eureka).** However, sea level rise trends underestimate the risk of coastal flooding if they do not incorporate tide and storm surge anomalies.

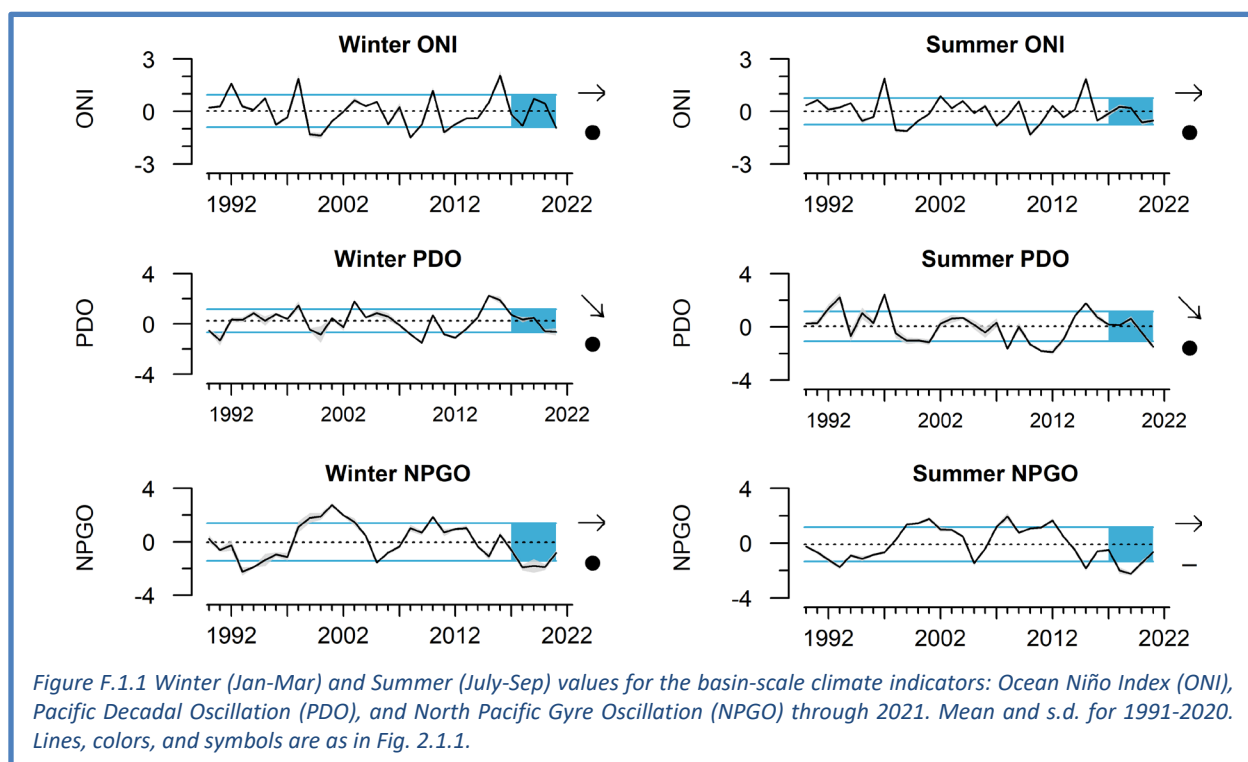
High resolution topography data can be used to predict areas that will become inundated as sea levels increase, using projections based on conventional climate change scenarios. (See below, map of social vulnerability in Eureka under a 4-foot sea level rise scenario.) These tools can help identify at-risk areas at event scales (storms, high tides) and into the future.



Appendix F CLIMATE AND OCEAN INDICATORS

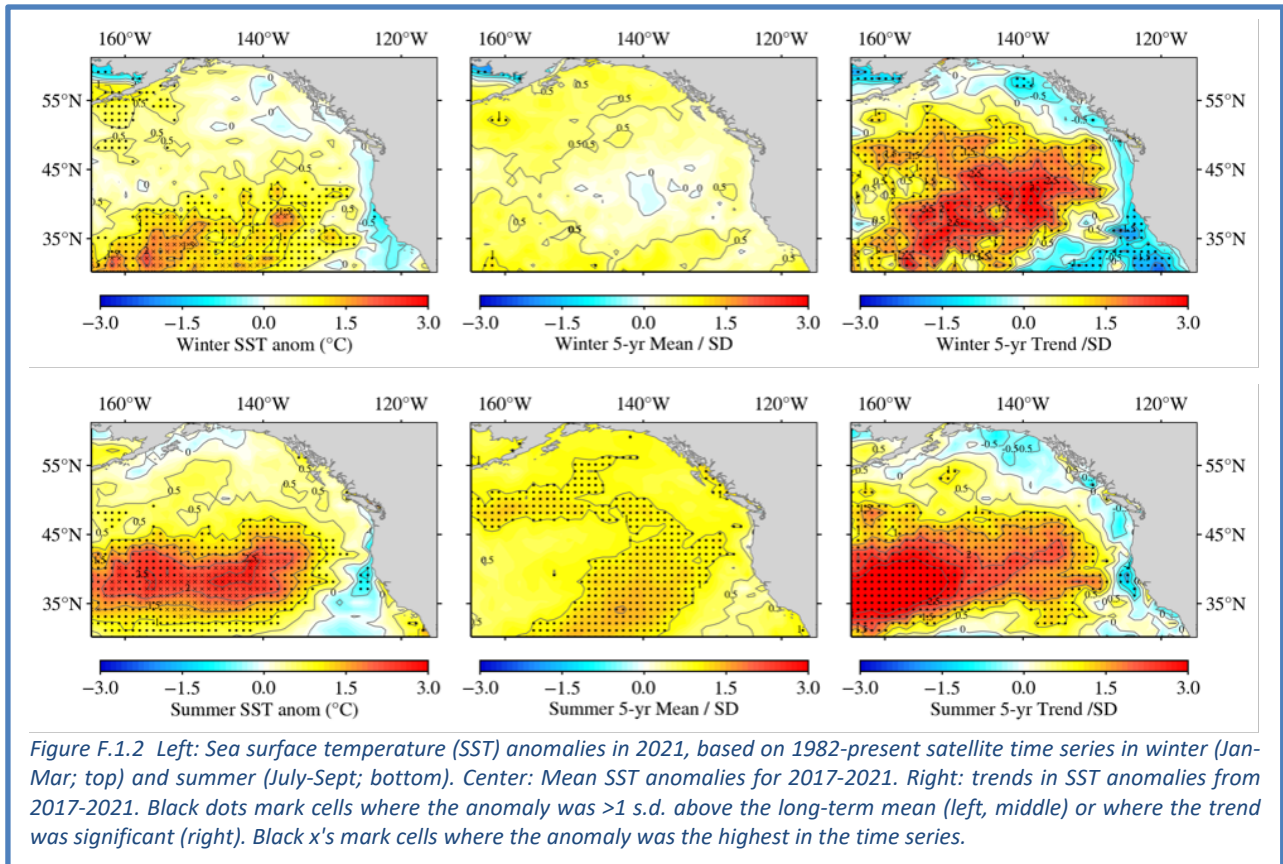
F.1 BASIN-SCALE CLIMATE/OCEAN INDICATORS AT SEASONAL TIME SCALES

These plots show seasonal averages and trends of the three basin-scale climate forcing indicators shown in the main report in Figure 2.1.1. The first notable outcome is that the Ocean Niño Index (ONI) is in a La Niña state (strongly negative) in 2021 (Figure F.1.1, top). We expect the forthcoming winter 2022 ONI to also be negative given current La Niña conditions, which are 67% likely to continue into the spring according to the NOAA Climate Prediction Center. PDO trends are negative in both winter and summer since 2015 (Figure F.1.1, middle), illustrating the decline from the strongly positive PDO signal of the 2013-2016 marine heatwave, and the emergence of a negative PDO during 2020. Finally, the most recent 5-year trends in NPGO are neutral (Figure F.1.1), and NPGO values in both winter and summer 2021 were closer to neutral, following several below-average years for winter and especially summer NPGO values (Figure F.1.1, bottom).



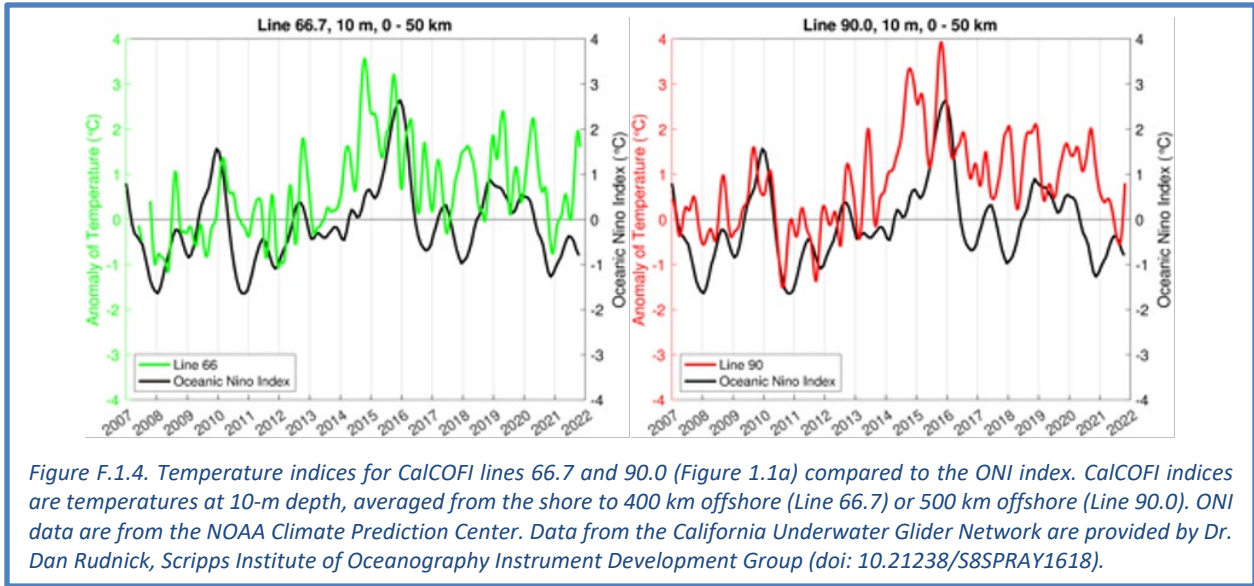
Winter sea surface temperature anomalies in 2021 were negative (between 0 to 0.5°C below average) within 150 km of the coast extending from Washington to southern California (Figure F.1.2, upper left). Winter sea surface temperature anomalies from San Francisco Bay to the Southern California Bight were below -0.5°C, which were the coolest anomalies along the coast. Farther offshore into the subtropical gyre, the winter temperature anomalies were warmer, with anomalies over 1 s.d. (marked with a black dot in Figure F.1.2, upper left), some of which were the largest of the time series (marked with a black X). Summer temperature anomalies in 2021 had a different coastal pattern, with negative anomalies in the Northern CCE and positive anomalies in the Southern CCE (Figure F.1.2, lower left). Further offshore, summer temperature anomalies south of 45°N were more than 1 s.d. above average in 2021, and many locations had the largest positive anomaly since 1982.

Winter 5-year average SST anomalies from 2017-2021 were warmer than average along the coast, though by <0.5°C except for the southernmost extent of the Southern California Bight (Figure F.1.2, top middle). Over most of the region, the 5-year winter mean SST anomalies were positive, generally

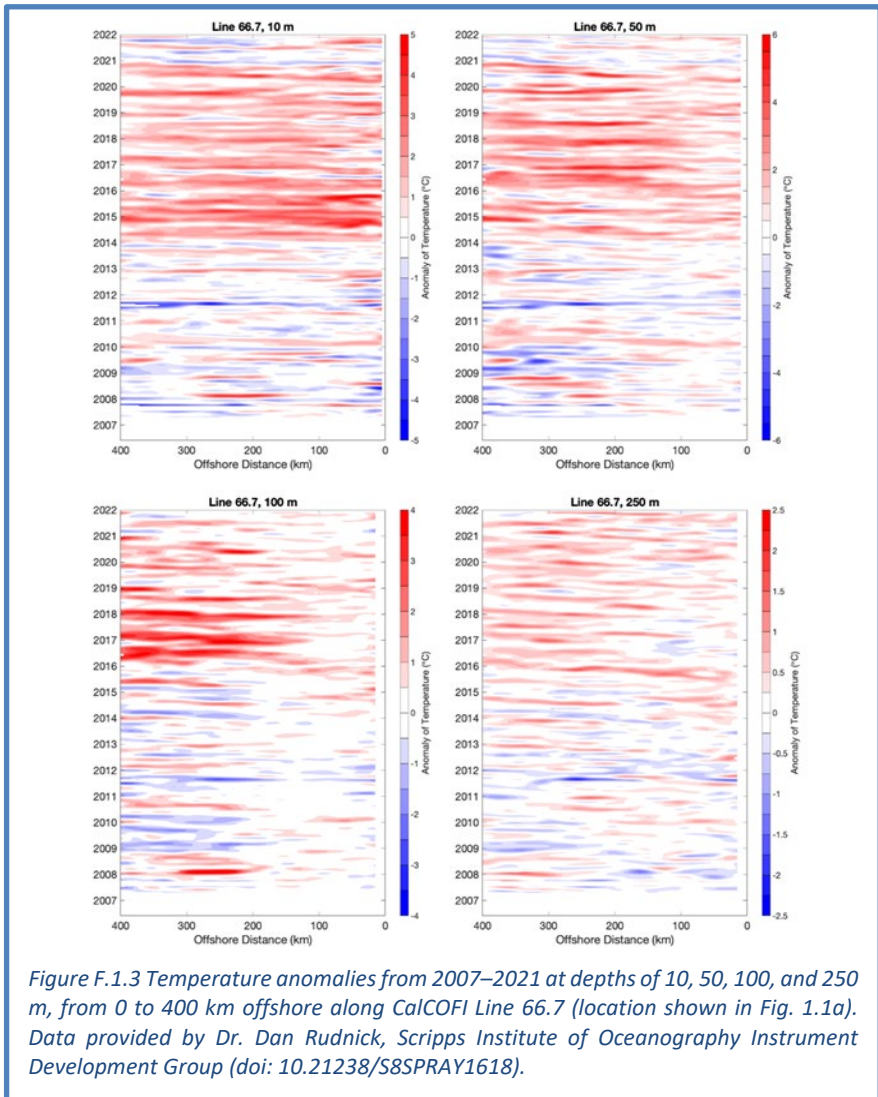


around 0.5°C. Summer 5-year means along the coast were also warmer than average, but anomalies were <0.5°C from Washington to the Southern California Bight; from the Bight to the Mexican border the means increased with some areas exceeding 0.5°C (Figure F.1.2, bottom middle). A large offshore portion of the region had summer 5-year mean SST anomalies exceeding 1 s.d. Winter SSTa trends from 2017-2021 were strongly positive offshore and negative along the coast, particularly for coastal California (Figure F.1.2, top right). The winter 5-year trends stem from reversals of 2017 SST anomalies that resulted in warm nearshore temperatures and cooler temperatures in the subtropical gyre. Summer 5-year trends had a similar pattern to the winter 5-year trends (Figure F.1.2, bottom right). The coastal trends in parts of central and northern California were significantly negative. The negative coastal SST anomalies are typical of La Niña conditions (Figure F.1.1, top).

Jacox et al. (2017) demonstrated that El Niño events were strong predictors of CCE surface temperature. The ONI is formed from the time average of equatorial SST. In a similar manner, Rudnick et al. (2017) created indices along the autonomous glider transects on CalCOFI Lines 66.7 (off Monterey Bay) and 90.0 (off Dana Point) by averaging the 10 m data from the coast out to the seaward extent (400 km for Line 66.7, 500 km for Line 90.0). The glider data demonstrate the relatively strong correlation with the ONI prior to the 2013 marine heatwave, especially at Line 90.0 in the Southern California Bight (Figure F.1.4). Since then, however, both the Line 66.7 and Line 90.0 temperature indices have remained warmer than the ONI and have not reflected the ONI cycling. Causes of this change are still being investigated.



While the figures and text above focus on surface and near-surface temperatures, the North Pacific has stored large amounts of heat in subsurface waters over the past several years (e.g., Scannell et al. 2020). Since 2007, subsurface gliders have enabled continuous sampling of temperature at depth off of Monterey Bay (CalCOFI Line 66.7) and Dana Point (CalCOFI Line 90; see Figure 1.1a). Glider sampling was not affected by the COVID-19 pandemic. Glider-based temperature data have been aggregated to construct monthly time-depth temperature anomaly figures from the coast to the offshore zone. Temperature anomalies along Line 66.7 (to 400 km offshore) generally were negative to neutral in the upper 100 m of the water column in 2021 (Figure F.1.4). Anomalies at greater depths remained neutral to



positive for the full year.

Time-depth temperature anomaly profiles were different to the south along Line 90 in the Southern California Bight. The 10-m temperature anomalies in 2021 were positive nearshore and negative offshore (Figure F.1.5). At greater depths, anomalies were very close to zero, showing both weakly positive and weakly negative values, and the cool anomalies in 2021 remained primarily offshore.

Glider data from the Trinidad Head Line (Figure 1.1a), averaged over from the coast to 200 km offshore, provide a picture of the changing conditions since 2015 (Figure F.1.6). The 2014-2016 marine heatwave produced the highest temperature anomaly of the period of observation, while the El Niño events of 2016 and 2019 show positive temperature anomalies down to 400 m. The La Niña conditions of 2020-2021 appear as the negative anomaly close to the surface.

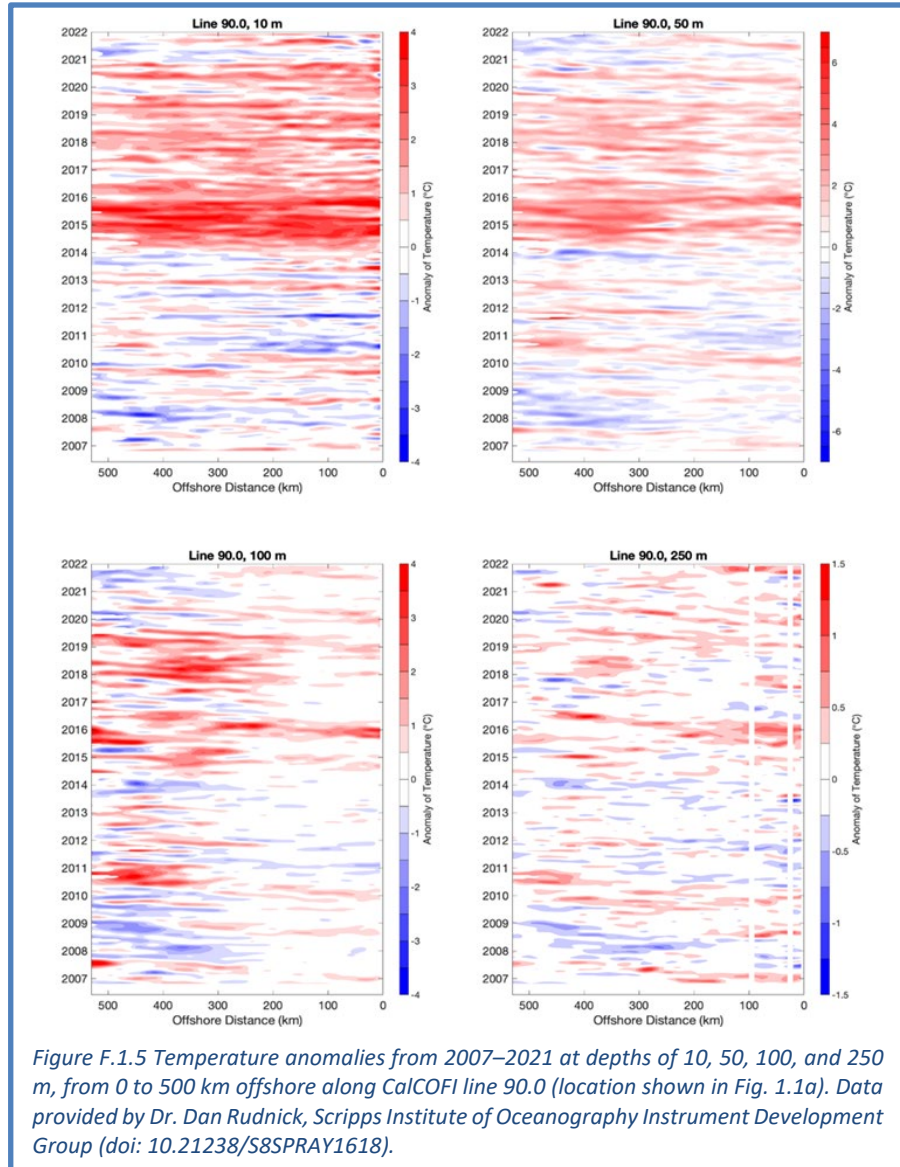


Figure F.1.5 Temperature anomalies from 2007–2021 at depths of 10, 50, 100, and 250 m, from 0 to 500 km offshore along CalCOFI line 90.0 (location shown in Fig. 1.1a). Data provided by Dr. Dan Rudnick, Scripps Institute of Oceanography Instrument Development Group (doi: 10.21238/S8SPRAY1618).

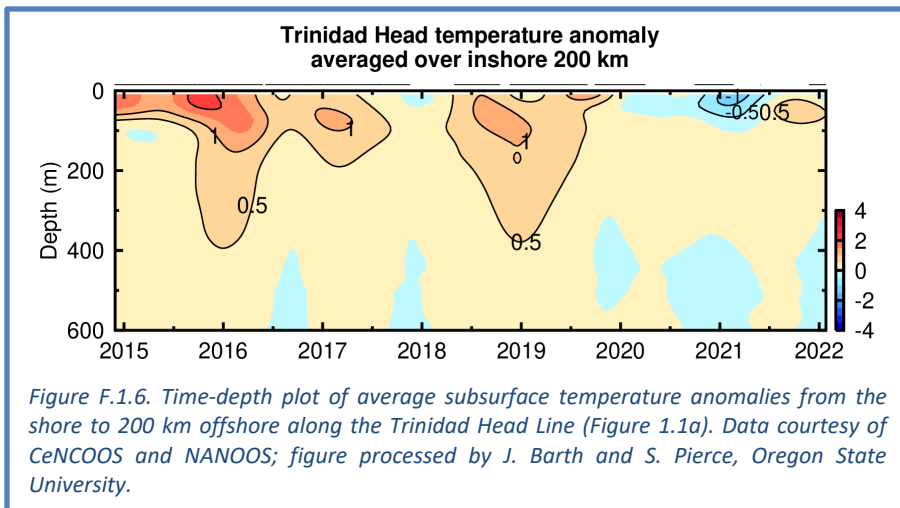
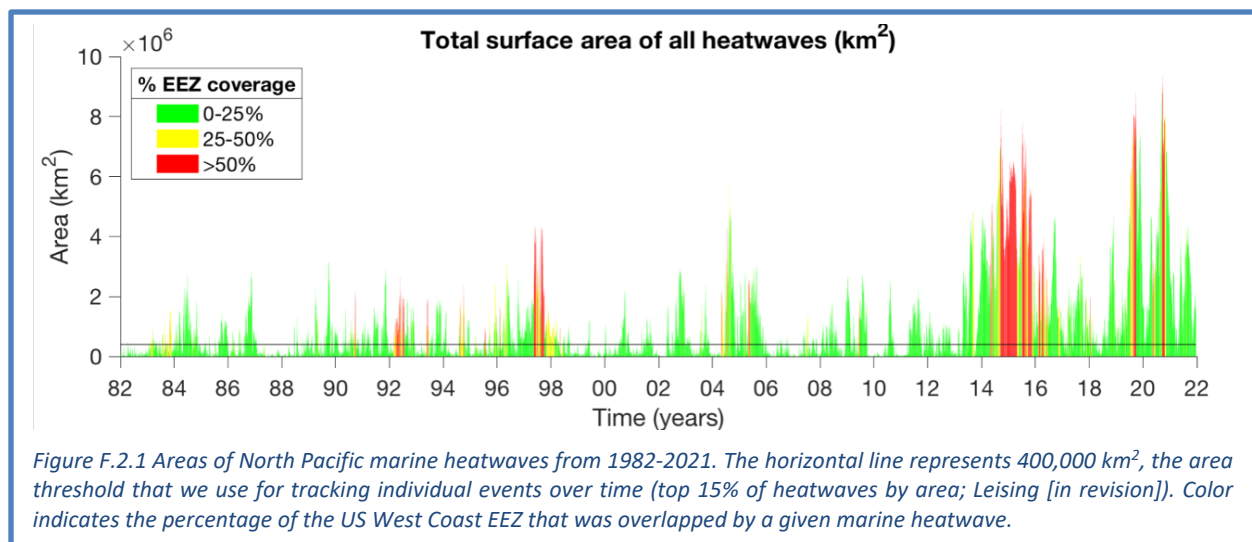


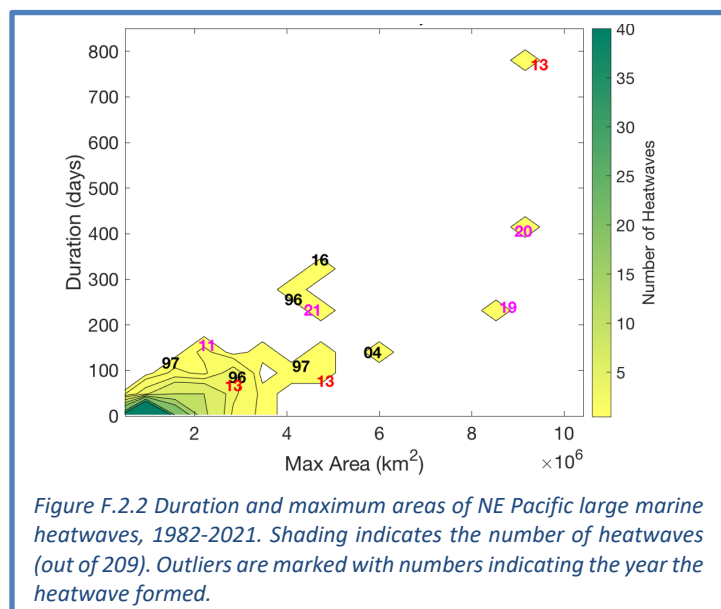
Figure F.1.6 Time-depth plot of average subsurface temperature anomalies from the shore to 200 km offshore along the Trinidad Head Line (Figure 1.1a). Data courtesy of CeNCOOS and NANOOS; figure processed by J. Barth and S. Pierce, Oregon State University.

F.2 ASSESSING MARINE HEATWAVES IN 2021

There is growing recognition that marine heatwaves can have strongly disruptive short-term impacts on the CCE (e.g., Morgan et al. 2019). Based on an analysis of sea surface temperature anomalies (SSTa) from 1982–2019, a marine heatwave has the potential to cause impacts in the CCE that are comparable to those from the 2013–2016 event if the anomalous feature: 1) has statistically normalized SSTa >1.29 s.d. (90th percentile) of the long-term SSTa time series at a location; 2) is $\geq 3.5 \times 10^6$ km² in area; 3) lasts for >5 days; and 4) comes within 500 km of the coast (Hobday et al. 2016; Leising in revision). Events in the North Pacific have met or surpassed these criteria every year since 2013 (Figure F.2.1). That streak includes 2021, which featured a large marine heatwave (designated NEP21A) that began in late April 2021, in the same region where the 2020 MHW declined. NEP21A remained intact through late 2021 in far offshore waters of the North Pacific. Satellite imagery in December 2021 showed warm coastal anomalies separate from the marine heatwave; such anomalies are typical of the succession from summertime upwelling to wintertime downwelling and do not constitute a heatwave as defined above.



After forming in April 2021 and strengthening and increasing in size in May, NEP21A broke into smaller fragments in early June. A relaxation of strong upwelling winds in June also allowed parts of NEP21A to reach the U.S. West Coast, producing anomalously warm conditions along much of the coast. It then reformed in late June, continued to expand, and reached the Canadian coast in August. Upwelling winds, leading to cooler coastal temperatures, resumed by mid-July 2021, during which NEP21A receded from the coast. However, NEP21A remained fairly strong in offshore waters and reached an area of approximately 4,100,00 km² by late August, placing it within the top 10 heatwaves in terms of area since monitoring began in 1982 (Figure F.2.2). Surface waters in the



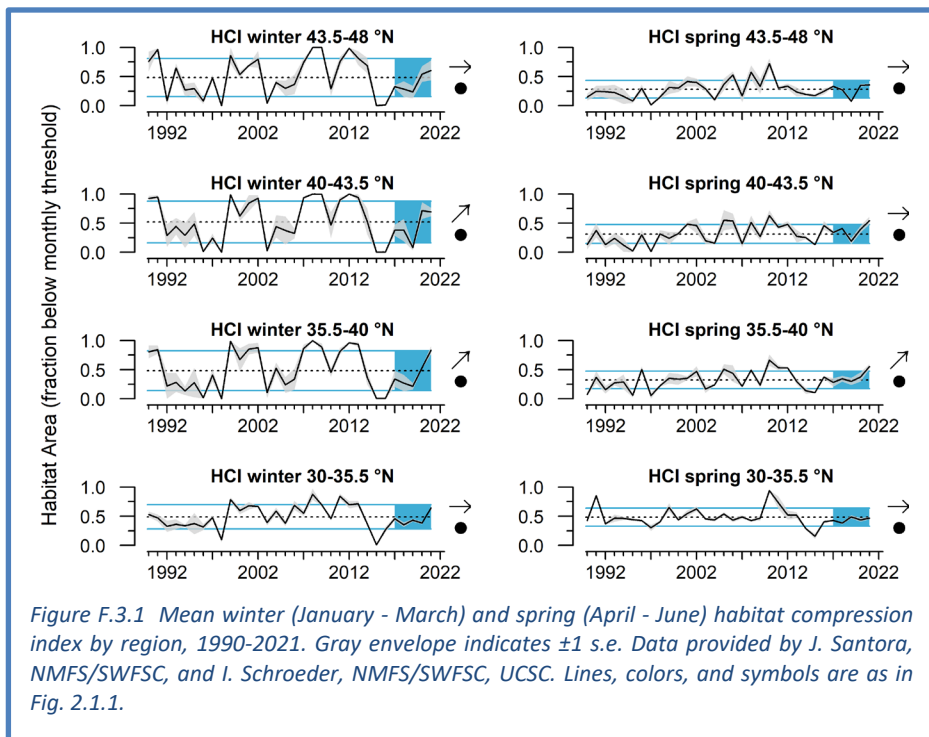
southern California Bight were also warmer than normal during much of the spring and summer, a separate feature from NEP21A. We continue to monitor the area, duration, and coastal proximity of surface water temperatures for these features in the northeast Pacific and communicate with other researchers and policy-makers to understand the array of possible West Coast impacts.

F.3 HABITAT COMPRESSION INDEX

Spatial variability in patterns of upwelling, including the distribution of upwelled water and associated development of hydrographic fronts, is important for ecosystem monitoring and assessment of marine heatwaves and ecosystem shifts that can impact coastal fishing communities. Coastal upwelling creates a band of relatively cool coastal water, which is suitable habitat for a diverse and productive portion of the CCE food web. Monitoring the area and variability of upwelling habitat provides regional measures of habitat compression—an indicator to monitor the incursion of offshore warming (e.g., from heatwaves or reduced upwelling conditions) over shelf waters, which relates to shifts in the pelagic forage species community in space and time. Santora et al. (2020) applied principles of ecosystem oceanography and integration of fisheries surveys to develop the Habitat Compression Index (HCI) to quantify how offshore warming during the 2013–2016 marine heatwave and previous warming events restricted the cool upwelling habitat to a narrower-than-normal band along the coast. This compression of habitat consequently altered prey community composition and distribution, spatial aggregation patterns of top predators, and contributed to increased rates of whale entanglements in fixed fishing gear.

HCI is derived from the CCE configuration of the Regional Ocean Modeling System (ROMS) model with data assimilation (Neveu et al. 2016), and is estimated in four biogeographic provinces within the CCE: 30°–35.5°N, 35.5°–40°N, 40°–43.5°N, and 43.5°–48°N. HCI is defined as the area of monthly averaged ROMS model temperatures at a depth of 2 m that fall below a temperature threshold. Each region/month has a unique temperature threshold, based on its distinct historic climatology. Winter and spring means for central California are shown in the main body of the report (Figure 2.2.2). Winter and spring means for all four regions are shown here, in Figure F.3.1.

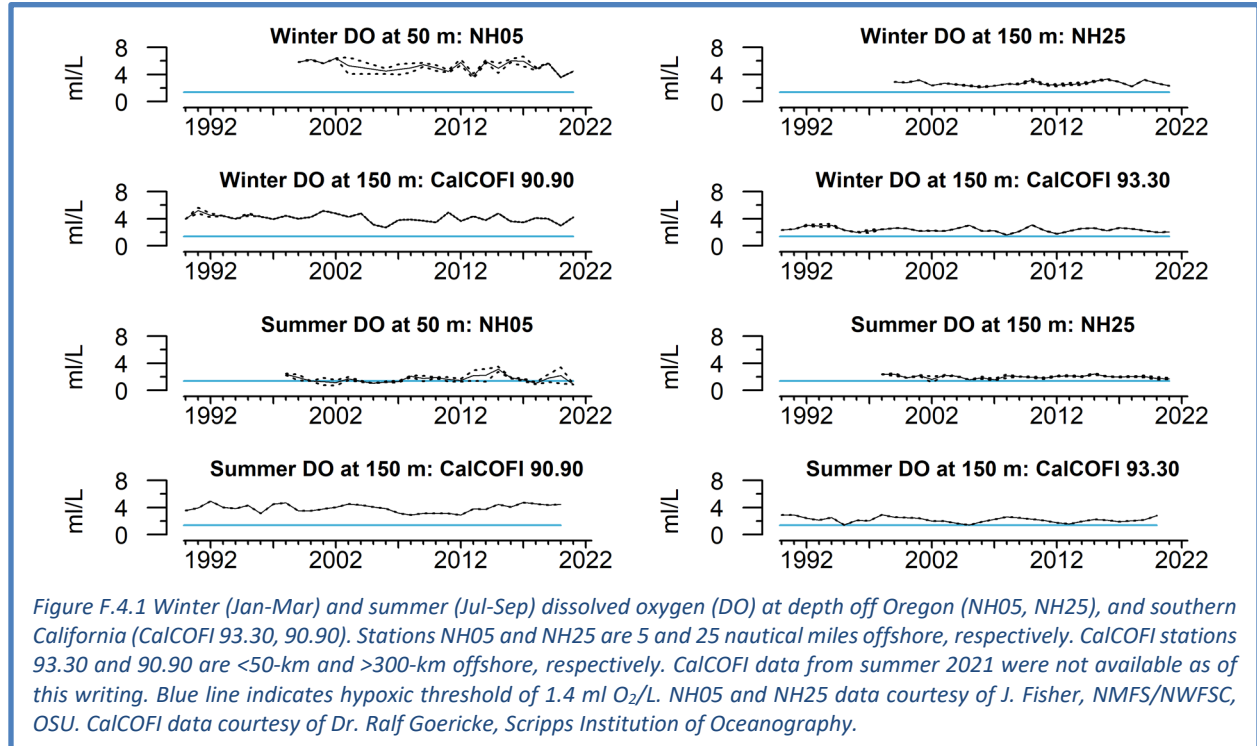
The most evident pattern in Figure F.3.1 is the increase in HCI in all four regions since the very low HCI (= strong compression) in 2015–2016, during the height of the 2013–2016 marine heatwave. Five-year trends are neutral to positive in all regions, with the strongest trends in winter. In 2021, all three northerly regions all had high HCI (= weak compression) in winter and spring, consistent with the early and strong upwelling season.



F.4 SEASONAL DISSOLVED OXYGEN AND OCEAN ACIDIFICATION INDICATORS

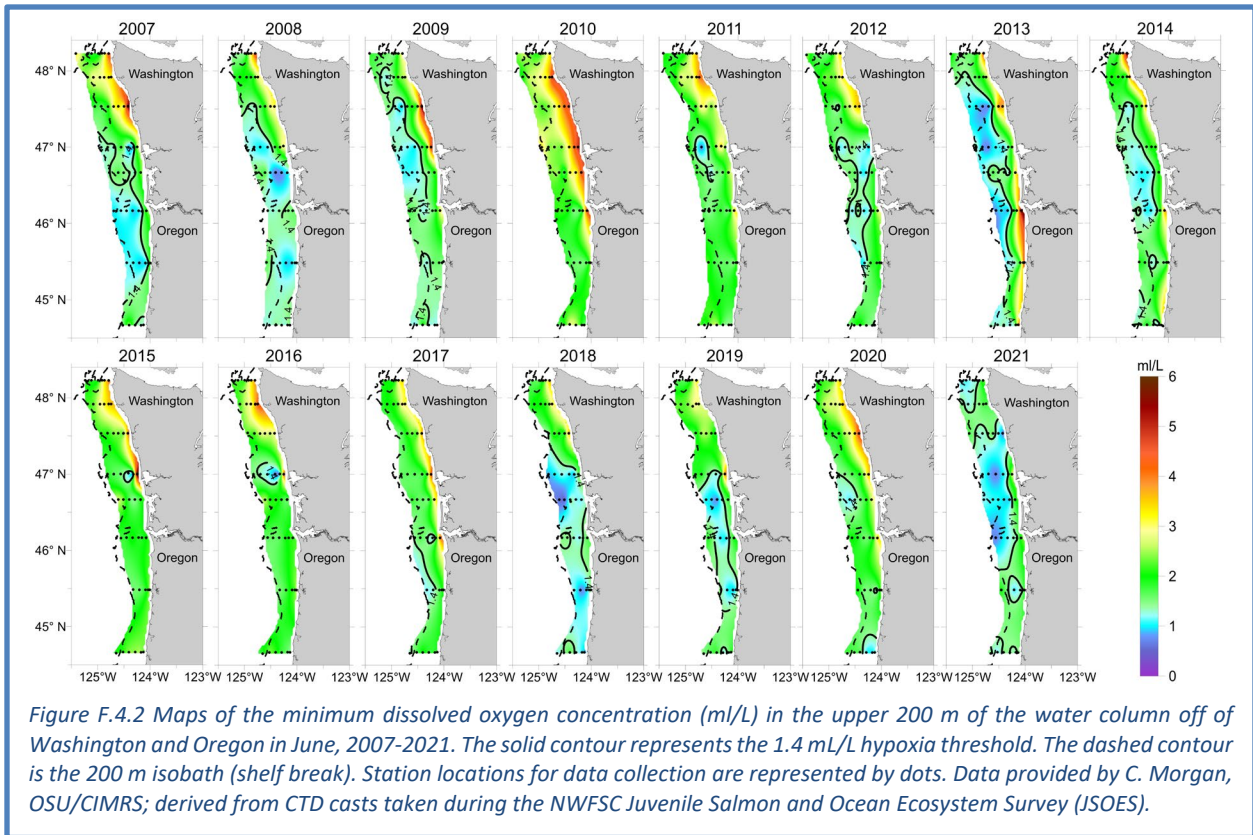
Nearshore dissolved oxygen (DO) depends on many processes, including currents, upwelling, air-sea exchange, and community-level production and respiration in the water column and benthos. DO is required for organismal respiration; low DO can compress habitat and cause stress or die-offs for sensitive species. Waters with DO levels <1.4 mL/L (or 2 mg/L) are considered to be hypoxic; such conditions may occur on the shelf following the onset of spring upwelling, and continue into the summer and early fall months until the fall transition vertically mixes shelf waters. Upwelling-driven hypoxia occurs because upwelled water from deeper ocean sources tends to be low in DO, and microbial decomposition of organic matter in the summer and fall increases overall system respiration and oxygen consumption, particularly closer to the seafloor (Chan et al. 2008).

The first series of plots in this section (Figure F.4.1) shows summer and winter averages for dissolved oxygen (DO) data off Newport, OR (stations NH05 and NH25, 5 and 25 nautical miles off the coast respectively) and in the Southern California Bight (stations CalCOFI 90.90 and CalCOFI 93.30). In 2021, winter DO concentrations (Figure F.4.1, top panels) were consistently above the hypoxia threshold (1.4 ml O_2 per L water) at each of the stations at the depths measured (near bottom at NH05; 150 m at the other stations). These results were fairly typical for winter in each time series.



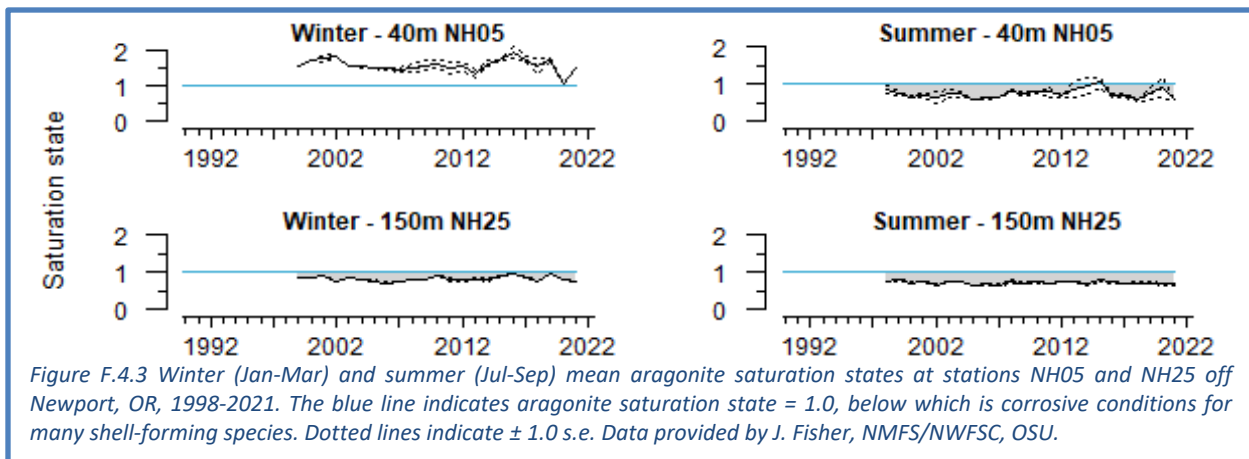
In contrast, summer near-bottom DO values at Newport station NH05 fell below the hypoxia threshold in 2021 (Figure F.4.1). They remained below the threshold into the fall for the first time on record. In fact, near-bottom DO values at NH05 were at or below the hypoxia threshold for much of May to October 2021, which was the longest hypoxic period observed at this station since monitoring began in 2006. Summer DO concentrations at station NH25 were close to the hypoxia threshold in 2021 but generally remained above it (Figure F.4.1), although data were not available beyond July. Summer DO values for the CalCOFI stations in 2021 were not available to us as of this writing.

Additional information from the Juvenile Salmon and Ocean Ecosystem Survey (JSOES), which operates off of Washington and northern Oregon in June (see Figure 1.1a), shows how widespread hypoxia was in the Northern CCE in 2021. Figure F.4.2 shows maps of the minimum DO concentration



in the water column, based on data collected at each sampling station and a kriging approach used by Peterson et al. (2013). Hypoxic conditions occurred on much of the shelf off of Washington and patches off Oregon in June 2021 (Figure F.4.2, blue shaded areas). While this was not unprecedented over the time series shown, the extent of the hypoxia was relatively high for Washington in June, and in some places the hypoxic conditions came closer to shore in 2021 than is typical.

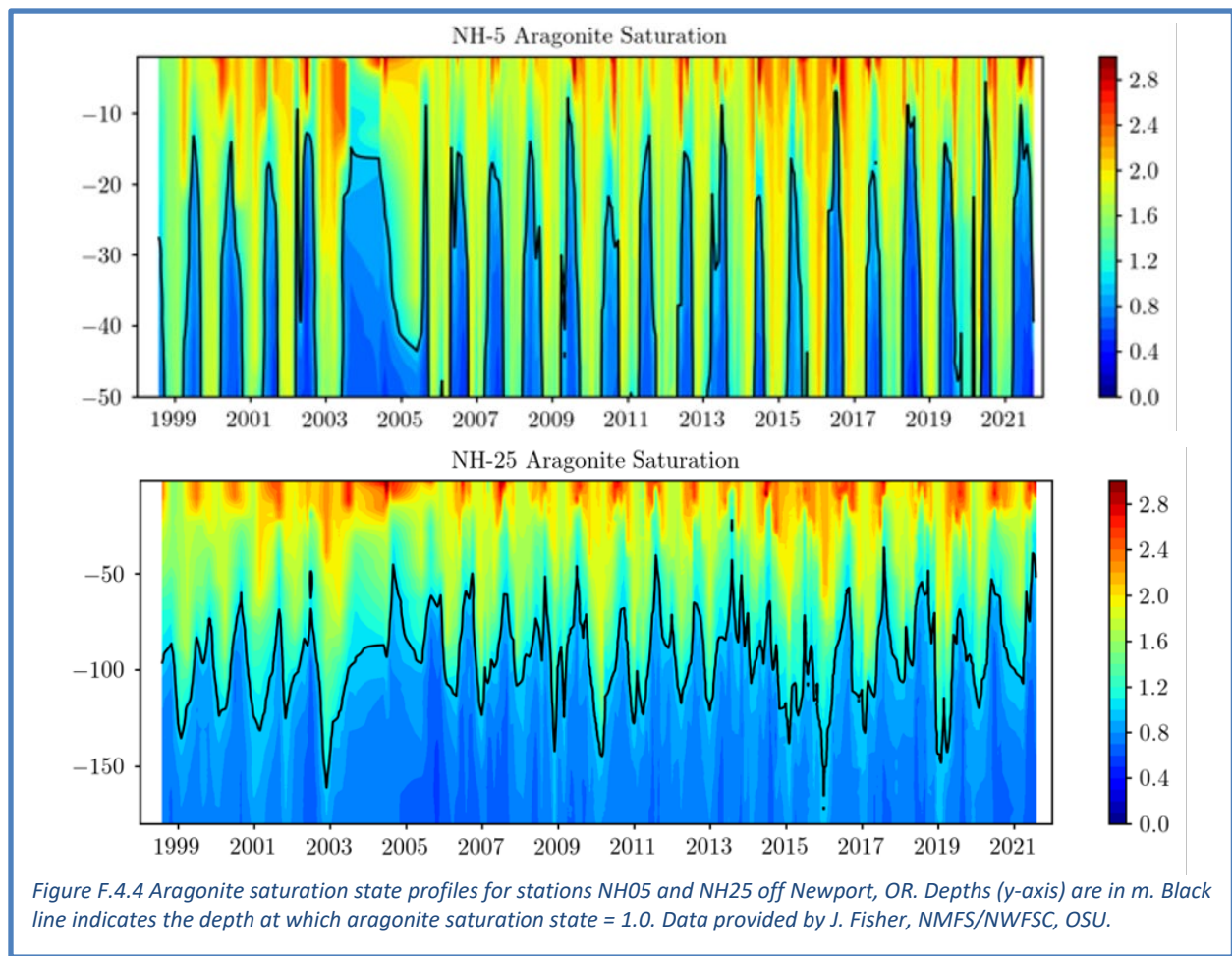
Ocean acidification (OA), which occurs when anthropogenically increased levels of atmospheric CO₂ dissolve into seawater, reduces seawater pH and carbonate ion levels. Upwelling transports hypoxic, acidified waters from offshore onto the continental shelf, where increased community-level metabolic activity can further exacerbate OA (Feely et al. 2008). A key indicator of OA is aragonite saturation state, a measure of the availability of aragonite (a form of calcium carbonate). Aragonite saturation <1.0 indicates relatively acidified, corrosive conditions that are stressful for many CCE



species, particularly shell-forming invertebrates. OA impacts on these species can propagate through marine food webs and potentially affect fisheries (Marshall et al. 2017). Aragonite saturation states tend to be lowest during spring and summer upwelling, and highest in winter.

Figure F.4.3 shows time series of winter and summer aragonite saturation from near bottom at stations NH05 and NH25. Aragonite saturation states in 2021 followed the expected pattern: higher levels in fall/winter and lower values in spring/summer. Winter saturation state at both stations has been trending down in recent years, due to high saturation levels in 2016 and lower saturation levels in recent years, including one of the lowest observations of the time series in winter 2020 at NH05 (Figure F.4.2, left). Winter values in 2021 were nonetheless fairly typical for both stations. Summer aragonite saturation levels were <1.0 at both stations (Figure F.4.2, right).

The corrosive water on the shelf at NH05 is largely driven by seasonal upwelling, where upwards of 80% of the water column becomes corrosive each summer. In 2021, this corrosive layer peaked within ~ 10 m of the surface (Figure F.4.4, top), and aragonite saturation was depressed in the water column for a longer period of time than normal for station NH05, consistent with the extended upwelling season. The offshore station over the slope at NH25 is slightly influenced by seasonal upwelling and downwelling, and much of the upper 100 m of the water column remains undersaturated year-round (Figure F.4.4, bottom). In 2021, the aragonite saturation threshold shoaled to shallower depths than in 2018-2020.



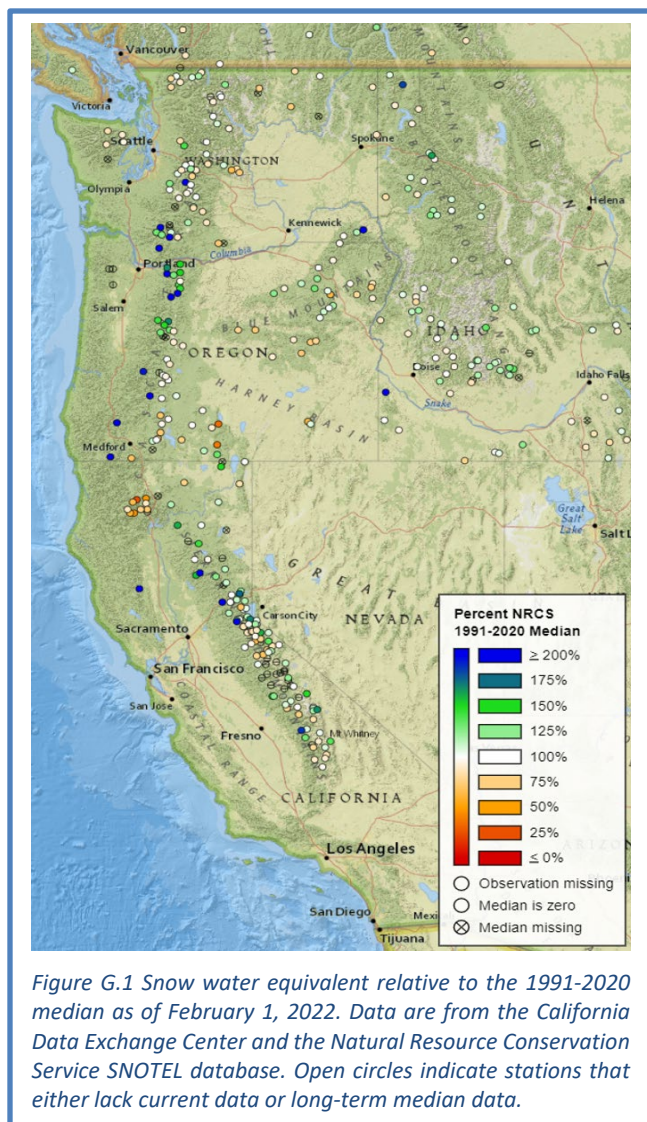
Appendix G SNOWPACK, STREAMFLOW, AND STREAM TEMPERATURE

Freshwater habitat indicators are reported based on a hierarchical spatial framework. The framework facilitates comparisons of data at the right spatial scale for particular users, whether this be the entire California Current, ecoregions within the CCE, or smaller spatial units. The framework we use divides the region encompassed by the CCE into ecoregions (Figure 1.1b), and ecoregions into smaller physiographic units. Freshwater ecoregions are based on the biogeographic delineations in Abell et al. (2008; see also www.feow.org), who define six ecoregions for watersheds entering the California Current, three of which comprise the two largest watersheds directly entering the California Current (the Columbia and the Sacramento-San Joaquin Rivers). Within ecoregions, we summarized data at scales of evolutionary significant units (ESUs) and 8-field hydrologic unit classifications (HUC-8). Status and trends for all freshwater indicators are estimated using space-time models that account for spatial and temporal autocorrelation (Lindgren and Rue 2015).

Snow-water equivalent. Snow-water equivalent (SWE) is measured using data from the California Department of Water Resources snow survey program (California Data Exchange Center, cdec.water.ca.gov) and The Natural Resources Conservation Service's SNOTEL sites across Washington, Oregon, California and Idaho. Snow data are converted into SWEs based on the weight of samples collected at regular intervals using a standardized protocol. Measurements on April 1 are considered the best indicator of maximum extent of SWE; thereafter snow tends to melt rather than accumulate.

April 1 SWE in 2021 was mixed across the West's mountain ranges, with northerly ecoregions receiving above-average SWE and the southerly Sierra Nevada receiving below-average levels (Figure 2.4.1 in the main report). However, 2021 was the second-warmest year on record, which led to early and rapid snowmelt, low soil moisture, high river temperatures, widespread drought, and disastrous forest fires in much of the region.

The outlook for snowpack in 2022 is limited to examination of current SWE, which is an imperfect predictor of SWE in April due to variable precipitation and atmospheric temperature. As of February 1, 2022, SWE in the CCE region was mixed (Figure G.1), despite numerous winter storms that have generated substantial snows in many parts of the Cascades and Sierra Nevada. It remains too soon to say whether patterns will change this winter, although a La Niña currently is in progress, and recent La Niña events have generally featured drier-than-normal winters for much of California and wetter-than-normal conditions in the Pacific Northwest. The NOAA seasonal drought outlook as of January 31, 2022 is for persistent drought in



nearly all of California and parts of southernmost Oregon and Idaho between now and April. Drought is expected to continue but improve during that time in most of Oregon and parts of central Washington and central Idaho.

Stream temperature. Mean maximum stream temperatures in August were determined from 446 USGS gages with temperature monitoring capability. While these gages did not necessarily operate simultaneously throughout the period of record, at least two gages provided data each year in all ecoregions. Stream temperature records are limited in California, so two ecoregions (Sacramento/San Joaquin and Southern California Bight-Baja) were combined. Maximum temperatures exhibit strong ecoregional differences in absolute temperature (for example, Salish Sea and Washington Coast streams are much cooler on average than California streams).

The most recent 5 years have been marked by stream temperatures that varied within and across regions (Figure G.2). Streams in the Salish Sea and Washington Coast ecoregion have cooled in the last five years, while the Columbia Unglaciaded and Oregon/Northern California Coast have experienced warming. The Columbia Glaciaded ecoregion has averaged warm anomalies that are barely statistically significant over the most recent five years. Coastwide, average summer water temperatures have generally trended upward since the early 2010s.

Minimum and maximum streamflow. Flow is derived from active USGS gages with records that are of at least 30 years' duration (waterdata.usgs.gov/nwis/sw). Daily means from 213 gages were used to calculate annual 1-day maximum and 7-day minimum flows. These indicators correspond to flow parameters to which salmon populations are most sensitive. We use standardized anomalies of streamflow time series from individual gages.

Most ecoregions of the California Current experienced below-average annual 7-day minimum streamflow anomalies in 2021 (Figure G.3). Several ecoregions experienced fairly extreme lows: since 1981, water year 2021 was the 4th lowest for the Oregon/Northern California Coast, the 4th lowest for the Southern California Bight, and the 7th lowest for the Sacramento/San Joaquin basin. Minimum streamflows have declined over the past five years in three of the six ecoregions (Columbia Unglaciaded, Oregon/Northern California Coast, Sacramento/San Joaquin). The Salish Sea & Washington Coast ecoregion has had a stable recent trend, but has experienced below-average minimum flows for much of the recent 5 years; similarly, streams in the Southern California Bight ecoregion have a stable recent trend, but minimum flows have been near the lower end of the range

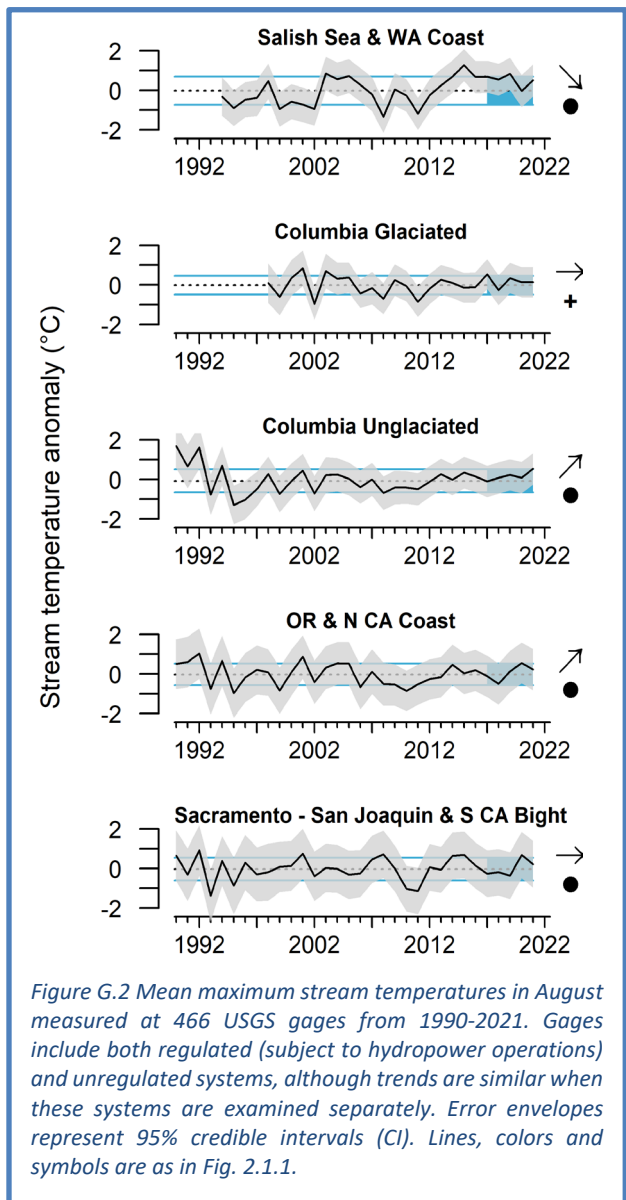
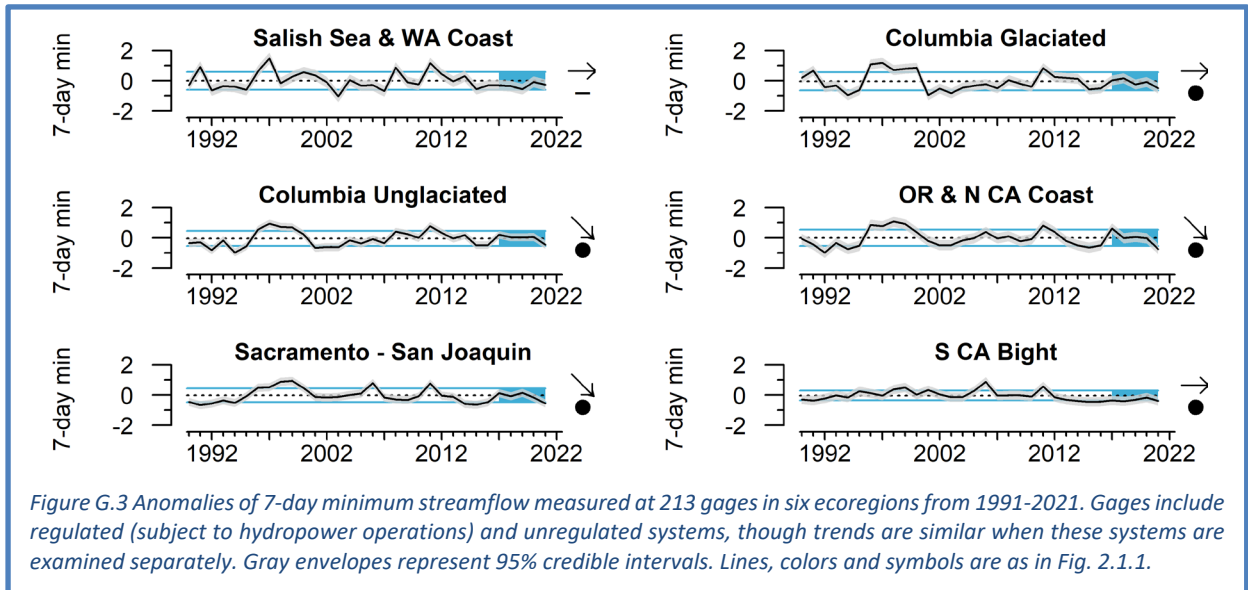
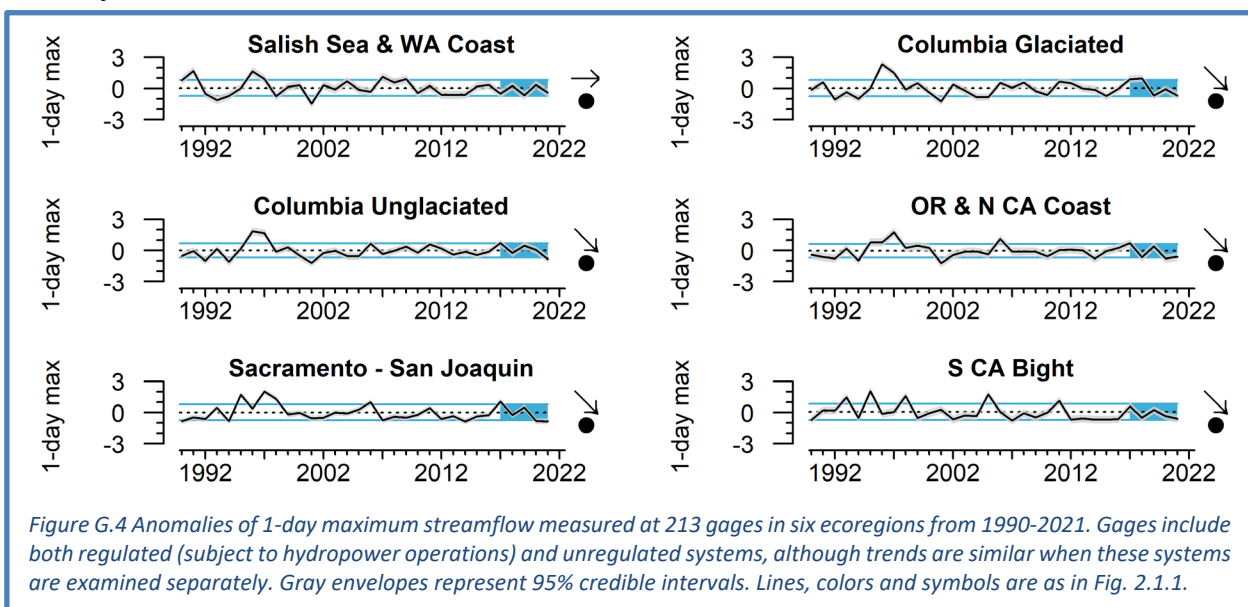


Figure G.2 Mean maximum stream temperatures in August measured at 466 USGS gages from 1990-2021. Gages include both regulated (subject to hydropower operations) and unregulated systems, although trends are similar when these systems are examined separately. Error envelopes represent 95% credible intervals (CI). Lines, colors and symbols are as in Fig. 2.1.1.

for the period of record. Within individual ecoregions, there is basin-scale variability in 7-day minimum flow patterns; see Figure G.5 for minimum flow trends by Chinook salmon ESU.



Similarly, 1-day maximum flows in 2021 declined in much of the California Current’s rivers relative to 2020, contributing to declining recent trends in five out of the six ecoregions (Figure G.4). The only (slight) increase from 2020 to 2021 at the ecoregion scale was in the Oregon/Northern California Coastal ecoregion. In the Sacramento-San Joaquin, maximum flows were lower even than the marine heatwave year of 2015. Since 1981, water year 2021 ranked the 10th, 4th, 9th, and 2nd worst years for the Columbia Glaciated, Columbia Unglaciaded, Oregon/Northern California Coast, Southern California Bight, and Sacramento/San Joaquin ecoregions, respectively. The maximum flow values for Salish Sea/Washington Coast, Columbia Glaciated and Columbia Unglaciaded in 2021 are inconsistent with 2021 SWE patterns, which were average to above average for those three ecoregions (Figure 2.4.1). Variability across basins exists within each ecoregion; see Figure G.6 for flows by Chinook salmon ESU.



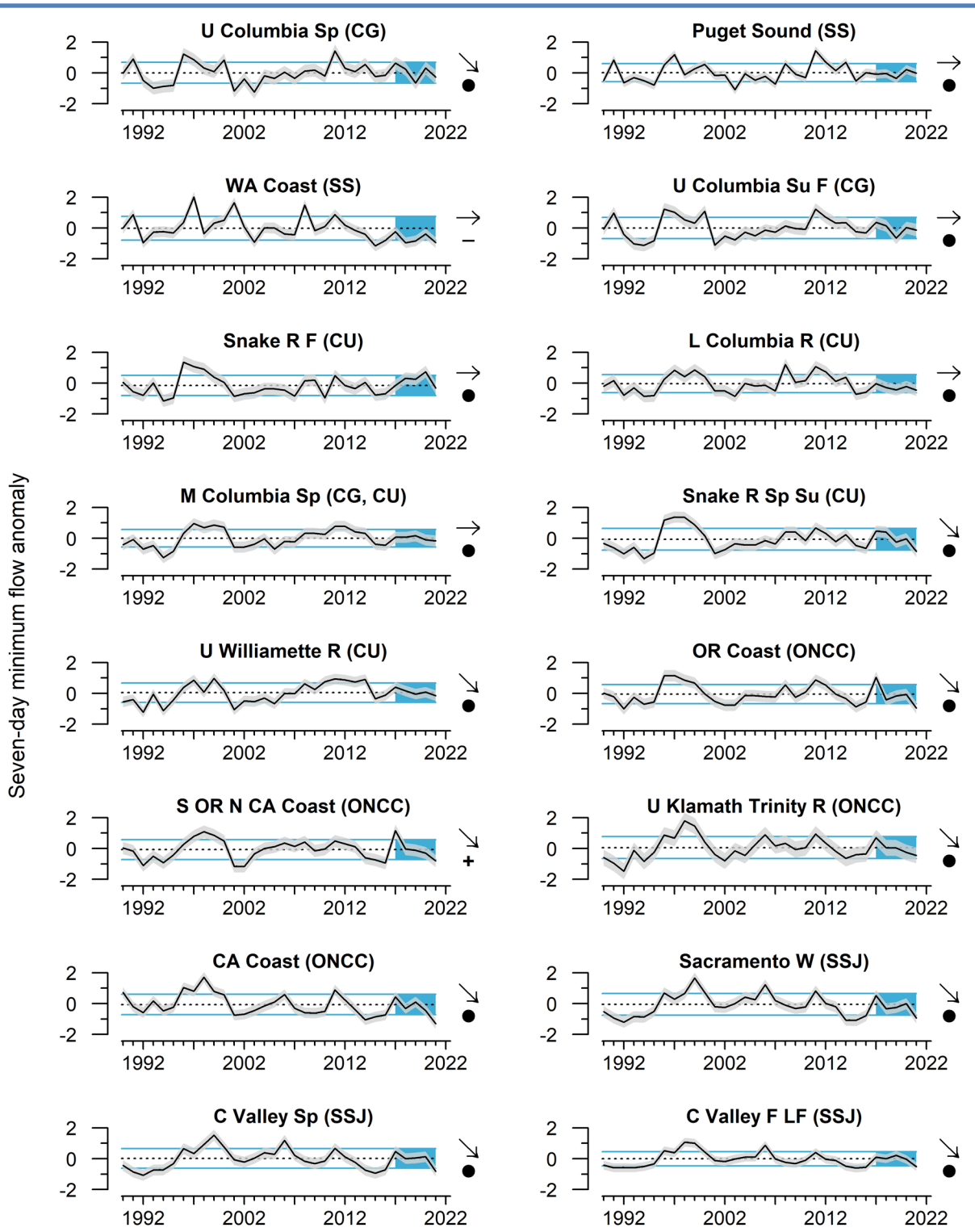


Figure G.5 Anomalies of the 7-day minimum streamflow measured at 213 gages in 16 Chinook salmon ESUs for 1990-2021. Gages include both regulated (subject to hydropower operations) and unregulated systems, although trends were similar when these systems were examined separately. Error envelopes represent the 95% credible intervals (CI). Lines, colors and symbols are as in Fig. 2.1.1. Acronyms in parentheses refer to freshwater ecoregions, shown in Figure 1.1.b.

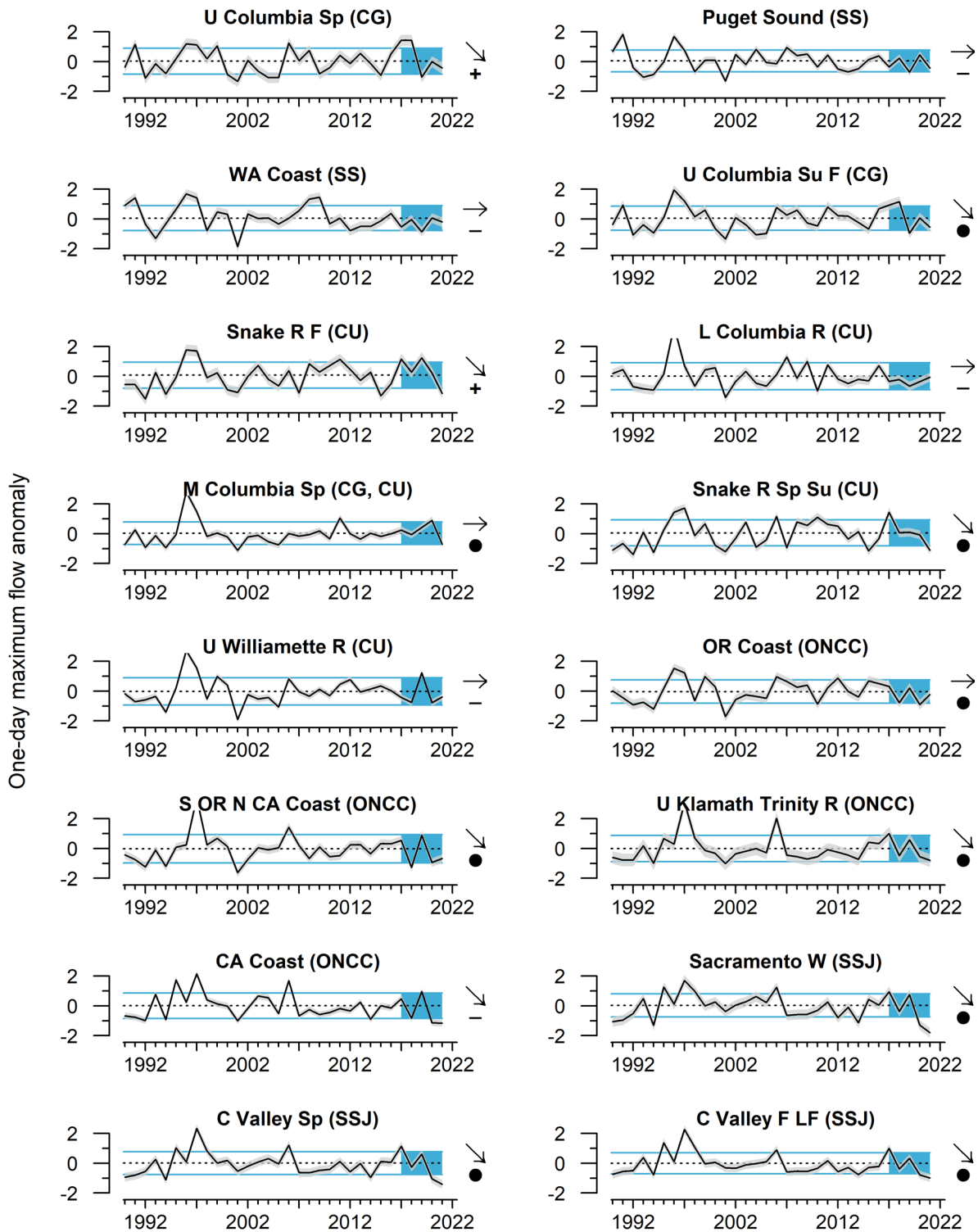


Figure G.6 Anomalies of the 1-day maximum streamflow measured at 213 gages in 16 Chinook salmon ESUs for 1990-2021. Gages include both regulated (subject to hydropower operations) and unregulated systems, although trends were similar when these systems were examined separately. Error envelopes represent the 95% credible intervals (CI). Lines, colors and symbols are as in Fig. 2.1.1. Acronyms in parentheses refer to freshwater ecoregions, shown in Figure 1.1.b.

Appendix H REGIONAL FORAGE AVAILABILITY

H.1 NORTHERN CALIFORNIA CURRENT FORAGE

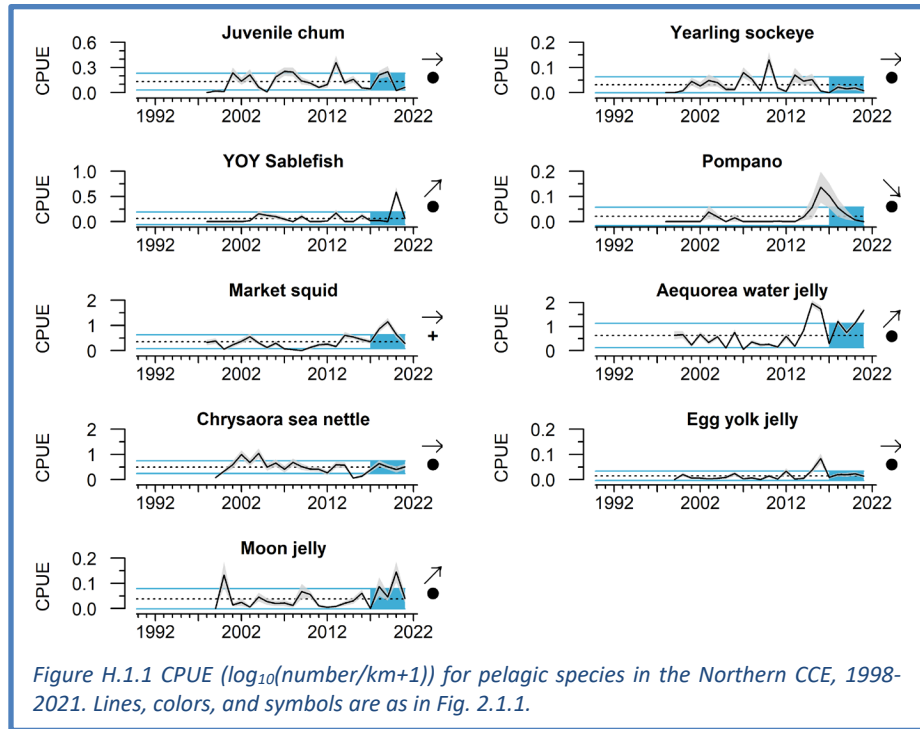
The Northern CCE survey (known as the Juvenile Salmon Ocean Ecology Survey, JSOES) occurs in June and targets juvenile salmon in surface waters off Oregon and Washington, but also collects adult and juvenile (age 1+) pelagic forage fishes, market squid, and gelatinous zooplankton with regularity. A Nordic 264 rope trawl is towed at the surface (upper 20 m) for 15 - 30 min at approximately 6.5 km/hr. The gear is fished during daylight hours in near-surface waters, which is appropriate for targeting juvenile salmon.

In 2021, catches of juvenile chum salmon and juvenile sockeye salmon were nearly >1 s.d. below the long-term survey mean; both had non-significant 5-year trends (Figure H.1.1). As noted in Section 3.3, catches of juvenile subyearling and yearling Chinook salmon and juvenile coho salmon were all very close to average in 2021 (data not shown here).

Among non-salmonids, catches of many species have been dynamic since the values associated with the 2013-2016

marine heatwave. Catches of market squid in 2021 returned to the time series average, down from the very high catches from 2018 to 2020. Similarly, catches of pompano (butterfish), which peaked in 2016, have declined to just below the time series mean. Egg yolk jellyfish also peaked in 2016, but have been close to average catches since then. *Aequorea* jellyfish, which were very abundant during the heatwave years of 2015-2016, have been highly variable since but were >1 s.d. above the mean again in 2021. Catches of *Chrysaora* jellyfish (sea nettles) have been at near-average values since the lows in 2015-2016, associated with the marine heatwave. Moon jellies have increased in recent years, but were close to the time series average in 2021 and down from the very high catches in 2020. Catches of age-0 sablefish were above average in 2021, though not as anomalously high as in 2020.

Researchers on a related survey in May 2021 in the same region noted that larval and juvenile sardines were encountered at more stations and in greater numbers than is typical for that survey (data not shown). In the past, this has indicated warmer ocean conditions. Researchers on this same May survey also observed higher numbers of juvenile lingcod, Pacific sandlance, juvenile greenlings, and adults of the krill species *Thysanoessa spinifera*, all of which are associated with relatively cooler ocean conditions.



H.2 CENTRAL CALIFORNIA CURRENT FORAGE

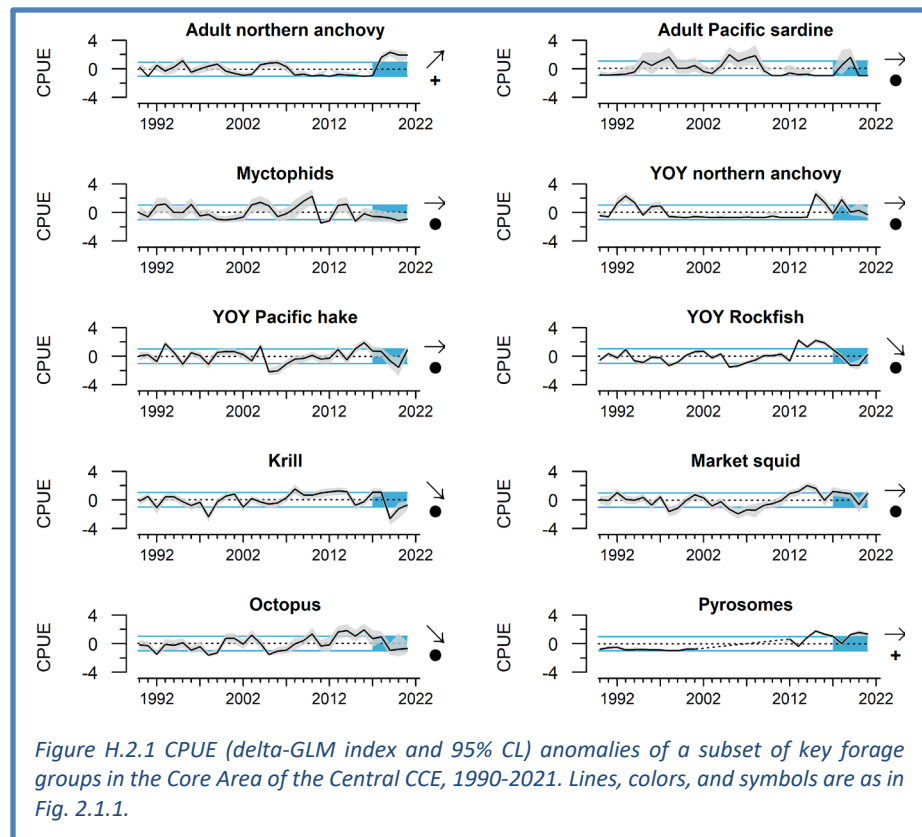
The Central CCE forage survey (known as the Rockfish Recruitment and Ecosystem Assessment Survey, RREAS) samples much of the West Coast each May to mid-June, using midwater trawls to collect young-of-the-year (YOY) rockfish species and a variety of other YOY and adult forage species, market squid, adult krill, and gelatinous zooplankton. Juvenile rockfish, anchovy, krill, and market squid are among the most important prey for CCE predators (Szoboszlai et al. 2015). Time series presented here are from the “Core Area” of that survey, centered off Monterey Bay (Figure 1.1a).

Catches were standardized by using a delta-GLM to estimate year effects while accounting for spatial and temporal covariates to yield relative abundance indices, shown with their approximate 95% confidence limits (Santora et al. 2021). Although data were very limited in 2020 due to the COVID-19 pandemic, effort was closer to normal (typically on the order of ~60 trawls in the Core Area, ~150 coastwide) in 2021. As the model could not estimate a variance when no fish were encountered, data points with no confidence limits in Figure H.2.1 indicate years in which none of a given taxon were caught (e.g., most recent years for adult sardines; 2012 and 2016 for adult anchovy).

Standardized anomalies of log-transformed catch indices indicate that in 2021, catches of YOY rockfish, sanddabs and Pacific hake in the Core Area increased from the very low levels observed in 2019 and 2020, although they remained well below the peak abundance levels that occurred during and shortly after the 2015-2016 large marine heatwave (Figure H.2.1). The relative abundance of adult northern anchovy remained at very high levels observed in recent years. No adult Pacific sardine were encountered in the Core Area in either 2020 or 2021, consistent with the observed decline in their abundance seen in other surveys. Catches of YOY anchovy were lower than in recent years in the Core Area (Figure H.2.1), but were considerably higher in the southern survey area (not shown). Survey results suggest that the relative abundance of krill in this region also increased, but remained slightly below long-term average levels; a similar trend was observed for myctophids.

Market squid catches increased substantially from 2020 to 2021, although we note that uncertainty around the 2020 value was very high due to sparse sampling (Santora et al. 2021). Pelagic juvenile octopus catches, which often covary strongly with YOY groundfish and market squid (Sakuma et al. 2016), remained low in 2021.

Pyrosome catches in 2021 were again far above the time series average, as they frequently have been at least since the onset of marine heatwaves in the mid-2010s.

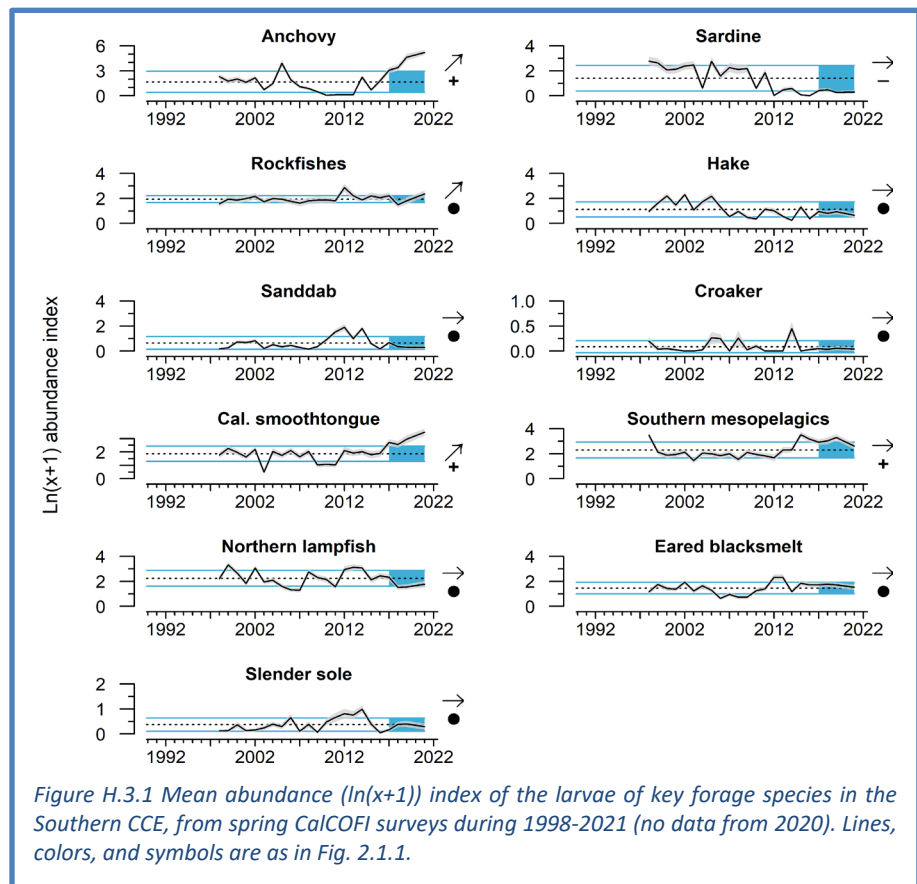


The cumulative results of these trends indicate a fairly productive ecosystem with abundant forage that is dominated by northern anchovy. Ocean conditions in 2021 were not highly conducive to groundfish recruitment, which is generally higher during periods of greater transport and more subarctic source waters in the California Current (Ralston et al. 2013, Schroeder et al. 2019).

H.3 SOUTHERN CALIFORNIA CURRENT FORAGE

Abundance indicators for forage in the Southern CCE come from fish and squid larvae collected in the spring (May-June) across all core stations of the CalCOFI survey (Figure 1.1a). Larval data are indicators of the relative regional abundances of adult forage fish, such as sardines and anchovy, and other species, including certain groundfish, market squid, and mesopelagic fishes. The survey samples a variety of fish and invertebrate larvae (<5 d old) from several taxonomic and functional groups, collected via oblique vertical tows of fine mesh Bongo nets to 212 m depth. In 2020, the spring larval survey was cancelled due to COVID-19, and thus no data are available for that year, but survey operations resumed in 2021.

Catches of larval anchovy in spring 2021 were the highest in the time series for this region, and larval anchovy numbers continued their strongly significant increase in recent years (Figure H.3.1). Larval California smoothtongue (a mesopelagic species) also continued a strongly increasing trend and had record high catches in 2021. Other notable results include that larval rockfish catches in 2021 were the highest since 2012, and that catches of larval sardines remained very low. Southern mesopelagic species also remained relatively abundant in 2021. Recent trends for most species or species groups were non-significant.



Appendix I COASTAL PELAGIC SPECIES DATA FROM SPRING 2021

Acoustic-trawl method (ATM) surveys have been used in most years since 2006 to map the distributions and estimate the abundances of coastal pelagic fish species (CPS) in the coastal region from Vancouver Island, Canada, to San Diego, California (e.g., Demer et al. 2012, Zwolinski et al. 2014, Stierhoff et al. 2020). Surveys cover waters to at least the 1,000-fathom (1829 m) isobath, or 65 km from shore. The five most abundant CPS in this domain are northern anchovy, Pacific herring, Pacific sardine, jack mackerel, and Pacific mackerel. The ATM combines data from echosounders, which record CPS echoes, and trawls, which produce information about the fish species and their sizes and ages contributing to the CPS echoes. This survey also samples the density of CPS eggs in near-surface water, using a continuous underway fish egg sampler (CUFES) mounted on the ship's hull at 3-m depth (Stierhoff et al. 2020).

Presented here are the results of the spring 2021 survey (Zwolinski et al., in press); 2021 summer survey data are still being processed. Because of its shorter duration (25 days) compared to the summer surveys (80+ days), the spring 2021 survey focused on sampling the central stock of northern anchovy. The survey area encompassed the expected distribution of anchovy and spanned the waters between San Diego and San Francisco, out to as far as 150 km off southern California. In the Southern California Bight, sampling from FSV *Reuben Lasker* was augmented by nearshore transects sampled by F/V *Long Beach Carnage*. The reduced latitudinal extent of the spring survey, relative to the aforementioned summer surveys, only allowed an assessment of the status of anchovy.

In the surveyed area, anchovy made up the majority of the trawl catches (Figure I.1c) and consequently dominated the acoustically derived biomass density (Figure I.1a). Anchovy eggs far outnumbered sardine eggs at the near-surface (Figure I.1b). The estimated anchovy biomass of 1,363,094 t (CV = 0.17) indicates that the central stock has continued to grow since 2019, when it was estimated at 810,634 t (CV = 0.13; Stierhoff et al., 2020). The increase in anchovy biomass is largely due to age-0 and age-1 fish in the ATM survey, indicating two strong consecutive recruitments in 2019 and 2020 (Zwolinski et al., in press).

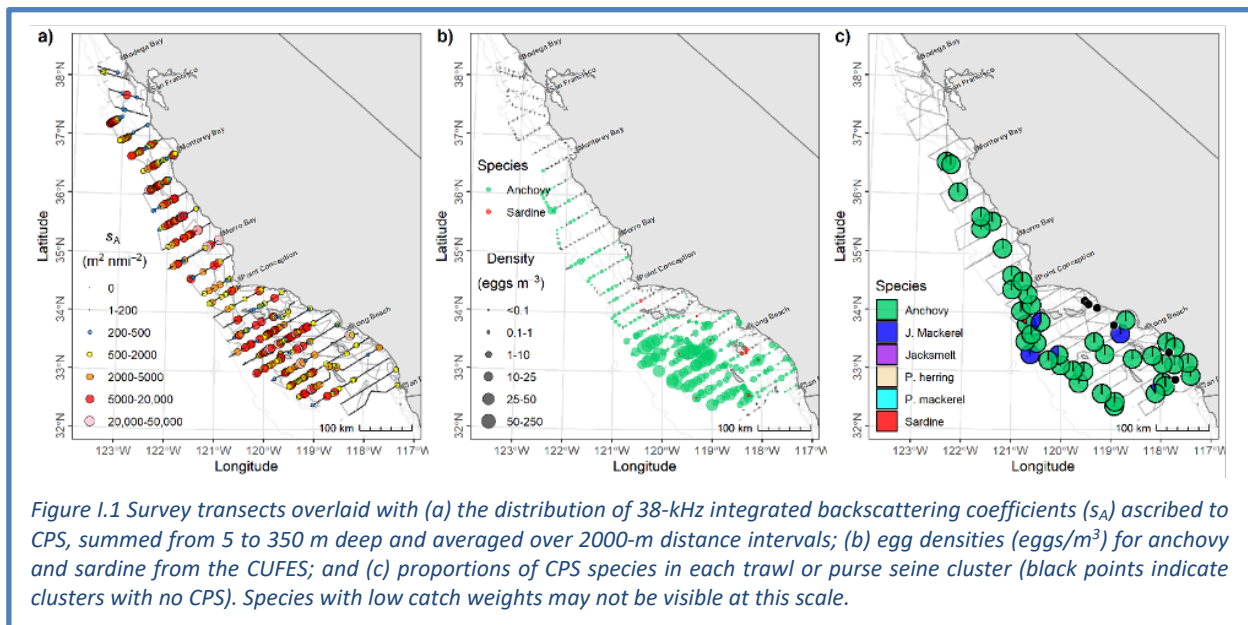


Figure I.1 Survey transects overlaid with (a) the distribution of 38-kHz integrated backscattering coefficients (s_A) ascribed to CPS, summed from 5 to 350 m deep and averaged over 2000-m distance intervals; (b) egg densities (eggs/ m^3) for anchovy and sardine from the CUFES; and (c) proportions of CPS species in each trawl or purse seine cluster (black points indicate clusters with no CPS). Species with low catch weights may not be visible at this scale.

Appendix J **INDICATORS OF SALMON RETURNS**

In past reports, we have included time series of Chinook and coho salmon escapements at the scale of ESUs. The SSC has voiced many technical concerns about these time series. Chiefly, the averages and trends within the scale of the time series available to us may not be representative of historic escapement levels and variability, or of the magnitude of change that may be needed to reach target reference points for particular stocks. Thus, short-term increases or “above average” escapements within our time series may appear overly optimistic. The CCIEA team shares these concerns, and has other concerns about how well these indicators fit in an ecosystem status report—that is, what elements of the ecosystem they are effectively indicative of. Finally, our time series have consistently been out of date by one or more years, and some ESUs have relatively few and possibly decreasing numbers of index populations to provide status data. We will therefore discontinue including escapement indicators until further discussion with the SSC and other committees and advisory bodies on how to improve the robustness and usefulness of indicators of salmon returns.

Instead, this Appendix focuses on indicator suites and analyses that may provide value in determining outlooks for salmon returns. These tools are related to the “stoplight tables” in Section 3.3 of the main body of the report.

J.1 ECOSYSTEM INDICATOR-BASED OUTLOOKS FOR CHINOOK SALMON ESCAPEMENT IN THE COLUMBIA BASIN

The main body of the report features a stoplight table (Table 3.3.1) that provides a qualitative, ecosystem-based outlook of returns of adult Columbia Basin Chinook salmon in 2022, based on indicators of conditions affecting marine growth and survival of outmigrating smolts. A related quantitative analysis, which has been refined this year in response to feedback from the SSC and other partners (see Appendix C), uses an expanded set of >40 ocean indicators and mark-recapture data to estimate smolt-to-adult survival of Chinook salmon from the Upper Columbia and Snake River basins.

In this analysis, models are fit to the smolt-to-adult return data, and these models use the most recent ecosystem indicator data to predict what smolt-to-adult survival will be for cohorts that have gone to sea but not yet returned. Separate models have been developed for spring and fall Chinook salmon from the Upper Columbia Basin and Snake River basins. The specific approach uses a Dynamic Linear Model, founded on linear regressions of single ecosystem indicators vs. survival rates of PIT-tagged fish that left Bonneville Dam as smolts and returned as adults (Figure J.1, black lines). Through a combination of ranking models based on predictive ability and eliminating potential variables using Variance Inflation Factors, the number of ecosystem indicators was iteratively reduced (arbitrarily to ~10) while minimizing the covariance among the remaining indicators. Rather than relying on any single model, we present results from multiple models (Figure J.1, colored points) that use: 1) the first Principal Component (PC1, derived from a Principal Components Analysis) of the NOAA stoplight chart; 2) the PC1 calculated from a new set of ocean indicator variables specific to each stock; or 3) the top five single-variable models for each stock.

For Snake River smolts that went to sea in 2020 (which should dominate adult returns in 2022), the survival estimates are at or below the averages for the past ten years. For Snake River spring/summer Chinook (Figure J.1, upper left), the 2020 smolt year is estimated to have survival that is similar to the 2019 cohort (the dominant cohort in last year’s returning adults). The 2020 cohort’s survival estimates are at or slightly below the average of the previous ten years, with moderate uncertainty relative to the overall time series. For Snake River fall Chinook salmon (Figure J.1, upper right), the 2020 smolt year is estimated to have survival that is greater than the 2019 smolt year, and similar to the average of the previous ten years, again with moderate uncertainty. The top

five single-indicator model estimates ranged from below the 10-year average to slightly above the 10-year average.

For Upper Columbia spring Chinook smolts that went to sea in 2020 (Figure J.1, lower left), estimated survivals is similar to the average of the past ten years, and greater than what was modeled or observed for the 2019 cohort. Uncertainty in the estimates (95% prediction intervals, Figure J.1) is high relative to the time series confidence intervals. Similarly, Upper Columbia summer/fall Chinook smolts from 2020 are estimated to have greater survival than the 2019 cohort, and average survival compared to the past ten years, with relatively high uncertainty (Figure J.1, lower right).

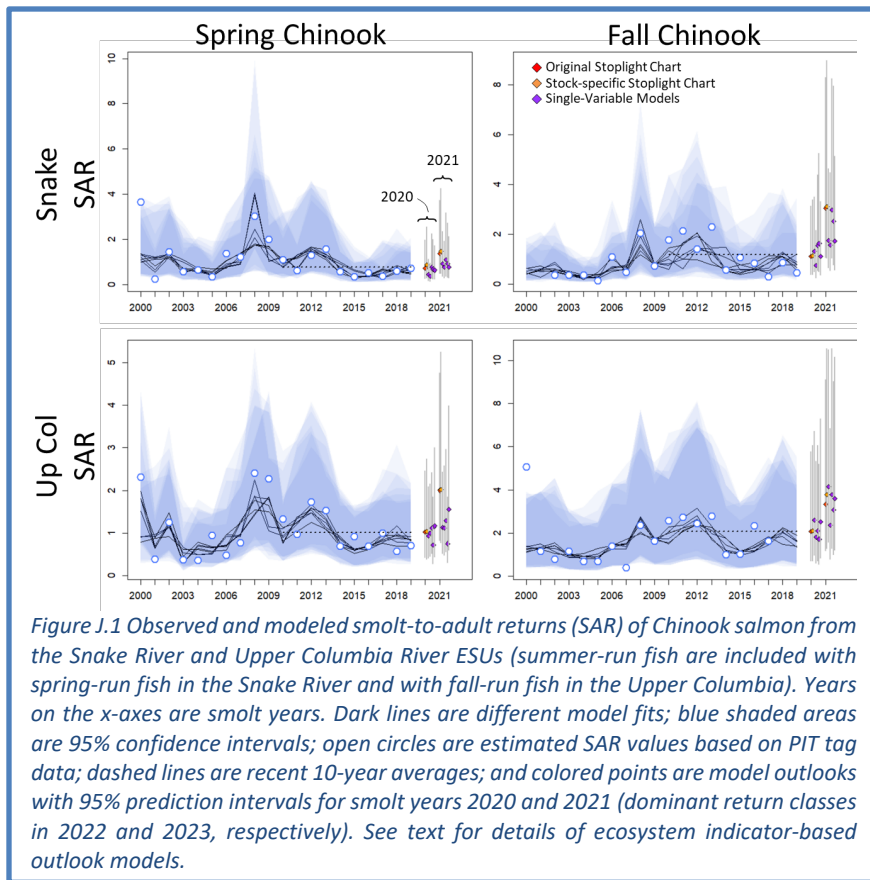


Figure J.1 Observed and modeled smolt-to-adult returns (SAR) of Chinook salmon from the Snake River and Upper Columbia River ESUs (summer-run fish are included with spring-run fish in the Snake River and with fall-run fish in the Upper Columbia). Years on the x-axes are smolt years. Dark lines are different model fits; blue shaded areas are 95% confidence intervals; open circles are estimated SAR values based on PIT tag data; dashed lines are recent 10-year averages; and colored points are model outlooks with 95% prediction intervals for smolt years 2020 and 2021 (dominant return classes in 2022 and 2023, respectively). See text for details of ecosystem indicator-based outlook models.

For all four ESUs, survivals of the 2021 smolt cohorts, which will dominate returns in 2023, are estimated to be above the 10-year average by the multi-indicator models and by most of the best single-indicator models, albeit with very high uncertainty. These increases in survival reflect the highly favorable ocean indicators observed in waters off of Washington and Oregon in late 2020 and the first half of 2021 (main report, Section 3.3, Table 3.3.1).

Although Table 3.3.1 represents a general description of ocean conditions related to multiple populations, we acknowledge that the importance of any particular indicator will vary among salmon species and runs. These new analyses represent progress toward greater distinction among different ESUs than some results shared in previous ecosystem status reports. NOAA scientists and partners are working toward stock-specific salmon projections by using both correlative and mechanistic methods that can optimally weight the indicators for each response variable in which we are interested. We will continue to work with the Council and advisory bodies to identify data sets for Council-relevant Pacific Northwest stocks for which analyses like these could be possible.

J.2 ECOSYSTEM CONDITIONS FOR FALL CHINOOK SALMON IN CALIFORNIA

Central Valley Fall Chinook salmon stoplight table: In our 2019-2020 ecosystem status report, we introduced a relatively simple “stoplight” table of ecosystem indicators that were shown by Friedman et al. (2019) to be correlated with returns of naturally produced Central Valley Fall Chinook salmon. An updated stoplight chart for adult Fall Chinook salmon returning to the Central Valley in 2022 is in Table 3.3.2. The focal ecosystem indicators are: spawning escapement of parent generations; egg incubation temperature between October and December at Red Bluff Diversion Dam (Sacramento

River); median flow in the Sacramento River in the February after fry emergence; and a marine predation index based on the abundance of common murrelets at Southeast Farallon Island and the proportion of juvenile salmon in their diets. Reflecting discussions with the SSC-ES in September 2020, we emphasize that the stoplight chart in Table 3.3.2 is strictly qualitative and contextual decision-support information. Qualitative descriptors (color-coded terms like “very poor” in Table 3.3.2) are based on recent time series and on expert opinion of how a given indicator relates to quantitative analysis of the relationship between the indicator and life-stage specific survival (Figure 5 in Friedman et al. 2019). The escapement descriptor is a qualitative evaluation of how escapement of a parent generation relates to the natural area + hatchery escapement goal of 122,000–180,000 fish, with 122,000 spawners as the MSY target (PFMC 2016). For example, in Table 3.3.2, February flows rated “very low” were near the low end of the range of observed values from 1982–2016, and are consistent with ~25% outmigrant survival, while the flows rated “high” were consistent with >50% outmigrant survival (see Friedman et al. 2019, Figure 5). Egg incubation temperatures in Table 3.3.2 were consistent with egg-to-fry survival ranging from ~50% (which we rated as “suboptimal”) to ~33% (“poor”). We have not been able to fully address the SSC-ES comments yet, and will work to refine these qualitative categories for future reports so that their basis is more explicit.

The qualitative nature of this stoplight table is in part due to the fact that some of the parameters used by Friedman et al. (2019) were estimated using information from both natural-origin and hatchery-origin fish, and while it is reasonable to assume that true parameter values would be similar, given correlations between natural and hatchery escapements, additional data specific to natural-origin fish are likely necessary in order to improve model fits, evaluate other potential covariates, and support adequate testing of model predictive skill.

Stoplight tables for Sacramento River and Klamath River Fall Chinook salmon: Rebuilding plans for four stocks of Pacific salmon in 2019 prompted evaluations of potential non-fishing related issues including environmental conditions and habitat changes that may have influenced poor stock performance. Many potential habitat issues were highlighted for Sacramento River and Klamath River fall Chinook salmon runs in rebuilding plans, and the Council’s Habitat Committee advocated an indicators-based approach to address this challenge. The goals for this new summary were to 1) illustrate multiple habitat factors in years that triggered the rebuilding plan, 2) document how habitat impacts will remain in years after rebuilding plan, 3) identify potential cumulative effects of multiple habitat stressors, and 4) identify potential avenues for Council engagement related to management actions that influence indicators.

After review by multiple scientists and members of various advisory bodies, members of the HC developed a suite of 22 indicators for Sacramento River fall Chinook salmon and 18 indicators for Klamath River fall Chinook salmon, spanning the full life history of natural-area fish and also including indicators related to hatchery-origin fish (Table J.2.1). Updates in 2021 include changes in some indicators to ensure more reliable and timely data updates, fixing a past error in directionality of one marine indicator, and new data for brood year 2020. The update also includes a new marine indicator for the Klamath River fall run, based on estimation of krill biomass along the Trinidad Head hydrographic line (see Section 3.1 of the main report). Both historical and recent indicator values changed slightly as a result of these updates.

Many of the indicators are already included in this ecosystem status report. The indicators have been shown in previous studies or were proposed in rebuilding plans to be strongly related with life-stage specific Chinook salmon productivity, and these studies helped determine expected directionality of indicators with stock productivity (Table J.2.1; see further explanations below). Four of the five broad categories of indicators in the new stoplight charts align with the simpler stoplight chart for Central Valley fall Chinook salmon presented in the main body of this report (Table 3.3.2): Adult Spawners, Incubation conditions, Freshwater/Estuarine Residence conditions, and Marine Residence

Table J.2.1 Habitat indicators, definitions, and key references for expanded stoplight charts for fall Chinook salmon. Months is the months for which indicators were summarized, Effect is the predicted direction of the indicator's effect on productivity, and Stock indicates whether indicators were summarized for the Sacramento (S) or Klamath (K) runs.

Life stage-specific indicator	Abbreviation	Months	Effect	Reference	Stock
Adult spawners					
Fall run spawners	Spawners		+	Friedman et al. 2019	S, K
Fall closures of Delta Cross Channel	CChannel.F	Sep-Oct	+	Rebuilding plan	S
Fall low flows	Flows.F	Sep-Oct	+	Strange et al. 2012	S, K
Fall temperatures in mainstem	Temp.F	Sep-Oct	-	Fitzgerald et al. 2021	S, K
Incubation and emergence					
Fall-winter low flows in tributaries	Flows.W	Oct-Dec	+	Jager et al. 1997	S, K
Egg-fry temperatures	Temp.W	Oct-Dec	-	Friedman et al. 2019	S, K
Egg-fry productivity	FW.surv		+	Hall et al. 2018	S, K
Freshwater/delta residence					
Winter-spring flows	Flows.S	Dec-May	+	Friedman et al. 2019	S, K
Delta outflow index	Delta	Apr-Jul	+	Reis et al. 2019	S
7-day flow variation (SD)	SDFlow.S	Dec-May	-	Munsch et al. 2020	S, K
Maximum flushing flows	Max.flow	Nov-Mar	+	Jordan 2012	K
Total annual precipitation	Precip	Annual	+	Munsch et al. 2019	S, K
Spring temperatures	Temp.S	May-Jun	-	Munsch et al. 2019	S, K
Spring closures of Delta Cross Channel	CChannel.S	Feb-Jul	+	Perry et al. 2013	S
Days Yolo Bypass was accessible	Yolo	Dec-May	+	Limm & Marchetti 2009	S
Hatchery releases					
Release number	Releases		+	Sturrock et al. 2019	S, K
Prop net pen releases	Net.pen		+	Sturrock et al. 2019	S
Release timing rel. to peak spring flow	FW.Timing	Jan-Aug	+	Sykes et al. 2009	S, K
Release timing rel. to spring transition	Mar.Timing	Jan-Aug	+	Satterthwaite et al. 2014	S, K
Marine residence					
Coastal sea surface temperature	SSTarc	Mar-May	-	Wells et al. 2008	S, K
North Pacific Index	NPI	Mar-May	+	Wells et al. 2008	S, K
North Pacific Gyre Oscillation	NPGO	Mar-May	+	Wells et al. 2008	S, K
Marine predation index	Predation		-	Friedman et al. 2019	S
Krill biomass	Prey	Mar-Aug	+	Robertson & Bjorkstedt 2020	K

conditions (for the first year of marine residence). The fifth category of indicators, Hatchery Releases, expands the scope of these tables relative to the simple stoplight chart (Table 3.3.2) that focuses only on natural area fish. These stoplight charts also share qualities with the stoplight chart developed for Columbia Basin Chinook salmon and Oregon coast coho salmon (Table 3.3.1) by including regional and basin-scale oceanographic indicators, as part of the Marine Residence conditions.

After indicator datasets were collected, all indicators were “directionalized” to account for inverse relationships with stock productivity (based on the “Effect” column in Table J.2.1) and converted into standardized values. These are reported in the stoplight charts below, where red (the bottom 33% of scores) represents poor conditions, yellow represents average conditions, and green (the top 33% of scores) represents beneficial conditions. The Sacramento River fall Chinook stoplight chart is shown in Table J.2.2 and the Klamath River fall Chinook stoplight chart is in Table J.2.3; both cover brood years 1983-2020. Descriptions and interpretations of the general categories of indicators are provided below.

Adults returning and migrating to spawning grounds. Spawning adults set the cohort size (Friedman et al. 2019) and potential for density-dependent habitat limitations at future life stages (Munsch et al. 2020), so we incorporated estimated escapements from PFMC pre-season forecasts. Adults must navigate multiple potential barriers to reach spawning grounds, including low river

flows and high temperatures at the end of summer. We used flow and temperature measurements from the lower portions of the Sacramento and Klamath Rivers in September and October. In the Sacramento River, adults must also navigate the channel network of the delta, and the rebuilding plan proposed examining potential effects of the Delta Cross Channel as a migration barrier. We used the proportion of time the Cross Channel was closed in September and October as the indicator.

In the Sacramento (Table J.2.2) and Klamath (Table J.2.3) stoplight tables, the four habitat indicators for spawners were mixed during the three brood years defined by the rebuilding plan. In years since, these indicators have generally worsened for both stocks. Habitat conditions for the 2021 outmigration year (brood year 2020) were mixed for Sacramento and generally poor for Klamath.

Incubation to emergence. After spawning, incubating eggs may be subject to dewatering in the river (Jager et al. 1997) and are sensitive to high temperatures (Friedman et al. 2019). For the Sacramento, the river flow indicator was derived from the seven-day 10th percentile of flow for the Sacramento River from October to December at Bend Bridge near Red Bluff. Because of previous observations of dewatering in portions of the Klamath, minimum flows from four gages (Klamath at Iron Gate, Scott River, Shasta River, and Trinity River at Lewiston Dam) were used, and the index was calculated from the average of standardized flow values. Incubation temperature records were obtained for both river systems, albeit for a much shorter time series in the Klamath. Sacramento incubation temperature estimates are from Red Bluff Diversion Dam (data in Friedman et al. 2019), while

Table J.2.2 Stoplight table of habitat indicators for Sacramento River fall Chinook salmon. Values are standardized values for the given indicator time series. Green cells represent values ranked in the upper third of all years ("good"), yellow cells rank in the middle third ("average"), and red cells rank in the bottom third ("poor") for a given indicator. The rebuilding plan period (brood years 2012-2014) is outlined. Table developed and provided by C. Greene (NMFS/NWFSC) and S. Munsch (NMFS/NWFSC, Ocean Associates Inc.).

Brood year	Freshwater conditions														Marine conditions							
	Adult spawners				Incubation			Freshwater/delta residence							Hatchery releases			Marine residence				
	Spawners	CChannel.F	Flows.F	Temp.F	Flows.W	Temp.W	FW.surv	Flows.S	Delta	SDFlow.S	Precip	Temp.S	CChannel.S	Yolo	Releases	Net.pen	FW.timing	Mar.timing	SSTarc	NPI	NPGO	Predation
1983	-0.53	-0.50	2.96	0.82	1.92	1.86	NA	0.59	-0.46	0.93	2.09	0.11	0.13	0.63	-1.63	-0.62	0.62	-0.21	-0.53	-1.06	0.95	0.05
1984	-0.19	-0.50	3.44	-0.32	2.31	1.39	NA	-0.56	-0.81	-0.91	0.28	-0.84	-0.66	-0.73	0.46	-0.85	0.60	1.66	0.19	1.67	0.24	2.73
1985	0.52	-0.10	0.74	NA	0.88	1.14	NA	0.51	1.21	1.57	-0.68	0.37	-0.24	0.60	0.28	-0.19	1.04	0.83	-0.59	-0.10	-0.65	0.34
1986	0.57	1.07	-0.53	0.15	-0.76	0.67	NA	-0.69	-0.71	-1.05	0.93	-0.47	-0.86	-0.73	-0.17	-1.09	0.55	0.83	-0.26	-0.87	0.34	2.73
1987	0.29	0.22	0.33	0.15	0.49	0.85	NA	-0.62	-0.85	-0.81	-1.26	0.16	-2.14	-0.73	-0.43	-1.02	-0.10	0.79	-0.15	-0.51	1.44	0.33
1988	0.46	-0.50	-0.86	1.58	-1.40	0.78	NA	-0.64	-0.48	-0.62	-0.77	0.06	-1.89	-0.53	-2.30	NA	1.14	0.76	-0.34	1.02	0.76	2.73
1989	-0.11	-0.50	-0.64	-1.75	-0.93	0.80	NA	-1.00	-0.88	-1.38	-0.09	0.11	-2.50	-0.73	-0.25	0.14	-1.40	0.79	-0.23	-0.25	0.26	-0.46
1990	-0.65	-0.50	0.79	1.58	-1.03	0.54	NA	-1.02	-0.73	-1.02	-0.85	1.48	-2.08	-0.73	0.31	-0.17	-0.31	0.43	-0.09	0.32	-0.36	-0.28
1991	-0.52	-0.50	-1.07	-0.32	-1.33	0.07	NA	-0.80	-0.82	-0.37	-0.89	-0.84	-0.87	-0.73	0.84	-1.32	-0.34	0.09	-0.71	-0.28	-1.35	0.33
1992	-1.07	-0.50	-1.04	-1.27	-0.96	0.36	NA	0.60	0.25	0.99	-0.82	1.32	0.11	0.41	-1.67	-1.29	0.34	-0.55	-0.60	-2.28	-1.20	0.20
1993	-0.27	-0.25	-1.47	-1.75	-1.74	0.60	NA	-0.96	-0.79	-1.33	0.97	-0.05	-0.07	-0.73	0.85	-1.10	1.27	0.93	-0.47	-0.31	-1.20	0.10
1994	-0.04	-0.50	0.20	-0.80	0.04	0.92	NA	1.76	2.74	1.45	-1.02	1.80	0.27	2.32	-0.40	-1.11	1.04	0.43	-0.41	-0.37	-1.79	-0.44
1995	0.76	-0.22	-0.76	-0.32	-1.11	0.24	NA	0.61	0.68	0.41	2.03	-0.10	0.55	1.04	0.36	-1.15	-3.55	-3.73	-0.86	-1.01	-0.95	-0.71
1996	0.83	-0.50	0.25	0.15	-0.14	0.30	NA	0.67	-0.46	1.35	0.62	-0.21	0.54	1.15	-1.45	-1.24	1.12	0.86	-0.75	-0.45	-0.67	-0.22
1997	0.89	0.35	0.47	2.05	0.32	0.53	NA	2.06	1.48	1.21	0.63	2.16	0.75	1.73	1.06	-0.62	0.21	0.83	-0.27	-0.49	0.56	-0.42
1998	0.29	4.75	0.28	0.15	-0.43	0.82	NA	0.90	0.19	0.48	1.92	1.32	0.68	0.70	-1.09	-1.21	0.08	-0.68	0.70	0.64	1.74	0.30
1999	1.20	-0.50	1.14	1.10	1.33	0.93	NA	0.56	0.29	0.90	-0.10	-0.05	0.03	0.34	-1.36	-1.22	0.00	-0.55	0.06	0.83	2.25	-0.16
2000	1.24	1.61	0.57	0.15	0.73	0.74	NA	-0.70	-0.60	-0.63	0.09	-0.31	-0.15	-0.73	-0.18	-0.04	-0.18	-0.11	0.28	0.30	2.18	0.02
2001	1.72	-0.12	0.09	0.63	0.53	0.66	NA	-0.22	-0.63	-0.06	-0.96	-0.36	0.60	-0.56	-1.15	-0.75	-0.23	-0.61	0.25	1.09	1.30	-0.15
2002	2.02	-0.21	-0.60	-0.80	0.26	-0.71	NA	0.95	-0.27	0.77	-0.36	0.32	0.57	-0.27	1.18	0.54	-1.06	-0.61	-0.33	-0.15	1.17	-0.33
2003	1.38	-0.50	-0.34	0.63	0.22	-0.56	0.60	0.66	-0.16	0.97	0.34	-0.42	0.69	0.11	0.22	0.18	-0.10	-1.05	-0.58	-0.16	0.24	-0.64
2004	0.50	-0.50	0.04	2.29	0.42	-0.98	-0.20	0.12	0.12	0.17	-0.23	0.90	0.64	-0.60	0.95	0.86	-1.45	-0.68	-0.69	-1.41	-1.32	-1.31
2005	0.55	-0.50	0.17	0.63	-0.49	-0.91	-0.18	2.23	2.58	1.12	0.40	-0.73	0.71	2.48	1.42	0.72	-0.73	-1.32	0.00	1.00	-0.47	-1.26
2006	0.43	-0.49	0.39	0.15	0.78	-0.28	-0.46	-0.78	-0.71	-1.10	1.33	-0.36	0.38	-0.73	1.32	0.96	0.03	-0.31	0.13	-0.67	0.13	-0.96
2007	-0.87	-0.50	0.17	-0.04	0.54	-0.93	0.11	-0.67	-0.75	-0.60	-1.00	0.06	0.39	-0.73	1.42	1.16	0.31	1.26	0.44	0.76	1.50	-0.83
2008	-1.37	-0.50	-0.34	-0.51	0.44	-1.30	-0.25	-0.79	-0.58	-0.46	-0.85	-0.26	0.33	-0.73	0.81	0.94	0.55	0.63	0.41	1.49	0.43	-0.62
2009	-2.19	-0.11	-0.93	-0.51	-1.27	-0.81	1.21	-0.28	-0.44	-0.07	-0.56	1.69	0.43	-0.60	0.90	0.81	0.75	-0.31	0.03	0.14	1.57	-0.55
2010	-0.54	-0.31	-0.64	-0.42	-1.00	-0.39	1.29	0.60	-1.24	0.74	0.03	2.06	0.75	0.50	1.24	0.87	0.23	0.16	0.07	-0.44	1.06	-0.68
2011	-0.74	0.48	0.09	-0.04	0.27	0.05	-0.12	-0.82	-0.46	-1.09	0.79	0.37	0.68	-0.73	1.26	0.49	0.31	-0.78	0.23	0.78	1.56	-0.43
2012	0.22	-0.50	0.57	NA	2.11	-0.36	0.16	-0.50	-0.73	-0.24	-0.73	-1.05	0.67	-0.37	0.25	0.09	-2.85	-0.88	-0.03	0.83	0.66	-0.04
2013	1.00	0.80	-0.20	-0.42	0.69	-0.43	0.29	-1.18	-0.80	-1.23	-0.45	-1.31	0.50	-0.73	0.25	1.48	0.55	-0.21	-0.93	-0.72	-0.28	0.41
2014	0.24	-0.31	-0.85	-1.37	-1.25	-2.43	-1.11	-0.74	-0.86	0.00	-1.19	-1.00	0.54	-0.69	-0.35	0.65	0.49	1.13	-1.40	0.50	-1.16	0.77
2015	-0.80	-0.41	-1.18	-0.61	-0.34	-1.03	0.41	-0.12	-0.10	0.61	-0.66	-0.84	0.47	-0.31	0.69	0.36	0.21	0.09	-1.18	-1.04	-0.20	-0.55
2016	-1.15	0.50	-1.37	-1.56	-0.84	-0.13	2.79	2.22	1.83	1.49	0.18	-0.79	0.75	2.74	-1.18	-0.04	0.60	-1.05	-0.77	-0.85	-0.49	NA
2017	-2.61	2.01	0.21	-0.51	0.25	-0.13	-0.43	-0.97	-0.25	-1.06	1.92	-0.89	0.68	-0.60	-0.41	1.07	-0.13	-0.34	-0.73	0.83	-2.01	NA
2018	-0.85	-0.50	0.23	0.25	0.61	-0.05	-0.22	1.19	1.44	1.56	-0.60	-0.26	0.75	0.67	-1.02	0.86	0.70	-0.41	-0.80	-1.01	-2.09	NA
2019	-0.17	-0.21	-0.36	-0.51	-0.62	0.31	-1.35	-0.93	1.07	-1.56	1.09	-0.79	0.65	-0.73	0.44	1.59	-0.34	1.73	-0.53	0.99	-1.57	NA
2020	-0.42	0.48	0.05	1.39	0.49	-3.13	-1.34	-1.26	-0.77	-1.14	-1.59	-2.37	-2.76	-0.73	0.24	2.24	0.06	0.17	-0.17	2.91	-1.14	NA

Klamath records are from Seiad Valley. Egg-fry productivity as measured by migrants per spawner were initiated in brood years 2003 and 2001 in the Sacramento and Klamath, respectively.

In both the Sacramento (Table J.2.2) and Klamath (Table J.2.3), the three incubation habitat indicators generally declined over the three brood years defined by the rebuilding plan. In years since, incubation habitat indicators have generally degraded in the Sacramento but improved in the Klamath. Incubation conditions were mixed for brood year 2020 (the 2021 outmigration year) for both stocks, although this was the worst year on record for at least one indicator in both stocks.

Freshwater and estuary residence. During migration to the ocean, fall Chinook salmon stocks take advantage of temporary residence in riverine and estuary habitats before transitioning to marine environments. We used a variety of indicators of habitat conditions during this stage. Freshwater conditions are set by precipitation and spring air temperatures, both of which influence snowpack

Table J.2.3 Stoplight table of habitat indicators for Klamath River fall Chinook salmon. Values are standardized values for the given indicator time series. Green cells represent values ranked in the upper third of all years ("good"), yellow cells rank in the middle third ("average"), and red cells rank in the bottom third ("poor") for a given indicator. The rebuilding plan period (brood years 2012-2014) is outlined. Table developed by C. Greene (NMFS/NWFSC) and S. Munsch (NMFS/NWFSC, Ocean Associates Inc.), with help from Justin Alvarez (Hoopa Tribe) for supplying several freshwater indicators.

Brood year	Freshwater conditions													Marine conditions				
	Adult spawners			Incubation			Freshwater residence					Hatchery releases			Marine residence			
	Spawners	Flows.F	Temp.F	Flows.W	Temp.W	FW.surv	Flows.S	SDFlow.S	Precip	Temp.S	Max.flows	Releases	FW.timing	Mar.timing	SSTarc	NPI	NPGO	Krill
1983	-0.63	1.25	NA	2.87	NA	NA	1.6	1.05	0.34	0.44	1.14	-0.14	2.17	1.03	-0.53	-1.06	0.95	NA
1984	-0.92	1.97	NA	1.89	NA	NA	0.1	-0.05	-0.07	-0.35	0.98	-0.96	0.51	1.80	0.19	1.67	0.24	NA
1985	-0.46	1.21	NA	-0.38	NA	NA	0.9	2.44	-0.87	-0.60	0.05	2.64	1.53	0.82	-0.59	-0.10	-0.65	NA
1986	1.18	1.14	NA	0.23	NA	NA	-0.5	-0.56	-1.16	0.06	1.75	2.27	1.56	1.40	-0.26	-0.87	0.34	NA
1987	1.29	1.15	NA	0.52	NA	NA	-0.7	-0.54	-0.34	0.91	-0.54	-0.38	-1.06	0.76	-0.15	-0.51	1.44	NA
1988	1.16	-0.23	NA	-0.07	NA	NA	0.3	0.27	0.53	2.24	-0.65	2.34	0.51	-0.46	-0.34	1.02	0.76	NA
1989	0.51	1.20	NA	-0.60	NA	NA	-0.7	-0.59	-0.38	0.69	0.97	0.31	-0.71	1.34	-0.23	-0.25	0.26	NA
1990	-1.33	-0.23	NA	0.40	NA	NA	-1.1	-0.98	-0.28	1.36	-0.54	-0.50	1.26	1.16	-0.09	0.32	-0.36	NA
1991	-1.47	-1.65	NA	-0.67	NA	NA	-1.1	-0.95	-1.28	-1.79	-0.76	-0.21	0.89	2.04	-0.71	-0.28	-1.35	NA
1992	-1.77	-3.14	NA	-0.96	NA	NA	0.8	0.48	0.71	0.76	-1.10	-0.24	1.35	0.00	-0.60	-2.28	-1.20	NA
1993	-0.64	1.25	NA	-0.44	NA	NA	-1.1	-1.14	-1.46	-0.19	1.21	-0.72	0.51	-0.30	-0.47	-0.31	-1.20	NA
1994	-0.47	-0.85	NA	-0.35	NA	NA	1.7	2.10	1.22	0.91	-0.90	0.23	1.06	0.09	-0.41	-0.37	-1.79	NA
1995	1.38	1.25	NA	-0.55	NA	NA	-1.7	-1.74	1.61	0.24	0.73	0.25	-0.19	-0.46	-0.86	-1.01	-0.95	NA
1996	1.03	0.52	NA	0.41	NA	NA	NA	NA	2.08	-0.37	1.50	0.40	-0.22	0.61	-0.75	-0.45	-0.67	NA
1997	-0.07	-0.21	NA	0.30	NA	NA	2.1	1.72	1.78	2.03	3.02	0.05	-0.31	-0.18	-0.27	-0.49	0.56	NA
1998	0.04	1.43	NA	0.51	NA	NA	1.4	0.73	0.85	0.14	0.72	-0.08	0.68	-0.36	0.70	0.64	1.74	NA
1999	-0.81	1.15	NA	0.82	NA	NA	0.2	0.08	0.18	-0.35	0.81	0.23	0.94	0.24	0.06	-0.83	2.25	NA
2000	1.35	0.06	NA	0.64	NA	NA	-1.2	-1.32	-1.57	-1.26	-0.13	0.22	-0.28	0.09	0.28	0.30	2.18	NA
2001	1.12	-0.26	NA	0.00	-1.20	-0.61	-0.1	-0.04	-0.20	-0.23	-1.00	0.23	-0.69	-0.21	0.25	1.09	1.30	NA
2002	0.90	-1.53	-1.00	-0.23	0.51	-1.43	0.4	0.40	0.57	-0.53	-0.60	0.35	0.27	-0.52	-0.33	-0.15	1.17	NA
2003	1.16	0.52	-0.64	-0.59	-2.34	-1.58	0.03	0.09	-0.49	-0.24	-0.34	0.24	0.33	-0.73	-0.58	-0.16	0.24	NA
2004	-0.16	-0.79	-2.27	-0.10	0.38	-0.78	-0.26	-0.43	0.25	1.20	-0.35	0.34	-1.68	-0.97	-0.69	-1.41	-1.32	NA
2005	-0.45	0.46	0.12	-0.19	0.34	1.39	1.89	1.99	2.34	-0.88	-0.87	0.65	-0.98	-0.88	0.00	1.00	-0.47	NA
2006	-0.54	-0.45	0.20	-0.36	0.33	-0.22	-0.27	-0.33	-0.61	-0.55	1.28	0.38	-0.05	-0.24	0.13	-0.67	0.13	NA
2007	0.60	-0.23	0.32	0.11	0.44	0.47	-0.19	-0.67	0.01	0.08	-0.38	0.34	-1.79	1.00	0.44	0.76	1.50	NA
2008	-0.33	-0.28	0.48	0.31	0.50	-0.64	-0.61	-0.59	-0.57	-0.29	-0.54	-0.13	0.16	0.21	0.41	1.49	0.43	1.29
2009	0.20	-0.41	3.09	-0.50	0.50	-0.01	-0.10	-0.52	-0.43	1.67	-0.90	0.02	-2.81	-1.43	0.03	0.14	1.57	-1.90
2010	0.05	-0.26	-0.08	-0.45	0.25	-0.13	0.72	-0.02	0.78	1.98	-0.91	-0.11	0.04	-0.64	0.07	-0.44	1.06	0.49
2011	0.22	-0.28	0.19	0.16	0.46	-1.39	-0.09	0.14	-0.60	0.34	-0.09	0.19	-0.22	-1.16	0.23	0.78	1.56	-1.29
2012	1.80	-0.32	-0.35	-0.14	0.08	0.43	-0.58	-0.47	-0.18	-0.27	-0.87	-0.14	-0.92	-1.12	-0.03	0.83	0.66	-0.21
2013	0.93	-0.38	-0.61	-0.35	0.76	0.38	-1.11	-0.72	-1.00	-0.85	-0.75	0.12	-0.13	-1.12	-0.93	-0.72	-0.28	0.55
2014	0.89	-0.38	0.67	-0.70	-0.17	-0.67	-0.67	-0.11	-0.13	-1.35	-0.88	-0.37	-0.48	0.43	-1.40	0.50	-1.16	0.45
2015	-0.18	-0.50	-0.28	-0.46	0.08	2.13	0.52	0.77	0.63	-0.50	-0.57	-0.26	0.25	-0.18	-1.18	-1.04	-0.20	-0.10
2016	-1.90	-0.52	-0.33	-0.45	0.31	NA	2.04	1.64	1.19	-0.94	0.93	-2.01	0.13	-1.12	-0.77	-0.85	-0.49	-0.33
2017	-1.45	-0.30	0.52	0.39	0.31	-0.09	-0.63	-0.67	-1.09	-1.03	1.05	0.00	-0.80	-1.28	-0.73	-0.83	-2.01	0.71
2018	0.05	-0.41	0.02	-0.09	0.25	0.86	0.23	0.40	0.13	-0.43	-0.83	-0.97	-0.86	-1.22	-0.80	-1.01	-2.09	-0.50
2019	-1.28	-0.45	0.15	-0.48	1.10	1.05	-1.07	-0.94	-1.34	-0.52	-0.75	-1.97	0.13	2.40	-0.53	0.99	-1.57	1.87
2020	-0.98	-0.50	-0.20	-0.31	-2.90	0.84	-1.02	-0.89	-1.14	-1.53	-0.90	-2.61	-0.10	-0.85	-0.17	2.91	-1.14	-0.95

and river flow (Munsch et al. 2019). In turn, flows from December to May (and their temporal variation) set conditions for rearing in river and estuary systems as fish move downstream, and have been linked to freshwater (Munsch et al. 2019) and life-cycle productivity (Michel 2019, Friedman et al. 2019). Higher flows also determine access to floodplain rearing in reaches such as the Yolo Bypass (Limm and Marchetti 2009), as well as the potential to flush polychaete hosts of the parasite *Ceratomyxis shasta* that infects juvenile salmon during outmigration (Jordan 2012). Flows also determine the outflow through the Sacramento delta (Reis et al. 2019), which can influence estuarine rearing opportunities (Munsch et al. 2020). To shift freshwater flows to pumping facilities, the Bureau of Reclamation opens the Delta Cross Channel, and this pathway can entrain salmon in pumps or otherwise expose them to higher mortality (Perry et al. 2013).

Over the three brood years defined by the rebuilding plan, habitat conditions during freshwater residence were generally poor for the Sacramento (Table J.2.2) but more mixed for the Klamath (Table J.2.3). In the years since, habitat conditions have been mixed but worsening, and brood year 2020 (smolts in 2021) experienced very poor stream residence conditions in both systems.

Magnitude and timing of hatchery releases. While much of the habitat indicators focus on natural-area fish, hatchery releases make up a significant contribution of each run and may also contribute to density dependence. We therefore included the annual total of hatchery releases (up to four hatcheries on the Sacramento but San Joaquin hatcheries were not included; two hatcheries in Klamath). While hatchery-origin juveniles are also sensitive to the conditions natural-origin juveniles face, they are generally raised until they are primed for rapid migration. Following concepts of match-mismatch theory (Cushing 1990), we compared release date with the date of peak spring flow in freshwater and the spring transition in the ocean, as Satterthwaite et al. (2014) showed that both timing of release relative to the spring transition and overall later release timing were positively correlated with survival rates. Fates of hatchery fish may be a consequence of release location (Sturrock et al. 2019), including locations external to the Sacramento River system, so we also included the proportion of releases that were seaward of Sherman Island in the lower delta.

Hatchery release indicators were mixed for both stocks in the three rebuilding plan years. Since then, indicators remain mixed for Sacramento fall Chinook, including brood year 2020 (outmigration year 2021) (Table J.2.2). In contrast, recent indicators of hatchery releases have been relatively poor for the Klamath system (Table J.2.3). Due to high river temperatures in spring 2021, most Sacramento River hatchery fish were released in estuarine or marine waters to reduce heat stress. This will provide an extreme comparison to determine whether this practice is beneficial for hatchery returns.

Marine residence. Marine residence of 1 to 5 years completes the life cycle for fall run Chinook salmon populations. While a broad number of marine habitat indicators have been examined (Wells et al. 2008), we focused on a limited subset of possible indicators representing initial set-up of ocean entry conditions (March-May), including sea surface temperature, the North Pacific Index, and North Pacific Gyre Oscillation. We also included an index of predation by common murre nesting at Southeast Farallon Island, which was a strong predictor in Friedman et al. (2019). Unfortunately, this indicator currently cannot be updated quantitatively, pending a data-sharing agreement. On the positive side, we now have the new krill prey indicator for Klamath River fall Chinook salmon.

Marine habitat indicators were generally average to below average for brood years in the rebuilding plan for both Sacramento (Table J.2.2) and Klamath (Table J.2.3) stocks. From brood years 2015-2018, these indicators generally worsened for both stocks. Marine habitat conditions for the two most recent outmigration years (brood years 2019-2020) have shown some signs of rebounds for both stocks.

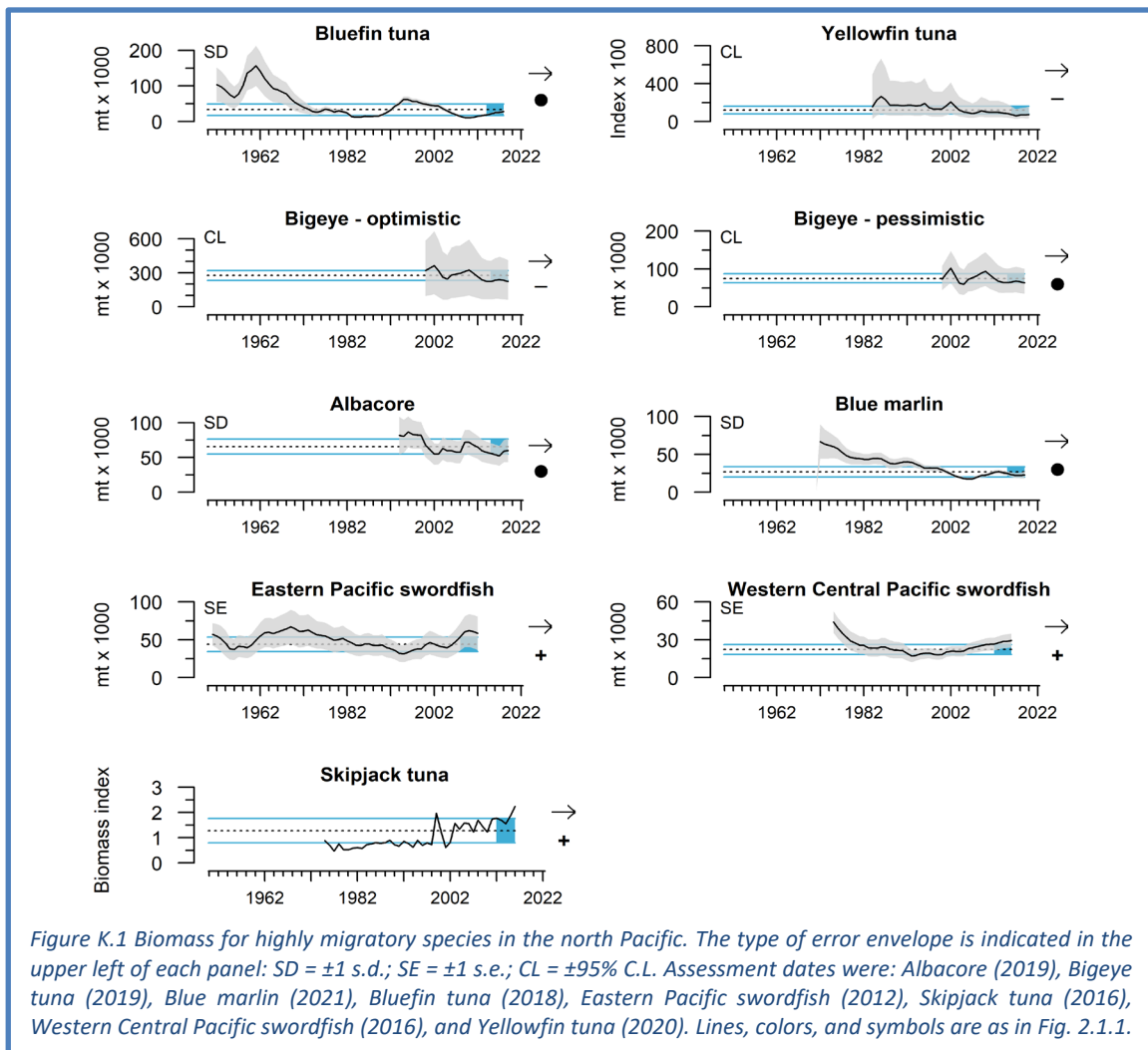
Management implications for the PFMC. The Council has a long history of engaging with other agencies to advocate for improved habitat conditions for the Sacramento and Klamath fall Chinook

salmon runs. While many possible management “dials” exist for improving habitat, few can easily be tracked annually. For both stocks, river flow is highly managed through reservoir operations, diversions and export pumping, and flows at particular stages can influence water temperature. Flow and water temperature indicators have shown evidence for long-term change as well as recent variability during brood years highlighted by the rebuilding plan and years thereafter. In particular, temperature conditions for the Sacramento River (during spawning and spring rearing) and flow conditions for the Klamath River (all types except maximum flushing flows) continue to remain at relatively low status, suggesting that improved flow management can support improvements for populations (Munsch et al 2020). The CCIEA team will work with the HC, the STT, and the SSC as necessary to continue to present and refine these indicators for these two important stocks.

Appendix K HIGHLY MIGRATORY SPECIES (HMS)

K.1 HMS STOCK ASSESSMENT INFORMATION

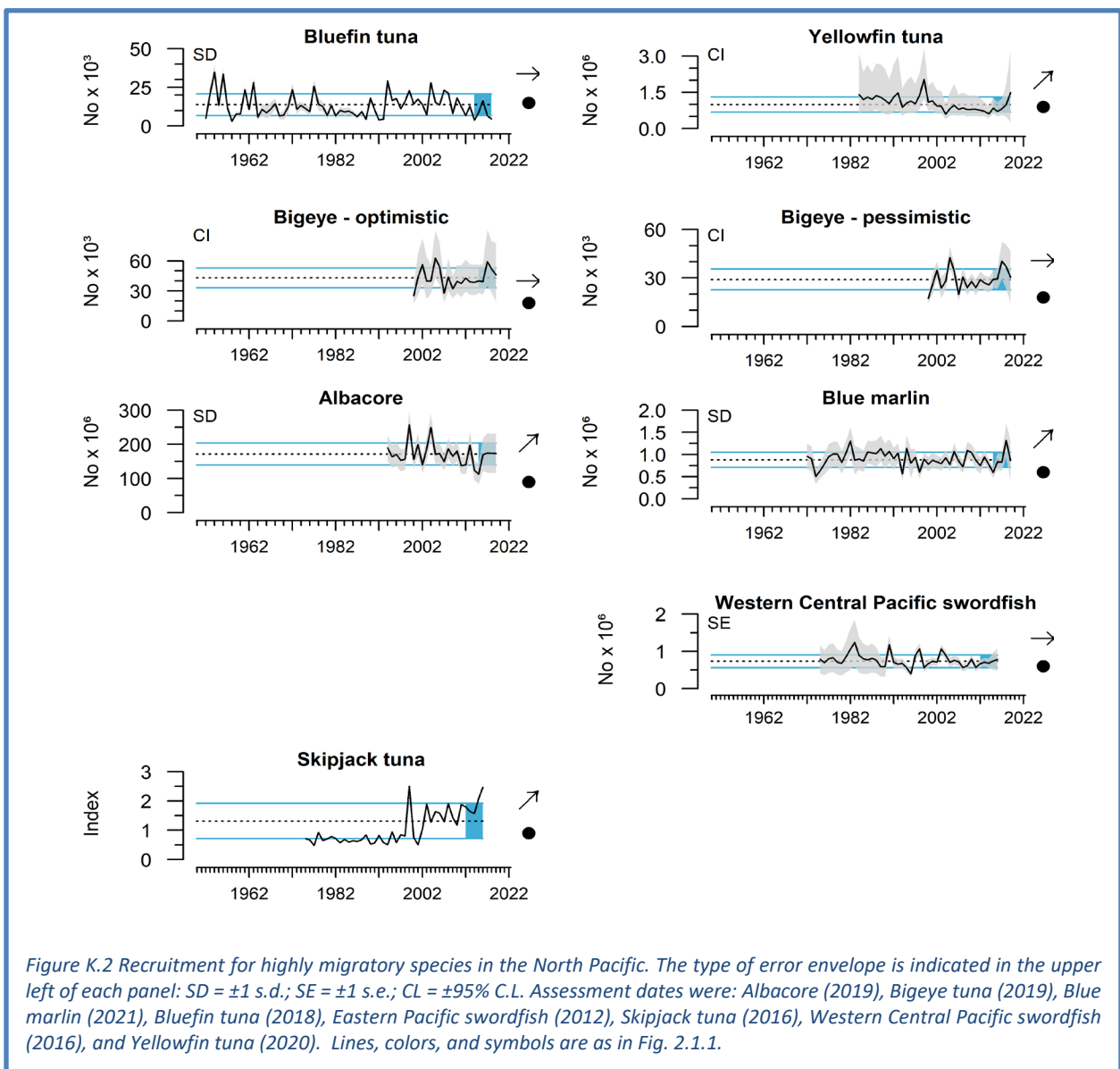
Highly migratory species are discussed in Section 3.5 of the main document. Time series for spawning stock biomass (Figure K.1) and recruitment (Figure K.2) are plotted here; the only benchmark assessment update since last year’s report is for blue marlin, with biomass and recruitment estimates now available through 2019. According to the most up-to-date assessments, biomass estimates range



from above the assessment time series average (skipjack, swordfish) to below average (yellowfin tuna, and bigeye tuna from the “pessimistic” assessment reference models) (Figure K.1). The updated blue marlin assessment (available at http://isc.fra.go.jp/reports/stock_assessments.html) indicates that biomass declined and then stabilized in the five most recent years analyzed, at levels roughly one-third those observed in the 1970s. The assessment indicated that blue marlin are likely not overfished, nor subject to overfishing.

HMS recruitment trends from the most recent assessments are generally trending positively, typically with high uncertainty (Figure K.2). This includes the updated blue marlin assessment.

We should emphasize that the status and trends symbols in Figures K.1 and K.2 reflect time series averages (with a period of reference of 1991-2020), and do not necessarily reflect reference points based on, e.g., unfished stock biomass; thus, for example, bluefin tuna are considered likely to be overfished (see our summary in last year’s report, Harvey et al. 2021a) even though it falls within 1 s.d. of the biomass time series average in Figure K.1.



K.2 HMS DIET INFORMATION

Quantifying the diets of highly migratory fishes in the CCE can complement existing assessments of the available forage, provide insight into how forage varies over time and space, as well as provide a direct metric of forage utilization. Albacore tuna and broadbill swordfish are both opportunistic predators that consume a wide variety of prey taxa across a range of depths and habitats. Albacore and swordfish stomachs were provided by commercial and recreational fishers, and prey were identified from whole or hard part remains and are reported as a mean percent abundance. A subset of prey species are described here, focusing on prey that are either themselves under a management plan, or considered key ecosystem components, to highlight their links to highly migratory species.

Juvenile albacore diets have been collected since 2009 off northern California, Oregon, and Washington in the summer and fall fishing season. Analysis of stomachs from 2021 is still ongoing, but data from the 15 already completed are described here and plotted in the main report (Figure 3.5.1) as preliminary insight into the most recent trends. The processed samples for 2021 represent 93% of the expected diversity at the family level based on rarefaction and extrapolation curves, so most of the expected diversity is already discovered (average among all years is 97%). The dominant prey from 2021 so far are northern anchovy, euphausiids, and Pacific saury. Anchovy consumption increased in 2020 and 2021 after a low in 2018-2019. Pelagic juvenile rockfish consumption demonstrated an opposing pattern, with consumption declining in 2020 and 2021 after a peak in 2019, coinciding with the anchovy low. Sardine consumption in 2020 and 2021 was well above the long term mean, though <10% of total stomach contents. The remaining CPS observed were of minimal importance across years. The most important contributors among prey items not targeted by fisheries were the squid *Onychoteuthis borealijaponica*, amphipods, and slender barracudina.

Swordfish (data not shown) have been collected off southern and central California during the commercial drift gillnet season (August 15th through January 31st), with data available from 2007-2014 and again from 2019-2020; analysis of samples from 2021 has been delayed due to COVID-19. Diets are classified by the year the fishing season began (stomachs collected in January are assigned to the previous year's fishing season). Swordfish that were studied fed mainly on fish and cephalopods. In 2019-2020, the dominant prey categories were anchovy, market squid, and slender blacksmelt, a mesopelagic species. Anchovy and market squid diet proportions were above the long term mean in 2019-2020, with anchovy well above the mean. Pacific hake fell near the mean in both years. Other CPS and juvenile rockfish were a minor part of swordfish diets across years. Across the whole time series, the most important other prey were various squids. Humboldt squid were the most important prey throughout the early portion of the time series, although their importance declined in 2010 during a peak in market squid consumption, and in both 2011 and 2014 as hake became more important. Fished species were less important in swordfish diets overall when compared with albacore. Future reports will include plots of swordfish diets, and we hope to include other HMS with different foraging ecology as well, as data become available.

Appendix L CALIFORNIA SEA LION PUP INDICATORS

California sea lion pup counts and pup growth rates are sensitive indicators of prey availability and composition in the Central and Southern CCE (Section 3.6). In September 2020, the SSC-ES requested: (1) more precise description of what these indicators represent about prey community dynamics and foraging conditions; (2) text explaining that California sea lion population size and carrying capacity are not affecting the value of these metrics as indicators of foraging conditions; and (3) a model-based estimate of total pups. We addressed the first two requests in the Supplement to the March 2021 ecosystem status report (Harvey et al. 2021a), and provide that information again below. Due to time constraints, we have not addressed the third request but will do so in the future.

Pup count and pup growth as indicators of foraging conditions: The San Miguel Island California sea lion indicators of pup births, pup condition, pup growth and nursing female diet are linked to the availability (a combination of abundance and distribution) and composition of the coastal pelagic forage community to nursing California sea lions foraging in the CCE from the northern California Channel Islands to Monterey Bay throughout the year. Nursing California sea lions are central place foragers for 11 months of the year, traveling to and from the breeding colonies in the Channel Islands, where their pups reside, to foraging areas within 200 km of the colonies. Consequently, they are sampling the coastal pelagic forage community throughout the year and their diet and resultant reproductive success measured by pup metrics depends on the availability of that forage community.

Nursing California sea lions consume a variety of fish and cephalopods but have a core diet of only seven taxa: Pacific hake, Pacific sardine, northern anchovy, rockfish, jack mackerel, Pacific mackerel, and market squid (Melin et al. 2008, Melin et al. 2012a). These taxa vary annually and seasonally in the diet. The nursing female diet index is based on the frequency of occurrence of these seven core taxa in scats collected at the San Miguel colony during the early lactation period (June-September). This index provides a relative measure of the availability of each prey taxa to nursing females within their foraging range because California sea lions consume prey relative to its abundance in the environment (Thompson et al. 2019a) but not necessarily proportionally. For example, an increase in the frequency of occurrence of anchovy from 5% in 1995 diets to 90% in 1996 diets means that almost no females consumed anchovy in 1995 because it was not available to them but almost all females consumed it in 1996; it does not necessarily mean that the biomass of anchovy increased nearly 20-fold in the CCE, just that the availability increased in the foraging range of nursing females. Nonetheless, it indicates that a change in the forage community occurred between the two years. A weakness of this index is that it only indicates presence or absence of a taxa in the diet; when sardine occurs in high frequency, it could be that sea lions are exploiting a small population of fish or it could be that sardine are ubiquitous in the environment. It also is a retrospective rather than forecasting index. It is thus important to view this as part of a suite of indicators about the prey community, along with ship-based catch or acoustic estimates of forage fish biomass. Strengths of the sea lion diet index are that it is easy to update annually and the core taxa comprise the core diet of many other top predators in the CCE that are difficult to sample or observe. Consequently, the annual variability and trends in the California sea lion diet can inform us on unusual patterns in the coastal pelagic forage community that may affect other top predators in the CCE.

Each of the pup indices in the report represents a different aspect of reproductive success that relies on successful foraging by reproductive females. As such, they are indirect qualitative measures of the forage available to reproductive females and do not provide specific forage community information. The annual number of pup births is an index of successful pregnancies, which are dependent on the nutritional condition of the female, which in turn, is dependent on the quality and quantity of prey available during the gestation period. Higher numbers of pup births indicates that females consumed a diet that provided sufficient quantity and nutrition to support the energetic cost of gestation. Pup condition and growth are dependent on milk intake. The more milk consumed the greater the better condition and growth rate. The amount of food consumed by a female on a foraging trip determines the amount of milk she has to deliver to the pup when she returns. Better pup condition and higher growth rates indicate abundant prey for nursing females during the lactation period.

Declines in pup births and pup growth have been associated with environmental events that reduced marine productivity at all trophic levels in the CCE for prolonged periods supporting the link between these indices and the status of the forage community (DeLong et al. 1991, Iverson et al. 1991, Melin et al. 2010, Melin et al. 2012b, DeLong et al. 2017). Other factors such as diseases (e.g., hookworm, Lyons et al. 2005), immune suppression from pollution (DeLong et al. 1973, Gilmartin et al. 1976) and natural environmental toxins (Goldstein et al. 2009) may affect pup growth or births, but these

factors are likely to have less of a population level effect than large-scale food supply issues that accompany anomalous oceanographic conditions.

The influence of population abundance and carrying capacity on these indicators: In discussions related to past reports, some Council advisory bodies expressed concerns that sea lion pup counts and growth may become less effective indicators when the population is close to carrying capacity, which it was in the 2010s: according to population modeling work by Laake et al. (2018), the San Miguel colony at that time had an estimated carrying capacity of ~275,000 animals (including pups), and annual population estimates between 2006 and 2014 ranged from 242,000 to 306,000 animals. Advisory bodies were concerned that changes in pup count or growth could be due to density dependent mechanisms within the sea lion population, rather than to changes in the prey community.

A linear mixed effects model of California sea lion pup growth that includes environmental variables, sea lion abundance, fish abundance and nursing female diet revealed that the abundance of California sea lions was not a significant factor in annual variability of pup growth rates (Melin et al. in preparation). The model also did not detect a declining trend in pup growth as the population size increased, which might occur if competition among nursing females for limited forage was affecting the ability of females to support the energetic demands of their pups. Elevated SST explained the greatest amount of variability for pup growth rates in the models: a 1°C increase in SST resulted in a 7% decline in the population growth rate, even when the population was much smaller (<100,000 animals) in the 1980s (Laake et al. 2018). The reverse effect was not apparent when SST decreased by 1°C. These analyses indicate that pup count and pup growth are not compromised as indicators by population size, but rather reflect the dynamic relationship between environmental conditions and California sea lion reproduction. We believe the key underlying mechanism is that elevated SST affects the distribution and abundance of the sea lion prey community thereby reducing access to food for nursing females, such that they cannot support the energetic demands of pregnancy, resulting in fewer births, or lactation, resulting in slower pup growth.

Appendix M **SEABIRD PRODUCTIVITY, DIET, AT-SEA DENSITY, AND MORTALITY**

M.1 **SEABIRD PRODUCTIVITY**

Seabird population productivity, as measured through indicators of reproductive success, tracks marine environmental conditions and often reflects forage production near breeding colonies. We monitor and report on standardized anomalies of fledgling production per pair of breeding adults for five focal species on Southeast Farallon Island in the Central CCE, and three species at Yaquina Head, Oregon in the Northern CCE. Collectively, the six focal species span a range of feeding habits and ways of provisioning their chicks, and thus a broad picture of the status of foraging conditions.

- Brandt's cormorants forage primarily on pelagic and benthic fishes in waters over the shelf, generally within 20 km of breeding colonies, returning to the colony during the day to deliver regurgitated fish to their chicks.
- Cassin's auklets forage primarily on zooplankton over the shelf break, generally within 30 km of colonies; they forage by day and night and return to the colony at night to feed chicks.
- Common murre forage primarily on pelagic fishes in deeper waters over the shelf and near the shelf break, generally within 80 km of colonies, returning to the colony during daylight hours to deliver single whole fish to their chicks.
- Pelagic cormorants forage primarily on pelagic and benthic fishes in waters over the shelf, generally within 20 km of breeding colonies, returning to the colony during the day to deliver regurgitated fish to their chicks.
- Pigeon guillemots forage primarily on small benthic and pelagic fishes over the shelf, generally within 10 km of colonies, returning to the colony during the day to deliver single fish to chicks.

- Rhinoceros auklets forage primarily on pelagic fishes in shallow waters over the continental shelf, generally within 50 km of colonies, returning to the colony after dusk to deliver multiple whole fish to their chicks.

Data and interpretation for fledgling production of the five species at Southeast Farallon Island are in the main body of the report in Section 3.7. Production was positive in 2021, with above-average production for Brandt’s cormorants, Cassin’s auklets, pigeon guillemots and rhinoceros auklets, and close-to-average production for common murres.

At Yaquina Head, fledgling production in 2021 was average to above average for the three monitored seabirds (Figure M.1.1). Brandt’s cormorant production was well above average, continuing an upward trend. Common murre chick production returned to the time series mean after near complete failure in 2020, high values in 2018-2019, and complete failure from 2015 to 2017. Pelagic cormorant chick production was above average, as it has been for four of the past five years. Bald eagles can be major drivers of seabird reproductive failures at Yaquina Head. While they contributed substantially to common murre reproductive failure in 2020, bald eagle disturbance and nest depredation rates were average in 2021.

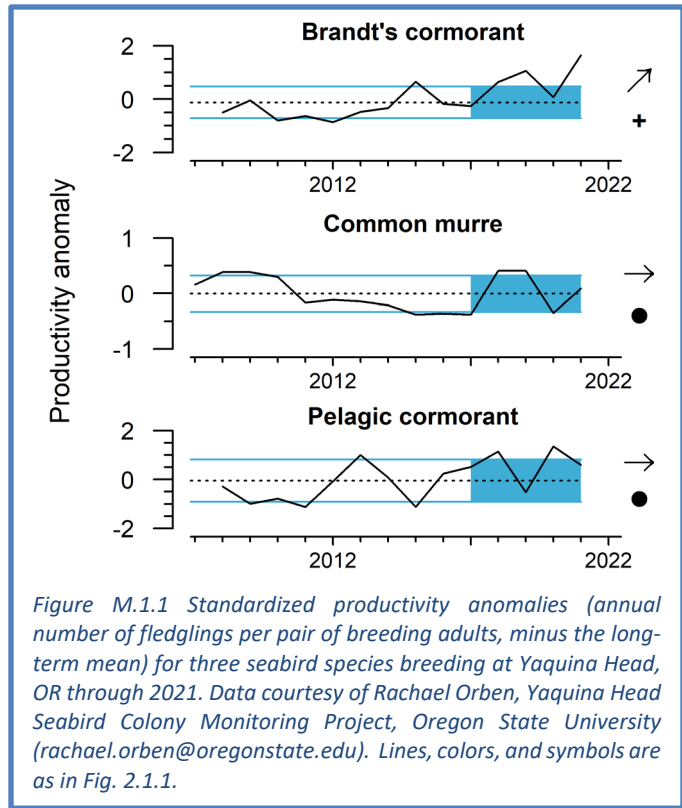


Figure M.1.1 Standardized productivity anomalies (annual number of fledglings per pair of breeding adults, minus the long-term mean) for three seabird species breeding at Yaquina Head, OR through 2021. Data courtesy of Rachael Orben, Yaquina Head Seabird Colony Monitoring Project, Oregon State University (rachael.orben@oregonstate.edu). Lines, colors, and symbols are as in Fig. 2.1.1.

M.2 SEABIRD DIETS

Seabird diet composition during the breeding season tracks marine environmental conditions and often reflects production and availability of forage within regions. Here, we present seabird diet data from the northern and central regions of the CCE that may shed light on foraging conditions in 2021.

In the Northern CCE, rhinoceros auklet chick diet data were collected in 2021 at Destruction Island, WA, following a sampling hiatus in 2020 due to COVID-19. The proportion of Pacific sandlance in the chick diet was the highest it has been since sampling started in 2008 and has been a prominent feature in the diet since 2016

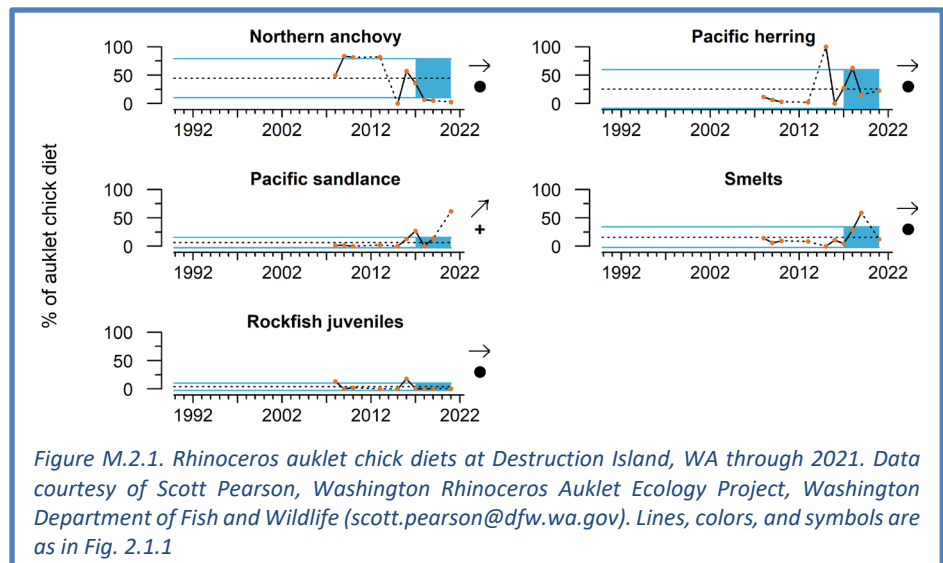


Figure M.2.1. Rhinoceros auklet chick diets at Destruction Island, WA through 2021. Data courtesy of Scott Pearson, Washington Rhinoceros Auklet Ecology Project, Washington Department of Fish and Wildlife (scott.pearson@dfw.wa.gov). Lines, colors, and symbols are as in Fig. 2.1.1

(Figure M.2.1). Proportions of anchovy and rockfish in the rhinoceros auklet chick diet were both near zero in 2021 and have been trending down since 2016, while the proportions of Pacific herring and smelts in the chick diet were average in 2021. This is consistent with forage and CPS surveys that show the bulk of the current anchovy population to be in the Central and Southern CCE (Section 3.2; Appendix H; Stierhoff et al. 2020). Pacific herring and smelts have been important prey items at Destruction Island in recent years, although with considerable year-to-year variability.

Also in the Northern CCE, diet observations of common murres provisioning chicks were collected at Yaquina Head. The proportion of smelts in the chick diet was average in 2021, and has trended

downward since 2017 (Figure M.2.2). The proportion of herring and sardines and Pacific sand lance were both rare. Other species, which are normally rare in murre chick diets at Yaquina Head, made up nearly 25% of the diets in 2021. This, included 15% Pacific salmon, which have trended upward in murre diets here in recent years.

In central California, long-term diet data are available for seabirds at breeding colonies on Southeast Farallon Island. These colonies are close to the most intense upwelling region in the CCE and thus a valuable source of information about system productivity and prey availability to higher trophic levels. Piscivorous birds have grown more reliant on

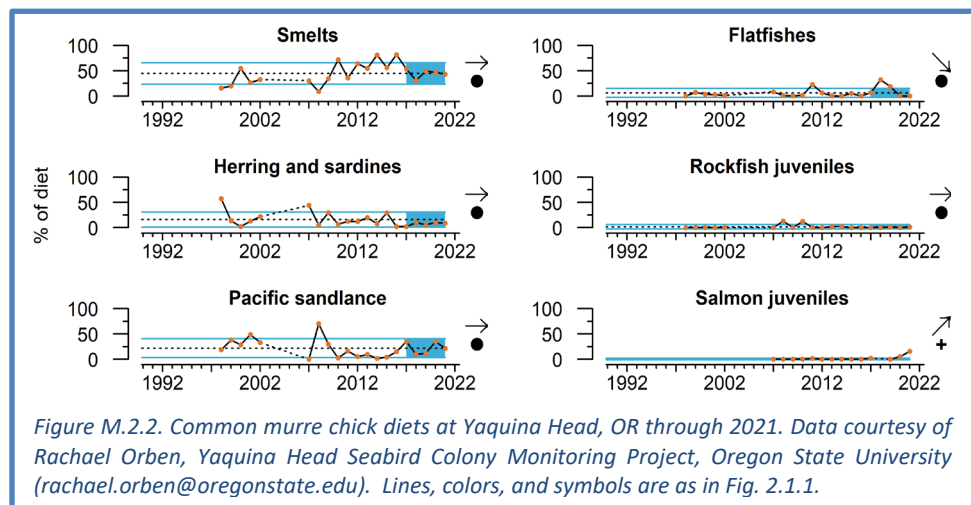


Figure M.2.2. Common murre chick diets at Yaquina Head, OR through 2021. Data courtesy of Rachael Orben, Yaquina Head Seabird Colony Monitoring Project, Oregon State University (rachael.orben@oregonstate.edu). Lines, colors, and symbols are as in Fig. 2.1.1.

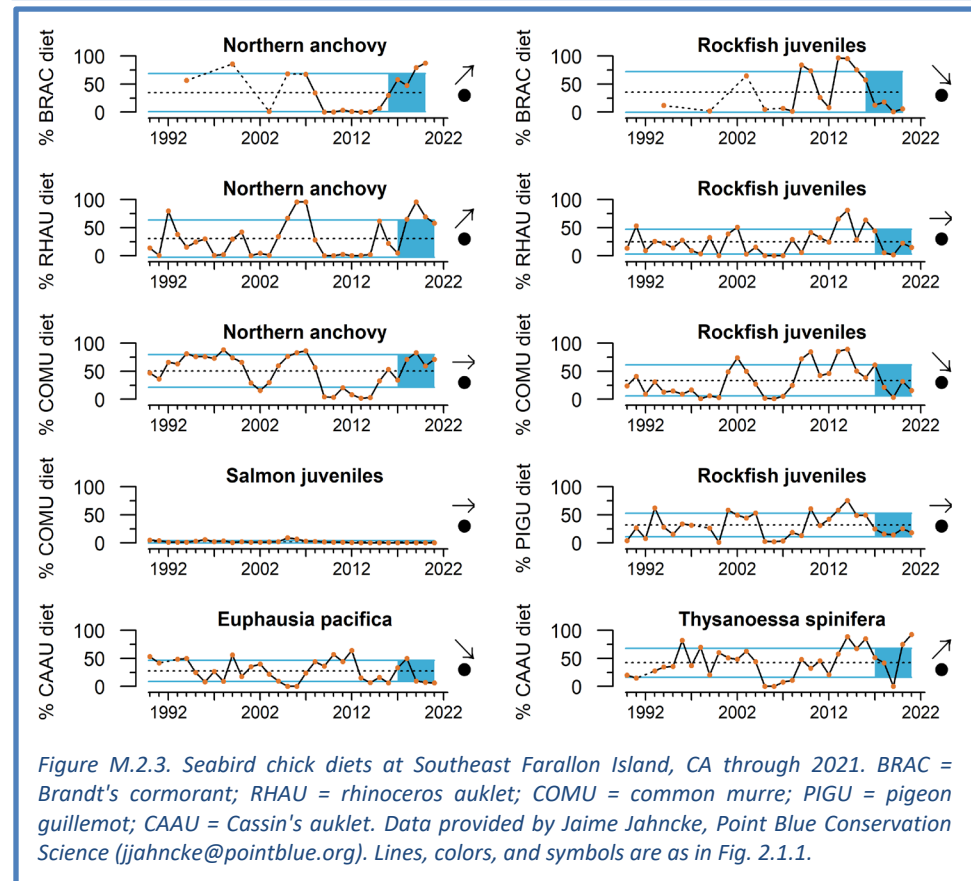
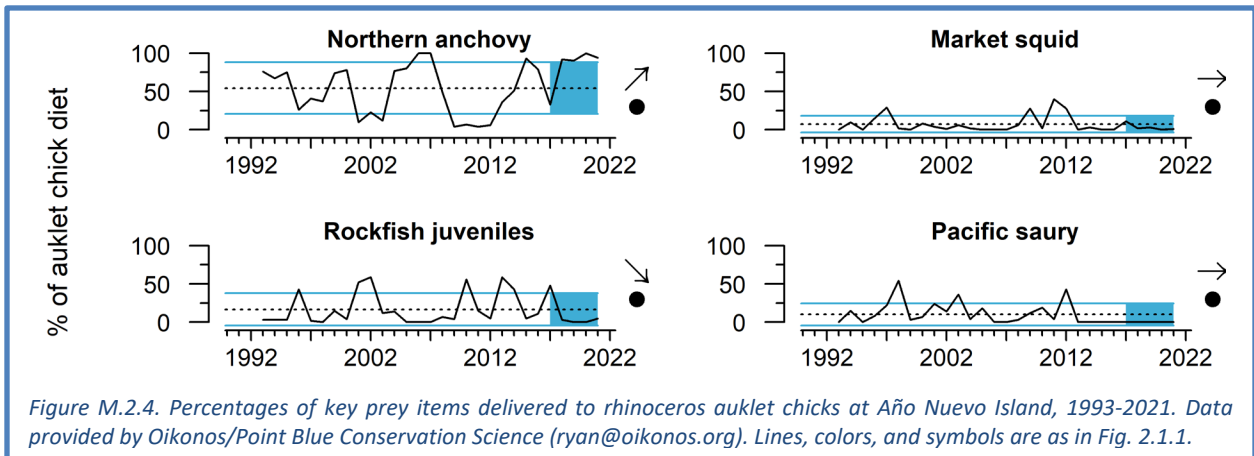


Figure M.2.3. Seabird chick diets at Southeast Farallon Island, CA through 2021. BRAC = Brandt's cormorant; RHAU = rhinoceros auklet; COMU = common murre; PIGU = pigeon guillemot; CAAU = Cassin's auklet. Data provided by Jaime Jahnncke, Point Blue Conservation Science (jjahnncke@pointblue.org). Lines, colors, and symbols are as in Fig. 2.1.1.

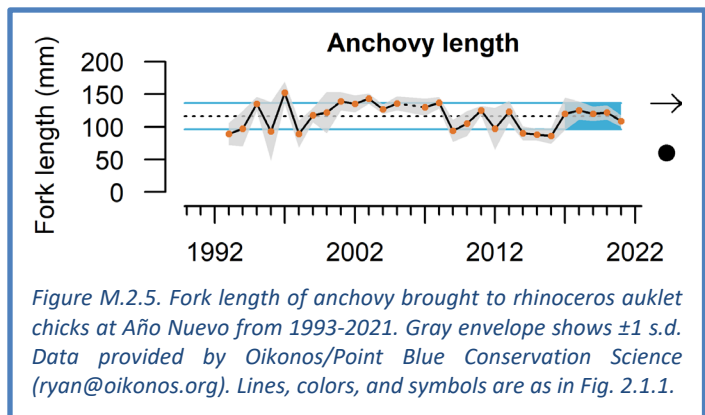
anchovy and less reliant on juvenile rockfish in recent years (Figure M.2.3), in contrast to 2009-2014 when anchovy were virtually absent from their diets. Proportions of anchovy in diets of Brandt’s cormorant, rhinoceros auklet, and common murre chicks on the island were above average in 2021. The proportion of anchovy in Brandt’s cormorant diets was the highest ever recorded at SEFI, and among the highest recorded for rhinoceros auklets and common murre. Proportions of juvenile rockfish in piscivore diets in 2021 were below average and have trended downward in recent years, consistent with relatively low catches of YOY rockfish in forage sampling off central California over the same time period (see Section 3.2 and Appendix H.2).

For common murres at Southeast Farallon Island the proportion of Pacific salmon was again very low in 2021 (Figure M.2.3; see also Central California salmon “stoplight” Table 3.3.2 and Appendix J.2). For Cassin’s auklets, which feed primarily on zooplankton, the proportion of the krill species *Euphausia pacifica* in the diet was below average in 2021, while the krill species *Thysanoessa spinifera* was close to 100% and has increased sharply since 2019 (Figure M.2.3, bottom). High prevalence of *T. spinifera* in the Cassin’s auklet chick diet is linked to increased late-winter upwelling and decreased habitat compression in spring of 2021 (Appendix F.3), which enhanced productivity in the cooler nearshore coastal habitats that *T. spinifera* inhabits.

Long-term diet data are also available for rhinoceros auklets breeding on Año Nuevo Island off central California. The proportion of anchovy in the diet of rhinoceros auklet in 2021 was close to 100%, well above average and continuing a recent upward trend, while the proportion of juvenile rockfish was below average and continued a recent downward trend (Figure M.2.4). The proportions of market squid and Pacific saury were below the long-term averages and close to zero.



The length of anchovy returned to rhinoceros auklet chicks at Año Nuevo in 2021 was slightly below the long-term average (Figure M.2.5). In recent years, researchers have expressed concern that anchovy, while abundant, may have been too large to be ingested by rhinoceros auklet and other colonial seabird chicks, and may have contributed to below-average fledgling production of some species in central California in recent years. However, fledgling production in the region was generally average to above average in 2021 (Figure 3.7.1), which may indicate that prey size was less of an issue last year.

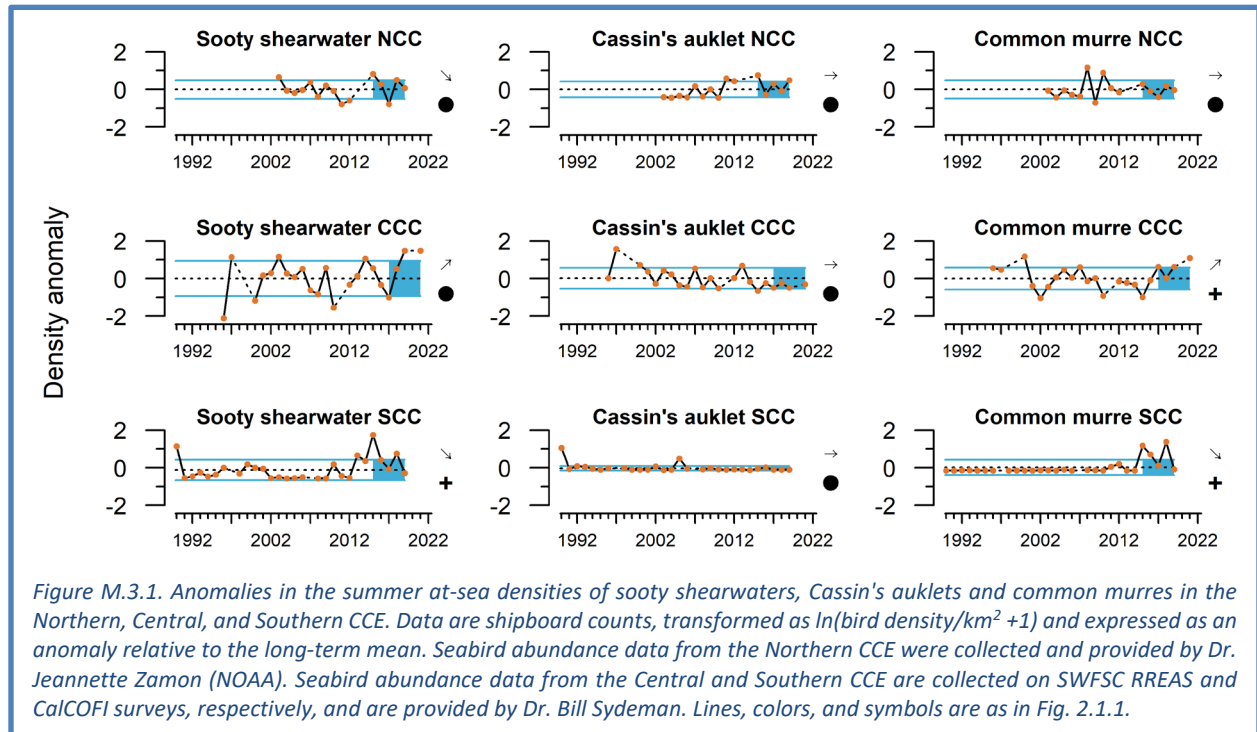


M.3 SEABIRD AT-SEA DENSITIES

Seabird densities on the water during the breeding season can track marine environmental conditions and may reflect regional production and availability of forage. Data from this indicator type can establish habitat use and may be used to detect and track seabird population movements or increases/declines as they relate to ecosystem change. We monitor and report on at-sea densities of three focal seabird species in the Northern, Central, and Southern CCE.

- Sooty shearwaters migrate to the CCE from the southern hemisphere in spring and summer to forage near the shelf break on a variety of small fish, squid and zooplankton.
- Common murres and Cassin’s auklets are resident species that feed primarily over the continental shelf; Cassin’s auklets prey mainly on zooplankton and small fish, while common murres target a variety of pelagic fish.

At-sea density patterns in the Central CCE varied among the three focal species in 2021. Sooty shearwater and common murre at-sea densities were well above average in the Central (CCC) region, and both species have trended upward since 2016 (Figure M.3.1). Cassin’s auklet at-sea density in 2021 was slightly below average, as it has been consistently in recent years. COVID-19 restrictions precluded data collection in the Northern (NCC) and Southern (SCC) regions in 2020 and 2021.

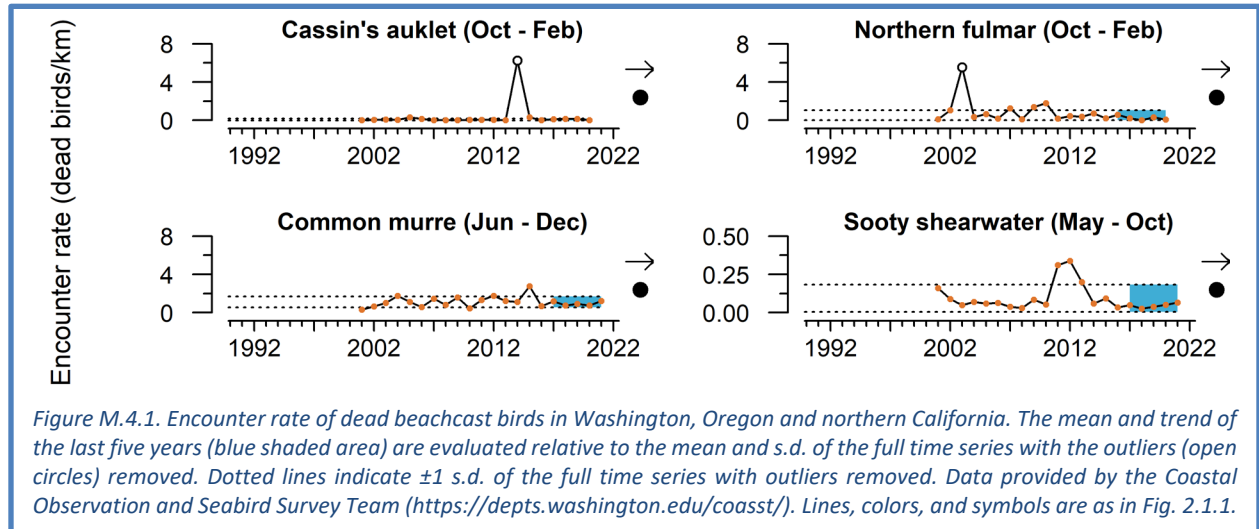


M.4 SEABIRD MORTALITY

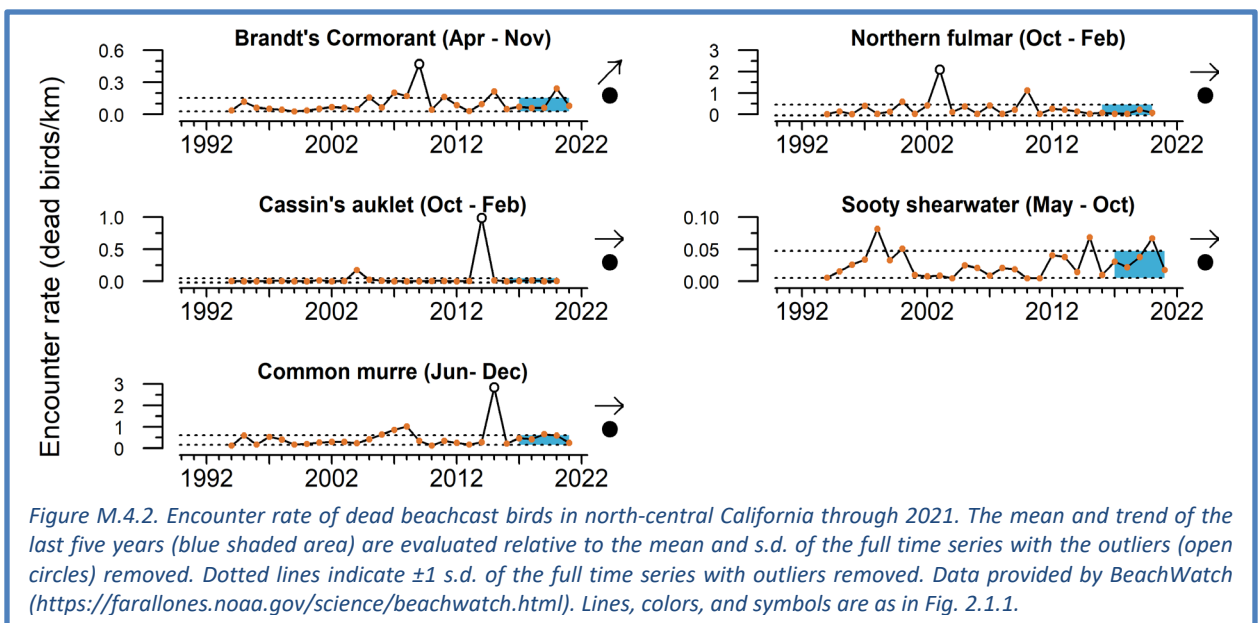
Monitoring of dead beached birds provides information on the health of seabird populations, ecosystem health, and unusual mortality events. CCIEA reports from the anomalously warm and unproductive years of 2014–2016 noted major seabird mortality events in each year. In 2021, seabird mortality monitoring efforts by citizen scientists returned to normal, following considerable reductions in sampling effort in 2020 due to the COVID-19 pandemic. No unusual mortality events were reported by any of the three beach monitoring programs in 2021.

The University of Washington-led Coastal Observation And Seabird Survey Team (COASST) documented average to below-average encounter rates for the seabird indicator species in the

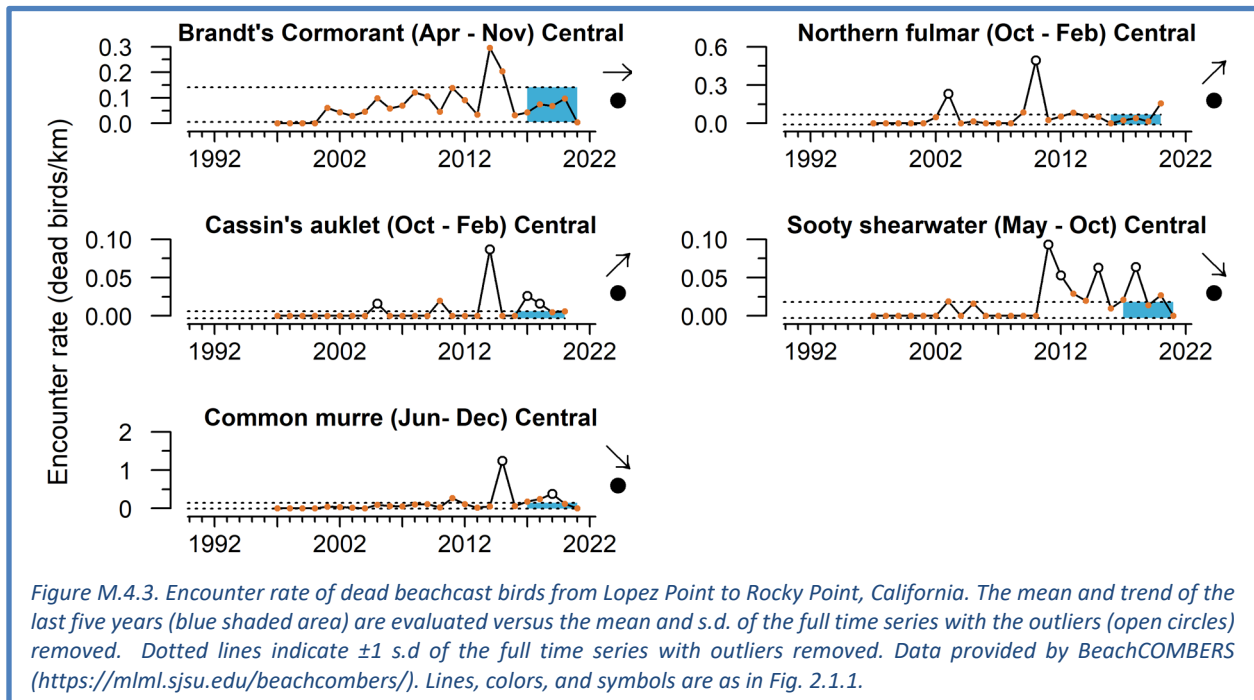
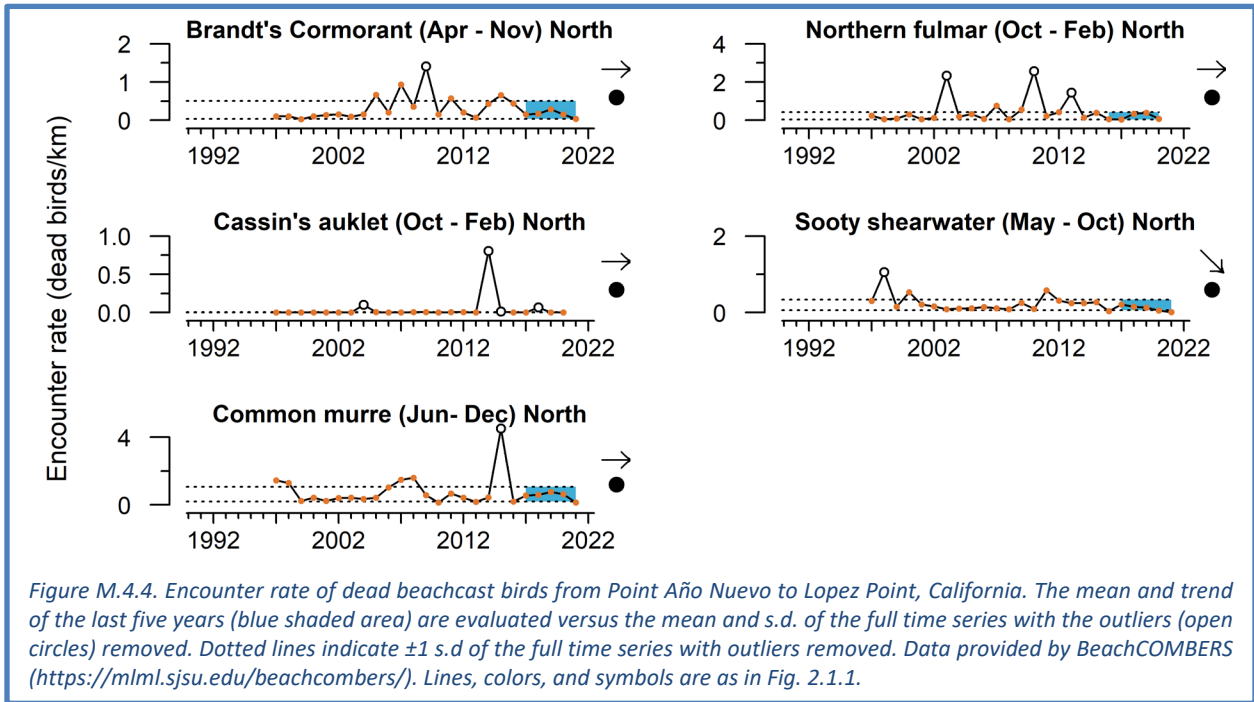
Northern CCE for 2021 (Figure M.4.1). The encounter rate of common murre in 2021 was average, while the encounter rate of sooty shearwater in 2021 was slightly below average. The encounter rates of Cassin’s auklet and northern fulmar are reported through 2020, as the data collection frame for 2021 includes the first two months of 2022. Preliminary data suggest elevated levels of beachcast northern fulmar and Cassin’s auklet in late 2021; however, it is unknown if these levels will remain elevated after including January and February 2022 data, which were unavailable as of this writing.



In the Central CCE (Point Arena to Point Año Nuevo, California), the Beach Watch program documented variable encounter rates for indicator species, but no unusual mortality events in 2021 (Figure M.4.2). Encounter rates for all species in the most recent year of data are within ± 1 s.d. of the long-term average, excluding outlier effects. Brandt’s cormorants and sooty shearwaters were down from 2020, but the encounter rate for Brandt’s cormorant has a positive recent trend. The encounter rates of Cassin’s auklet and northern fulmar are reported through 2020, as the data collection frame for 2021 includes the first two months of 2022. Preliminary data suggest elevated levels of beachcast northern fulmar in late 2021; however, it is unknown if they will remain elevated for 2021 after including January and February 2022 data, which were unavailable as of this writing.



The BeachCOMBERS program conducts surveys of beached seabirds on central and southern California beaches from Point Año Nuevo to Malibu, and we include data from two of their survey regions: North (Point Año Nuevo to Lopez Point, California) and Central (Lopez Point to Rocky Point, California). In the North region, Brandt's cormorant, common murre and sooty shearwater encounter rates were below average in 2021, and sooty shearwater showed a downward trend in recent years (Figure M.4.3). The encounter rates of Cassin's auklet and northern fulmar were average and low in 2020; data for both species will be updated after including January and February 2022 data, which were unavailable at the time of this writing.



In their Central region, BeachCOMBERS found Brandt’s cormorant, sooty shearwater and common murre encounter rates that were below average in 2021, and both common murre and sooty shearwater have a downward trend in recent years (Figure M.4.4). The encounter rates of Cassin’s auklet and northern fulmar were above average and trending upward in 2020, although the 2020 rates did not constitute unusual mortality events. Time series for both species will be further updated after including January and February 2022 data, which were unavailable at the time of this writing.

Appendix N HARMFUL ALGAL BLOOMS

Harmful algal blooms (HABs) of diatoms in the genus *Pseudo-nitzschia* have been a recurring concern along the West Coast. Certain species of *Pseudo-nitzschia* produce the toxin domoic acid, which can accumulate in filter feeders and extend through food webs to cause harmful or lethal effects on people, marine mammals, and seabirds (Lefebvre et al. 2002, McCabe et al. 2016). Because domoic acid can cause amnesic shellfish poisoning in humans, fisheries that target shellfish (including razor clam, Dungeness crab, rock crab, and spiny lobster) are delayed, closed, or operate under a health advisory in the recreational sector when domoic acid concentrations exceed regulatory thresholds for human consumption. Fishery closures can cost tens of millions of dollars in lost revenue, plus cause a range of sociocultural impacts in fishing communities (Dyson and Huppert 2010, Ritzman et al. 2018; Moore et al. 2020; Holland and Leonard 2020), and can also cause “spillover” of fishing effort into other fisheries.

Ocean conditions associated with El Niño events or positive PDO regimes may further exacerbate domoic acid toxicity and fishery impacts, and domoic acid toxicity also tracks anomalies of southern copepod biomass (Figure 3.1.1) (McCabe et al. 2016, McKibben et al. 2017). The largest and most toxic HAB of *Pseudo-nitzschia* on the West Coast occurred in 2015, coincident with the 2013-2016 marine heatwave, and caused the longest-lasting and most widespread HAB-related fisheries closures on record (McCabe et al. 2016, Moore et al. 2019, Trainer et al. 2020). Closures and delays in the opening of West Coast crab fisheries resulted in the appropriation of >\$25M in federal disaster relief funds (McCabe et al. 2016).

According to thresholds set by the U.S. Food and Drug Administration, domoic acid levels ≥ 20 parts per million (ppm) trigger actions for all seafood and tissues except Dungeness crab viscera, for which the level is >30 ppm (California applies this to rock crab viscera as well) (FDA 2011). Under evisceration orders, Dungeness crab can be landed when the viscera exceeds the threshold but the meat does not, provided that the crab are eviscerated by a licensed processor. Oregon was the first West Coast state to pass legislation allowing evisceration, in November 2017, followed by California in October 2021. Washington adopted an emergency evisceration rule in February 2021, and is considering legislation to grant long-term authority for issuing evisceration orders.

Domoic acid in Washington, 2021: As in 2020, domoic acid had impacts on Washington shellfish fisheries in 2021 (Figure N.1). Delays to the start of the 2020-21 Washington Dungeness crab fisheries and closures of the state and tribal recreational razor clam fisheries extended in 2021. On February 16, 2021, the non-tribal Dungeness crab fishery opened with evisceration requirements for all crab landed from Point Chehalis to the Oregon border. Evisceration requirements were extended to include crab landed inside Grays Harbor on February 26, 2021. All commercial evisceration requirements were lifted and the recreational Dungeness crab fishery re-opened coast wide in Washington on April 15, 2021. Limited tribal and recreational razor clam harvests began mid-spring on northern beaches only (Kalaloch, Mocrocks, and Point Grenville). Due to elevated domoic acid levels in razor clams from southern beaches, the Willapa spits commercial razor clam season was delayed until July 10, 2021. The recreational razor clam fishery was opened coast wide on September 17, 2021. Low levels of domoic acid remain present in Washington razor clams. The 2021-22 Washington commercial Dungeness crab fishery opened on time December 1, 2021.

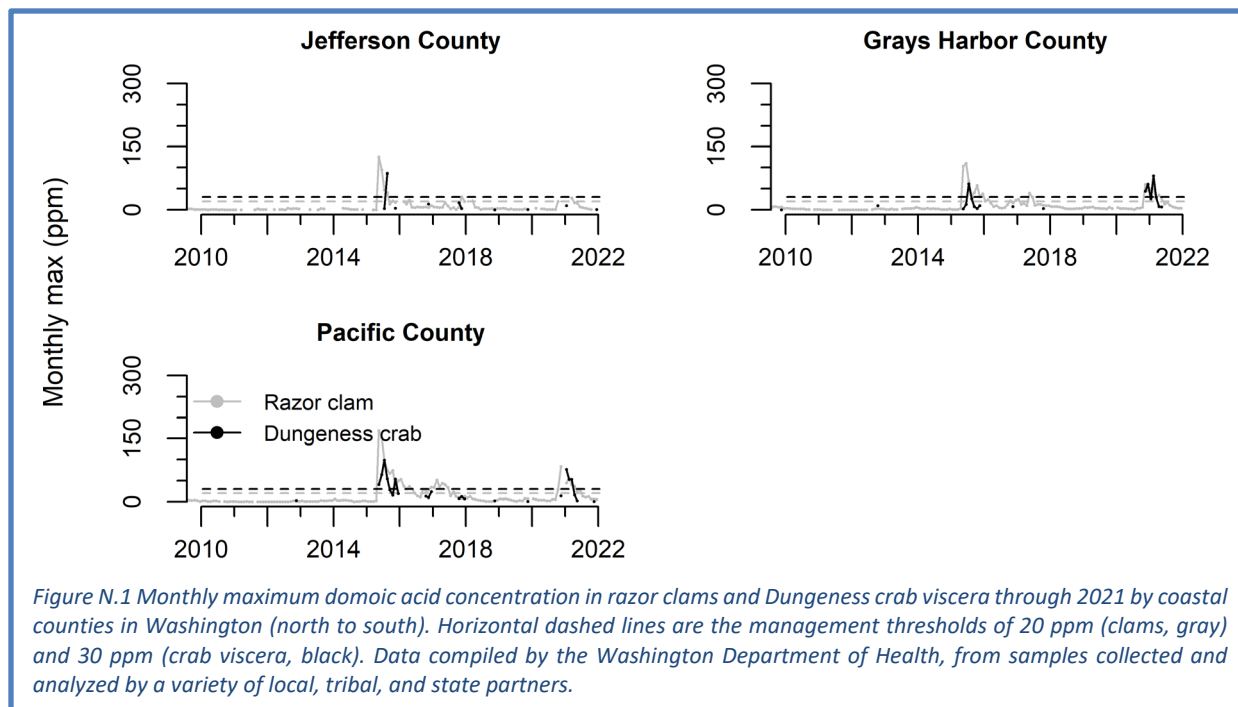


Figure N.1 Monthly maximum domoic acid concentration in razor clams and Dungeness crab viscera through 2021 by coastal counties in Washington (north to south). Horizontal dashed lines are the management thresholds of 20 ppm (clams, gray) and 30 ppm (crab viscera, black). Data compiled by the Washington Department of Health, from samples collected and analyzed by a variety of local, tribal, and state partners.

In Oregon, domoic acid exceedances resulted in some closures in razor clam fisheries (Figure N.2). A statewide closure of the razor clam fishery that was implemented in three stages during fall 2020 was lifted first for the south coast (Coos Bay to the OR/CA border) on April 16, 2021, followed closely by the central coast (Suislaw River to the OR/CA border) on April 30, 2021, then the most northern beaches (Cape Lookout to the WA/OR border) on June 11, followed finally by the remainder of the north coast on September 28, 2021. A razor clam fishery closure was implemented for the south coast from Cape Blanco to the OR/CA border on November 24 and remained in place for the remainder of 2021. The 2021-22 Oregon commercial Dungeness crab fishery opened on time December 1, 2021.

Domoic acid levels also affected some fisheries in California in 2021 (Figure N.3). The razor clam fishery in Del Norte County was re-opened in April 2021 and closed again in December 2021. The Humboldt County razor clam fishery was opened in mid-August 2021. The start of the 2021-22 commercial Dungeness crab fishery in the Central Management Area (Zones 3 and 4) was delayed to avoid marine life entanglements; however, exceedances of domoic acid were also observed in Dungeness crab from two regions: Monterey Bay, although samples cleared prior to the Dungeness crab season start date; and north of Bodega Bay, although samples eventually cleared prior to the delayed start date. The latter resulted in a health advisory for the recreational take of Dungeness crab between Point Reyes and the Sonoma/ Mendocino County line from November 5 to 29, 2021. In Southern California, there were no domoic acid-related closures of spiny lobster or rock crab in 2021 (Figure G.3). However, the northern rock crab fishery is still closed in two areas due to domoic acid concerns (data not shown; see <https://wildlife.ca.gov/Fishing/Ocean/Health-Advisories>). These areas have not been open since November 2015.

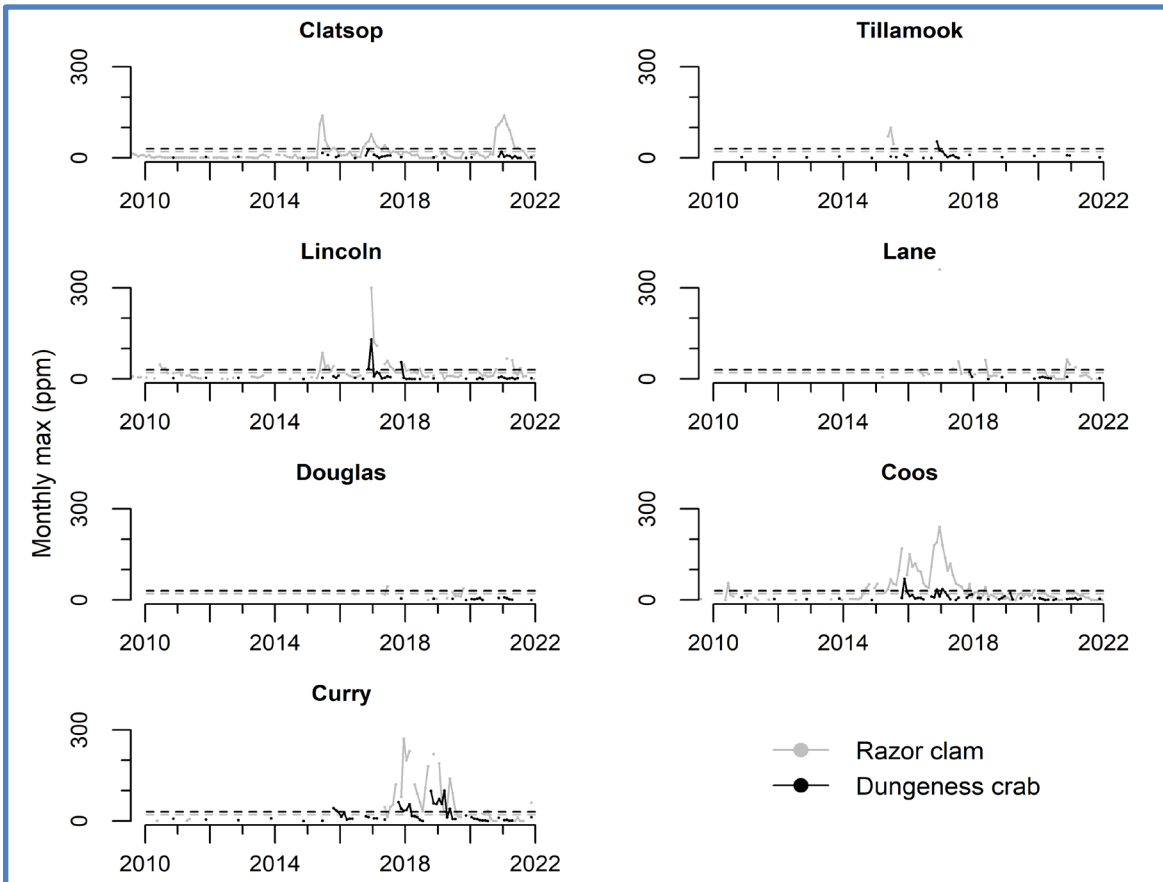


Figure N.2 Monthly maximum domoic acid concentration in razor clams and Dungeness crab viscera through 2021 by coastal counties in Oregon (north to south). Horizontal dashed lines are the management thresholds of 20 ppm (clams, gray) and 30 ppm (crab viscera, black). Razor clam tissue sampling is conducted twice monthly from multiple sites across the Oregon coast. Data compiled and reported by Oregon Department of Fish and Wildlife from analyses conducted by the Oregon Department of Agriculture.

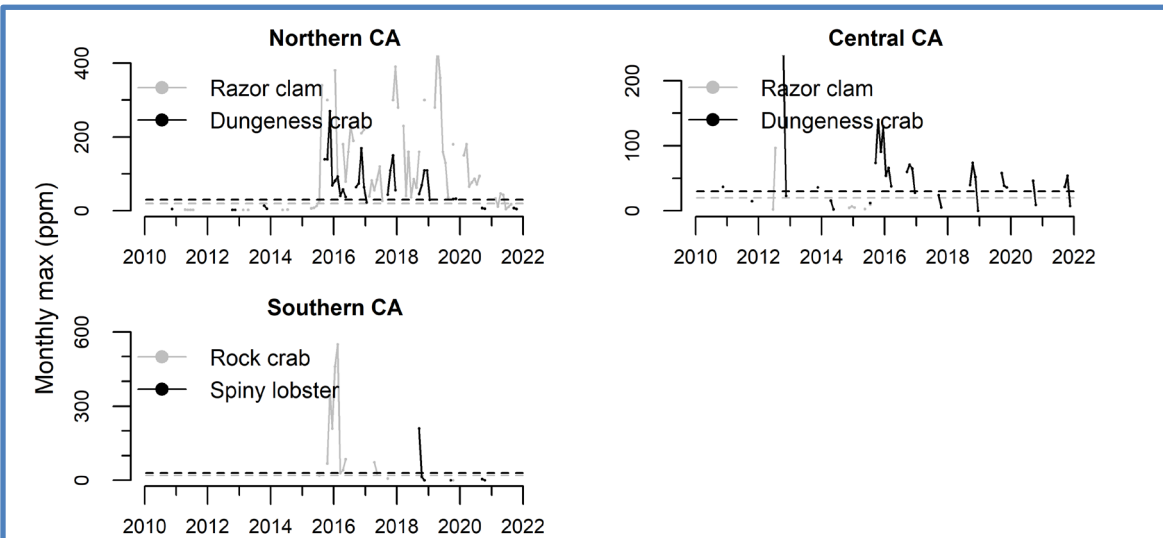


Figure N.3 Monthly maximum domoic acid concentration in razor clams, Dungeness crab, rock crab, and spiny lobster through 2021 in California (Northern CA: Del Norte to Mendocino counties; Central CA: Sonoma to San Luis Obispo counties; Southern CA: Santa Barbara to San Diego counties). Horizontal dashed lines are the management thresholds of 20 ppm (clams and lobsters, gray) and 30 ppm (crab viscera, black). Data compiled by the California Department of Public Health from samples collected by a variety of local, tribal, and state partners.

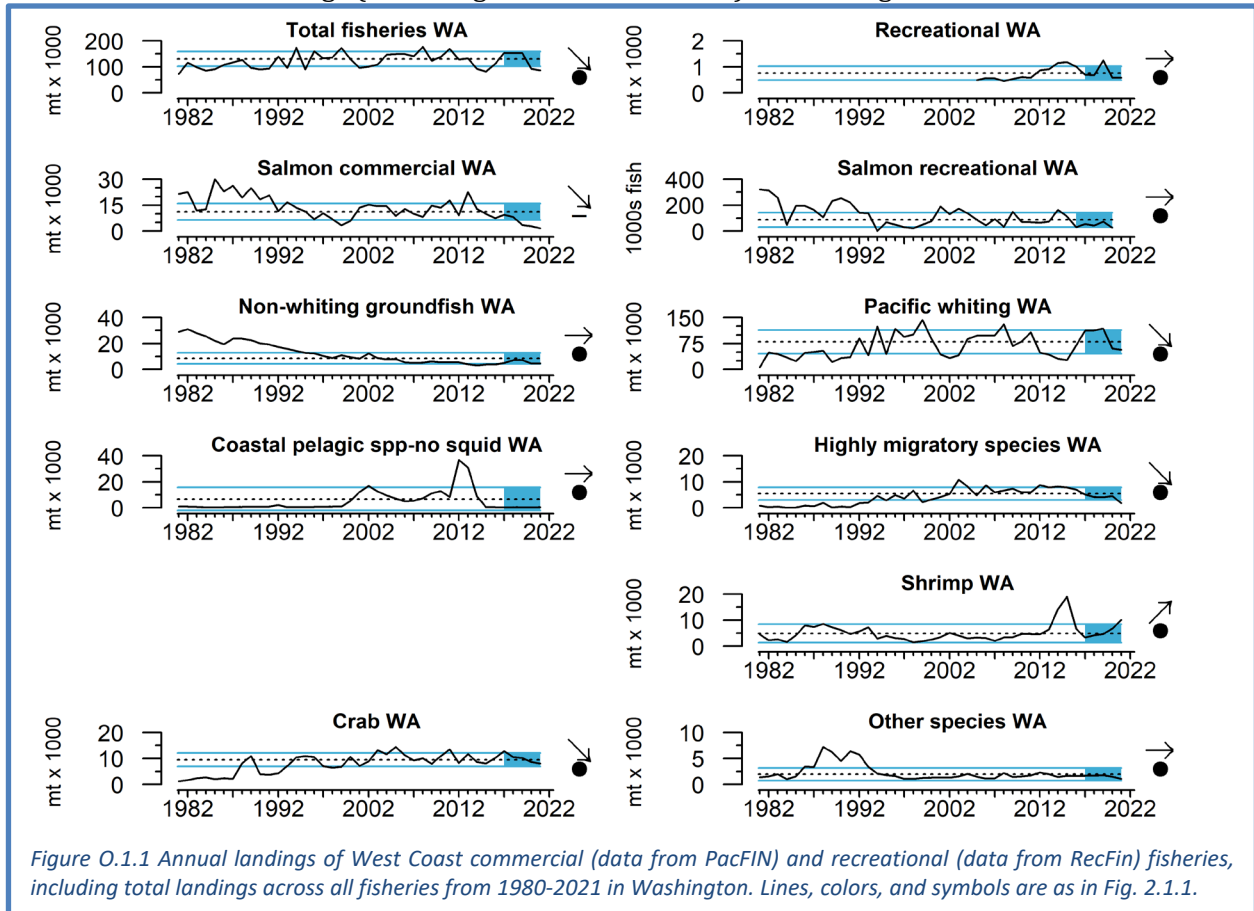
Appendix O STATE-BY-STATE FISHERY LANDINGS AND REVENUES

The Council and EWG have requested information on state-by-state fisheries landings and revenues; these values are presented here. Data through 2021 were nearly complete for all states at the March 2022 Briefing Book deadline. Commercial landings and revenue data are best summarized by the Pacific Fisheries Information Network (PacFIN; pacfin.psmfc.org), and recreational landings are best summarized by the Recreational Fisheries Information Network (RecFIN; www.recfin.org). Landings provide the best long-term indicator of fisheries removals. Revenues are based on consumer price indices for 2021. Status and trends are estimated relative to a frame of reference of 1991-2020.

0.1 STATE-BY-STATE LANDINGS

Commercial fisheries landings in Washington are >90% complete through November 2021. Total landings decreased from 2017 to 2021, with particularly low landings in 2020 and 2021 (Figure 0.1.1). These patterns were driven primarily by changes in Pacific whiting landings: the correlation coefficient between total fisheries landings and whiting landings in Washington over the last five years was 0.99 (0.92 across all years). Commercial landings of salmon, HMS and crab also have decreasing trends over the last five years. Shrimp landings were the only commercial fishery we included that had an increasing trend over the past five years. Commercial salmon landings remained >1 s.d. below the long-term average. All other commercial fisheries shown had no trends from 2017 to 2021, and were within ± 1 s.d. of the long-term average.

Recreational landings data for Washington in 2021 are >90% complete through October 2021; 2020 and 2021 both appear to be among the lowest recreational landings in Washington in our time series. Total recreational landings (excluding salmon and halibut) in Washington have been within 1 s.d. of



the long-term average in recent years except 2019 (Figure O.1.1), when albacore landings were at their greatest of the entire time series. Recreational landings of salmon (Chinook and coho) were mostly within 1 s.d. of the long-term average from 2016 to 2020, although they were also low relative to the average (2021 data were not available at time of this report).

Total fisheries landings in Oregon were consistently >1 s.d. above the time series average from 2017 to 2021 (Figure O.1.2), and these patterns were primarily driven by landings of whiting, which were also consistently >1 s.d. above the time series average for the last five years and were highly correlated with total landings ($r = 0.97$). Similar to Washington, commercial landings of shrimp increased and crab decreased from 2017-2021. Although market squid catches were slightly lower in 2021 than in 2020, market squid landings in Oregon ports have a strongly positive trend over the last five years. Commercial landings of all other individual fisheries showed no recent trends. Recent average landings for HMS were below the time series average, and landings of HMS, CPS finfish and salmon in Oregon were all near time series lows in 2021.

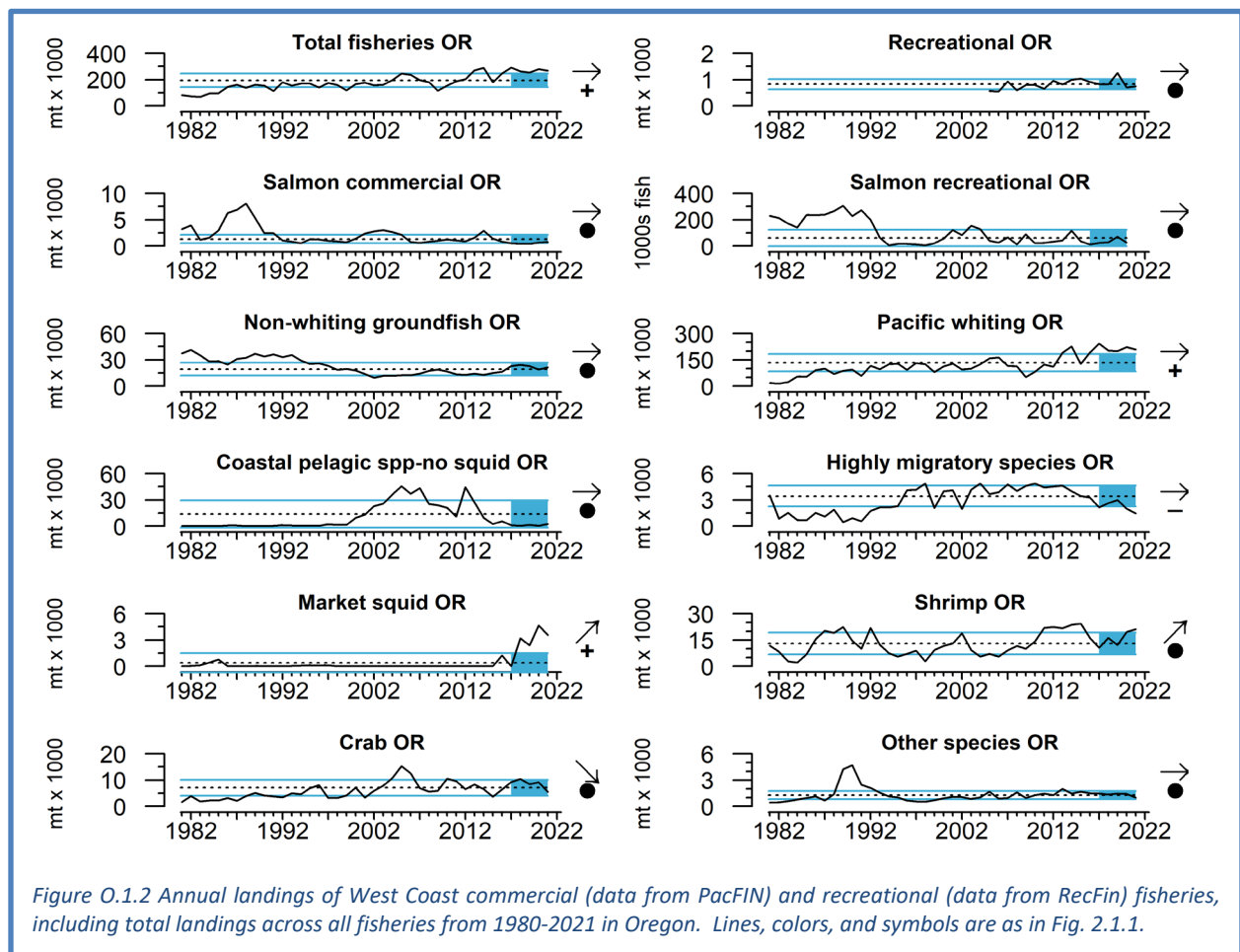
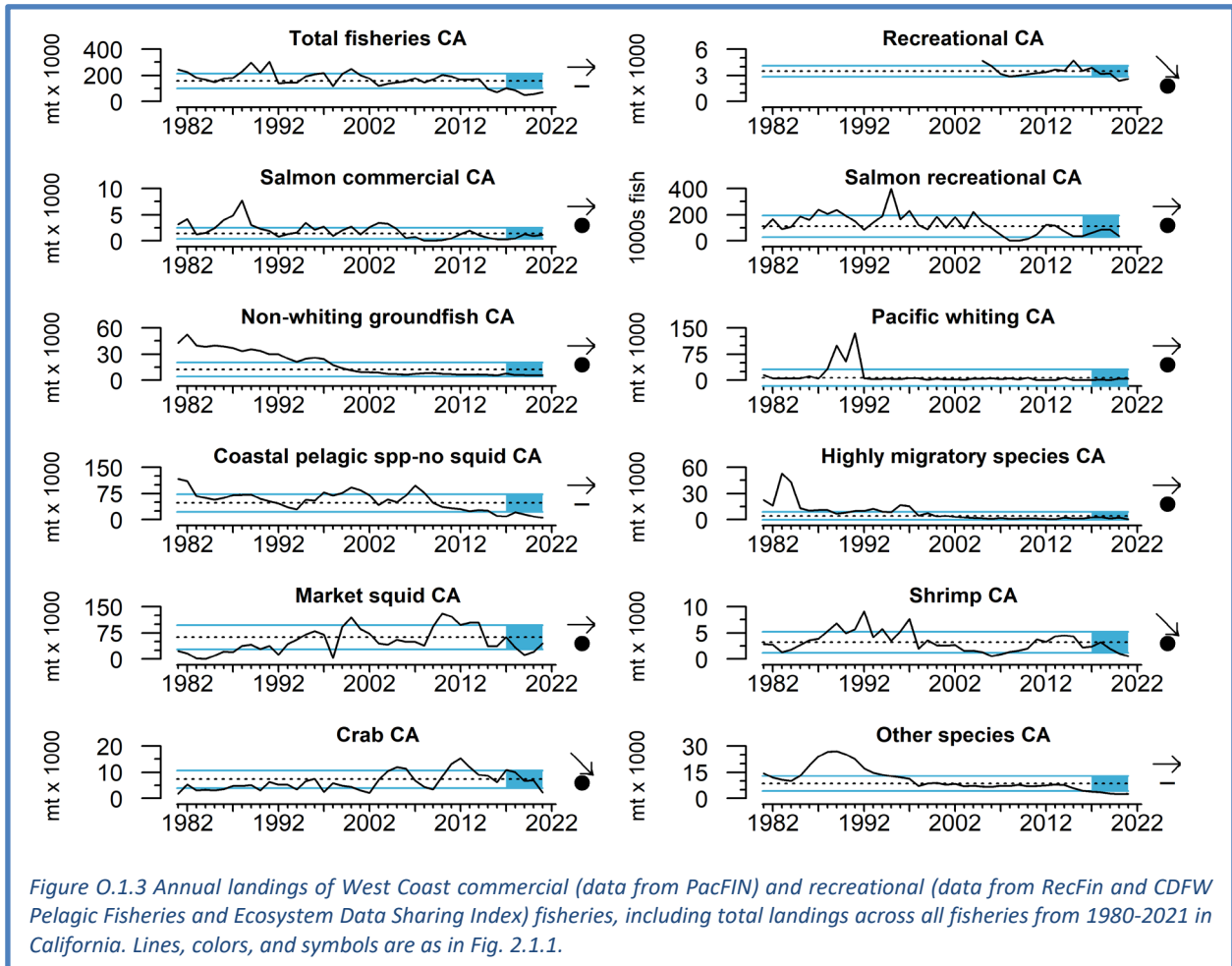


Figure O.1.2 Annual landings of West Coast commercial (data from PacFIN) and recreational (data from RecFin) fisheries, including total landings across all fisheries from 1980-2021 in Oregon. Lines, colors, and symbols are as in Fig. 2.1.1.

Recreational fisheries landings in Oregon for 2021 are >90% complete through October 2021. Similar to Washington, Oregon recreational fisheries landings (excluding salmon and Pacific halibut) have been within ± 1 s.d. of the time series average from 2017 to 2021, with the exception of 2019 when albacore landings were at their greatest of the entire time series (Figure O.1.2). Salmon recreational landings (Chinook and coho) showed no recent trends and were within ± 1 s.d. of the time series average since 2016 (2021 data were not available at time of this report).

Total commercial landings in California were relatively unchanged from 2017 to 2021, but were >1 s.d. below the time series average, primarily due to low levels of CPS landings over the last five years (Figure O.1.3). Commercial landings of shrimp and crab have declined in the past five years. There were no significant trends observed for any other commercial fisheries, but landings of CPS finfish and other species were >1 s.d. below time series averages, and landings of non-whiting groundfish were near the lowest recorded levels of their time series over the last five years.



Recreational fisheries landings in California for 2021 are >90% complete through October 2021. Recreational landings (excluding salmon, Pacific halibut, and HMS) in California decreased >1 s.d. of the long-term average from 2017-2021 (Figure O.1.3). Salmon recreational landings in California were within 1 s.d. of the time series average over the last 5 years of available data (2016-2020), although they were low relative to the average, and there was a sharp decrease in 2020 that may have been due to restrictions on sampling due to the COVID pandemic.

0.2 COMMERCIAL FISHERY REVENUES

Total revenue across West Coast commercial fisheries had a declining trend from 2017 to 2021, but was 6% higher in 2021 than in 2020, based on data currently available (Figure 0.2.1). The five-year decline was driven primarily by decreased revenue from crab, HMS, and non-whiting groundfish fisheries over the last five years, accounting for 75% of the total revenue decline. However, revenue for 6 of 9 commercial fisheries increased in 2021 from 2020 levels: market squid (+96%), whiting (+44%), non-whiting groundfish (+18%), Other species (+11%), salmon (+6%) and shrimp (+4%). In contrast, HMS (-35%), crab (-14%) and CPS finfish (-14%) fisheries generated less revenue in 2021 than in 2020. Despite a decreasing trend over the last five years, the mean revenue from crab fisheries from 2017-2021 remained >1 s.d. above the time series average. Recent average revenue from whiting was ~1 s.d. above the time series average, while recent average revenues from CPS finfish and HMS were ≥ 1 s.d. below time series averages, and HMS and non-whiting groundfish revenues have been trending down. All other fisheries' revenues showed no recent trends and had recent averages within ± 1 s.d. of time series averages. The increasing trend observed in landings of shrimp fisheries from 2017-2021 (Figure 4.1.1 in the main report) contrasted with the relatively constant levels of revenue over the same period (Figure 0.2.1), highlighting the importance of variation in price-per-pound within the fishery.

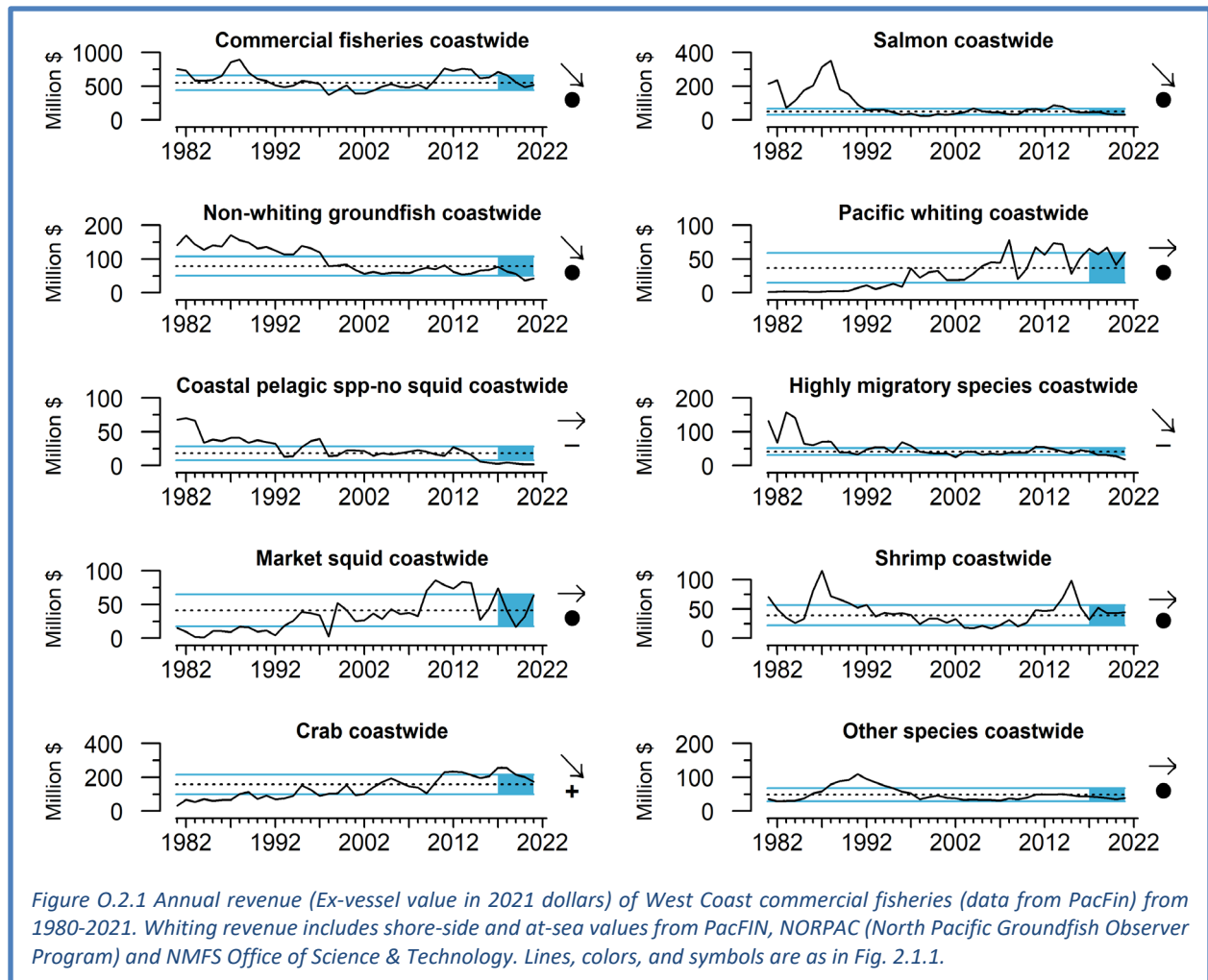
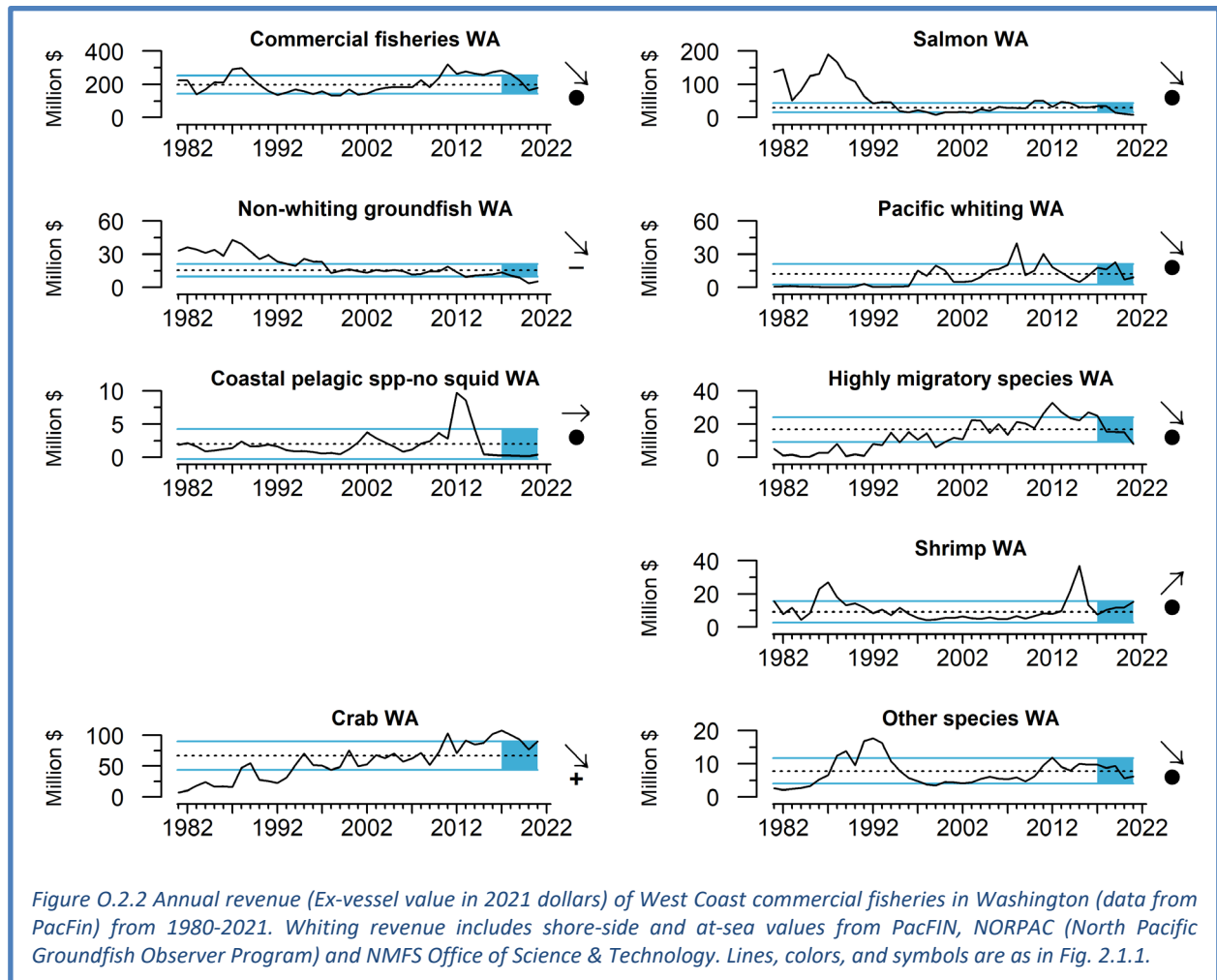
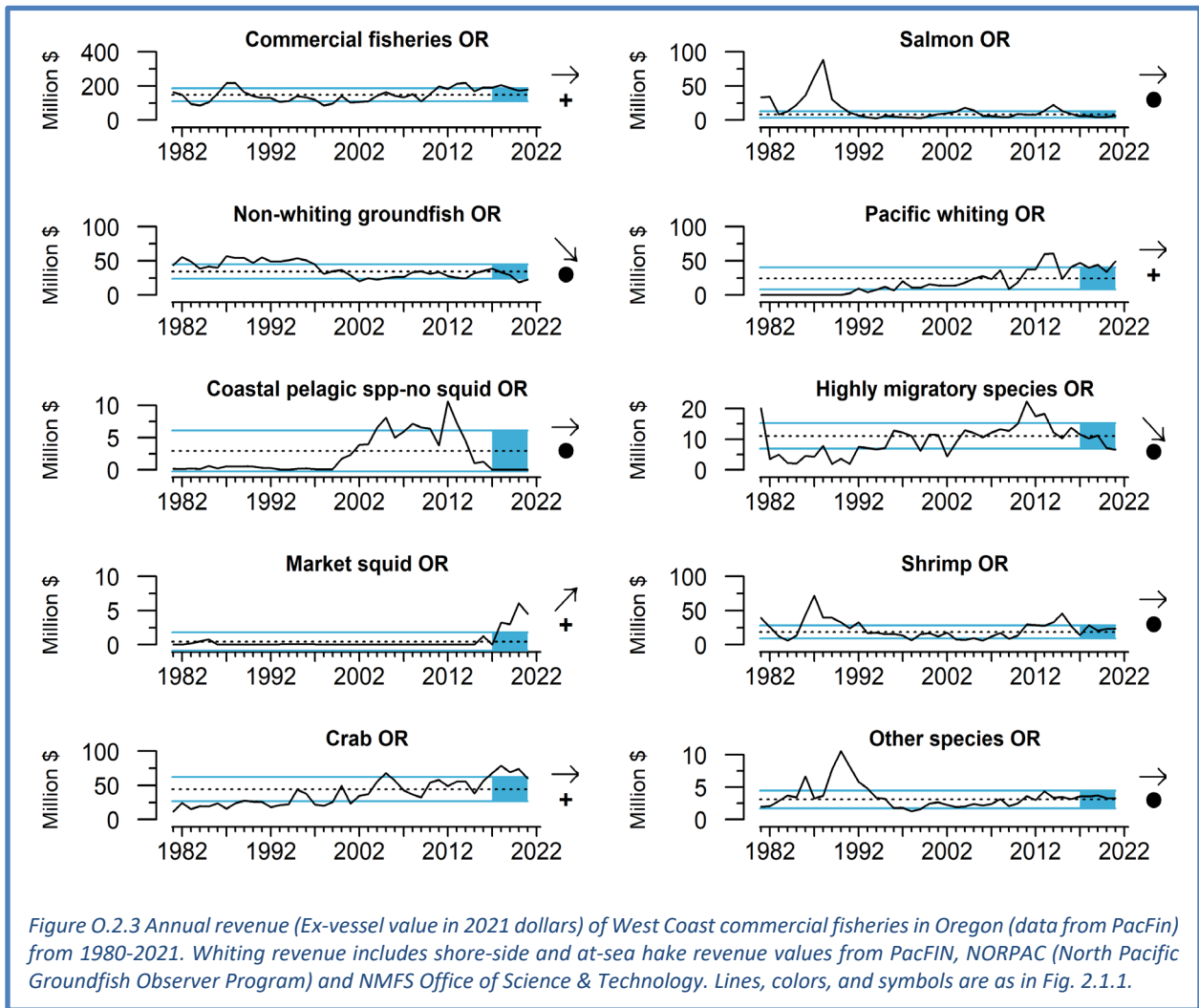


Figure 0.2.1 Annual revenue (Ex-vessel value in 2021 dollars) of West Coast commercial fisheries (data from PacFin) from 1980-2021. Whiting revenue includes shore-side and at-sea values from PacFIN, NORPAC (North Pacific Groundfish Observer Program) and NMFS Office of Science & Technology. Lines, colors, and symbols are as in Fig. 2.1.1.

Similar to coastwide patterns, total revenue across commercial fisheries in Washington decreased from 2017 to 2021, with a 36% drop in that time period (Figure 0.2.2). This pattern was driven by dynamics in salmon, crab, HMS, whiting, and non-whiting groundfish revenues over the last five years. However, 6 of 8 major fisheries had increases in revenue in 2021 over 2020 levels: CPS finfish (+147%), non-whiting groundfish (+45%), whiting (+29%), shrimp (+29%), crab (+16%) and Other species (+8%). In contrast, revenues from HMS (-47%) and salmon (-27%) fisheries were lower in 2021 than in 2020. Average crab fishery revenue from 2017-2021 was >1 s.d. above the time series mean, while non-whiting groundfish revenue was >1 s.d. below the mean. CPS finfish remained close to zero revenue from 2017-2021. Revenue from salmon, non-whiting groundfish, whiting, HMS, and Other species fisheries all declined from 2017-2021 in Washington. Only shrimp revenue showed a recent positive trend.

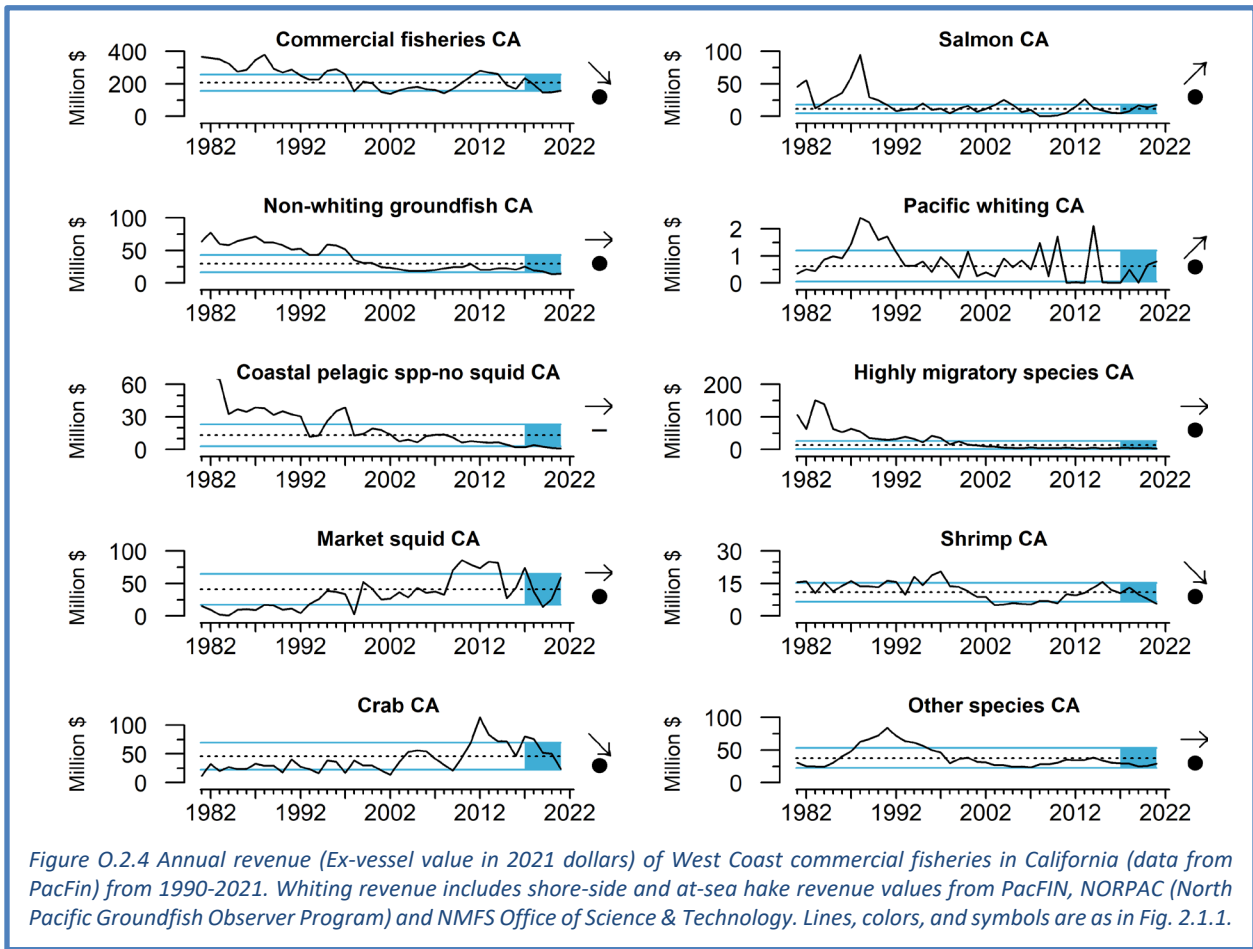


Total revenue across commercial fisheries in Oregon was relatively unchanged and ~1 s.d. above the time series average from 2017 to 2021 (Figure 0.2.3). This pattern was driven primarily by relatively high levels of revenue in the Pacific whiting and crab fisheries over the last five years. In 2021, revenue for 6 of 9 commercial fisheries increased from 2020 levels: CPS finfish (+428%), Pacific whiting (+47%), salmon (+26%), non-whiting groundfish (+20%), shrimp (+2%) and other species (+1). In contrast, market squid (-25%), crab (-18%) and HMS (-8%) fisheries generated less revenue in 2021 than in 2020 in Oregon. Revenue from non-whiting groundfish and HMS fisheries decreased from 2017-2021, while market squid was the only major fishery to show an increase in revenue over



the last five years. All other fisheries shown here had no significant recent trends and were within ± 1 s.d. of time series averages.

Total revenue across commercial fisheries in California decreased from 2017–2021 and was near the lower range of the time series (Figure O.2.4). These patterns largely reflect decreases in revenue observed in the shrimp and crab fisheries coupled with high variability in market squid revenue over the last five years. In 2021, revenue for 5 of 9 commercial fisheries increased from 2020 levels: market squid (+124%), salmon (+24%), whiting (+19%), Other species (+13%) and non-whiting groundfish (+7%). In contrast, revenue from crab (-54%), HMS (-35%), CPS finfish (-33%) and shrimp (-27%) fisheries generated less revenue in 2021 than in 2020. Average revenue from 2017-2021 for non-whiting groundfish, CPS finfish, HMS, and Other species were in the lower ranges for each time series. Revenue decreased over the last five years in the California shrimp and crab fisheries, while revenue increased in the last five years for salmon and also for the Pacific whiting fishery (from ‘at-sea’ sectors operating in California waters). All other major fisheries showed no trend and revenue was within ± 1 s.d. of time series averages. Delays and closures of the Dungeness crab fisheries in California as the result of harmful algal blooms, whale entanglement risk and low meat quality have all contributed to the overall decrease in revenue from 2017-2021.



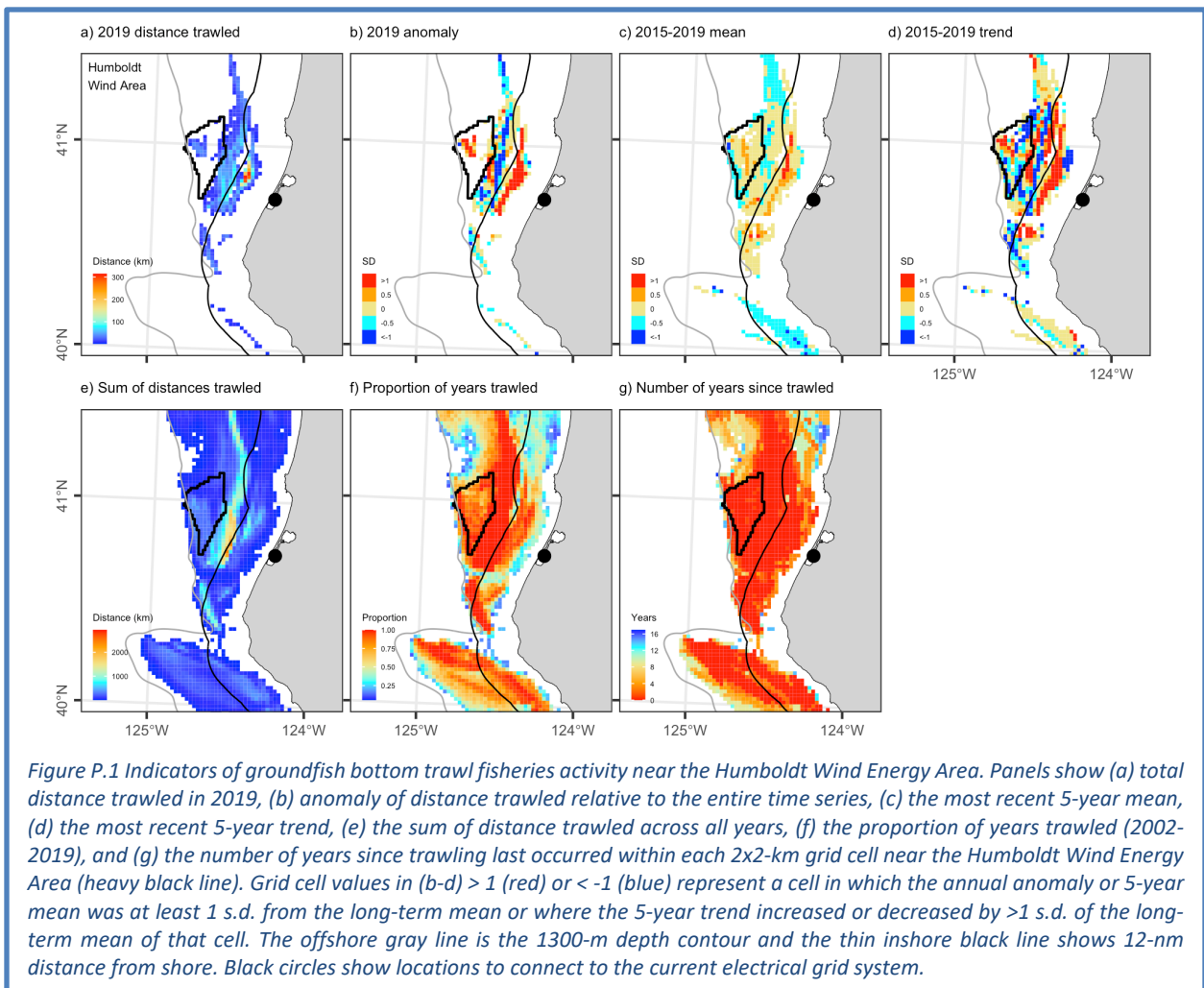
Appendix P POTENTIAL FOR SPATIAL INTERACTIONS AMONG OCEAN-USE SECTORS

New ocean-use sectors of the economy (e.g., offshore wind and hydrokinetic energy and offshore aquaculture) are becoming a reality off the U.S. West Coast, particularly with new offshore Wind Energy Area designations. This presents an urgent need to identify sources of conflict and trade-offs that might occur with existing marine uses, especially commercial fisheries, protected species, EFH and other managed resources. Understanding how fisheries, fishing communities, marine mammals, endangered species and EFH will be affected by new ocean-use sectors is needed to ensure transparent marine spatial planning and to minimize conflicts across the West Coast.

To introduce and illustrate these concepts to this report, we mapped seven indicators that describe spatial and temporal variation in bottom trawling activity from 2002-2019 in areas within and around newly established Wind Energy Areas (WEAs) in California, and the Wind Energy Planning Area in Oregon. We used logbook set and retrieval coordinates from the limited-entry/catch shares groundfish bottom trawl fisheries to estimate total distance trawled on a 2x2-km grid. These distances were then used to calculate (1) total distance trawled in the most recent year (2019), (2) the anomaly of the most recent year relative to the entire time series, (3) the most recent 5-year mean (2015-2019), (4) the most recent 5-year trend (2015-2019), (5) the sum of distance trawled across all years, (6) the proportion of years trawled, and (7) the number of years since trawling occurred within each grid cell. To maintain confidentiality, grid cells with <3 vessels operating within the grid

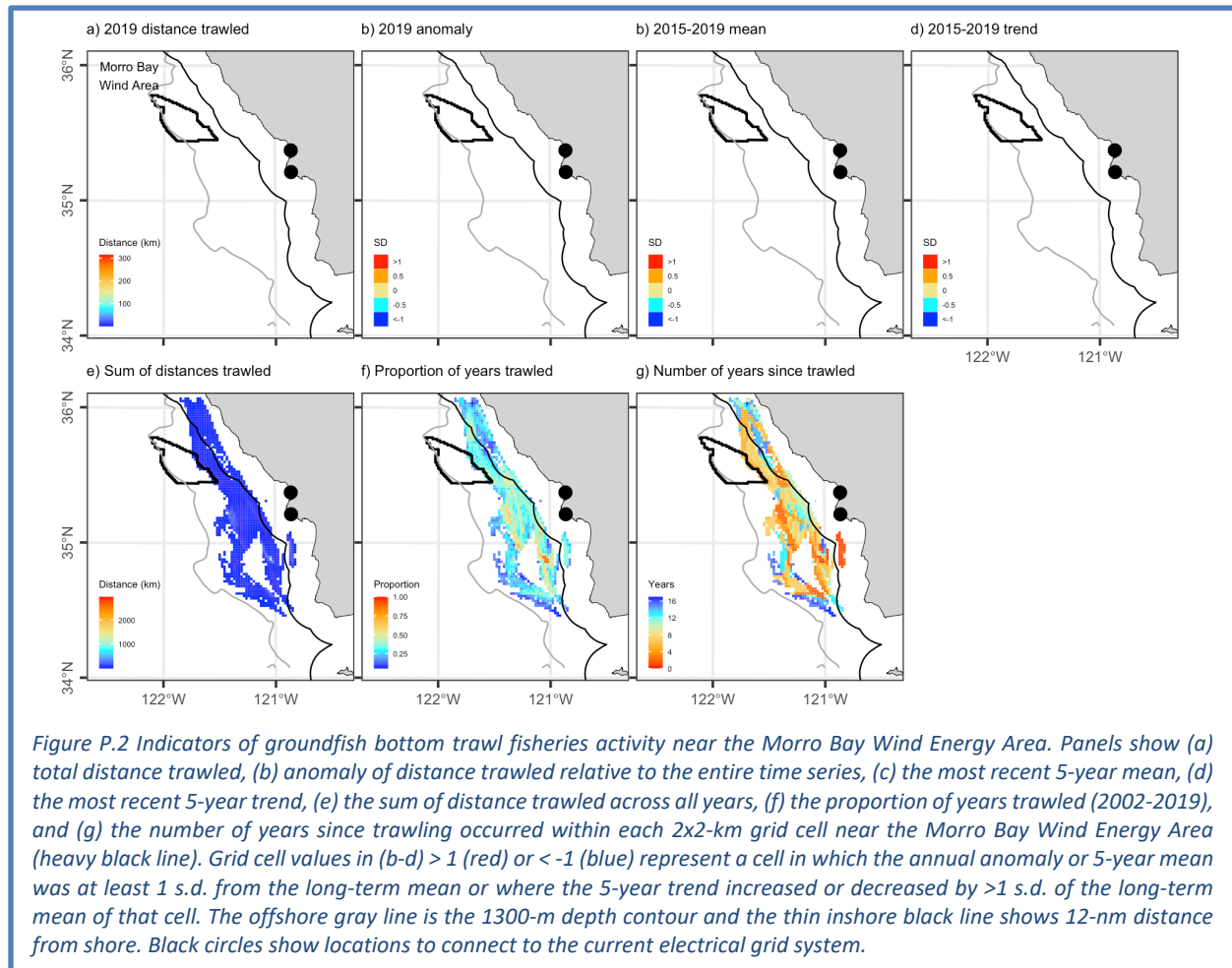
cell across the years associated with the indicator have been removed. The first four indicators have been presented in this report in previous years, while the last three have been developed as indicators to use within a risk analysis framework. These indicators account for only federal limited-entry/catch shares groundfish bottom trawl fisheries, but provide a useful framework for identifying the potential for overlap and conflict between day-to-day fisheries operations and offshore wind energy sites. Overlap with fixed-gear and mid-water trawl fisheries will be included in this framework as data becomes available.

Within the Humboldt WEA (HWEA; Figure P.1), recent groundfish bottom trawl activity occurred primarily in the westernmost portion (Figure P.1a), with above-average activity in 2019 (red cells in Figure P.1b) and an increasing trend over the last five years (red cells in Figure P.1d). Across the entire time series, bottom trawl activity was relatively low within the HWEA (compared to the scale of activity across the entire West Coast; Figure P.1e), but nearly all grid cells had bottom trawling activity in >60% of all years (Figure P.1f) and had activity within the last three years (Figure P.1g). Between the HWEA and the grid-connection locations onshore, there were large regions along the eastern boundary and inside of the 12-nm contour with above-average recent activity (Figure P.1b) and 5-year means (Figure P.1c) and increasing trends (Figure P.1d). Over the entire time series, bottom trawl activity was relatively high in areas between the HWEA and the 12-nm contour (Figure P.1e). Finally, a large majority of grid cells located between the HWEA and the grid-connection locations were used frequently (Figure P.1f) and within the last couple of years (Figure P.1g) by the



groundfish bottom trawling community.

The Morro Bay WEA (MBWEA; Figure P.2) did not have any non-confidential groundfish bottom trawling activity (i.e., no grid cells with ≥ 3 vessels operating) within its boundaries or in surrounding areas within the last five years (Figure P.2a-d). Across the entire time series, groundfish bottom trawl activity was relatively low in areas surrounding the MBWEA (Figure P.2e, which is scaled relative to groundfish trawling activity across the entire West Coast). Most grid cells between MBWEA and shore had bottom trawling activity in 25-50% of all years from 2002-2019 (Figure P.2f) and had activity within the last 4-8 years (Figure P.2g).



The Oregon Wind Energy Planning Area spans the entire north-south length of Oregon, between the 1300-m depth and 3-nm offshore contours. However, we label the 12-nm offshore contour in Figure P.3 based on the potential for objections to locating a wind farm visible from the shore, as has occurred in the siting processes in California. Recent groundfish bottom trawl activity occurred in several distinct north-south bands between the 12-nm offshore and 1300-m depth contours (Figure P.3a) with above-average activity in 2019 (red cells in Figure P.3b) and increasing trends from 2015-2019 (red cells in Figure P.3d) in several patches >12 nm offshore, the largest of which were off central Oregon. Lower 5-year means (blue cells in Figure P.3c) and decreasing 5-year trends (blue cells in Figure P.3d) were most concentrated at the southern and northern borders, where wind speeds are the highest and lowest, respectively, off Oregon. Across the time series, there was high variability in bottom trawling activity (Figure P.3e), with the greatest total activity generally occurring in the same areas having activity in 2019 (Figure P.3a). Highlighting the spatial and

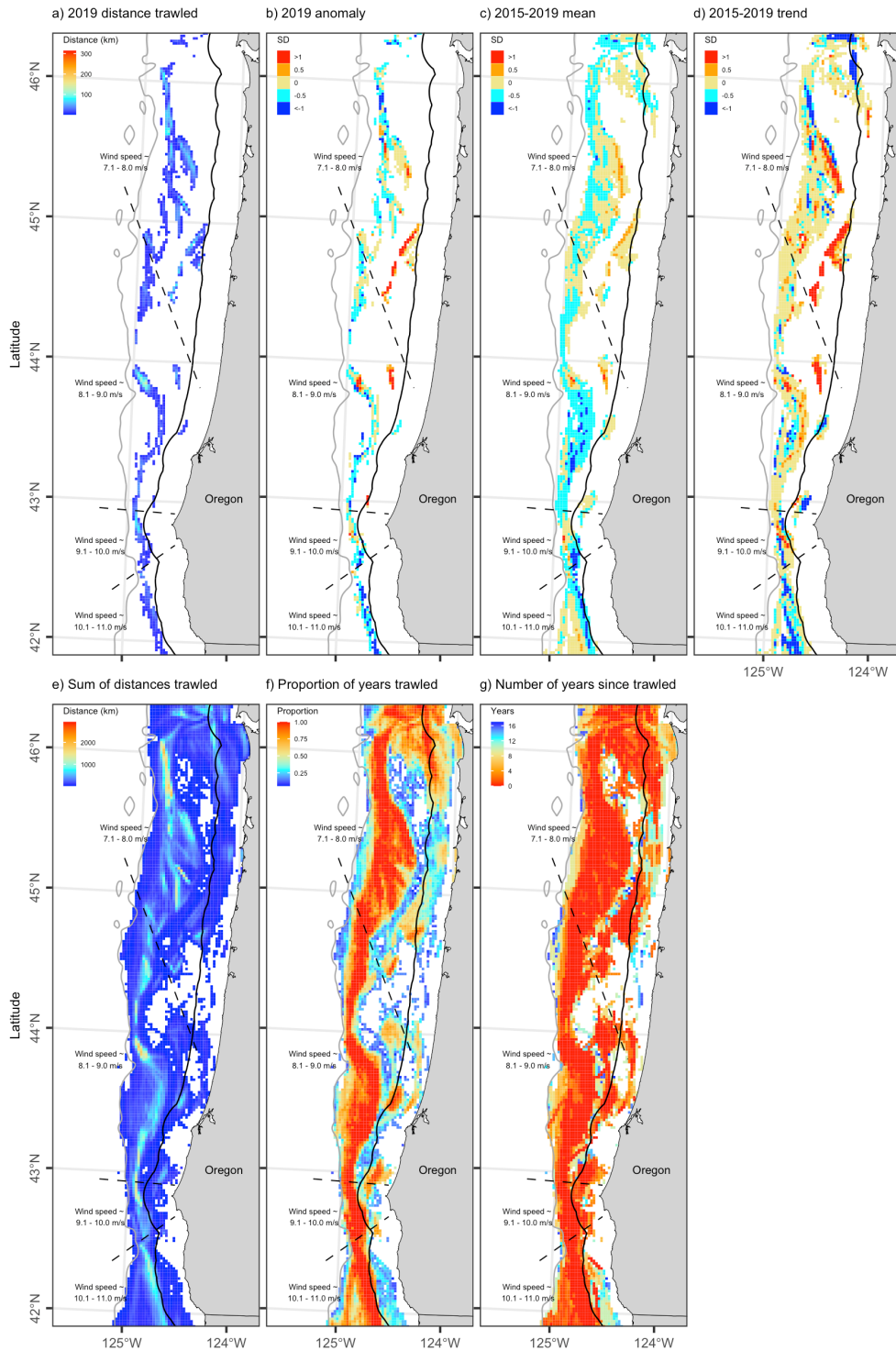


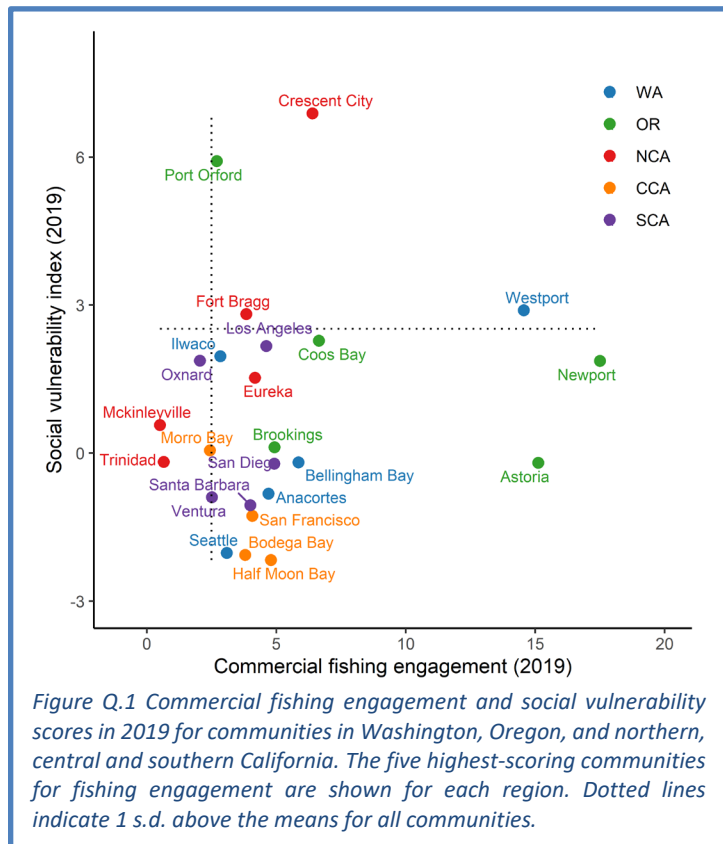
Figure P.3 Indicators of groundfish bottom trawl fisheries activity across the Oregon Wind Energy Planning Area. Panels show (a) total distance trawled in 2019, (b) anomaly of distance trawled in 2019 relative to the time series, (c) the most recent 5-year mean (2015-2019), (d) the most recent 5-year trend, (e) the sum of distance trawled across all years (2002-2019), (f) the proportion of years trawled (2002-2019), and (g) the number of years since trawling occurred within each 2x2-km grid cell. Grid cell values in (b-d) > 1 (red) or < -1 (blue) represent a cell in which the annual anomaly or 5-year mean was at least 1 s.d. from the long-term mean or where the 5-year trend increased or decreased by > 1 s.d. of the long-term mean of that cell. The offshore gray line is the 1300-m depth contour and the inshore black line is 12 nm distance from shore. Approximate latitudinal differences in annual wind speed averages are shown and separated by dashed lines.

grid cells that have been trawled frequently (Figure P.3f) and recently (Figure P.3g) between the 12-nm offshore and 1300-m depth contours. The most notable exception to this is off central Oregon, where significant amounts of hard and mixed habitat types around Stonewall and Heceta Banks have been closed to bottom trawling since 2006 because they are EFH Conservation Areas.

Appendix Q SOCIAL VULNERABILITY OF FISHING-DEPENDENT COMMUNITIES

In Section 5.1 of the main report, we present information on the Community Social Vulnerability Index (CSVI) as an indicator of social vulnerability in coastal communities that are dependent upon commercial fishing. Fishery *dependence* can be expressed in terms of engagement, reliance, or by a composite of both. *Engagement* refers to the total extent of fishing activity in a community; it can be expressed in terms of commercial activity (e.g., landings, revenues, permits, processing, etc.) or recreational activity (e.g., number of boat launches, number of charter boat and fishing guide license holders, number of charter boat trips, number of bait and tackle shops, etc.). *Reliance* is the per capita engagement of a community; thus, in two communities with equal engagement, the community with the smaller population would have a higher reliance on its fisheries activities.

In the main body of the report, Figure 5.1.1 plots CSVI in 2019 against commercial reliance for the five most reliant communities in 2019 from each of five regions of the CCE. Here, we present a similar plot of CSVI relative to commercial fishing engagement scores from 2019. Figure Q.1 shows highly engaged West Coast commercial fishing communities and the corresponding social vulnerability results. Communities above and to the right of the dashed lines are at least 1 s.d. above the averages of both indices, as averaged



across all commercial fishing communities. Of particular note are fishing-oriented communities like Westport, Crescent City, Fort Bragg, and Port Orford that have relatively high commercial fishing engagement results and also a high CSVI composite result. Communities in this region of the plot are both highly engaged and have relatively high social vulnerabilities, and thus may be highly vulnerable to commercial fishing downturns. Shocks due to ecosystem changes or management actions may produce especially high individual and community-level social stress in these communities. As discussed in past meetings, these data are difficult to groundtruth and require further study.

Information on community-level recreational fishing engagement (number of boat launches, number of charter boat and fishing guide license holders, total charter boat trips, bait shops, etc.) has not been updated beyond 2016. Thus we do not have updated comparisons of CSVI with recreational fishing reliance or engagement. Efforts are ongoing to develop new data sources to support recreational fishing analyses, and exclude inland recreational fisheries activities outside of Council purview.

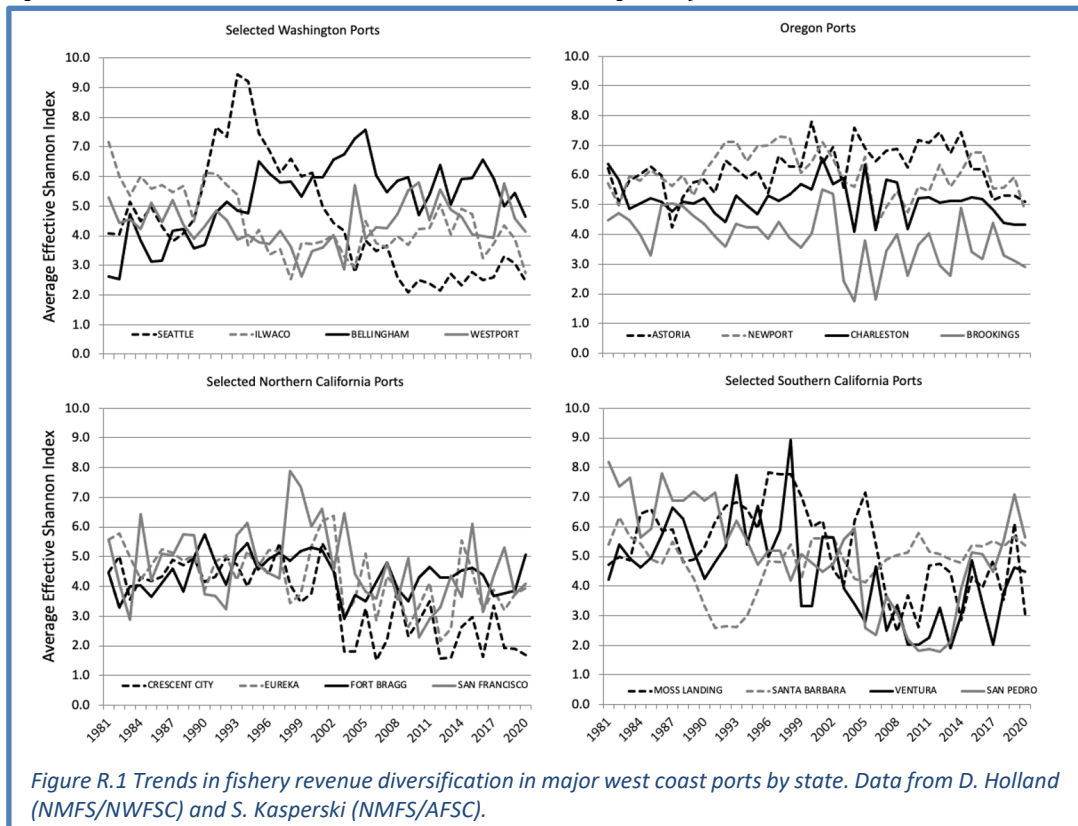
Appendix R FLEET DIVERSIFICATION INDICATORS FOR MAJOR WEST COAST PORTS

Catches and prices from many fisheries exhibit high interannual variability, leading to high variability in fishermen’s revenue, but variability can be reduced by diversifying activities across multiple fisheries or regions (Kasperski and Holland 2013). Individuals may have good reasons to specialize, including reduced costs or greater efficiency; thus while diversification may reduce income variation, it does not necessarily promote higher average profitability. We used the Effective Shannon Index (ESI; Figure 5.2.1) to examine diversification of fishing revenue for more than 28,000 vessels fishing off the West Coast and Alaska over the last 39 years. ESI increases as revenues are spread across *more* fisheries, and as revenues are spread more *evenly* across fisheries; ESI = 1 when a vessel’s revenues are from a single species group and region; ESI = 2 if revenues are spread evenly across 2 fisheries; ESI = 3 if revenues are spread evenly across 3 fisheries; and so on. If revenue is not evenly distributed across fisheries, then the ESI value is lower than the number of fisheries a vessel enters.

As is true with individual vessels and vessel classes, the variability of landed value at the port level is reduced with greater diversification of landings. Diversification of fishing revenue has declined over the last 20 years for some ports (Figure R.1). Examples include Seattle and most but not all ports in Southern Oregon and California. However, a few ports have become more diversified in recent decades, including Bellingham Bay and Westport in Washington. Diversification in Astoria, Oregon had been increasing but has decreased in recent years while Brookings has had an erratic trend. Diversification scores are highly variable year-to-year for some ports, particularly those in Southern Oregon and Northern California that depend heavily on the Dungeness crab fishery.

In 2020 (the most recent year of available data), most of the ports shown in Figure R.1 saw a decline in diversification. The exceptions were Eureka, Fort Bragg and San Francisco.

(These indices and plots do not include income from recreational charter fleets, which may be an important component of revenue and diversification for some ports.)

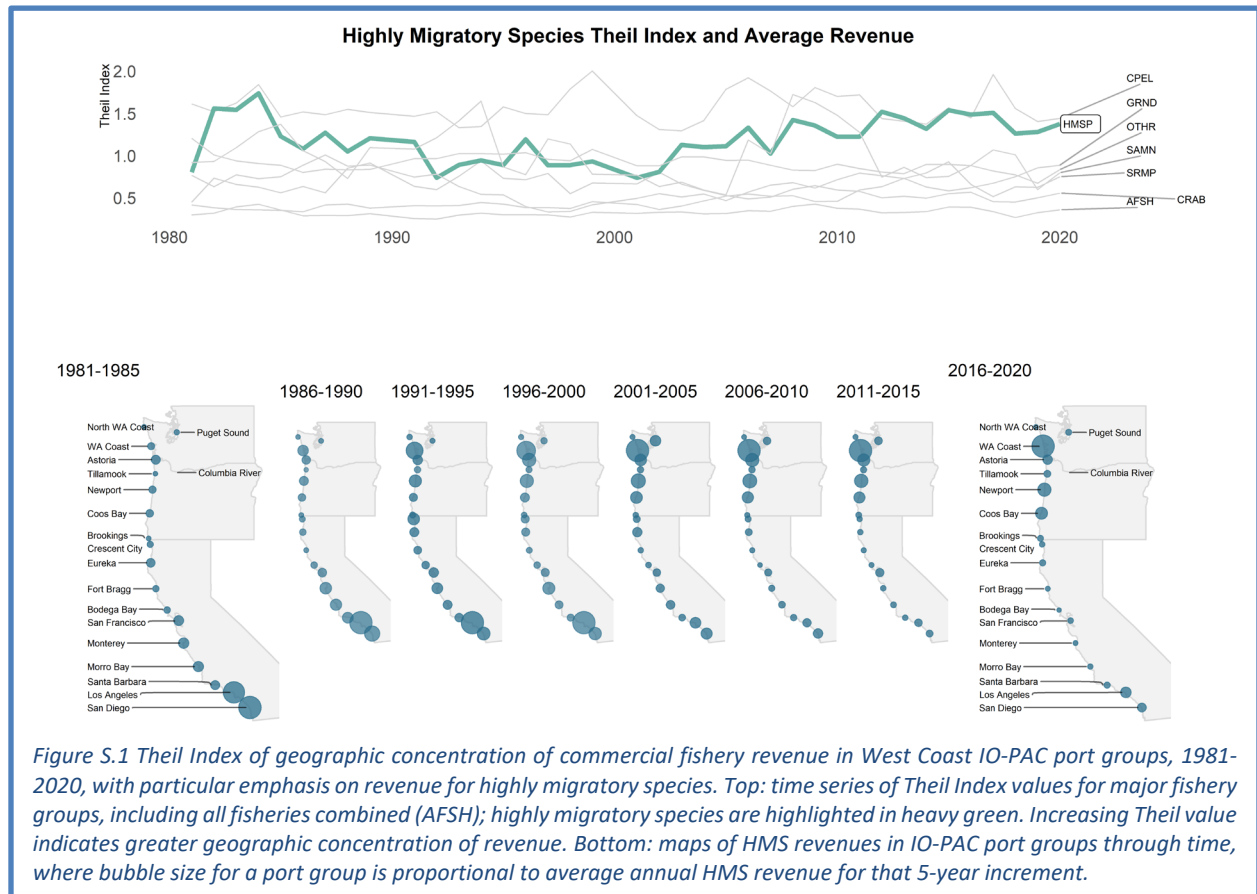


Appendix S THEIL INDEX OF FISHERY REVENUE CONCENTRATION

Over the past two reports, we have worked with the SSC-ES to develop an index of the concentration or consolidation of ex-vessel fishery revenue in ports on the West Coast. This index is one possible way of indicating if fishery access opportunities are changing within and across ports and/or FMPs, possibly in relation to meeting requirements of NS-8. We use the Theil Index (Theil 1967) as an annual measure of geographic concentration of fishery revenue. Though it typically measures economic inequality, the Theil Index may be developed and applied in varying contexts. Here, we use the Theil Index as an annual estimate of how observed revenue is concentrated within ports, relative to what revenues would be if they were distributed with perfect equality across those ports. An increase in the Theil Index for a particular fishery or group of fisheries indicates that revenue is becoming more concentrated in a smaller number of ports.

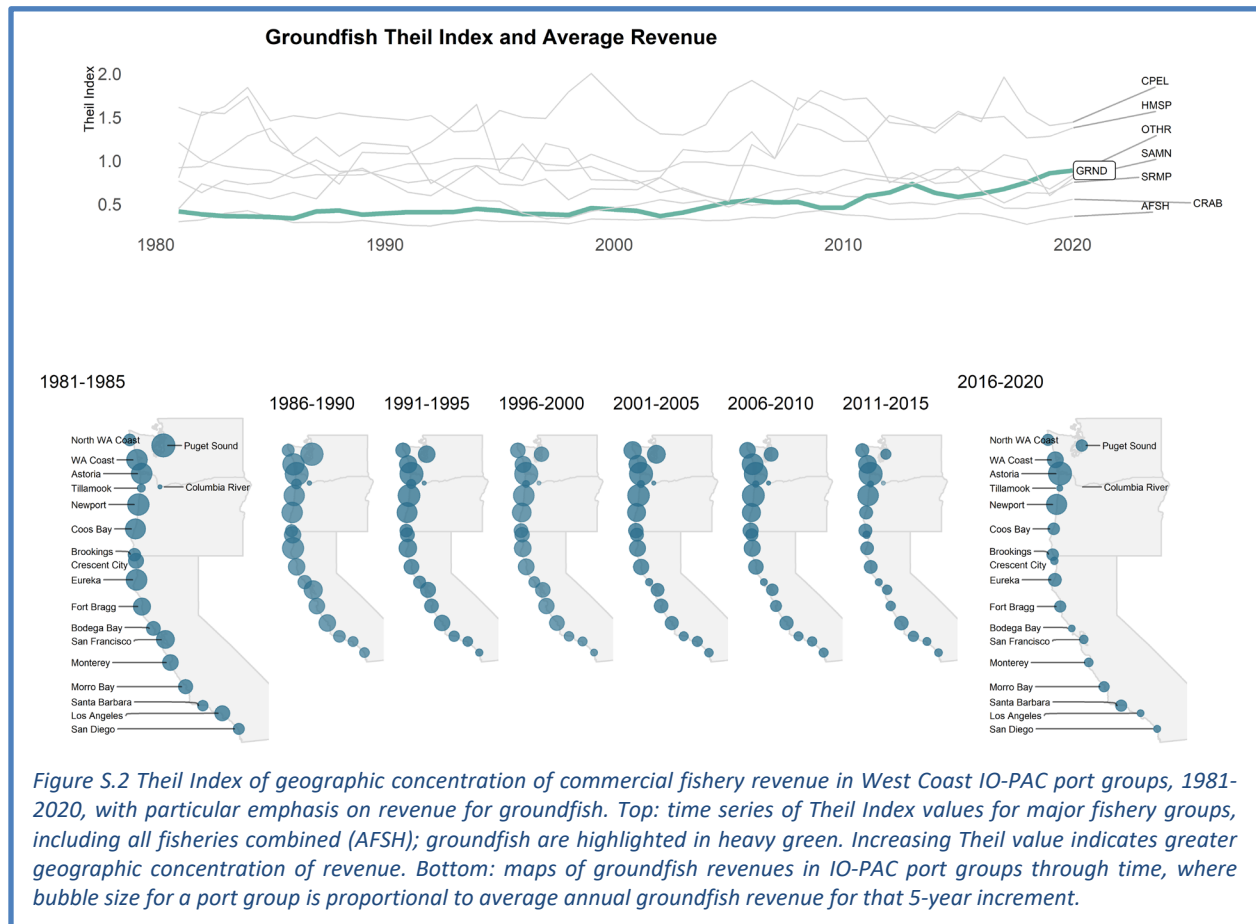
In the Section 5.3 of the main body, we show how total commercial fisheries revenue has not exhibited high levels or extended trends of geographic concentration, but that different fishery management groups demonstrated clearer trends or patterns of variability over the study period (Figure 5.3.1). Here, we more closely examine annual changes in the Theil Index for two important West Coast fishery management groups—HMS and groundfish—in more depth.

First, as shown in the main report in Figure 5.3.1 and here in Figure S.1 (top), Theil Index values for HMS generally decreased from 1981 to 2002, but then returned to higher annual values from 2003 to 2020. This U-shaped pattern appears to be a result of HMS revenues initially being concentrated in southern port groups, then gradually becoming more equally distributed, and finally becoming more concentrated in northern port groups (Figure S.1, bottom). In examining the annual Theil index measures for individual species in the HMS category (data not shown), we see evidence that shifts in



HMS revenue concentration were largely due to changes in revenue distribution of swordfish and albacore. Swordfish, which contributed most strongly to HMS revenues in the early portion of the time series and were concentrated in the south, were replaced in more recent years by albacore, the revenues for which have come to dominate the HMS category.

As also shown in Figure 5.3.1, Theil Index values for groundfish revenues on the West Coast have been trending fairly continuously toward increased geographic concentration over the time period examined. In general, increased concentration of groundfish revenues has occurred in northern ports (Figure S.2), both prior to and after the 2011 adoption of catch shares into groundfish management. Research suggests this increasing concentration is not distinct from trends for commercial fisheries generally (Speir and Lee 2021); that is, the implementation of catch shares is likely not driving the increase in geographic concentration of groundfish revenue.



We have made no effort yet to attribute changes in revenue concentration with management actions, environmental drivers, food web changes, or changes within coastal communities. It is therefore premature to conclude that this is an effective indicator in the context of NS-8, or what changes in the index mean for Council considerations. We also note that pooling coastal communities into IO-PAC port groups is a coarser scale than intended for NS-8 considerations, which are attuned to communities rather than port groups. Community-scale estimation of the Theil Index is possible, and we should anticipate different qualitative and quantitative outcomes than those presented here once the scale is refined to the community level. Community-scale estimation will increase the complexity of data analysis, presentation and visualization, which will be an important discussion point between the IEA team and the Council as we continue to develop this metric.

Appendix T FISHERIES PARTICIPATION NETWORKS

Fishery participants with diverse harvest portfolios create links between fisheries, even when ecological links between the harvested species are weak or absent. This results in networks of alternative sources of income. Undirected fisheries participation networks (e.g., Fuller et al. 2017, Fisher et al. 2021) offer one way to represent this information visually, with different fisheries depicted as nodes in the network; pairs of nodes can then be connected by lines that integrate information about vessels participating in both fisheries. Networks can be constructed in a variety of ways and across different spatial and temporal scales, and can be compared for differences before and after events such as environmental or management changes (Anderson et al. 2017, Fuller et al. 2017, Addicott et al. 2018, Beaudreau et al. 2019, Kroetz et al. 2019, Fisher et al. 2021, Frawley et al. 2021, Nomura et al. 2021). Fisheries participation networks may add levels of detail or context to other analyses in this report, such as those related to the community vulnerability (Appendix Q), fishery diversification (Appendix R), and port-level revenue concentration (Appendix S). As such, fisheries participation networks offer one way to respond to requests from the EAS and EWG for deeper characterization of social and economic conditions in West Coast fishing communities, and information relevant to meeting NS-8 under the Magnuson–Stevens Act.

Fisheries participation networks representing IO-PAC port groups in the past year (November 2020 to November 2021) consisted of one to ten fisheries nodes, with 0–29 links between the fisheries within each network (Washington, Figure T.1; Oregon, Figure T.2; northern and central California, Figure T.3; southern California, Figure T.4); all IO-PAC port groups are illustrated in these figures except for Other Coastal WA and Unknown Ports.) These snapshots in time depict the portfolios of fisheries that are economically important to individual vessels within a port group, based on a diversity of behaviors and choices at the level of individual vessels over the past year.

These networks clearly demonstrate the important role crab, groundfish, Pacific halibut, pink shrimp, and skate/dogfish/shark fisheries play in creating high levels of cross-fishery participation across the coast: these target groups’ relatively large “eigenvector centralities” (Figure T.5) signify that they themselves are

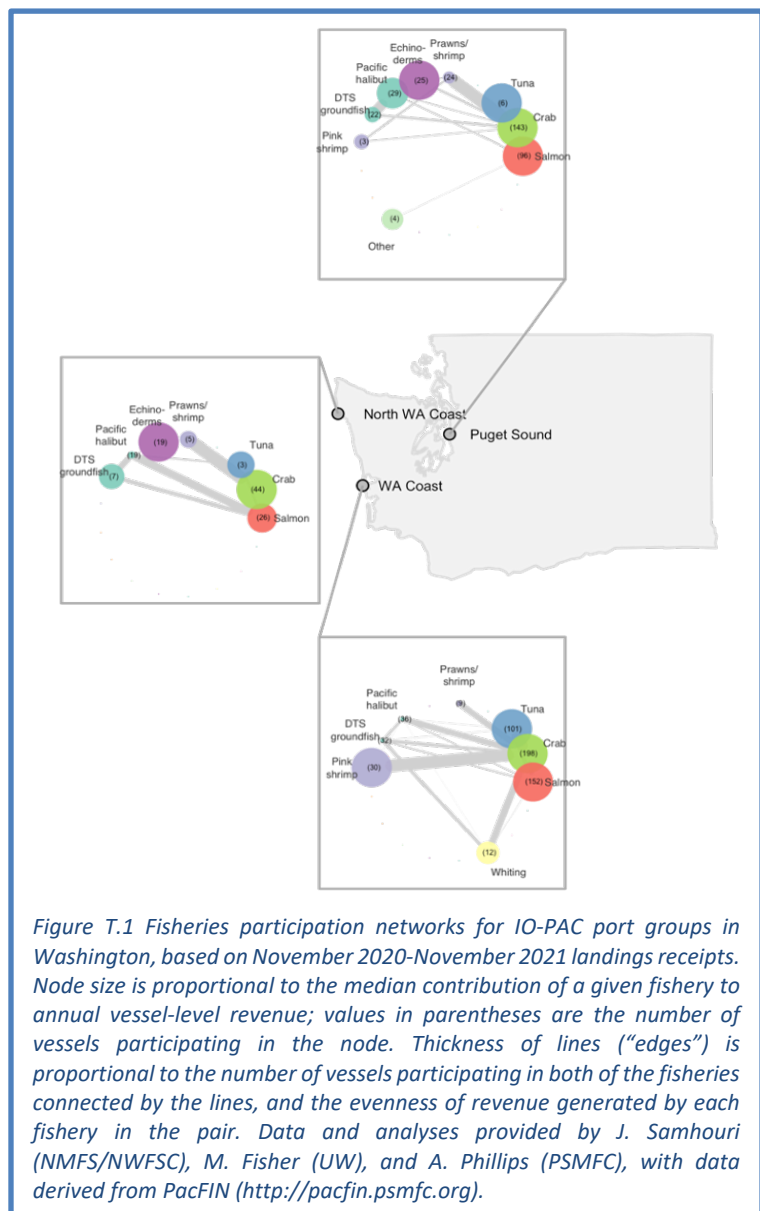
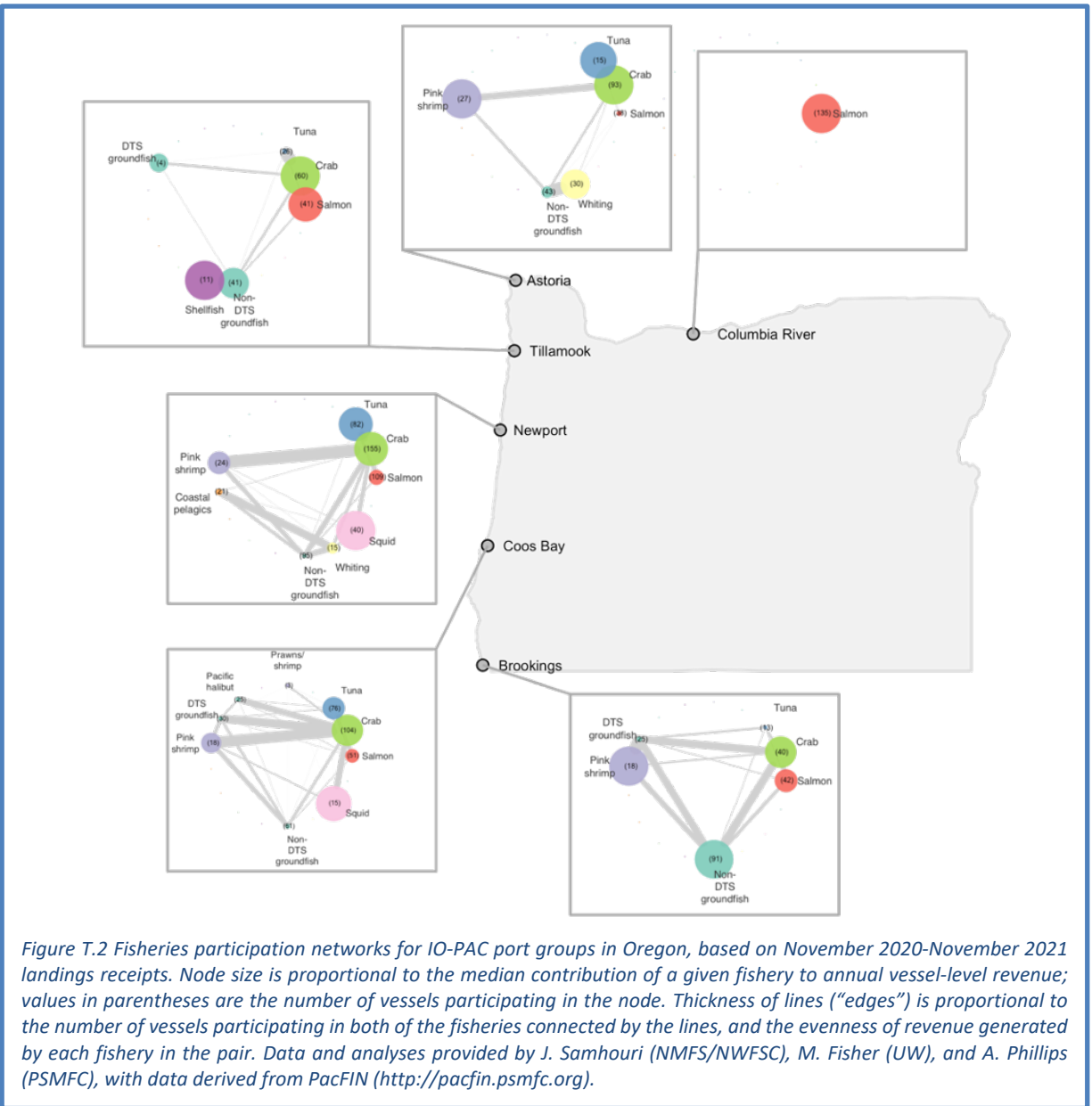
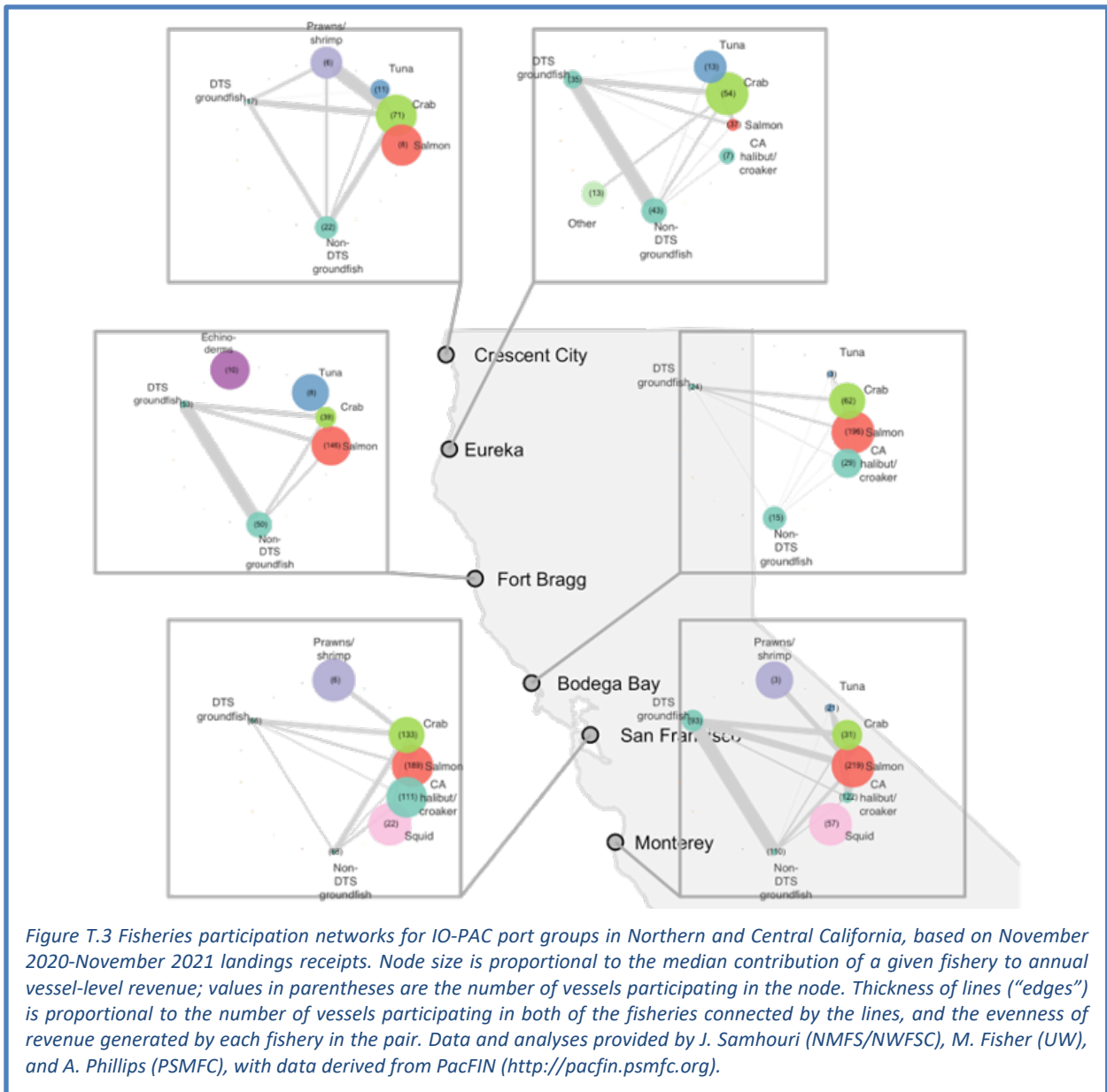


Figure T.1 Fisheries participation networks for IO-PAC port groups in Washington, based on November 2020–November 2021 landings receipts. Node size is proportional to the median contribution of a given fishery to annual vessel-level revenue; values in parentheses are the number of vessels participating in the node. Thickness of lines (“edges”) is proportional to the number of vessels participating in both of the fisheries connected by the lines, and the evenness of revenue generated by each fishery in the pair. Data and analyses provided by J. Samhuri (NMFS/NWFSC), M. Fisher (UW), and A. Phillips (PSMFC), with data derived from PacFIN (<http://pacfin.psmfc.org>).



well-connected to other well-connected fisheries. By contrast, echinoderms generate a large proportion of revenue of participating vessels in many port groups (Figure T.1, Figure T.3 and Figure T.4), but contribute less to overall network connectivity in those port groups (Figure T.5). Similar contrast between total revenue generated by a fishery for a port group, and the extent to which it is strongly connected to other fisheries, is clear from the examination of the non-DTS groundfish fishery described in the main report (Figure 5.4.2). Thus, not only do these networks provide a visual representation of the portfolios of fisheries that are economically important to individual vessels within a port group, they can also suggest where regulatory changes to one fishery (such as the non-DTS groundfish fishery) are likely to have indirect, cross-fishery consequences (spillover or leakage; Kroetz et al. 2019, Fisher et al. 2021).

Finally, tracking changes in networks over time may support the Council’s Climate and Communities Initiative and other activities by providing insight into how fishing communities are changing and potentially adapting to external forces such as changing stock availabilities, climate, regulations



(such as rebuilding plans), and economic and social systems. To that end, we present time series of a network metric called Edge Density within these participation networks from 2004–2021 (Figure T.6). Edge Density represents the extent to which nodes within a networks are connected (the lines in the networks in Figures T.1–T.4) by vessels that participate in multiple fisheries. Declines in Edge Density imply a simplification of network structure, which can in turn reduce resilience to environmental or regulatory shocks (e.g., Fisher et al. 2021). For West Coast networks, some communities show directional change in Edge Density (e.g., increasing over time in Bodega Bay, declining over time in North WA Coast) while others show more cyclical patterns (e.g., many Oregon port groups; Figure A7). Future work to evaluate the causes and potential impacts of these trends could prove fruitful, especially in the context of historical or potential management actions.

The networks presented here, along with those for the years 2005–21, can be viewed on Github: https://github.com/jameals/cciea_networks/tree/main/data/networks/participation_vessel_ports/plots/comparable.

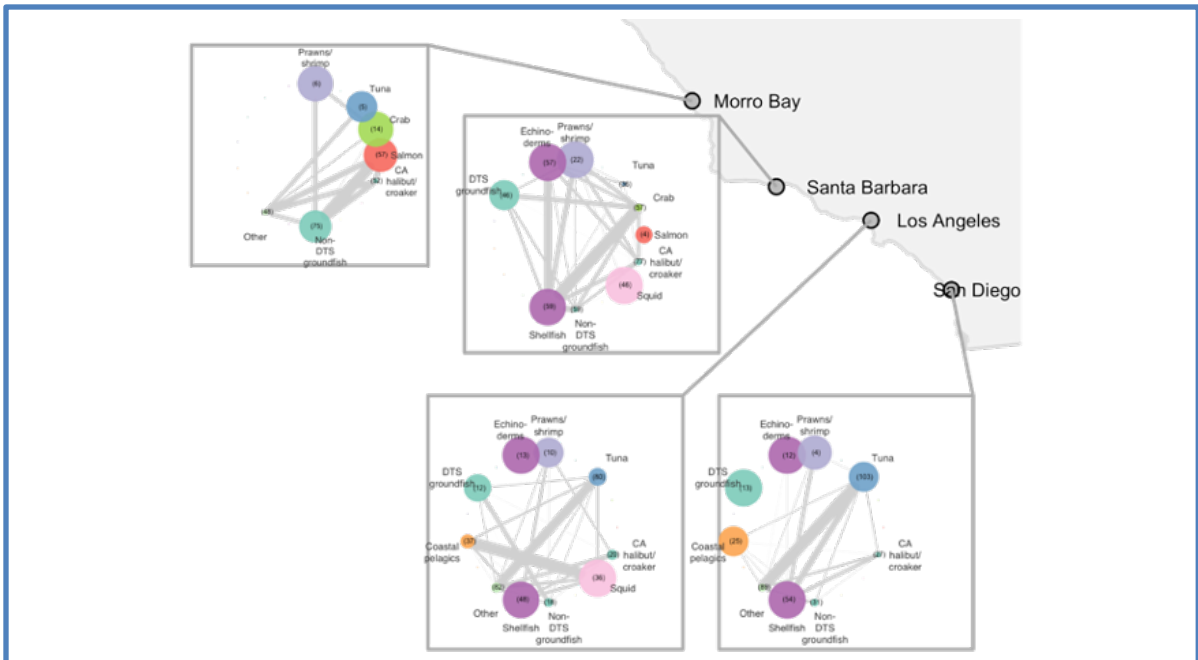


Figure T.5 Fisheries participation networks for IO-PAC port groups in Southern California, based on November 2020–November 2021 landings receipts. Node size is proportional to the median contribution of a given fishery to annual vessel-level revenue; values in parentheses are the number of vessels participating in the node. Thickness of lines (“edges”) is proportional to the number of vessels participating in both of the fisheries connected by the lines, and the evenness of revenue generated by each fishery in the pair. Data and analyses provided by J. Samhouri (NMFS/NWFSC), M. Fisher (UW), and A. Phillips (PSMFC), with data derived from PacFIN (<http://pacfin.psmfc.org>).

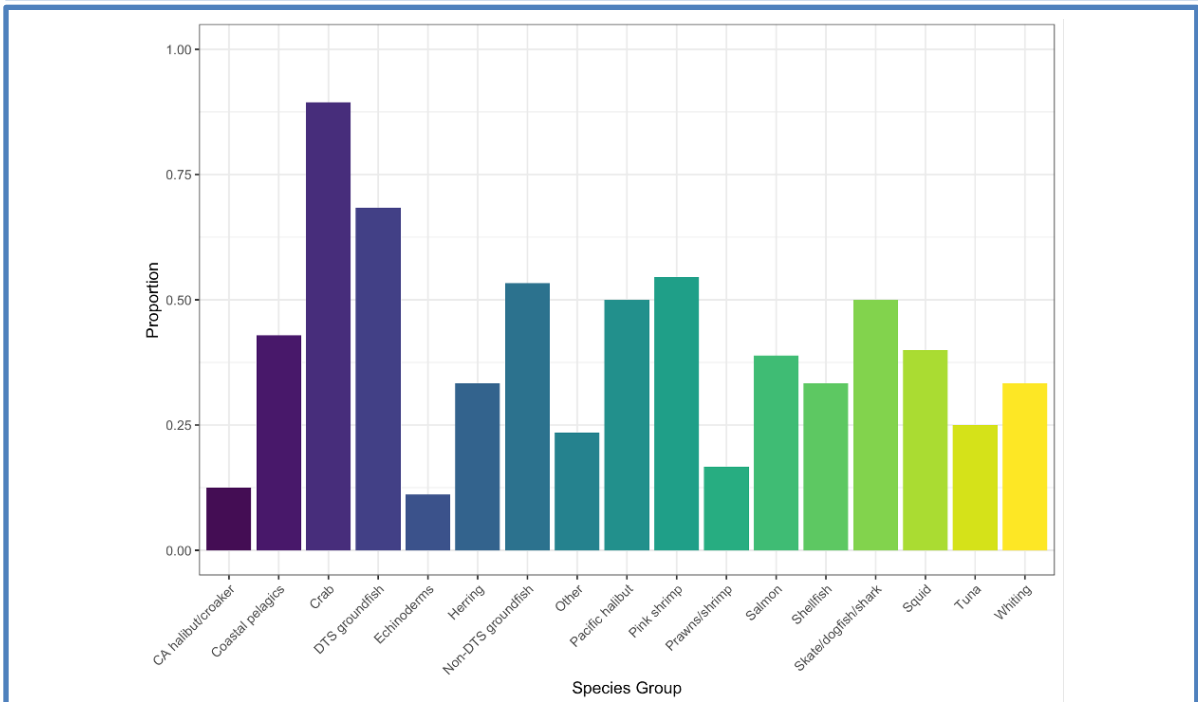


Figure T.4 Proportion of IO-PAC port groups in which a fishery (species group) is highly connected with other highly-connected fisheries (defined as having eigenvector centrality ≥ 0.25 for the fishery) within fisheries participation networks from 2017–2021. Data and analyses provided by J. Samhouri (NMFS/NWFSC), M. Fisher (UW), and A. Phillips (PSMFC), with data derived from PacFIN (<http://pacfin.psmfc.org>).

Edge Density in Fisheries Participation Networks
2005-2021

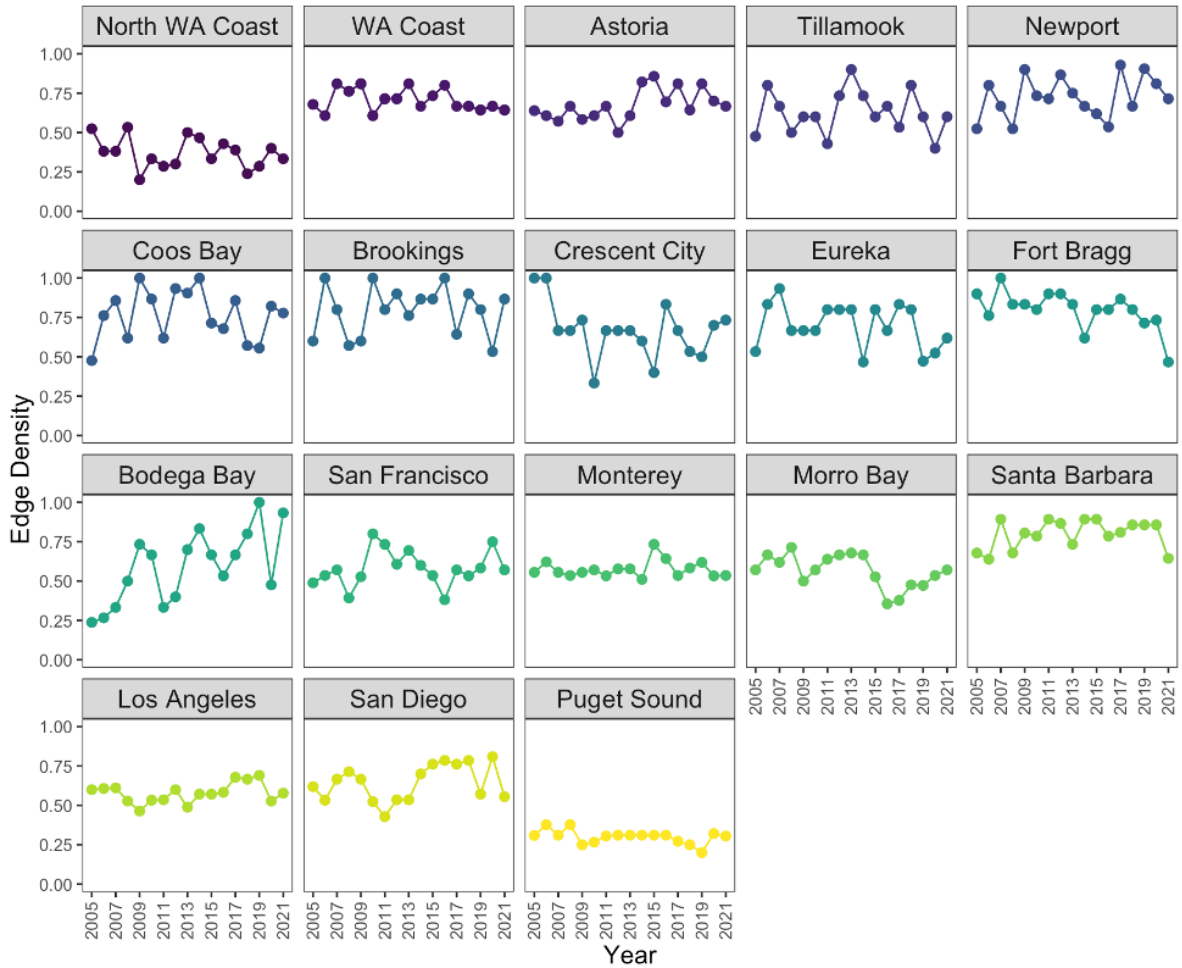


Figure T.6 Edge Density in fisheries participation networks for IO-PAC port groups from Nov 2004 - Nov 2021. Higher edge densities correspond to greater flexibility in fishery participation among all vessels represented in the network. Each year represents landings from November of the previous year through November of the labeled year. Note that edge density scales with network size (it is easier to achieve a high density in a low complexity network), so comparisons across networks of different sizes should be interpreted carefully. The following port groups are not shown: Other Coastal Washington, Columbia River, and Unknown Ports. Data and analyses provided by J. Samhuri (NMFS/NWFSC), M. Fisher (UW), and A. Phillips (PSMFC), with data derived from PacFIN (<http://pacfin.psmfc.org>).

Appendix U REFERENCES

- Abell, R., *et al.* 2008. Freshwater ecoregions of the world: A new map of biogeographic units for freshwater biodiversity conservation. *BioScience* 58:403-414.
- Addicott, E.T., *et al.* 2018. Identifying the potential for cross-fishery spillovers: a network analysis of Alaskan permitting patterns. *Canadian Journal of Fisheries and Aquatic Sciences* 76:56–68.
- Anderson, S.C., *et al.* 2017. Benefits and risks of diversification for individual fishers. *Proceedings of the National Academy of Sciences* 114:10797-10802.
- Beaudreau, A.H., *et al.* 2019. Thirty years of change and the future of Alaskan fisheries: shifts in fishing participation and diversification in response to environmental, regulatory and economic pressures. *Fish and Fisheries* 20: 601-619.
- Busch, D.S., and P. McElhany. 2016. Estimates of the direct effect of seawater pH on the survival rate of species groups in the California Current ecosystem. *PLoS ONE* 11:e0160669.
- Burke, B.J., *et al.* 2013. Multivariate models of adult Pacific salmon returns. *PLoS ONE* 8:e54134.
- Chan, F., *et al.* 2008. Emergence of anoxia in the California Current large marine ecosystem. *Science* 319:920-920.
- Cushing, D.H. 1990. Plankton production and year-class strength in fish populations: an update of the match/mismatch hypothesis. *Advances in Marine Biology* 26: 249-293
- DeLong, R.L., *et al.* 1973. Premature births in California sea lions: Association with high organochlorine pollutant residue levels. *Science* 181:1168-1170.
- DeLong, R.L., *et al.* 1991. Effects of the 1982-1983 El Niño on several population parameters and diet of California sea lions on the California Channel Islands. Pages 166-172 in F. Trillmich and K. A. Ono, editors. *Pinnipeds and El Niño: Responses to environmental stress*. Springer-Verlag, Berlin.
- DeLong, R.L., *et al.* 2017. Age-and sex-specific survival of California sea lions (*Zalophus californianus*) at San Miguel Island, California. *Marine Mammal Science* 33:1097-1125.
- Demer, D.A., *et al.* 2012. Prediction and confirmation of seasonal migration of Pacific sardine (*Sardinops sagax*) in the California Current Ecosystem. *Fishery Bulletin* 110:52-70.
- Dyson, K., and Huppert, D.D. 2010. Regional economic impacts of razor clam beach closures due to harmful algal blooms (HABs) on the Pacific coast of Washington. *Harmful Algae* 9: 264-271.
- FDA, 2011. Fish and Fishery Products Hazards and Controls Guidance. Appendix 5: FDA and EPA Safety Levels in Regulations and Guidance. Department of Health and Human Services, Food and Drug Administration.
- Feely, R.A., *et al.* 2008. Evidence for upwelling of corrosive "acidified" water onto the continental shelf. *Science* 320:1490-1492.
- Fisher, J.L., *et al.* 2015. The impact of El Niño events on the pelagic food chain in the northern California Current. *Global Change Biology* 21:4401-4414.
- Fisher, M.C., *et al.* 2021. Climate shock effects and mediation in fisheries. *Proceedings of the National Academy of Sciences* 118:e2014379117.
- FitzGerald, A.M., *et al.* 2021. Quantifying thermal exposure for migratory riverine species: Phenology of Chinook salmon populations predicts thermal stress. *Global Change Biology* 27:536-549.
- Frawley, T.H., *et al.* 2021. Changes to the structure and function of an albacore fishery reveal shifting social-ecological realities for Pacific Northwest fishermen. *Fish and Fisheries* 22: 280-297.
- Friedman, W.R., *et al.* 2019. Modeling composite effects of marine and freshwater processes on migratory species. *Ecosphere* 10:e02743.
- Fuller, E.C., *et al.* 2017. Characterizing fisheries connectivity in marine social-ecological systems. *ICES Journal of Marine Science* 74:2087-2096.
- Gilmartin, W.G., *et al.* 1976. Premature parturition in the California sea lion. *Journal of Wildlife Diseases* 12:104-115.
- Goldstein, T., *et al.* 2009. The role of domoic acid in abortion and premature parturition of California sea lions (*Zalophus californianus*) on San Miguel Island, California. *Journal of Wildlife Diseases* 45:91-108.
- Hall, J.E., *et al.* 2018. Large river habitat complexity and productivity of Puget Sound Chinook salmon. *PLoS ONE* 13(11):e0205127.

- Harvey, C., *et al.* 2021. California Current Integrated Ecosystem Assessment (CCIEA) California Current ecosystem status report, 2021. Report to the Pacific Fishery Management Council. March 2021, Agenda Item I.1.a.
- Harvey, C.J. *et al.* 2021. Ecosystem status report of the California Current for 2020-21: a summary of ecosystem indicators compiled by the California Current Integrated Ecosystem Assessment team (CCIEA). NOAA Tech. Memo. NMFS-NWFSC-170.
- Hobday, A.J., *et al.* 2016. A hierarchical approach to defining marine heatwaves. *Progress in Oceanography* 141:227-238.
- Holland, D.S. and J. Leonard. 2020. Is a delay a disaster? Economic impacts of the delay of the California Dungeness crab fishery due to a harmful algal bloom. *Harmful Algae* 98:101904.
- Hunsicker *et al.*, in press. Tracking and forecasting community responses to climate perturbations in the California Current Ecosystem. *PLoS Climate*.
- Iverson, S. J., *et al.* 1991. The effect of El Niño on pup development in the California sea lion (*Zalophus californianus*). Pages 180-184 in F. Trillmich and K. A. Ono, editors. *Pinnipeds and El Niño: Responses to environmental stress*. Springer-Verlag, Berlin.
- Jacox, M.G., *et al.* 2017. On the skill of seasonal sea surface temperature forecasts in the California Current System and its connection to ENSO variability. *Climate Dynamics* 53:7519-7533.
- Jacox, M.G., *et al.* 2018. Coastal upwelling revisited: Ekman, Bakun, and improved upwelling indices for the U.S. west coast. *Journal of Geophysical Research: Oceans* 123:7332-7350.
- Jager, H.I., *et al.* 1997. Modelling the linkages between flow management and salmon recruitment in rivers. *Ecological Modelling* 103:171-191.
- Jepson, M., and L.L. Colburn. 2013. Development of social indicators of fishing community vulnerability and resilience in the U.S. Southeast and Northeast Regions. NOAA Tech. Memo. NMFS-F/SPO-129.
- Jordan, M.S. 2012. Hydraulic predictors and seasonal distribution of *Manayunkia speciosa* density in the Klamath River, CA, with implications for ceratomyxosis, a disease of salmon and trout. MS thesis, Oregon State University, 79 pp.
- Kasperski, S., and D.S. Holland. 2013. Income diversification and risk for fishermen. *Proceedings of the National Academy of Sciences* 110:2076-2081.
- Keister, J.E., *et al.* 2011. Zooplankton species composition is linked to ocean transport in the Northern California Current. *Global Change Biology* 17:2498-2511.
- Kroetz, K., *et al.* 2019. Defining the economic scope for ecosystem-based fishery management. *Proceedings of the National Academy of Sciences* 116:4188-4193.
- Laake, J.L., *et al.* 2018. Population growth and status of California sea lions. *Journal of Wildlife Management* 82:583-595.
- Lefebvre, K.A., *et al.* 2002. From sanddabs to blue whales: the pervasiveness of domoic acid. *Toxicon* 40:971-977.
- Leising, A.W., in revision. Marine heatwaves of the North East Pacific from 1982-2019: a Blobtrospective. *Journal of Geophysical Research: Oceans*.
- Leonard, J., and P. Watson. 2011. Description of the input-output model for Pacific Coast fisheries. NOAA Tech. Memo. NMFS-NWFSC-111.
- Limm, M.P. and M.P. Marchetti. 2009. Juvenile Chinook salmon (*Oncorhynchus tshawytscha*) growth in off-channel and main-channel habitats on the Sacramento River, CA using otolith increment widths. *Environmental Biology of Fishes* 85:141-151.
- Lindgren, F., and H. Rue. 2015. Bayesian spatial modelling with R-INLA. *Journal of Statistical Software* 63:1-25.
- Lyons, E., *et al.* 2005. Seasonal prevalence and intensity of hookworms (*Uncinaria* spp.) in California sea lion (*Zalophus californianus*) pups born in 2002 on San Miguel Island, California. *Parasitology Research* 96:127-132.
- McCabe, R.M., *et al.* 2016. An unprecedented coastwide toxic algal bloom linked to anomalous ocean conditions. *Geophysical Research Letters* 43:10366-10376.
- McKibben, M., *et al.* 2017. Climatic regulation of the neurotoxin domoic acid. *Proceedings of the National Academy of Sciences* 114:239-244.

- Mantua, N., *et al.* 2021. Mechanisms, impacts, and mitigation for thiamine deficiency and early life stage mortality in California's Central Valley Chinook salmon. North Pacific Anadromous Fish Commission Technical Report No. 17:92–93.
- Marshall, K.N., *et al.* 2017. Risks of ocean acidification in the California Current food web and fisheries: ecosystem model projections. *Global Change Biology* 23:1525-1539.
- Melin, S.R., *et al.* 2008. The effects of El Niño on the foraging behavior of lactating California sea lions (*Zalophus californianus californianus*) during the nonbreeding season. *Canadian Journal of Zoology* 86:192-206.
- Melin, S.R., *et al.* 2010. Unprecedented mortality of California sea lion pups associated with anomalous oceanographic conditions along the central California coast in 2009. *CalCOFI Reports* 51:182-194.
- Melin, S.R., *et al.* 2012a. California sea lions: an indicator for integrated ecosystem assessment of the California Current system. *CalCOFI Reports* 53:140-152.
- Melin, S.R., *et al.* 2012b. Age-specific recruitment and natality of California sea lions at San Miguel Island, California. *Marine Mammal Science* 28:751-776.
- Moore, S.K., *et al.* 2019. An index of fisheries closures due to harmful algal blooms and a framework for identifying vulnerable fishing communities on the U.S. West Coast. *Marine Policy* 110:103543.
- Moore, S.K., *et al.* 2020. Harmful algal blooms and coastal communities: socioeconomic impacts and actions taken to cope with the 2015 U.S. West Coast domoic acid event. *Harmful Algae* 96:101799.
- Morgan, C.A., *et al.* 2019. Recent ecosystem disturbance in the northern California Current. *Fisheries* 44:465-474.
- Munsch, S.H., *et al.* 2019. Warm, dry winters truncate timing and size distribution of seaward-migrating salmon across a large, regulated watershed. *Ecological Applications* 29:p.e01880.
- Munsch, S.H., *et al.* 2020. Science for integrative management of a diadromous fish stock: interdependencies of fisheries, flow, and habitat restoration. *Canadian Journal of Fisheries and Aquatic Sciences* 77:1487-1504.
- Munsch, S.H., *et al.* 2022. One hundred-seventy years of stressors erode salmon fishery climate resilience in California's warming landscape. *Global Change Biology*, DOI: 10.1111/gcb.16029.
- Neveu, E., *et al.* 2016. An historical analysis of the California Current circulation using ROMS 4D-Var: system configuration and diagnostics. *Ocean Modelling* 99:131-151.
- Nomura, K., *et al.* 2021. Fisheries connectivity measures of adaptive capacity in small-scale fisheries. *ICES Journal of Marine Science*, DOI: 10.1093/icesjms/fsab178.
- Perry, R.W., *et al.* 2013. Sensitivity of survival to migration routes used by juvenile Chinook salmon to negotiate the Sacramento-San Joaquin River Delta. *Environmental Biology of Fishes* 96:381-392.
- Peterson, J.O., *et al.* 2013. Seasonal and interannual variation in the extent of hypoxia in the northern California Current from 1998–2012. *Limnology and Oceanography* 58:2279-2292.
- Peterson, W.T., *et al.* 2014. Applied fisheries oceanography ecosystem indicators of ocean condition inform fisheries management in the California Current. *Oceanography* 27:80-89.
- PFMC. 2016. Pacific Coast Salmon Fishery Management Plan for commercial and recreational salmon fisheries off the coasts of Washington, Oregon, and California as amended through Amendment 19. Pacific Fishery Management Council, Portland, OR.
- Ralston, S., *et al.* 2013. Interannual variation in pelagic juvenile rockfish (*Sebastes* spp.) abundance—going with the flow. *Fisheries Oceanography* 22:288-308.
- Reis, G.J., *et al.* 2019. Clarifying effects of environmental protections on freshwater flows to—and water exports from—the San Francisco Bay Estuary. *San Francisco Estuary and Watershed Science* 17(1).
- Ritzman, J., *et al.* 2018. Economic and sociocultural impacts of fisheries closures in two fishing-dependent communities following the massive 2015 US West Coast harmful algal bloom. *Harmful Algae* 80:35-45.
- Robertson, R.R., and E.P. Bjorkstedt. 2020. Climate-driven variability in *Euphausia pacifica* size distributions off northern California, *Progress in Oceanography* 188:102412.
- Rudnick, D.L., *et al.* 2017. A climatology using data from the California Underwater Glider Network - Dataset. Scripps Institution of Oceanography. doi: 10.21238/S8SPRAY7292
- Sakuma, K.M., *et al.* 2016. Anomalous epipelagic micronekton assemblage patterns in the neritic waters of the California Current in spring 2015 during a period of extreme ocean conditions. *CalCOFI Reports* 57:163-183.

- Santora, J.A., *et al.* 2020. Habitat compression and ecosystem shifts as potential links between marine heatwave and record whale entanglements. *Nature Communications* 11:536.
- Santora, J.A., *et al.* 2021. Diverse integrated ecosystem approach overcomes pandemic-related fisheries monitoring challenges. *Nature Communications* 12:6492.
- Satterthwaite, W.H., *et al.* 2014. Match-mismatch dynamics and the relationship between ocean-entry timing and relative ocean recoveries of Central Valley fall run Chinook salmon. *Marine Ecology Progress Series* 511:237-248.
- Scannell, H.A., *et al.* 2020. Subsurface evolution and persistence of marine heatwaves in the Northeast Pacific. *Geophysical Research Letters* 10.1029/2020GL090548.
- Schroeder, I.D., *et al.* 2019. Source water variability as a driver of rockfish recruitment in the California Current Ecosystem: implications for climate change and fisheries management. *Canadian Journal of Fisheries and Aquatic Sciences* 76: 950-960.
- Speir, C. and Lee, M. 2021. Geographic distribution of commercial fishing landings and port consolidation following ITQ implementation. *Journal of Agricultural and Resource Economics* 46:152-169.
- Stierhoff, K.L., *et al.* 2020. Distribution, biomass, and demography of coastal pelagic fishes in the California Current Ecosystem during summer 2019 based on acoustic-trawl sampling. NOAA Tech. Memo. NMFS-SWFSC-626.
- Strange, J.S., 2012. Migration strategies of adult Chinook salmon runs in response to diverse environmental conditions in the Klamath River basin. *Transactions of the American Fisheries Society* 141:1622-1636.
- Sturrock, A.M., *et al.* 2019. Eight decades of hatchery salmon releases in the California Central Valley: factors influencing straying and resilience. *Fisheries* 44:433-444.
- Sykes, G.E., *et al.* 2009. Temperature and flow effects on migration timing of Chinook salmon smolts. *Transactions of the American Fisheries Society* 138:1252-1265.
- Szoboszlai, A.I., *et al.* 2015. Forage species in predator diets: synthesis of data from the California Current. *Ecological Informatics* 29:45-56.
- Theil, H. 1967. *Economics and Information Theory*. Rand McNally, Chicago.
- Thompson, A.R., *et al.* 2019a. Indicators of pelagic forage community shifts in the California Current Large Marine Ecosystem, 1998–2016. *Ecological Indicators* 105:215-228.
- Thompson, A.R., *et al.* 2019b. State of the California Current 2018-19: a novel anchovy regime and a new marine heatwave? CalCOFI Reports 60:1-65.
- Tommasi, D., *et al.* 2017. Managing living marine resources in a dynamic environment: the role of seasonal to decadal climate forecasts. *Progress in Oceanography* 152:15-49.
- Trainer, V.L., *et al.* 2020. Pelagic harmful algal blooms and climate change: lessons from nature's experiments with extremes. *Harmful Algae* 91:101591.
- Wells, B.K., *et al.* 2008. Relationships between oceanic conditions and growth of Chinook salmon (*Oncorhynchus tshawytscha*) from California, Washington, and Alaska, USA. *Fisheries Oceanography* 17:101-125.
- Zwolinski, J.P., *et al.* 2014. Building on fisheries acoustics for marine ecosystem surveys. *Oceanography* 27:68-79.
- Zwolinski, J.P., *et al.* in press. Distribution, biomass, and demography of coastal pelagic fishes off Central and Southern California during spring 2021 based on acoustic-trawl sampling. NOAA Tech. Memo. NMFS-SWFSC-xxxx.